Aβ's effect on long term memory: A top-down approach in *Lymnaea stagnalis*

LENZIE KATHERINE FORD

A thesis submitted for the degree of Doctor of Philosophy

University of Sussex

July 2015

Declaration

The work presented in this thesis is entirely my own, except where acknowledgement and reference was made. This thesis has not been, and will not be, submitted in whole or in part to another University for the award of any other degree.

Lenzie Ford

(July 2015)

Acknowledgements

I would like to express my sincere gratitude to my supervisors George Kemenes and Louise C. Serpell for their intellectual support, mentorship, patience, and time. Their positive influence played a very important role in shaping not only my PhD experience, but also my scientific career. For this, I am extremely grateful.

I would like to thank Dr. Michael Crossley, Dr. Tom Williams, and Devkee Vadukul for their work referenced in this thesis. I would also like to thank the past and present members of the G. Kemenes, L.C. Serpell, I. Kemenes, K. Staras, P. Benjamin, J.R. Thorpe, and S. Morley labs; whilst there are too many to name here, many colleagues offered both academic and friendly support which has been invaluable to my experience at Sussex.

Finally, I would like to thank my wonderful family, friends, and partner for their never-ending love and support; as well as the American Friends of the University of Sussex for their financial support.

Table of contents

List of Figures and Tables

Abbreviations

CNQX (6-cyano-7-nitroquinoxaline-2, 3-dione)

AMPAR (α-Amino-3-hydroxy-5-methyl-4-isoxazolepropionic acid)

AChE (acetycholinesterase)

AHP (after-hyperpolarisation)

AD (Alzheimer's disease)

Aβ (amyloid β)

ADDLs (amyloid-β derived diffusible ligands)

APP (amyloid precursor protein)

ANOVA (analysis of single variance)

APOE4 (apolipoprotein E4)

APV ((2R)-amino-5-phosphonovaleric acid)

BME (β-Mercaptoethanol)

bZIP (basic leucine zipper)

BCA (bicinchoninic acid)

Bis (Bisindolylmaleimide I)

BSA (bovine serum albumin)

Ca^{2+} (calcium)

CaMKII (Ca^{2+}/calmodulin-dependent kinase II)

CRE (cAMP response element)

CREB (cAMP response element binding protein)

C/EBP (CCAAT element binding protein)

CNS (central nervous system)

CPG (central pattern generator)

CGC (cerebral giant cell)

CSF (cerebrospinal fluid)

CM (colour marker)

CS (conditioned stimulus)

CTGF (corrected total ganglia fluorescence)

CBP (CREB binding protein)

cAMP (cyclic adenosine monophosphate)

cGMP (cyclic guanosine monophosphate)

DNA (deoxyribonucleic acid)

DNQX (6,7-dinitroquinoxaline-2,3-dione)

dUTPs (deoxyuridine triphosphates)

DAG (diacyl-glycerol)

MK-801 (dizocilpine)

ER (endoplasmic reticulum)

ELISA (enzyme-linked immunosorbent assay)

EtOH (ethanol)

ERK (extracellular signal regulated kinase)

FBS (foetal bovine serum)

GABA (γ-aminobutyric acid)

GPCRs (G-protein-coupled receptors)

GSK-3 (glycogen synthase kinase 3)

HEPES (4-(2-hydroxyethyl)-1-piperazineethanesulfonic acid)

HFIP (hexafluoroisopropanol)

HRP (horseradish peroxidase)

IEGs (immediate early genes)

IA (inhibitory avoidance)

IMS (industrial methylated spirits)

IP (immunoprecipitation)

IP3 (inositol triphosphate)

KID (kinase inducible domain)

LTD (long-term depression)

LTF (long-term facilitation)

LTM (long-term memory)

LTP (long-term potentiation)

L-LTP (late-LTP)

Mg^{2+} (magnesium)

MAGUK (membrane-associated guanylate kinase)

mRNAs (messenger ribonucleic acids)

MeOH (methanol)

MAPK (mitogen-activated protein kinase)

NMDA (N-methyl-D-aspartate)

nNOS (neuronal nitric oxide synthase)

nAChRs (nicotinic acetylcholine receptors)

NO (nitric oxide)

OCT (optical cutting temperature)

OD (optical density)

PMA (phorbal 12-myristate 13-acetate)

PACAP (pituitary adenylate cyclase-activating peptide)

PP1 (phosphatase protein 1)

PP2A (phosphatase protein 2A)

PBS (phosphate buffered saline)

PAGE (polyacrylamide gel electrophoresis)

PVDF (polyvinylidene fluoride)

PSD (postsynaptic density)

PSP (postsynaptic potential)

K^+ (potassium)

PKA (protein kinase A)

PKC (protein kinase C)

PKM (protein kinase M)

ROS (reactive oxygen species)

RPM (revolutions per minute)

5-HT (serotonin)

STF (short-term facilitation)

STM (short-term memory)

Na^+ (sodium)

SDS (sodium dodecyl sulphate)

SEM (standard error mean)

TEM (transmission electron microscope)

TCA (trichloroacetic acid)

TBS (tris buffered saline)

TBS-T (tris buffered saline + Tween 20)

THB (tris homogenisation buffer)

US (unconditioned stimulus)

VDCCs (voltage-dependent calcium channels)

Abstract

Amyloid β (Aβ)-induced synaptic and neuronal degeneration has been linked to the memory loss observed in Alzheimer's disease (AD). Although Aβ-induced impairment of synaptic and nonsynaptic plasticity is known to occur before any cell death, the links between these neurophysiological changes and the loss of specific types of behavioural memory are not fully understood. This thesis introduces a behaviourally and physiologically tractable animal model to the Aβ field for the first time, allowing for an in-depth approach to investigating Aβ-induced memory loss to be explored. In Aβ 1-42- and Aβ 25-35-treated *Lymnaea stagnalis*, retrieval of consolidated memory is disrupted after single-trial conditioning and single-injection of synthetic peptide. All succeeding work builds upon these findings using a top-down approach to investigate how Aβ disrupts retrieval of consolidated memory. Neuronal and synaptic health were monitored over a 24 hour *in vivo* incubation period and other memory stages were considered to determine time points of memory vulnerability. In brains that displayed healthy neurons and degenerating synapses, only animals that were exposed to Aβ during the 24-48 hour post-training time points exhibited any behavioural deficits. All other behavioural responses remained normal.

Focus then shifted to investigate the peptide, as opposed to behaviour, involved in the above mentioned experiments. After systemic injection, Aβ was found to penetrate the ganglia, enter cells, and localise to specific organelles by 24 hours exposure. Aβ morphology and structure were also monitored over the 24 hour incubation period, using transmission electron microscopy (TEM), formic acid extraction, silver stain, and western blot. A large distinction between the two peptides, Aβ 1-42 and Aβ 25-35, became apparent at this point and even when peptides were prepared using the same procedure, their effects on behaviour became drastically different. However, it is interesting to note that although the two peptides used are very different, under different preparation procedures they will both produce predominantly tetramer species after 24 hour *in vivo* incubation.

Finally, investigations into disruptions of molecular signalling cascades were considered in order to correlate these disruptions to the observed Aβ-induced behavioural deficits. Specifically, molecular, pharmacological, and biochemical techniques were used to measure protein alterations and post-translational modifications, and to inhibit key protein components, involved in cAMP response element binding protein (CREB)-signalling pathways in *Lymnaea* brain after 24 hour *in*

vivo incubation of Aβ. Phosphorylated CREB was found to be decreased in both Aβ-treated groups; this decrease pattern was also found in active protein kinase A (PKA) experiments. These experiments correlate memory deficits to Aβ-induced disruptions in PKA and CREB activity; however, PKA inhibition experiments indicate that this molecular cascade disruption is not sufficient to cause the observed behavioural deficits.

Taken together, this work correlates Aβ-induced changes from a wide range of components involved in learning and memory, with Aβ-disrupted memory recall. Importantly as well, this work develops *Lymnaea stagnalis* as a novel model for Aβ research and continues to distinguish the two commonly used peptides, Aβ 1-42 and Aβ 25-35. By linking the effects of Aβ on defined neuronal circuits to behavioural deficits in a novel model, the Aβ field has been further developed in an important and unique way.

Publications

The following published article and abstracts contain key results from Chapters 3, 4, 5, 6, and 7:

Ford, L., Crossley, M., Williams, T., Thorpe, J.R., Serpell, L.C., and Kemenes, G. Effects of Aβ exposure on long-term associative memory and its neuronal mechanisms in a defined neuronal network. *Scientific Reports* 5, 10614 (2015).

Ford, L., Crossley, M., Thorpe, J.R., Serpell, L.C., and Kemenes, G. A novel amyloid beta model: Linking long term memory defects to altered signalling in CREB pathways. *Society for Neuroscience Abstracts*, programme number 483.07 (2014).

Ford, L., Thorpe, J.R., Serpell, L.C., and Kemenes, G. Amyloid beta's effect on long term memory: A top-down approach in Lymnaea stagnalis. *Society for Neuroscience Abstracts*, programme number 343.24 (2012).

The following published article does not contain any results described in this thesis.

Al-Hilaly, Y.K., Williams, T.L., Stewart-Parker, M., Ford, L., Skaria, E., Cole, M., Bucher, W.G., Morris, K.L., Sada, A.A., Thorpe, J.R., and Serpell, L.C. A central role for dityrosine crosslinking of Amyloid-β in Alzheimer's disease. *Acta Neuropathologica Communications* **1**, 83 (2013).

1. General Introduction

1.1 Learning and memory

After the seminal work of Wilder Penfield (Penfield, 1952), further scientific investigation of the localisation of learning and memory within the brain was greatly facilitated by the case of patient H.M. (Scoville and Milner, 1957). The patient had severe epilepsy and was treated by removal of the medial temporal lobe. While treatment eradicated the seizures, he developed anterograde amnesia. Studies with H.M., and subsequent research, lead to an understanding that memory is acquired and consolidated in the hippocampus (Zola-Morgan and Squire, 1990; Kim et al., 1995; Anagnostaras et al., 1999). Once fully consolidated, memories are stored in the neocortex (for review, see Frankland and Bontempi, 2005). Cortical storage allows for further categorisation and generalisation of memories, which is advantageous for advanced cognitive function (for review, see Dudai, 2004).

1.1.1 Synaptic and nonsynaptic plasticity

These influential early studies, together with early seminal findings concerning the electrical properties of neurons and the role of synapses and neurotransmitters (Hodgkin and Huxley, 1952; Dale, 1934; Loewi, 1935) have lead to an increasing understanding of how signalling between neurons and storage of engrams in the brain leads to behavioural memory. During chemical transmission, an electrical signal in the presynaptic neuron will cause an influx of calcium (Ca^{2+}) into the presynapse. This increase in Ca^{2+} will cause neurotransmitter-filled vesicles to dock at presynaptic active zones and release neurotransmitters into the synaptic cleft. Neurotransmitters will then be received by postsynaptic receptors, which will cause postsynaptic Ca^{2+} influx and further downstream signalling to occur (Figure 1.1; for review, see Purves et al., 2008). Electrical transmission can occur together, or instead of chemical transmission. This signalling does not involve chemical neurotransmission, but instead is dependent upon gap junctions (for review, see Purves et al., 2008) and ultimately, the direct depolarisation of the postsynaptic neuron by a presynaptic action potential. Signal transmission will lead to long-term memory (LTM) or long-term potentiation (LTP), the cellular correlate of LTM, if a sufficient signal is propagated. LTM/ LTP are often split into two temporal stages; the early stage lasts for 1-3 hours and the protein synthesis-dependent late stage can last more than 24 hours (Frey et al., 1988; Frey et al., 1993). Coordination between the pre- and postsynapse is crucial for LTP and can be enhanced by increased presynaptic neurotransmitter release and/or increased postsynaptic responsiveness (Figure 1.2; for review, see Abraham and Williams, 2003;

Glanzman, 2010). Once LTP has been achieved in a circuit, these neurons are then capable of propagating the same signal with much less stimulation. This is in part due to the increased probability of quantal release, increased numbers of release sites at the presynapse (Oliet et al., 1996), increased synaptic vesicle fusion time, and/or increased fusion pore size (Zahkarenko et al., 2001) of the presynaptic neuron and the enlargement of the synapse and increased receptor insertion of the postsynaptic neuron. Another important aspect of this chemical communication between the synapses is the use of retrograde messengers sent from the postsynapse to feed information back to the presynapse (for review, see Glanzman, 2010).

Postsynaptic depolarisation is often caused by the integration of both synaptic and nonsynaptic (or intrinsic) plasticity changes. This depolarisation is thought to influence the postsynapse by relieving the magnesium (Mg^{2+}) block from N-methyl-D-aspartate (NMDA) receptors, allowing Ca^{2+} influx to the postsynaptic neuron (for review, see Bliss and Collingridge, 1993). For the purposes of this chapter, only a brief description of postsynaptic molecular signalling cascades involved in learning and memory will be considered. A more in-depth background will be considered in Chapters 5 and 6. The initial point of chemical signal entry to the postsynapse occurs at receptors, including NMDARs, nicotinic acetylcholine receptors (nAChRs), α-Amino-3-hydroxy-5-methyl-4-isoxazolepropionic acid (AMPARs), and voltage-dependent calcium channels (VDCCs). NMDAR-dependent, and α7-nAChR-facilitated, LTP will lead to insertion of AMPARs into the postsynapse (Gu and Yakel, 2011). Addition of AMPA receptors into the postsynaptic membranes strengthens signalling, taking the postsynapse from a “silent”, NMDA-only state to a more active NMDA and AMPA state. The insertion of and conductance properties of AMPA receptors are dependent upon ratios of downstream protein kinases and phosphatases, which is swayed from equilibrium depending upon neurotransmitter binding, depolarisation, state of silencing, and more (Malinow and Malenka, 2002; Benke et al., 1998). NMDAR-independent LTP exists as well, with chemical signal entering via VDCCs. Both forms of LTP result in Ca^{2+} entry into the cell which will then signal downstream elements, eventually activating transcription factors, such as cAMP (cyclic adenosine monophosphate) response element binding protein (CREB), and up-regulating gene expression. This results in a rise in immediate early genes (IEGs) and eventual increases in synapses, dendritic spines, and protein rearrangement of the postsynapse for appropriate LTP storage and maintenance.

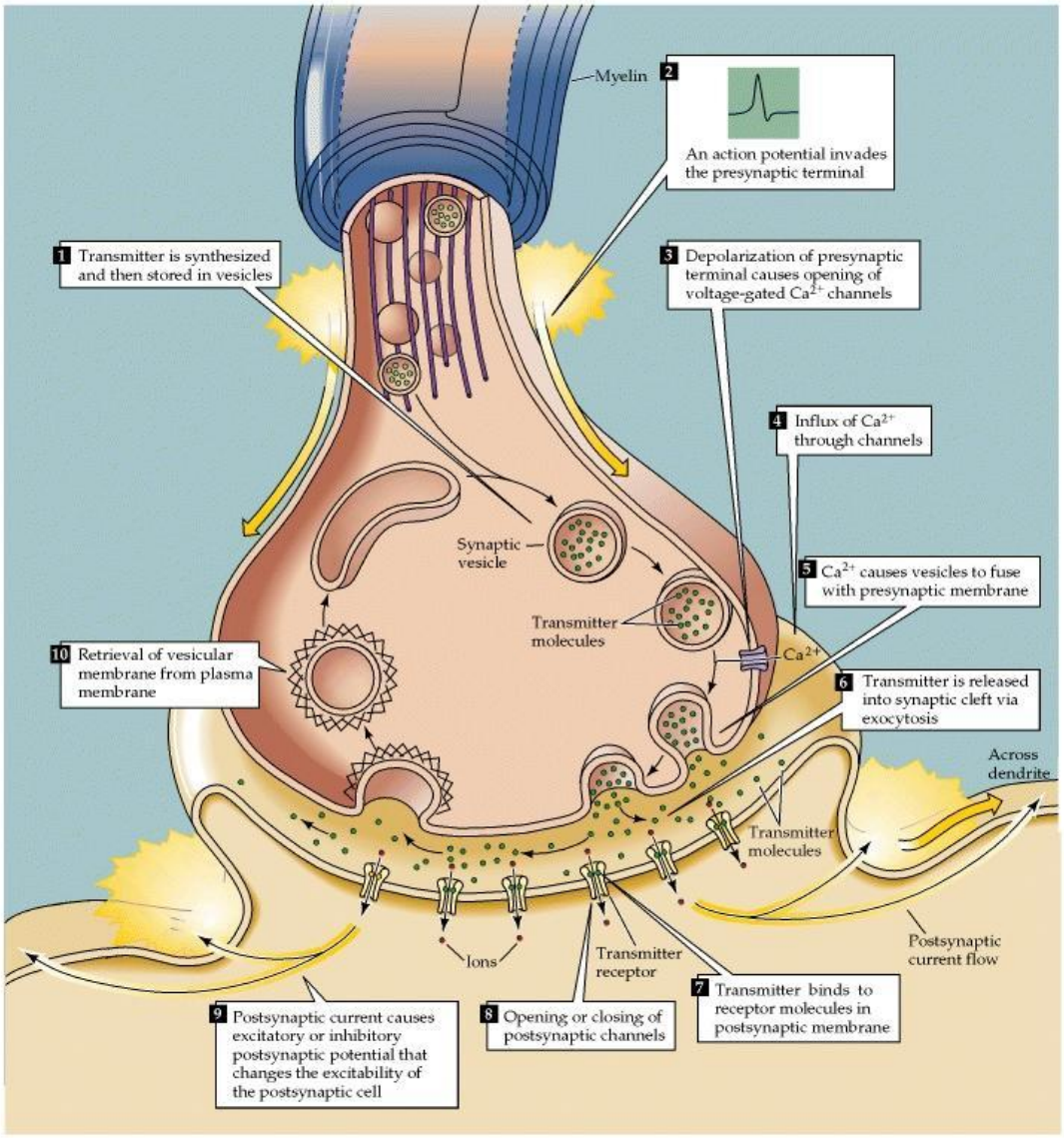

Figure 1.1 Sequence of events in chemical transmission. Representation of a typical synapse during chemical transmission. Sequence of events follows the numbered boxes 1-10 (reproduced from Purves et al., 2008).

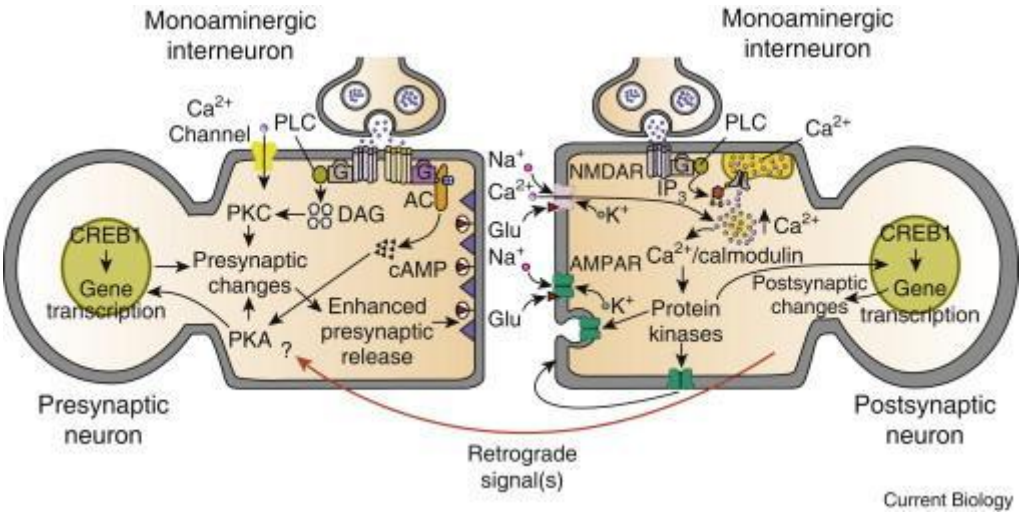

Figure 1.2 Model of excitatory glutamatergic synapse after learning-related enhancement. Presynaptic series of events: Modulatory interneurons release neurotransmitters, often in the form of monoamines which bind to G protein-coupled receptors on the presynaptic neuron. This stimulates several kinases, such as PKA and PKC. Both kinases phosphorylate K^+ channels and enhance presynaptic vesicle mobilisation. Prolonged activation causes PKA to translocate into the nucleus, where is activates CREB and triggers LTP. Postsynaptic series of events: paired pre- and postsynaptic stimulation allows influx of Ca^{2+} into the postsynapse via NMDARs. Ca^{2+} is also released from intracellular Ca^{2+} stores after monoaminergic input at the postsynapse. This Ca^{2+} influx activates several kinases such as CaMKII, PKA, MAPK, and PKC, as well as triggers retrograde signalling to the presynapse. Kinase activation causes "AMPA-fication" at the postsynaptic terminal and prolonged activation results in kinase translocation to the nucleus and activation of CREB, resulting in increased protein synthesis and LTP (reproduced from Glanzman, 2010).

Depolarisation of the postsynapse also results in nonsynaptic plasticity changes. Training produces increases in cell excitability; this excitability can manifest as a reduction in spike threshold, spike accommodation, and amplitude of burst-evoked after-hyperpolarisation (AHP) (for review, see Zhang and Linden, 2003). Each of these components of excitability suggests modulation of potassium (K^+) channels as a potential nonsynaptic mechanism. Other intrinsic properties may also contribute to changes in postsynaptic excitability, such as the resting membrane potential, leakage conductance, membrane capacitance, membrane pumps, action potential back-propagation, and time- and voltage-dependent membrane conductance (for review, see Mozzachiodi and Byrne, 2010). As mentioned previously, LTP "primes" circuits for stimulation and it is believed that increased neuronal excitability may serve as a "label" to identify these cells as recently active (for review, see Janowitz and van Rossum, 2006). Synaptic and nonsynaptic plasticity often coincide, making it difficult to distinguish which proteins are involved in strictly synaptic or nonsynaptic functioning.

1.1.2 Dendritic alterations and new synaptic growth

While synaptic and nonsynaptic biochemical changes play an important role in LTM/ LTP formation, dendritic structural rearrangements are ultimately how a memory trace is encoded. These structural rearrangements take the form of increased perforated postsynapses; formation of new dendritic spines; enlargement of spine heads; increase in number, size, and vesicle complements at presynaptic active zones; and modulation of the total number of presynaptic varicosities per presynaptic neuron (Bailey and Chen, 1988; Bosch and Hayashi, 2012; Maletic-Savatic et al., 1999; Nagerl et al., 2004). The synaptic tag hypothesis was created to explain this process; specifically, how newly synthesised proteins in the soma make their way to the correct synapses during this LTM/ LTP-induced dendritic growth or rearrangement. Potentiated synapses are "tagged", allowing them to capture newly synthesised proteins as they are being transported through dendritic trees (Frey and Morris, 1997). Frey and Morris were the first to demonstrate the synaptic tag hypothesis in rat hippocampus (Frey and Morris, 1997), showing that once transcription dependent LTP has been induced in one pathway, this LTP can be captured at a second pathway receiving very weak stimuli. While many in the field believe the synaptic tag hypothesis, the specifics of how synaptic tagging and capture works are still unknown. Local protein synthesis also occurs in potentiated dendritic spines to regenerate proteins, which are naturally turned over within hours to days. Local protein synthesis is known to occur, due to the observation that ribosomes move to activated synaptic areas (for review, see Abraham and Williams, 2003). This localised protein synthesis is very important for developing

dendrites that are far from the soma to combat spatial restrictions. Spatial and temporal restrictions are also combated in the form of key proteins being made continuously activate or proteins that are able to catalyse its own kind, instead of being reliant upon naturally upstream molecules or protein turnover. The newly formed synaptic structures can be stable for at least a year (Grutzendler et al., 2002).

1.1.3 Invertebrates used in learning and memory studies

Many of the key factors in signalling cascades, such as transcription factors, protein kinases, and homeobox domains, retain high levels of conservation since the evolution of bilateral symmetry (for review, see Alberini, 2009). For this reason, invertebrates possess many genes that are highly homologous to human disease-linked genes. The well-studied fruit fly, *Drosophila*, and nematode, *C. elegans*, have about 70% genetic homology in these genes in humans (for review, see Alberini, 2009). Thus, invertebrates offer a simplified, but relevant, model to study human diseases and other highly evolutionarily conserved aspects of human biology. In fact, some of the most important learning and memory research has used invertebrates. The first compelling evidence for nonsynaptic changes associated with learning was provided in the mollusc *Hermissenda*. Crow and Alkon found that classical conditioning in this mollusc produced several changes in membrane properties that were retained even after these neurons were isolated from the nervous system (Crow and Alkon, 1980). The *Hermissenda* model has since been developed to study alterations of synaptic structure and molecular signalling cascades following associative conditioning, as well (for review, see Crow, 2004). A selection of the most important *Hermissenda* findings include: anisomycin pre-treatment can disrupt structural remodelling of photoreceptor terminal branches following conditioning (Kawai et al., 2003); protein kinase C (PKC), involved in short-term memory (STM), and extracellular signal-regulated protein kinase (ERK), involved in later memory stages, modify both neuronal excitability and synaptic efficacy (Crow et al., 1991; Crow et al., 1998); and actin interacts with other cytoskeleton-related proteins to influence intermediate- and long-term excitability change (Crow and Xue-Bian, 2002). Non-molluscan models have also been influential to the field. *Drosophila* odour-related learning, combined with gene mutation, uncovered the necessity for the *dunce* (cAMP phosphodiesterase), *rutabaga* (calcium/calmodulin-dependent adenylate cyclase), *amnesiac* (pituitary peptide which activates adenylate cyclase), and *linotte* (a deoxyribonucleic acid helicase) genes in learning and memory (Preat, 1998; Folkers, 1982; Dura et al., 1993). The use of heat shock promoters in *Drosophila* has also uncovered the necessity of PKA catalytic activity and found that mutating *turnip* (PKC) inhibits memory acquisition but not LTM

(Kane et al., 1997; Horiuchi et al., 2008). These kinases converge on transcription factors to influence protein synthesis and the best studied transcription factor in *Drosophila* is CREB. Besides the seminal *dunce* and *rutabaga* studies previously mentioned, a direct study of CREB using dominant negative mutation deemed this transcription factor specific and necessary for LTM formation (Yin et al., 1994).

The use of the mollusc, *Aplysia californica*, has helped to develop much of the current knowledge of LTM and its accompanying field, often preceding mammalian studies on the same topic. The tail-siphon withdrawal reflex paradigm is used to model facilitation in identified sensory neurons. When neurons are stimulated with only one pulse of serotonin (5-HT), giving rise to short-term facilitation (STF), PKA is activated and will phosphorylate K^+ S channels which increase the intracellular Ca^{2+} levels and thus increases membrane excitability and broadens spikes (for review, see Lee et al., 2008). Repeated 5-HT application to sensory neurons will produce a long lasting increase in synaptic transmission called long-term facilitation (LTF) (for review, see Burrell and Sahley, 2001) and this facilitation is dependent upon increased protein synthesis of sensory neurons (Barzilai et al., 1989), specifically at cAMP response element (CRE) sites (Dash et al., 1990). LTF is believed to follow this series of events in *Aplysia* presynapses (Figure 1.2): First, 5-HT is released by facilitating neurons once appropriate signal is received, which then activates 5-HT -sensitive adenylyl cyclase in the presynaptic membrane of sensory neurons (Brunelli et al., 1976; Cedar et al., 1972; Levitan and Barondes, 1974; Klein and Kandel, 1978). This increases the amount of cAMP at the synaptic terminal and activates PKA, which allows the catalytic subunit to phosphorylate a number of different proteins, including K^+ channels (Backsai et al., 1993; Dash et al, 1990) and CREB. Phosphorylation of K^+ channels decreases the K^+ currents, which increases membrane resistance and depolarises membrane potential; decrease of K^+ currents therefore prolongs action potentials (termed broadening), which allows more Ca^{2+} to enter the neuron and thus, more neurotransmitters to be released into the synaptic cleft (Klein and Kandel, 1978; Klein and Kandel, 1980). PKA translocation to the nucleus and activation of CREB results in an up-regulation of protein synthesis.

Since the early *Aplysia* facilitation studies, the animal has been further developed for studying LTP and postsynaptic neuronal change (Wainwright et al., 2004) using classical conditioning of the siphon-withdrawal reflex. These paradigms result in both nonsynaptic and synaptic plasticity (Scholz and Byrne, 1987). Researchers have found that the sensory neuron to motor neuron post synaptic potentials (PSP) are glutamatergic and that these PSPs can be initiated by application

of L-glutamate to the culture (Dale and Kandel, 1993). It was also found that these PSPs have NMDAR-like properties (Antonov et al., 2003), similar to many vertebrate glutamatergic PSPs (Dale and Kandel, 1993; Glanzman, 1994; Conrad et al., 1999). Importantly, this LTP is dependent upon presynaptic and postsynaptic coincidence, as evidenced by reduction of associative plasticity after application of a presynaptic PKA inhibitor or a postsynaptic Ca^{2+} chelator (Bao et al., 1998). Besides phosphorylating channels that alter nonsynaptic plasticity, as mentioned previously, PKA can also be activated in the postsynapse causing it to phosphorylate proteins involved in synaptic plasticity, such as the transcription factor CREB. Injection of cloned, phosphorylated *Aplysia* CREB into the postsynapse will initiate the LTM process (Pittenger et al., 2002). Also similarly to mammalian models, AMPA receptors are incorporated into the postsynaptic membrane as neurons are potentiated (Chitwood et al., 2001), CREB-signalling cascades increase IEG production (for review, see Reissner et al., 2006), and retrograde signalling occurs to increase presynaptic neurotransmitter release (for review, see Kandel and Pittenger, 1999), all leading to synaptic rearrangements and new synaptic growth following LTP. These new synaptic formations can take place from 12-18 hours after the initial 5-HT application in *Aplysia* (Kim et al., 2003).

1.2 *Lymnaea stagnalis*, a learning and memory model

Lymnaea stagnalis, the freshwater pond snail, is in the phylum Mollusca and has a relatively simple brain consisting of about 20,000 neurons, many of which are large (~100 μm diameter) and readily identifiable (for review, see Kemenes and Benjamin, 2009) (Figure 1.3). The circuit involved in the generation of feeding behaviour is well defined and contains approximately 100 neurons (for review, see Benjamin, 2012) located in the cerebral and buccal ganglia. For this reason, after using behavioural classical or operant conditioning, the underlying mechanisms can be investigated on a behavioural, circuitry, and single neuron level.

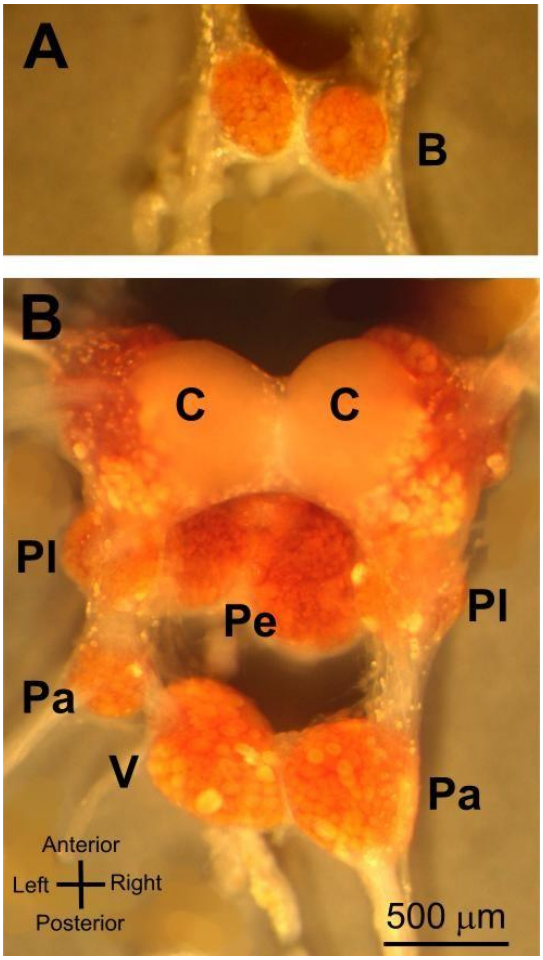

Figure 1.3 Photograph of the *Lymnaea* brain. The *Lymnaea* brain contains (**A**) a pair of buccal ganglia (B, connected to the cerebral ganglia) and (**B**) a ring of other ganglia. C = cerebral ganglia. Pe = pedal ganglia. Pl = pleural ganglia. Pa = parietal ganglia. V = visceral ganglia (reproduced from Benjamin and Kemenes, 2010).

1.2.1 Circuitry involved in feeding and memory

This thesis specifically considers the single-trial food-reward classical conditioning paradigm, in which the same circuitry is involved in the generation of the feeding motor programme in untrained and trained animals (Straub et al., 2004). This gives rise to either unconditioned or conditioned feeding behaviour, with the implicit memory trace acquired and stored in the feeding network (Straub et al., 2004). The three-phase rhythmic feeding motor programme is driven by bursting of cerebral pattern generator (CPG) interneurons which leads to activation of buccal ganglia motoneurons (Benjamin and Rose, 1979; McCrohan and Benjamin, 1980). These motoneurons, B1-10, generate the rhythmic feeding pattern which includes a protraction, retraction, and swallow phase (Rose and Benjamin, 1979). Specifically, *Lymnaea* feeding involves the mouth opening and the toothed radula scraping forward over the food (protraction phase), followed by food being lifted into the mouth (rasp phase) and finished by mouth closure while the food is swallowed (swallow phase) (for review, see Benjamin, 2012) (Figure 1.4A). The CPG neurons, types N1-3, each control one of these phases of feeding (Rose and Benjamin, 1981; Yeoman et al., 1995; Brierley et al., 1997). The cerebral giant cells (CGC) are higher order neurons that modulate these CPG and motoneuron functions (McCrohan and Benjamin, 1980; Yeoman et al., 1996) (Figure 1.4B-C).

Analyses of the CGCs in this circuit revealed a correlation between cellular activity and behavioural effects (McCrohan and Benjamin, 1980). While unable to drive CPG activity via rates of firing, the continuous (called tonic) spiking of the CGC provides an increase in background excitatory modulation, lowering the threshold for activation of the downstream feeding network and thus the behavioural response (for review, see Benjamin, 2012). These CGCs are extremely important for the feeding network; CGC properties alone are capable of altering motoneuron bursting (Kemenes et al., 1989) which controls the feeding motor program of intact animals' feeding behaviour (Yeoman et al., 1994) and this feeding is critically dependent on the CGCs (Yeoman et al., 1994; McCrohan and Benjamin, 1980). Importantly, when an animal learns to associate an unconditioned stimulus with a conditioned stimulus, CGC properties change (I. Kemenes et al., 2006). As early as 20 hours after training, CGCs are depolarised due to an up-regulation of persistent sodium (Na^+) currents (Nikitin et al., 2008); this membrane depolarisation will persist for as long as the memory trace exists.

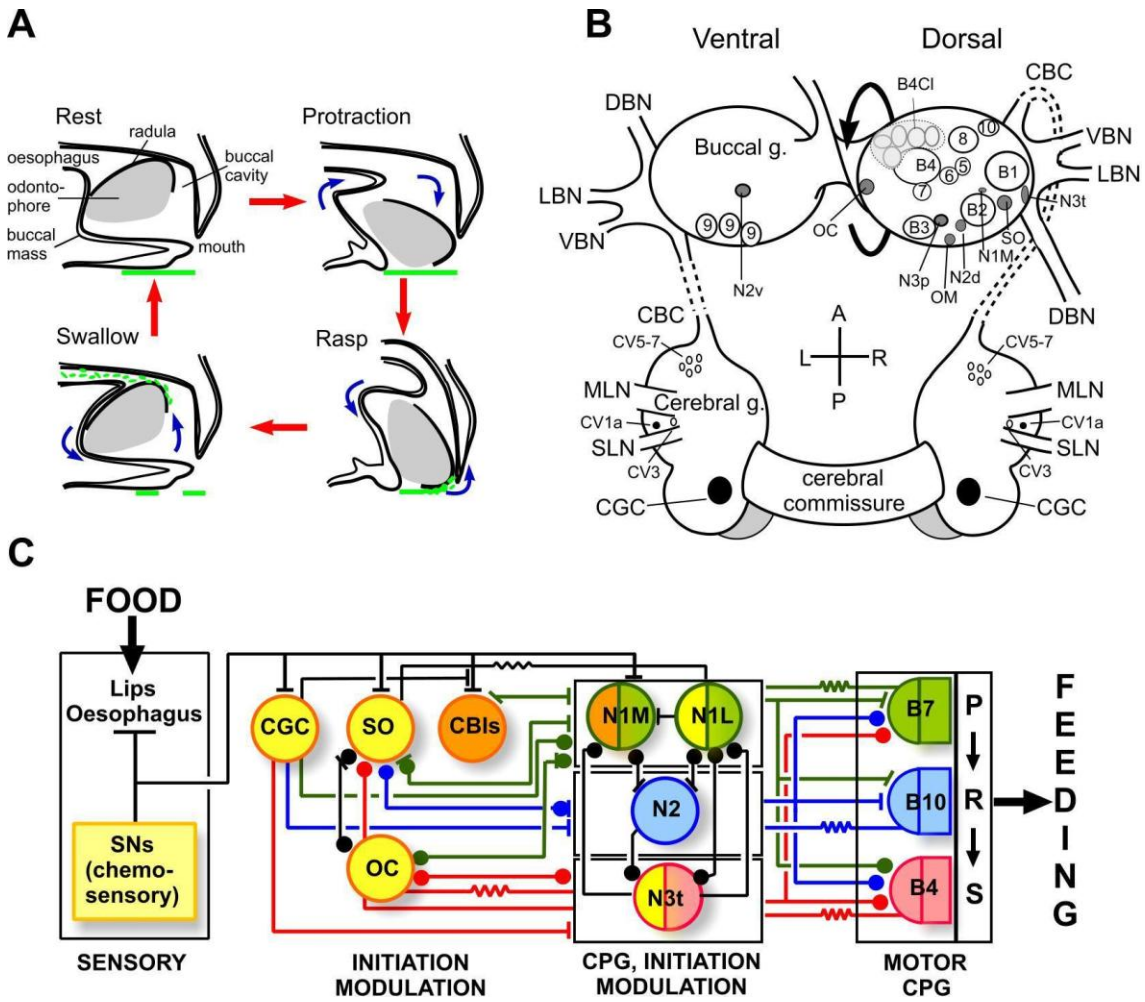

Figure 1.4 Diagram of feeding movements, cellular location, and circuitry. (**A**) The four phases of feeding in *Lymnaea*: rest, protraction, rasp, swallow. (**B**) Feeding neurons located in the buccal and cerebral ganglia. Unshaded neurons are motoneurons. Shaded neurons are interneurons/ initiating neurons/ or sensory neurons. A=anterior, CBC= cerebrobuccal connective, DSN= dorsobuccal nerve, L=left, LBN= laterobuccal nerve, MLN= median lip nerve, OM= oesophageal mechanoreceptor, P=posterior, R=right, SLN= superior lip nerve, VBN= ventrobuccal nerve. (**C**) Circuitry involved in the feeding behaviour. Dots indicate inhibitory chemical synapses, bars indicate excitatory chemical synapses, and resistor symbols indicate electrical synapses. CGC= cerebral giant cells, CBIs= cerebral-buccal interneurons, OC= octopamine-containing interneuron, P= protraction, R= rasp, SO= slow oscillator, S= swallow (reproduced from Benjamin, 2012).

1.2.2 Molecular signalling cascades involved in memory

Besides the well-studied nonsynaptic, electrophysiological properties of key neurons within the feeding circuitry, there is a growing understanding of synaptic/nonsynaptic molecular components as well. Like *Aplysia*, *Lymnaea* maintains highly evolutionarily conserved molecular memory biology. Crucially for the postsynaptic component of LTP, the above mentioned NMDA-like receptors (Moroz et al., 1993), AMPA-like receptors (Darlison et al., 1993; Naskar et al., 2014), and nACh-like receptors (van Nierop et al., 2006) have all been found in *Lymnaea*, as have many of the other kinases and transcription factors noted previously (Figure 1.5; Sadamoto et al., 2003; Naskar et al., 2014; I. Kemenes et al., 2002; Ribeiro et al., 2003; Fulton et al., 2005; Ribeiro et al., 2005; Korneev et al., 2005; G. Kemenes et al., 2006; Michel et al., 2008; Ribeiro et al., 2008; Wan et al., 2010; Pirger et al., 2010 a,b). It is important to note that while other behavioural conditioning paradigms exist; such as chemical or touch classical conditioning, aversive classical conditioning, or operant conditioning (Kemenes and Benjamin, 2009; Kemenes and Benjamin, 1989; Andrew and Savage, 2000; Sakakibara, 2006; Lukowiak et al., 1996; Martens et al., 2007; Kojima et al., 1997; for review, see Benjamin and Kemenes, 2010); the single-trial food-reward classical-conditioning paradigm has been used most prominently for molecular studies in *Lymnaea* (for review, see Kemenes, 2013). For this reason, only the single-trial food-reward classical-conditioning paradigm-based molecular signalling cascade results will be further considered in this thesis.

In *Lymnaea*, as in other animals used in learning and memory research, LTM is known to be dependent on transcription and translation, as has been shown by anisomycin- and actinomycin-D-induced LTM disruption when administered 10 minutes to 1 hour after conditioning (Fulton et al., 2005; Marra et al., 2013). Protein synthesis is initiated by transcription factors; CREB is the best-known transcription factor involved in *Lymnaea* LTM. Both CREB-1 (further referred to as CREB) and CREB-2 orthologues have been found (Ribeiro et al., 2003; Sadamoto et al., 2004) as well as CREB binding protein (CBP) (Hatakeyama et al., 2005) and CCAAT element binding protein (C/EBP) (Hatakeyama et al., 1996). Importantly, animals that have undergone single-trial food-reward classical-conditioning have neurons within the feeding network that express increased phosphorylation of CREB (Ribeiro et al., 2005); all of these findings in *Lymnaea* coincide with the mammalian literature. Many pathways involved in LTM involve CREB-signalling and have been detailed in *Lymnaea*. Starting at the receptor level, memory acquisition is dependent on NMDARs; however, NMDARs are not important for late memory consolidation (Wan et al., 2010). AMPARs have also been

studied in *Lymnaea* and levels of the subunit GluA1 are found to be increased 6 hours after conditioning (Naskar et al., 2014). Finally, pituitary adenylate cyclase-activating peptide (PACAP) receptors have been investigated in *Lymnaea* as well and found that application of a PACAP receptor antagonist during training blocked LTM (Pirger et al., 2010 a,b). Using semi-intact preparations, which involve 6+ trials to learn, PACAP was able to reduce the amount of training trials needed (Pirger et al., 2010 a); these experiments suggest that PACAP helps to boost memory formation. Downstream from receptors, there have been four key kinases studied in *Lymnaea*, one of which is PKA. Blocking catalytic PKA will inhibit LTM at the 24 hour post-conditioning time point in *Lymnaea*, as well as at earlier 5 minute, 10 minute, and 1 hour time points (Michel et al., 2008). These experiments were furthered by finding that injecting cAMP into the CGC soma will enhance the neuron's output, similarly to artificial depolarisation (Nikitin et al., 2006). Importantly, behavioural pharmacology experiments were used to connect PKA to CREB; it was found that activating adenylyl cyclase using forskolin resulted in a large increase in CREB phosphorylation (Ribeiro et al., 2003). Another important kinase involved in *Lymnaea* LTM is mitogen-activated protein kinase (MAPK). Inhibiting phosphorylation of MAPK will disrupt 24 hour LTM; however, MAPK increases in response to the conditioned stimulus (CS) + unconditioned stimulus (US), or CS and US alone, suggesting that MAPK is necessary but not sufficient for LTM in *Lymnaea* (Ribeiro et al., 2005). PKC, along with its atypical isoform protein kinase M (PKM), have also been considered in *Lymnaea*. Both are important for STM recall, however at 24 hours LTM is independent of both PKC and PKM (Marra et al., 2013). Finally, Ca^{2+}/calmodulin-dependent kinase II (CaMKII), as well as its autophosphorylation of Thr286, is necessary for acquisition and late consolidation of memory (Wan et al., 2010; Naskar et al., 2014). Also, CaMKII Thr305 studies in *Lymnaea* suggest that phosphorylation of CaMKII at this site is necessary for the increased GluA1 levels observed in the feeding network 6 hours after conditioning (Naskar et al., 2014). These experiments suggest a possible "AMPA-fication" of neurons in the memory network, as mentioned previously. Alongside these studies, the nitric oxide (NO)/cyclic guanosine monophosphate (cGMP) pathway has also been investigated in *Lymnaea*. The NO/cGMP pathway appears to be critical for LTM up to 5 hours after conditioning (I. Kemenes et al., 2002) and has been found to be important in memory consolidation using behavioural pharmacology (I. Kemenes et al., 2002), a network-level approach examining neuronal nitric oxide synthase (nNOS) messenger ribonucleic acids (mRNAs) (Korneev et al., 2005; Ribeiro et al., 2008), and electrophysiology to measure the role of the NO/cGMP pathway in the CGC (I. Kemenes et al., 2006; Ribeiro et al. 2008).

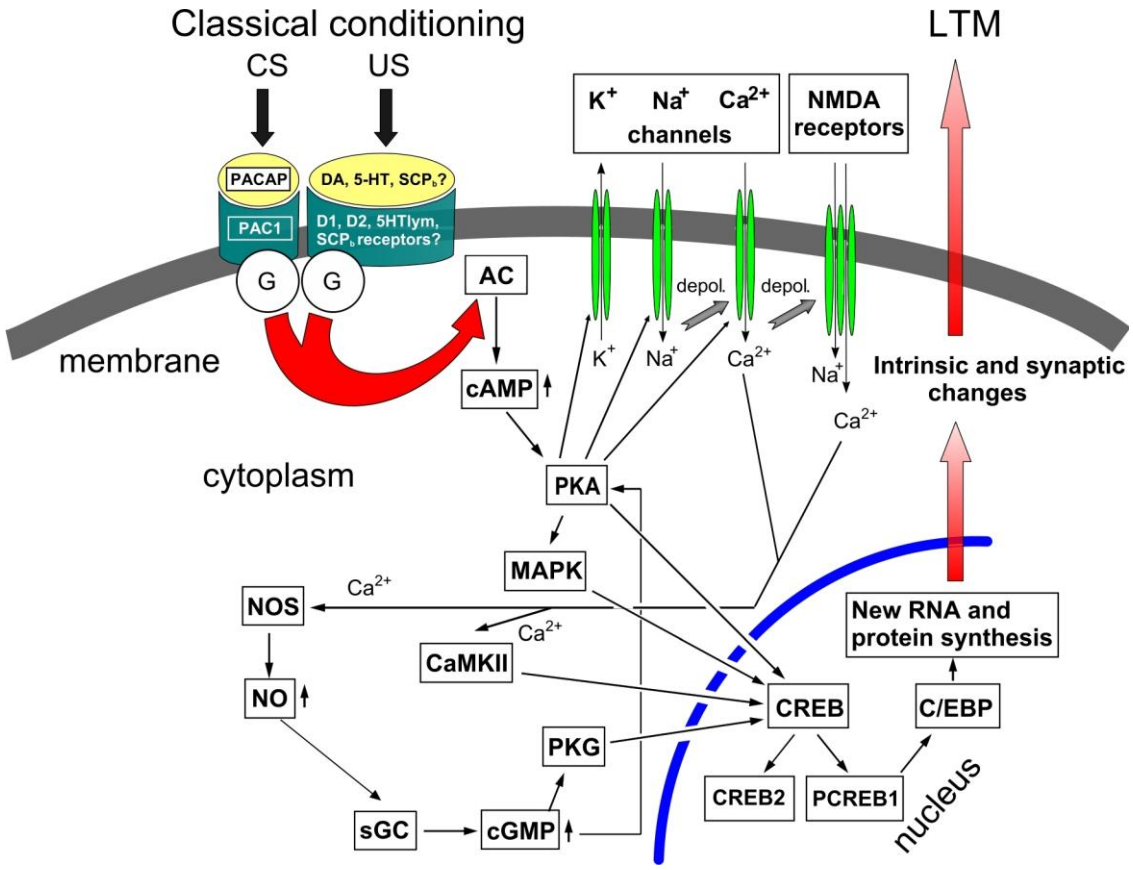

Figure 1.5 CREB-signalling cascades involved in *Lymnaea* LTM. Schematic of key proteins involved in *Lymnaea* CREB-signalling pathways of LTM (reproduced from Kemenes, 2013).

1.3 Alzheimer's Disease

An estimated 30 million+ individuals currently suffer from dementia worldwide; these estimates are largely based on the United States statistics, with 4.5 million individuals within the United States diagnosed with AD prior to 2000 (Alzheimer's Association, 2012). These numbers are staggering, with AD being the sixth leading cause of death in the United States and the fifth leading cause in individuals aged 65 and over. The country is facing an aged population where 13% of those 65 and over, and 45% of the population over 85, have AD. Worse yet, the figures of individuals diagnosed are predicted to increase by 50% by 2030 and 130% by 2050 (Alzheimer's Association, 2012).

The preclinical stage of AD, up to 20 years before any symptoms have developed, already exhibits early neuropathologies which can be measured in the brain, cerebrospinal fluid (CSF), and blood (Alzheimer's Association, 2012). The earliest symptoms manifest as a progressive loss of episodic memory which are often over-looked as normal age-related lapses. As the disease spreads and dementia grows, executive function declines, correct language use becomes obscured, and emotion becomes unstable (for review, see Selkoe, 2013). The final stage of AD brings loss of motor and sensory functions, often ending in death from minor respiratory complications. By this end stage the AD brain has enlarged ventricles and an atrophied hippocampus and cerebral cortex (for review, see Walsh and Selkoe, 2004), causing a 10-20% brain volume decrease (for review, see Selkoe, 2013). The post-mortem diagnosable neuropathology of AD is the appearance of extracellular senile plaques made of Aβ and the intracellular neurofibrillary tangles made of tau (for review, see Walsh and Selkoe, 2004).

The cells most likely to be targeted in AD are those with cholinergic, glutamatergic, noradrenergic, and γ-aminobutyric acid-ergic (GABA) phenotypes. Within these diseased cells, there are alterations in Ca^{2+}, increased free radical formation and oxidative injury, changes in membrane lipids and signalling, deregulation of metal ions, and possibly other changes and dysfunctions (for review, see Selkoe, 2013). Inflammation has also been documented in AD, likely due to the excessive glutamate build up between neurons (for review, see Parameshwaran et al., 2007). Synapses are heavily disrupted; there is a drastic increase in synaptic loss in AD, far more than can be explained simply by the loss of neurons (for review, see Walsh and Selkoe, 2004). In fact, there is a 15-35% decrease in the number of synapses per cortical neuron in AD only a few years after disease onset and pre-mortem cognitive

deficits correlate more with synapse loss than with numbers of plaques or tangles (Terry et al., 1991). Yet even before synaptic loss, synaptic function is highly compromised (for review, see Walsh and Selkoe, 2004). This cellular and network dysfunction can manifest into compromised excitatory synaptic transmission and plasticity (for review, see Parameshwaran et al., 2007). Individuals with AD experience the early symptom of memory loss and in studies where Aβ is extracted from post-mortem AD brains, LTP in rat hippocampus and entorhinal cortex has been found to be disrupted (Walsh et al., 2002).

1.3.1 Neuropathological characteristics of AD

To reiterate, the diagnosable neuropathological characteristics of AD are the presence of Aβ plaques and neurofibrillary tangles. The major component of neurofibrillary tangles is tau. Tau protein is soluble and belongs to the microtubule-associated protein family, localised predominantly in neurons (for review, see Mietelska-Porowska et al., 2014). Its normal function is to stabilise axonal microtubules and does so by either being an isoform with increased binding domains or through phosphorylation. There are six tau isoforms in the human brain and each is distinguished by the amount of binding domains. There are 79 tau phosphorylation sites; at most, 30 sites are phosphorylated in normal tau proteins (for review, see Mietelska-Porowska et al., 2014). Functionally, tau facilitates the polymerisation of α and β tubulin into microtubules. In AD, tau is hyperphosphorylated and detaches from microtubules to form paired-helical and straight filaments, which self-assemble to form tangles (for review, see Selkoe, 2013). Tau disruption can also lead to impaired transport of mitochondria, which can lead to mitochondria-induced non-apoptotic caspase activation (Eckert et al., 2010). This may be involved in the synaptic loss seen in AD (Eckert et al., 2010). Hyperphosphorylation of tau is believed to be a secondary effect of Aβ-induced increase in intracellular Ca^{2+} (Ekinci et al., 1999); therefore, this thesis focuses on Aβ.

The other neuropathological hallmark of AD is Aβ plaques. These plaques are not only composed of fibrillised Aβ peptides (these peptides will be considered in greater detail in section 1.4 of this chapter). Other substances are also found in these plaques, such as proteoglycans, inflammatory molecules, serum-related molecules, heavy metals, protease and clearance-related elements, antioxidant defence proteins, cholinesterases, and other miscellaneous proteins (for review, see Atwood et al., 2002). In both human AD and in AD transgenic mice (Appendix I.1), synaptic loss is greatest near Aβ plaques, which suggests a link between Aβ and synaptotoxicity *in*

vivo (Lacor et al., 2004). In healthy brains, Aβ can be detected in the picomolar to nanomolar range (Haass et al., 1992; Wilson et al., 1999; Seubert et al., 1993). However, AD brains exhibit a 70% increase in Aβ oligomers (Gong et al., 2003), which can also be found in the CSF to a lesser extent (Georganopoulou et al., 2005).

Aβ peptides are believed to induce the Ca^{2+} dyshomeostasis seen in AD, resulting in increased reactive oxygen species (ROS) levels (for review, see Simonian and Coyle, 1996). ROS build-up damages membranes by compromising its integrity which allows for an increased permeability of several ions, including Ca^{2+}, and this loop of increasing Ca^{2+} influx and ROS production renders the intracellular environment excitotoxic (Dykens, 1994; Khodorov et al., 1993). The ROS-induced disruption of cells is believed to be a secondary effect of Aβ (for review, see Mattson, 2007).

1.4 Amyloid β

1.4.1 Amyloid precursor protein (APP)

Aβ is cleaved from APP, a type-1 transmembrane protein of unknown function (for review, see Wilson et al., 1999). The gene is located on human chromosome 21q (for review, see Shirwany et al., 2007) and in humans, the protein is expressed as three isoforms. APP695 is the isoform most prominent in the brain (for review, see Hsiao et al., 1996) and is expressed in neurons, astrocytes, microglia, and endothelial cells (Haass et al., 1992; Busciglio et al., 1993). Low levels of Aβ have been found to be secreted by each of these cell types (Ouimet et al., 1994; Busciglio et al., 1993). Glutamatergic neurons specifically express high levels of APP (Ouimet et al., 1994), both presynaptically and postsynaptically with high localisation at synaptic puncta (for review, see Hoe et al., 2012). APP is highly evolutionarily conserved, with >95% sequence homology existing across mammalian species and high homology within invertebrate species as well, with low sequence homology in the Aβ region (Finch and Sapolsky, 1999; Tharp and Sarkar, 2013). *Drosophila* has an APP orthologue, APPL (Rosen et al., 1989), an α-secretase orthologue (Allinson et al., 2003), and components of γ-secretase (Boulianne et al., 1997; Francis et al., 2002; Hong and Koo, 1997). The *Drosophila* γ-secretase can process human APP (Fossgreen et al., 1998; Greeve et al., 2004) and human APP can be cleaved to produce Aβ in flies, suggesting an endogenous β-secretase-like protease (Greeve et al., 2004).

Although the function of APP is currently unknown, it is believed to play a role in neuromuscular junction formation, synaptic transmission, ion channel function (for review, see Hoe et al., 2010), and blood clotting regulation (Xu et al., 2005). At picomolar levels, Aβ 1-42 has been shown to enhance learning and memory formation (Puzzo et al., 2008) and monomeric Aβ is suggested to play a neuroprotective role in the brain (for review, see Randall et al., 2010). Kamenetz and colleagues have hypothesised that Aβ is involved in a feedback loop regulated by neuronal intrinsic excitability (Kamenetz et al., 2003). They believe that Aβ is produced after action potentials have propagated, increasing the amount of extracellular Aβ at the synapse and reducing postsynaptic excitatory transmission (Kamenetz et al., 2003). However, there are others in the field who do not agree with this hypothesis. Some researchers believe that natural Aβ may facilitate presynaptic transmitter release in neurons with low activity (Puzzo et al., 2008).

APP cleavage and the functional end-products produced are well defined (Figure 1.6). APP is predominantly cleaved through the non-amyloidogenic pathway in healthy brains; the protein is first cleaved by α-secretase (also called ADAM) in the trans-Golgi apparatus (Lammich et al., 1999) and then cleaved by γ-secretases (including the proteins presenilin, PEN2, APH1, niscatrin) (Xia et al., 1998). This process results in production of the p3 peptide and sAPPα, which are thought to be neuroprotective, neurotrophic, and prevent Aβ formation (for review, see Pearson and Peers, 2006). However, APP can also naturally be processed through the amyloidogenic pathway and it is the up-regulation of this processing that increases Aβ in AD. β-secretase first cleaves APP in the trans-Golgi apparatus (Xu et al., 1997; Xia et al., 1998; Greenfield et al., 1999) and then by γ-secretase in either the trans-Golgi apparatus (for Aβ 1-40 production) or the endoplasmic reticulum (for Aβ 1-42 production) (Xia et al., 1998). This process results in Aβ and sAPPβ (for review, see Pearson and Peers, 2006). Aβ 1-40 and Aβ 1-42 are the dominant products produced via amyloidogenic APP processing, but it is thought that other fragments may be produced through proteolytic degrading enzymes (for review, see Kaminsky et al., 2010). These fragments include, but are not limited to, Aβ 2-14, 1-17, 1-18, 1-33, 1-34, 1-37, 1-38, 1-39, 1-43, and 1-46 (Maddalena et al., 2004). It is possible that these fragments play a role in pathology. Importantly, APP can also be cleaved by caspases, but this will not be further investigated in this thesis (for review, see Kaminsky et al., 2010).

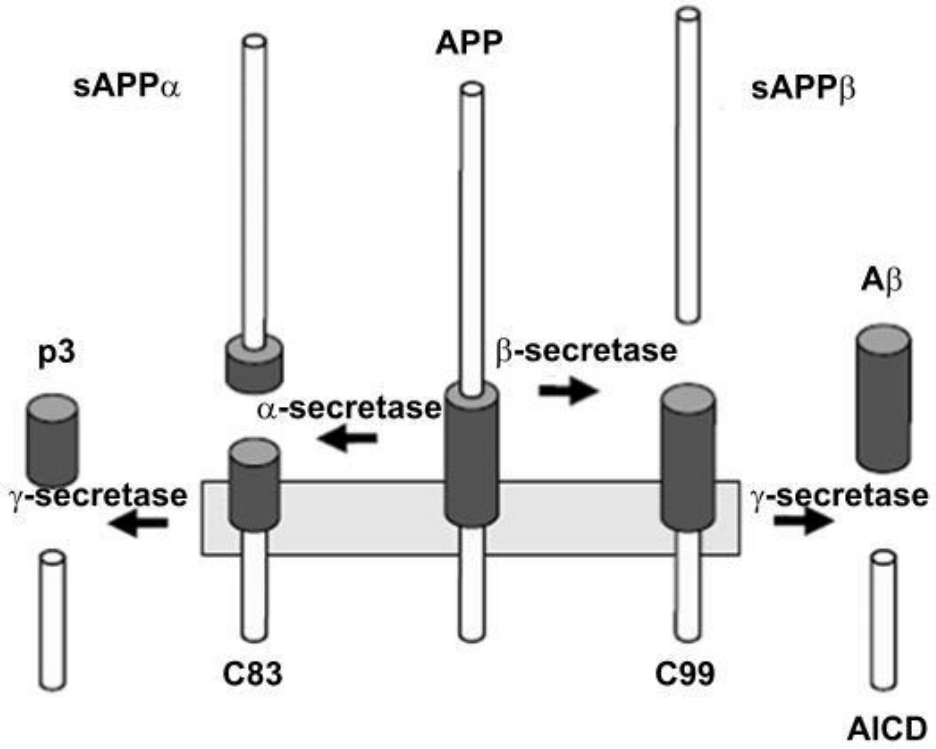

Figure 1.6 APP processing. APP may be processed through the amyloidogenic or non-amyloidogenic pathway. Amyloidogenic processing involves BACE-1 (or β-secretase) cleavage, followed by γ-secretase cleavage. Non-amyloidogenic processing involves α-secretase (or ADAM) cleavage followed by γ-secretase cleavage. Each secretase cleavage produces a fragment of APP (adapted from Linchtenthaler, 2012).

1.4.2 Amyloid β peptide

Aβ is categorised as an amyloid-like protein, indicating that these peptides fibrillise and do not crystallise, and fold into a cross-β structure (Figure 1.7) (for review, see Dobson, 2003). Monomeric Aβ is predominantly unstructured, at least in aqueous solution (Baumketner et al., 2006), and fibrillisation involves a structural change to β-sheet formation, followed by self-assembly to form amyloid fibrils. These fibrils are composed of multiple protofilaments with cross-β structure in which the β-strands run perpendicular to the fibre axis and are held together by hydrogen bonds along the length of the fibril (for review, see Serpell, 2014). Side chains play an important role in associating several β-sheets between protofilaments (for review, see Serpell, 2014). An example of one specific interaction that holds strands together occurs at the β-strands at residues 18-26 and 31-42, which forms salt bridges between Asp23 and Lys28 (for review, see Tycko, 2011). Other influencers include side chains that π stack with identical side chains of other peptides, self-association due to high net charge, changes in the number of aromatic side chains, exposed surface area, and dipole moments (for review, see Chiti and Dobson, 2006). This thesis specifically investigates Aβ 1-42, which is an amphipathic peptide. Of the two physiologically relevant Aβs, Aβ 1-42 is more neurotoxic and more redox active (for review, see Naylor et al., 2008), fibrillises much more quickly (for review, see Roychaudhuri et al., 2006), and has an increased “sticky” characteristic due to exposed hydrophobic residues (for review, see Chiti and Dobson, 2006). The primary sequence for Aβ 1-42 is Asp-Ala-Glu-Phe-Arg-His-Asp-Ser-Gly-Tyr-Glu-Val-His-His-Gln-Lys-Leu-Val-Phe-Phe-Ala-Glu-Asp-Val-Gly-Ser-Asn-Lys-Gly-Ala-Ile-Ile-Gly-Leu-Met-Val-Gly-Gly-Val-Val-Ile-Ala.

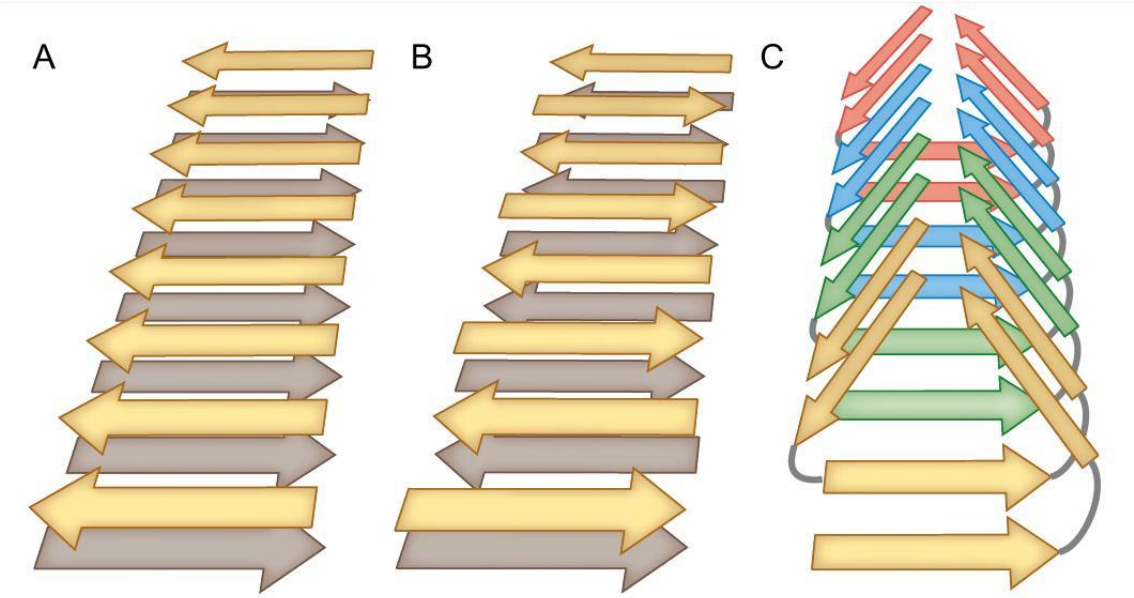

Figure 1.7 Examples of cross-β structure. Schematic examples of (**A**) parallel β-sheets (**B**) antiparallel β-sheets, and (**C**) β-helix formed into cross-β structures (reproduced from Tycko, 2011).

1.4.3 Aβ's involvement in AD

Aβ peptide is believed to be the main toxic element in AD, as detailed by the amyloid cascade hypothesis of AD (for review, see Hardy, 2009). The first evidence for Aβ's role in the disease is its presence in senile plaques, which are found in all AD brains. More recently, soluble extracts of AD brains show Aβ monomers, dimers, and other low-n oligomers at higher concentrations than in healthy brains (McDonald et al., 2010; McDonald et al., 2012) and many different length Aβ peptides have been found in the CSF of those with AD (Maddalena et al., 2004). Secondly, synthetic Aβ peptides are known to be toxic to cells. The next line of evidence comes from Down's Syndrome, or trisomy 21, patients. These individuals exhibit typical AD neuropathology unless they are diploid for the distal location of chromosome 21q, where the APP gene is located, which then relieves the brain of any AD neuropathology (for review, see Ness et al., 2012). Further research has shown that soluble Aβ 1-42 peptides precede senile plaques in the brains of these individuals (Russo et al., 1997). The fourth argument for the amyloid cascade hypothesis of AD states that familial mutations in APP, which are located within or near the Aβ region, will alter aggregation properties of Aβ and are sufficient to cause early-onset AD. Another set of familial mutations, within the presenilin 1 and 2 genes, increase the Aβ 1-42/ Aβ 1-40 ratio in favour of the more neurotoxic Aβ 1-42 species which, again, leads to early-onset AD. Presenilins are the catalytic site of the γ-secretase complex which cleaves the C-terminus of Aβ (for review, see Walsh and Selkoe, 2007). Yet another inheritable factor, the cholesterol-transporter apolipoprotein E4 allele (APOE4), is a strong risk factor for AD and increases cerebral Aβ in diseased brains (for review, see Holtzman et al., 2012). Finally, mice transgenic for mutant human APP show a time-dependent increase in Aβ and develop neuropathological and behavioural changes similar to AD (for review, see Webster et al., 2014).

As well as its central role in AD pathogenesis, Aβ is believed to induce early stage synaptic dysfunction which leads to memory deficits (for review, see Selkoe, 2002). The idea that Aβ disrupts synapse function, which leads to synaptic degeneration and thus memory loss, is known to precede cell death (Lambert et al., 1998; Walsh et al., 2002). Synaptic disruption has been found specifically at postsynaptic, as opposed to presynaptic, terminals (Lacor et al., 2007). This Aβ-induced memory dysfunction has been studied by many labs, using many different models. Aβ-overproducing transgenic mice (including Tg2576; APP+PS1) have been seen to disrupt memory acquisition using a wealth of different training paradigms,

including the Morris water maze, Y-maze, fear conditioning, and social object recognition tasks (Hsiao et al., 1996; Westerman et al., 2002; Chapman et al., 1999; Arendash et al., 2001; Barnes and Good, 2005; Puolivali et al., 2002) (see Appendix I.1). Similar findings of memory acquisition inhibition have been found in animals treated with Aβ (Delobette et al., 1997). However, some consolidated memory experiments indicate that Aβ specifically affects this form of memory, and not memory acquisition (McDonald et al., 1994; Lesne et al., 2006; Tucci et al., 2014; Cleary et al., 2005); while others suggest that neither memory acquisition nor retrieval of consolidated memory are inhibited by Aβ, but instead memory is disrupted during the consolidation process, specifically at time points important for synaptic remodelling (Freir et al., 2011).

Aβ is also known to affect the cellular correlates of memory and forgetting, LTP and long-term depression (LTD). There is a great consensus that Aβ-treatment impairs LTP (Walsh et al., 2002; Shankar et al., 2008; Lambert et al., 1998) and enhances LTD (Kim et al., 2001; Li et al., 2009; Shankar et al., 2008). This induction of LTD is believed to occur through internalisation of receptors or desensitisation of receptors, followed by collapse of the desensitised spines (Snyder et al., 2005; Hsieh et al., 2006).

1.4.4 Oligomeric Aβ

Fibrillisation requires a nucleation event to initiate assembly from monomeric species. This event creates intermediate species, including oligomers and protofibrils, and then elongates before mature fibrils are fully formed. Toxic oligomers may be created via this pathway; however, there is possibly off-pathway production of these toxic species. Importantly, buffer-soluble bioactive Aβ oligomers have been found in synthetic Aβ preparations (Lambert et al., 1998; Bitan et al., 2001), cell culture media (Walsh et al., 2002), Tg2567 mice (Lesne et al., 2006), and AD brains (Gong et al., 2003; Shankar et al., 2008). One of the first studies to suggest that fibrillar Aβ species were not affecting cognitive functions was the Nun Study. Researchers cognitively tested one convent of nuns every year over their lifespan. The nuns brains were then studied post-mortem for the presence of neurofibrillary tangles and amyloid plaques. Sister Mary, the study's "gold star", maintained high cognitive abilities throughout her lifetime and had a brain that contained many plaques and tangles (Snowdon, 1997). This study suggested that the presence of plaques, and thus fibrillar Aβ, does not correlate to the cognitive decline observed in AD. Another important piece of evidence

in support of this hypothesis occurred in 1994 when Oda and colleagues treated Aβ fibrils with clusterin to de-fibrillise them. This dismantling of Aβ fibrils caused an increase in ROS in PC12 cells (Oda et al., 1994). Four years later, Lambert and colleagues found that a fibril free solution of Aβ was neurotoxic to cells and caused a rapid inhibition of LTP which eventually resulted in cell death (Lambert et al., 1998). In 2002, Walsh and colleagues were able to further the findings of Lambert et al. by separating monomers from oligomers and demonstrating that oligomers specifically, and not monomers, inhibit LTP (Walsh et al., 2002). However, not all oligomers are necessarily toxic. While many labs believe that low-n oligomers are neurotoxic (McLean et al., 1999; Hepler et al., 2006), two specific oligomeric species are suggested to be the toxic species. These toxic oligomers are dodecamers and dimers. Dodecamers have been found in human AD brain extracts (Gong et al., 2003) and these species have been found to bind neuronal cultures similar to Aβ derived diffusible ligands (ADDLs; also known as soluble Aβ oligomers) (Lacor et al., 2004). They can also be extracted from Tg2576 mice, which will disrupt LTM when injected into healthy mice (Lesne et al., 2006); other labs have found similar results in synthetic Aβ at this size (Bernstein et al., 2009; Reed et al., 2011). Dimers are also believed to be neurotoxic. When Aβ dimers are extracted from AD brains and applied to rat hippocampal slices, LTP is inhibited (Shankar et al., 2008). Besides LTP inhibition, AD brain-derived Aβ dimers inhibit synaptic remodelling and impair memory consolidation (Shankar et al., 2008). These dimers will also induce degenerative effects when applied to neuronal cultures (Selkoe, 2008). It has more recently been suggested that protofibrils may also be neurotoxic, as seen by the enhancement of protofibril formation in the aggressive Arctic APP mutation (Nilsberth et al., 2001) (Appendix I.1). These toxic protofibrils may be linked to dimers (O'Nuallain et al., 2010). When Aβ 1-40 is mutated to have Ser26 replaced with cysteine and cross-linked with disulphide bonds, dimers will form. The dimers in this study did not block LTP; however, when the dimers were allowed to form protofibrils, this more matured structure did block LTP. Thus, O'Nuallain and colleagues hypothesised that dimers are a crucial building block to form toxic protofibrillar Aβ species (O'Nuallain et al., 2010).

Since the initial studies of Oda, Lambert, and Walsh, much more work has furthered the hypothesis of oligomer-induced toxicity. One area of important findings is that oligomers directly bind to neurons. There are three possible oligomer-neuron interactions that may be involved in toxicity. First, oligomers may interact directly with membranes, forming toxic gain-of-function pores in the lipid bilayer (for review, see Wilcox et al., 2011) and possibly increasing membrane conductance by the dielectric

barrier property of the membrane (Sokolov et al., 2006). Aβ has been shown to specifically bind to GM1 gangliosides and the lipid rafts they inhabit (Zampagni et al., 2010). This pore formation not only allows aberrant concentrations of Ca^{2+} into the cell, a known phenomenon in AD, but also disrupts certain aspects of nonsynaptic plasticity, such as inactivation of K^{+} channels (for review, see Mattson, 2007; Randall et al., 2010). This binding is believed to occur through the hydrophobic residues on Aβ 1-42 interacting with the hydrophobic membrane lipids (Williams and Serpell, 2011). A second group of thought considers intracellular Aβ to be the toxic species, directly altering synapses (Takahashi et al., 2004; Walsh et al., 2000). Intracellular Aβ is found in AD brains (Gouras et al., 2000), can be produced intracellularly (for review, see Wilcox et al., 2011), and has been shown to cause synaptic degeneration (Oddo et al., 2008). Specifically, intracellular oligomeric Aβ was suggested through studies that showed that the intracellular peptides exist in a non-mature, non-fibrillar structure; this was examined with a lack of Bielschowsky silver staining, lack of Congo Red staining, and lack of thioflavin S staining (Gouras et al., 2000). What complicates this hypothesis is that this intracellular Aβ is not necessarily in an oligomeric structure, although some oligomeric species have been discovered (Leon et al., 2010). The final suggestion for Aβ oligomer binding to neurons is their binding to specific extracellular sites. This coincides with the finding that not all areas of the human brain are equally affected by AD (Braak and Braak, 1991) and that Aβ will bind excitatory hippocampal neurons *in vitro*, but will bind with very low affinity to cerebellar neurons (Gong et al., 2003; Lacor et al., 2004). Extracellularly applied, naturally prepared Aβ oligomers at physiological concentrations alter synaptic plasticity, lead to abnormal tau phosphorylation, cause neurite dystrophy, and disrupt memory (Cleary et al., 2005; Lesne et al., 2006; Shankar et al., 2008; Li et al., 2009). Recent studies have indicated that soluble oligomers will only bind to extracellular synaptic components, even when the membrane has been permeabilised (Lacor et al., 2004), and multiple studies have shown that Aβ specifically binds to postsynaptic receptors and will pull-down with these receptors during immunoprecipitation (IP) (Lacor et al., 2004; Lacor et al., 2007; Gong et al., 2003; Renner et al., 2010; De Felice et al., 2007; Roenicke et al., 2011; Wang et al., 2000). Moreover, this final field of thought agrees with the hypothesis put forward by Kamenetz and colleagues for natural APP and Aβ function as feedback loop regulators, as mentioned earlier (see section 1.4.1). An increase in APP cleavage to produce Aβ would allow for greater Aβ at the synapse and an even greater reduction of postsynaptic excitatory transmission after action potential production (Kamenetz et al., 2003).

1.4.5 Aβ affects nonsynaptic plasticity

Besides synaptic plasticity disruption, Aβ is also believed to disrupt nonsynaptic plasticity. Many Aβ-treated or APP-over expressing transgenic mouse models (APdE9; hAPP; APP+PS1; Tg2576) have shown that Aβ alters intrinsic neuronal excitability (for review, see Randall et al., 2010) (Appendix I.1). Aberrant neuronal excitability likely arises due to deregulation of ion channels or pore formation within the membrane. As mentioned previously, pore formation increases Ca^{2+} influx and inactivates K^+ channels. However, application of Aβ to neuronal cultures has been shown to enhance Ca^{2+} and K^+ channel activity in some experiments (Ramsden et al., 2002). Pore formation is only one suggestion as to why intracellular Ca^{2+} is increased with Aβ treatment. Controlled Ca^{2+} influx is a normal, rapid process involved in many different cell functions (for review, see Mattson, 2007). However, the Aβ-induced influx of Ca^{2+} is not controlled and this prolonged influx of Ca^{2+} is toxic to cells, leading to generation of ROS and disruption of energy metabolism (for review, see Mattson, 2007).

1.5 Thesis outline

This thesis considers Aβ peptide and its effect on long term memory using a top-down experimental approach in the pond snail *Lymnaea stagnalis*; combining the two fields of study for the first time. The four results chapters develop this animal model for use in behavioural, structural, molecular, and biochemical investigations in order to answer the question "How does Aβ effect long term memory in *Lymnaea*?". The top-down approach is used to link Aβ structural changes and molecular signalling cascade changes to behavioural deficits observed, while maintaining tight methodological consistency to reduce experimental error. Throughout the thesis, both Aβ 1-42 and Aβ 25-35 are investigated and comparisons and contradictions are noted. Chapter 3 utilises both behavioural, molecular, and imaging techniques to monitor behavioural abnormalities, neuronal health, and synapse health in the snail brain 24 hours post-Aβ injection. Chapter 4 utilises imaging, molecular, biochemical, and behavioural techniques to monitor peptide localisation, peptide structure, peptide morphology, and the effect of differing structure on animal behaviour in snail brain or haemolymph after 24 hour post-Aβ injection. Chapter 5 and Chapter 6 utilise molecular, behavioural, and biochemical techniques to measure protein alterations and post-translational modifications, and to inhibit key protein components, involved in CREB-signalling pathways in *Lymnaea* brain after 24 hour *in vivo* incubation of Aβ. These chapters

include a large amount of necessary background information on CREB-signalling pathways, explained only when each protein is investigated experimentally. Thus, the introduction and results are intertwined in these two chapters. Multiple conclusions are drawn throughout the results sections and in the main discussion.

2. Materials and methods

2.1 Experimental animals

Pond snails, *Lymnaea stagnalis*, were bred at the University of Sussex and maintained in large holding tanks containing 18-22°C copper-free water, at a 12:12 hour light-dark cycle. The animals were fed Tetra-Phyll (TETRA Werke) twice a week and lettuce three times a week.

2.2 Preparation and systemic application of Aβ peptides

Aβ 1-42 was prepared in normal saline solution (50 mM NaCl, 1.6 mM KCl, 2 mM $MgCl_2$ x $6H_2O$, 3.5 mM $CaCl_2$ x $2H_2O$, 10 mM HEPES [4-(2-hydroxyethyl)-1-piperazineethanesulfonic acid]. pH 7.9) (Benjamin and Winlow, 1981) for maximally soluble oligomeric morphology, as previously described (Soura et al., 2012). Briefly, 0.2 mg Aβ 1-42 (rPeptide) was solubilised in 200 μL HFIP (hexafluoroisopropanol) (Sigma-Aldrich) to disaggregate the peptide. The solution was then vortexed on high for one minute and sonicated in a 50/60 Hz bath sonicator for one minute. The HFIP was then dried completely using a low stream of nitrogen gas for five to ten minutes. To ensure complete removal of HFIP, the sample was placed in a dessicator for 30 minutes. Once completely dried, 200 μL dry DMSO (Sigma-Aldrich) was added to the Aβ 1-42, vortexed for one minute, and sonicated for one minute. The Aβ 1-42 was then added to a prepared Zeba buffer-exchange column with 40 μL normal saline solution as a stacking buffer and centrifuged for 30 minutes at 16k RPM. Using a molar absorption coefficient of 1490 M^{-1} cm^{-1}, protein concentration was assessed by measuring at 280 nm using a NanoDrop spectrophotometer. The peptide was then diluted using normal saline to an injected concentration of 1 μM. The peptide control,

created in the Serpell Lab, was prepared for systemic injection in the same manner as Aβ 1-42 and diluted to the same injected concentration of 1 μM.

To prepare Aβ 25-35 for systemic injection, 0.25 mg Aβ Fragment 25-35 (Sigma- Aldrich) was mixed with 1.25 mL copper-free water and left to incubate for two hours to allow the peptide to solubilise and assemble. After two hours, the sample was diluted with 1.25 mL normal saline solution to an injected concentration of 1 μM or 0.1 mM.

To prepare oligomeric Aβ 25-35, 0.25 mg Aβ Fragment 25-35 (Sigma-Aldrich) was prepared as described above for Aβ 1-42. Optical density (OD) was measured at 220 nm using a NanoDrop spectrophotometer before the Zeba buffer exchange column run, and again after, to determine peptide concentration (Millucci et al., 2009). Final concentration was determined using the equation $(OD_{before}-OD_{after})/OD_{before}$ x 100% (Millucci et al., 2009). The peptides were administered to the animals directly after preparation. Using a 1 mL syringe with 30 gauge precision glide needles (Becton Dickinson), 100 μL of the Aβ 25-35 or Aβ 1-42 peptide solution was injected into the haemolymph (~ 1 mL in volume) of each snail. The estimated final concentration in the animal was 0.1 μM for Aβ 1-42 and 0.1 μM or 10 μM for Aβ 25-35. As there is no blood-brain barrier in *Lymnaea* (Sattelle and Lane, 1972), the injected peptides have direct access to the animal's central nervous system. For vehicle-injected control animals, 100 μL of normal saline was injected.

2.3 Single-trial food-reward classical (CS+US) conditioning

Using well-established methods (I. Kemenes et al., 2006), four-to six-month-old snails were removed from their home tanks and starved in new tanks for two days at the same temperature and light dark cycle as the home tanks. After the starvation period, the animals underwent single-trial food-reward classical conditioning (Alexander et al., 1984) in which the CS (amyl acetate: 0.004% final concentration) and

the US (sucrose: 0.6% final concentration) were paired. Initially, each individual snail was left to acclimatise in a 14 cm diameter Petri dish with 90 mL of 18-22°C copper-free water for ten minutes. After the acclimatisation period, 5 mL of amyl acetate was added to the dish and after thirty seconds, 5 mL of sucrose was added. The snails were then left in their Petri dishes for two minutes, and then removed to their starvation tanks. Both the vehicle-injected and Aβ-injected groups were trained. The naïve groups were not trained, but underwent the same starvation/feeding schedule and handling.

All animals were tested with the CS. Each individual snail was left to acclimatise in a 14 cm-diameter Petri dish with 90 mL of 18-22°C copper-free water for ten minutes. After the acclimatisation period, 5 mL of 18-22°C copper-free water was added to the dish. Rasps, the animals' feeding movements, were manually counted for two minutes to determine a baseline rasping rate (number of rasps per two minutes) for each individual. After two minutes, 5 mL amyl acetate was added to the dish. Rasping was tracked for two minutes. Rasping rates were determined by subtracting the individual animal's baseline rasp from the amyl acetate induced rasp. As a control, a separate group of Aβ-treated naïve animals were tested for their ability to produce the unconditioned feeding motor response to the US 24 hours post injection. Snails from the same home tanks as those used in the classical conditioning paradigm were submitted to the same starvation and acclimatisation procedures. However, these animals did not undergo training, only Aβ or vehicle-injection and testing. After the acclimatisation period, 5 mL of 18-22°C copper-free water was added to the dish. Rasping was tracked for two minutes to determine a baseline rasping rate for each individual. After two minutes, 5 mL sucrose was added to the dish. Rasping was tracked for a further two minutes.

2.4 TEM immunolabelling

Buccal and cerebral ganglia were dissected and prepared for immunogold labelling using a previously described protocol involving minimal, cold fixation and embedding in Unicryl resin (Soura et al., 2012; Thorpe, 1999). Briefly, thin (100 nm) sections were labelled with either 1 μg/mL mouse antibody specific for Nu1 (Klein lab), Nu2 (Klein lab), Nu4 (Klein lab), or 1 μg/mL rabbit antibody specific for AlexaFluor 488 (Molecular Probes). They were then labelled with either goat anti-mouse 10 nm gold-conjugated secondary antibody or goat anti-rabbit 10 nm gold-conjugated secondary antibody (BBI Solutions OEM Ltd., Cardiff, UK) and stained with 2% aqueous uranyl acetate. The labelled thin sections were examined in a Hitachi 7100 TEM at 100 kV and digital images acquired with an axially mounted (2K x 2K pixel) Gatan Ultrascan 1000 CCD camera (Gatan UK, Oxford, UK).

2.5 Cell death and apoptosis measurements

To test the integrity of the feeding network, behavioural testing with sucrose was used as described in 2.3.

For the cell morphology analysis, TEM was used to examine buccal and cerebral ganglia as detailed above in 2.4. Images were then qualitatively scored for the health of the nucleolus, nuclear envelope, cellular membrane, and chromatin on a scale of 0 to 2, with 0= unhealthy 1= uncertain 2= healthy.

For the TUNEL assay (Roche) analysis, buccal and cerebral ganglia were dissected and pinned on to a sylgard square. Samples were immediately placed in 4% paraformaldehyde (in 0.2 M phosphate buffer, pH 7.2) for 1 hour and then transferred into 30% sucrose in phosphate buffered saline (PBS) solution overnight at 4^{o}C. Samples were removed from the sylgard square, coated in OCT (optical cutting temperature) embedding medium (VWR), and frozen in liquid nitrogen. Samples were sliced to 14 μm thickness using a Cryostat and placed on to SuperFrost Plus slides (VWR). Slides were then allowed to dry for at least 30 minutes before being washed

three times for two minutes each in PBS. Slides were permeabilised in 0.1% Triton-X in PBS for 2 minutes on ice. The positive control slide was then treated with DNase I in Tris-HCl for 10 minutes, and all slides were labelled with TUNEL reaction mixture for 60 minutes at 37^{o}C except for the negative control, which was only labelled with the Label Solution. Slides received two final washes in PBS for two minutes each before 6 drops of Fluoroshield (Sigma-Aldrich) was added to each slide, along with a cover slip. Slides were allowed to dry and samples were imaged using an Olympus BX61WI with a 10x 1.0 NA dipping objective and excitation and emission filters 470/22. Images were taken using an EMCCD camera (Andor iXon), processed using μManager software (Edelstein et al., 2010), and binned at 2x2. Images were analysed using ImageJ software and measured for area, mean, integrated density, and background signal mean all on the same ImageJ default setting for threshold. Final signal intensity was calculated using the Corrected Total Ganglia Fluorescence (CTGF) formula: CTGF=Integrated Density – (Area of selected ganglia X Mean fluorescence of background reading).

2.6 SDS-PAGE and membrane immunolabelling

First, *Lymnaea* ganglionic samples were prepared. Buccal and cerebral ganglia were dissected, pooled so that there were 5 buccal + cerebral ganglia per eppendorf tube, and stored at -80^{o}C until use. For use, ganglia were homogenised in Tris Homogenisation Buffer (THB) (240 mM Trizma base, HCl to pH 6.8) and then Laemelli Buffer (BioRad) + 10% β-Mercaptoethanol (BME) was added to the sample and pipette mixed. Samples were heated at 95^{o}C for 5 minutes and centrifuged for 30 minutes at 13K revolutions per minute (RPM) and 4^{o}C. Only the supernatant was retained. For rat sample preparation, 1 part PEPI (1x PBS, 5mM EDTA, 1x Protease Inhibitor) to 1 volume tissue were homogenised. Samples were vortexed, centrifuged at 14K for 10 minutes, and only supernatant was retained. Samples were then treated the same as

Lymnaea samples, starting with the addition of Laemelli Buffer and finishing with centrifugation. Protein concentration was measured using a bicinchoninic acid (BCA) assay (see below) and samples were diluted (often to 20-40 μg per well).

For dot blot experiments, polyvinylidene fluoride (PVDF) membranes were prepared by allowing incubation in methanol (MeOH), water, and tris buffered saline (TBS) until fully immersed. Prepared samples were then dotted on to the membrane and allowed to dry for 1 hour. Membranes were then put into blocking solution (Table 2.1) for 1 hour with gentle rocking, and incubated in primary antibody + blocking solution (Table 2.1) overnight at 4^{o}C with gentle rocking. After the primary antibody labelling, membranes were washed in 20 mL TBS-Tween 20(T) (24.2 g Trizma base, 80 g $NaCl_2$, in 1 L H_2O. pH 7.5. + 0.15% Tween 20) for 5 minutes three times, with moderate rocking. Membranes were then allowed to incubate with 5 mL blocking solution + horseradish peroxidase (HRP)-conjugated secondary antibody (Cell Signalling) (Table 2.1) for 1.5 hours with gentle rocking. The membranes were then washed with 20 mL TBS-T for 10 minutes three times, with moderate rocking. Finally, 4 mL HRP substrate (Millipore) was added to the membranes and allowed to incubate for 5 minutes. Membranes were then removed from the substrate, immediately exposed to x-ray film, and developed.

For sodium dodecyl sulphate (SDS)-polyacrylamide gel electrophoresis (PAGE) experiments, prepared sample was run either on a hand cast gel (8.25%, 10%, or 12%) or on a Tris-glycine 4-20% gradient gel (BioRad), placed into a mini-PROTEAN tank (BioRad) with Running Buffer (30.3 g Trizma base, 144 g glycine, 10g SDS, in 1 L H_2O. pH 8.3), and run at 120 V, 40 mA until the dye front reached the bottom of the gel. Gels were then either silver stained or transferred for western blot.

For silver stain experiments, gels were subjected to a Proteo-Silver Silver Stain Kit (Sigma-Aldrich) and the manufacturer's instructions were followed. Briefly, gels were fixed for 1 hour, followed by an ethanol (EtOH) wash and then a water wash. Next, Sensitisation Solution was added to the gel, followed by a water wash. Then,

Silver Equilibration was added to the gel, followed by a water wash. Finally, Developer Solution was added to the gel until bands were visible. Once developed, Stop Solution was added to the gel. Finally, the gel was imaged using a Gel Doc EZ System (BioRad), and used for qualitative analysis.

For western blot experiments, the prepared sample was run using SDS-PAGE as described above. Gels were then wet transferred in Transfer Buffer (5.8 g Trizma base, 2.9 g glycine, 0.37 g SDS, 200 mL MeOH, 800 mL H_2O. pH 8.3) on to a PVDF membrane at either: 80 V, 200 mA for 2 hours; 20V, 200 mA for 16 hours; or 25 V, 200 mA for 2 hours. Membranes were then removed from the tank and allowed to incubate in an appropriate blocking solution (Table 2.1) for one hour with gentle rocking. After the block, membranes were then allowed to incubate in blocking solution + primary antibody (Table 2.1) at 4^{o}C overnight with gentle rocking. After the primary antibody labelling, membranes were washed in 20 mL TBS-T for 5 minutes three times, with moderate rocking. Membranes were then allowed to incubate with 5 mL blocking solution + HRP-conjugated secondary antibody (Table 2.1) for 1.5 hours with gentle rocking. The membranes were then washed with 20 mL TBS-T for 10 minutes three times, with moderate rocking. Finally, 4 mL HRP substrate was added to the membranes and allowed to incubate for 5 minutes. Membranes were then removed from the substrate, immediately exposed to x-ray film, and developed.

All membranes were stripped at least once and no more than three times. Membranes were allowed to incubate in Stripping Buffer (12.5 mL Tris/HCl [12.11 g Trizma base, in 100 mL H_2O. pH 6.8], 1.426 mL BME, 4 g SDS, in 200 mL H_2O) for 15 minutes at 65^{o}C with vigorous shaking, twice. Membranes were then vigorously washed with TBS-T for 10 minutes. The washing step was repeated until all Stripping Buffer was removed.

All dot blots and western blots were quantified using ImageJ software. Every result was normalised to an appropriate loading control; steady state proteins were

normalised to α tubulin and phosphorylated proteins were normalised to an appropriate steady state protein.

Protein of interest	**Blocking solution**	**Primary antibody**	**Secondary antibody**
α tubulin	3% Milk in TBS-T	1/7000. Anti- α-Tubulin antibody, Sigma Aldrich	1/3000. Goat anti mouse
PSD-95	5% Milk in TBS-T	1/1000. PSD95 antibody, Novus Biological	1/1000. Goat anti mouse
Nu1	5% Milk in TBS-T	1 μg/mL. Nu1, Klein Lab	1/1000. Goat anti mouse
Nu4	5% Milk in TBS-T	1 μg/mL. Nu4, Klein Lab	1/1000. Goat anti mouse
CREB	3% bovine serum albumin (BSA) in TSB-T	1/1500. CREB, Cell Signalling	1/1000. Goat anti rabbit
pCREB Ser133	3% Milk in TBS-T	1/5000. Anti-phospho-CREB (Ser133), Millipore	1/1000. Goat anti mouse
H3	5% Milk in TBS-T	1/10000 Anti-Histone H3, Sigma Aldrich	1/1000. Goat anti rabbit
GluA1	3% Milk in TBS-T	1/1000. Anti-GluR1, Millipore	1/1000. Goat anti rabbit
pGluA1 Ser845	3% Milk in TBS-T	1/1000. Anti-	1/1000. Goat anti

		GluR1-S845, Abcam	rabbit
pGluA1 Ser831	3% Milk in TBS-T	1/1000. Anti-GluR1-S831, Abcam	1/1000. Goat anti rabbit
NMDA NR1 (1)		Anti-NMDAR1 antibody, Abcam	Goat anti rabbit
NMDA NR1 (2)		NMDAR1 Antibody, Novus Bio	Goat anti mouse
α7-nAChR	3% BSA/ 10% fetal bovine serum (FBS) in TBS-T	1/7000. Anti-Nicotinic Acetylcholine Receptor alpha 7 antibody, Abcam	1/5000. Goat anti rabbit
Adenylyl cyclase	5% Milk in TBS-T	1/2000. Anti-Adenylate cyclase 1 antibody, Abcam	1/1000. Goat anti rabbit
cAMP	3% Milk in TBS-T	1/2000. Anti- cAMP antibody, Abcam	1/1000. Goat anti mouse
PKC	5% Milk in TBS-T	1/4000. Anti- PKC (α,β,γ), Millipore	1/1000. Goat anti mouse
PKA	3% Milk in TBS-T	1/6000. PKAα cat antibody, Santa Cruz Biotech	1/1000. Goat anti rabbit
MAPK	5% BSA in TBS-T	1/1000. p44/p22 MAPK (Erk 1/2) Antibody, Cell	1/1000. Goat anti rabbit

		Signalling	
pMAPK	5% BSA in TBS-T	1/3500. Phospho-p44/42 Map Kinase (Thr202/Tyr204) Antibody, Cell Signalling	1/1000. Goat anti rabbit

Table 2.1 Optimisation for antibodies used in this thesis. Proteins of interest and the corresponding blocking solution; primary antibody concentration, name, and company; and secondary antibody concentration and name are indicated.

2.7 Measurement of protein concentration

A BCA Protein Assay Kit (Pierce) was used to measure protein concentration in samples. The procedure followed the manufacturer's suggestions completely. Briefly, fresh standards and samples were prepared for each BCA. Working Reagent was added to all standards and samples, which were then heated to 37^{o}C for 30 minutes. All standards and samples were then measured at 562 nm using a spectrophotometer. A standard curve was created using the results from the standards, allowing protein concentration of the sample to be identified.

2.8 Preparation and imaging of AlexaFluor 488 tagged Aβ 1-42

The protocol for preparation was fully described previously (Soura et al., 2012). Briefly, an AlexaFluor 488 Protein Labelling Kit (Invitrogen) was used to label the freshly solubilised Aβ 1-42 (described above), following the manufacturer's instructions. Aβ 1-42 was prepared as normal up to the DMSO stage, where kit components were added to the vial and allowed to incubate for 15 minutes at 21^{o} C. Tagged-peptide was then run on a 2 mL Zeba buffer-exchange spin column with 40 μL normal saline solution as a stacking buffer and centrifuged for 30 minutes at 16k RPM, to remove any free tag from the solution. Protein concentration was measured as described for Aβ 1-

42 preparation with the addition of a measurement at 495 nm and 0.11 correction factor to account for the added AlexaFluor 488 tag, and degree of labelling was then assessed using the molar extinction coefficient of the AlexaFluor 488 of 71,000 M−1 cm−1. Protein labelling was low, 0.042 moles dye per moles protein, likely due to the low concentration of peptide (less than 2 mg/mL) used, as suggested by the manufacturer. Tagged-Aβ 1-42 was diluted to 1 μM, 25 μM, or 50 μM in normal saline solution.

For whole mount fluorescent imaging of AlexaFluor 488 tagged Aβ 1-42, snail brains were dissected and the desheathed brains were immediately placed on glass slides with cover slips and imaged using an Olympus BX61WI with a 10x 1.0 NA dipping objective and excitation and emission filters 470/22. Images were taken using an EMCCD camera (Andor iXon), processed using μManager software (Edelstein et al., 2010), and binned at 1x1.

2.9 Formic acid extracted haemolymph preparation

After 24 hours *in vivo* incubation of either Aβ 1-42, Aβ 25-35, or oligomeric Aβ 25-35, a 1 mL syringe with 30 gauge precision glide needles (Becton Dickinson) was used to extract roughly 1 mL of haemolymph from each snail. 10 mL of haemolymph was pooled to create one sample. Each sample was submitted to formic acid extraction, a method of removing soluble Aβ from tissue samples (McDonald et al., 2012). 1 mL of pooled haemolymph sample was mixed with 1 mL 0.4% diethylamine/100 mM NaCl. 400 μL was then centrifuged at 14K RPM for 1 hour at 4^{o} C. The supernatant was removed and 200 μL 1M Tris Base pH 7.4 was added to the pellet. 400 μL cold formic acid was then added. The sample was sonicated for 20 seconds and then 400 μL was centrifuged at 14K RPM for 1 hour at 4^{o} C. 210 μL of the supernatant was diluted into 4mL Formic Acid Neutralization Buffer (1M Tris Base, 0.5 M Na_2HPO_4) and 2 mL of this mixture was centrifuged at 14K RPM for 1 hour at 4^{o} C.

The supernatant was then neutralised with 1/10 volume 1M Tris Base (pH 6.8). The samples were stored at -80^{o} C until used for imaging.

2.10 TEM negative stain

Formic acid extracted haemolymph samples were prepared for TEM negative stain to quantify soluble, oligomeric Aβ within the animals' body fluids. 4 μL of each sample were pipetted on to Formvar/carbon coated 400-mesh copper grids (Agar Scientific, Essex, UK) for 1 minute. Excess liquid was removed with Whatman paper. Grids were washed with 4 μL of Milli-Q water and blotted, followed by 4 μL of filtered 2% (w/v) uranyl acetate for 1 minute and blotted again. Grids were allowed to air dry before being examined in a Hitachi 7100 TEM at 100 kV and digital images acquired with an axially mounted (2K x 2K pixel) Gatan Ultrascan 1000 CCD camera (Gatan UK, Oxford, UK). After initial imaging, the samples were immunogold labelled (as previously described in Section 2.4) to determine oligomeric structure. A 1 μg/mL mouse Nu1 primary antibody (Klein lab) and a goat anti-mouse 10 nm gold-conjugated secondary antibody (BBI Solutions OEM Ltd., Cardiff, UK) were used and grids were imaged as stated previously.

Negative staining of Aβ 1-42, Aβ 25-35, or oligomeric Aβ 25-35 was used to determine peptide morphology. Aliquots of 94 μM Aβ 25-35, 100 μM Aβ 1-42, and 100 μM oligomeric Aβ 25-35 were allowed to incubate in normal saline solution for 0, 3, or 24 hours. Samples were prepared and images acquired as stated above.

2.11 Behavioural pharmacology

Four animal groups were assessed in all behavioural pharmacology studies: trained, inhibitor-injected; trained, vehicle-injected; naïve, inhibitor-injected; naïve, vehicle-injected. Trained animals were trained, injected 24 hours post-training, and tested 24 hours post-injection, as stated in 2.2 and 2.3. Naïve animals were injected

during the same experimental time points as trained animals. The inhibitors used in this thesis include 10^{-4}M Anisomycin (Sigma-Aldrich) (Fulton et al., 2005), 20 μM MK-801 (Sigma-Aldrich) (Wan et al., 2010), 0.04 μM Bisindolylmaleimide I (Calbiochem) (Marra et al., 2013), and 5 μM H-89 (Sigma-Aldrich) (Michel et al., 2008).

2.12 S^{35}-methionine labelling

Animals were trained, injected with 200 μL of Aβ. 10 μCi/mL S^{35}-methionine (ICN Biomedicals), and tested, as stated in 2.3 and 2.4. Brains were dissected after testing and 5 buccal + cerebral ganglia were pooled to create one sample. Each sample was transferred to 60 μL PBS; 10 μL was used for BCA to determine protein concentration. The remaining 50 μL solution was centrifuged at 10K RPM for 3 minutes. The supernatant was retained and 1 mL 25% trichloroacetic acid (TCA) was added, along with 1 mL H_2O. The mix was vortexed and precipitated on to cellulose paper using 10% TCA. The sample was then air dried in 100% industrial methylated spirits (IMS) and the sample was measured using a scintillator. Results were normalised to the appropriate BCA results.

2.13 Chromatin Extraction

An Episeeker Chromatin Extraction Kit (Abcam) was used to extract chromatin from tissue samples; the manufacturer's instructions were followed. Briefly, 5 buccal + cerebral ganglia were homogenised and 500 μL Working Lysis Buffer was added. Tissue was further homogenised, followed by centrifugation at 5K RPM for 5 minutes at 4^{o}C. Supernatant was completely removed from the pellet and retained as the cytosolic fraction. 100 μL Working Extraction Buffer was then added to the chromatin pellet and resuspended by pipette mixing. The sample was then allowed to incubate on ice for 10 minutes and occasionally vortexed before being resuspended by pipette mixing and sonicated for 20 seconds, twice. The sample was then centrifuged at 12K RPM for 10

minutes at 4°C and the supernatant was retained as the chromatin fraction. A 1:1 ratio of Chromatin Buffer was added to the chromatin extract. Both the cytosolic extract and chromatin extract were measured for protein concentration using BCA and were maintained at -80°C until further use in western blot or ELISA.

2.14 Enzyme-linked immunosorbent assay (ELISA)

For the CREB and pCREB ELISAs, sandwich ELISAs were used. To begin, a Nunc MaxiSorp flat-bottom 96-well plate (eBioscience) was coated with 100 μL of Coating Buffer (1x PBS) + either 1/1500 rabbit anti CREB (Cell Signalling) or 1/1000 mouse anti pCREB Ser133 (Millipore). The plate was covered with plastic wrap and allowed to incubate at 37°C for 2 hours. After incubation, the wells were washed with 200 μL Washing Buffer (1x PBS + 0.05% Tween 20) three times, and then 200 μL Blocking Buffer (10 mg/mL BSA) was added to each well. The plate was again covered with plastic wrap and allowed to incubate at 37°C for 1 hour. After incubation, the wells were washed with 200 μL Washing Buffer three times, and then 100 μL of samples were applied to the appropriate well. The plate was covered with plastic wrap and allowed to incubate at 37°C for 2 hours. After incubation, the wells were washed with 200 μL Washing Buffer three times, and then 100 μL Dilution Buffer + 1/1000 goat anti rabbit HRP-conjugated secondary antibody (Cell Signalling) or 1/1000 goat anti mouse HRP-conjugated secondary antibody (Cell Signalling) was applied to each well. The plate was covered with plastic wrap and allowed to incubate at 37°C for 30 minutes. After incubation, the wells were washed with 200 μL Washing Buffer three times, and 75 μL HRP substrate (Millipore) was added to each well and allowed to incubate in the dark for 10 minutes. The absorbance of each well was then read at 450 nm using a plate reader and values were normalised to BCA measurements of the appropriate sample.

For the cAMP ELISA, a cAMP Direct ELISA kit (Enzo) was used, and manufacturer's instructions were followed. Briefly, standards and samples were added to a 96-well plate along with colourimetric reagents. Once substrate was added and proper colour development was achieved, wells were measured at 405 nm using a plate reader. Sample values were determined by comparing to standard measurements.

For the PKA ELISA, a PKA Kinase Activity Assay kit (Abcam) was used, and manufacturer's instructions were followed. Briefly, samples were added to a 96-well plate along with kinase reagents. Once HRP substrate was added and proper colour development was achieved, wells were measured at 450 nm using a plate reader. Sample values were normalised to BCA measurements of the appropriate sample.

2.15 Statistical analysis

Data that passed the D'Agostino and Pearson omnibus normality test were subjected to parametric tests (one-way analysis of single variance [ANOVA] with Tukey's multiple comparison, or t-tests) to establish significance (criterion, $p < 0.05$). Data that did not pass this normality test were subjected to nonparametric tests (Kruskal-Wallis with Dunn's multiple comparison, or Mann-Whitney) to establish significance (criterion, $p<0.05$). All datasets were analysed for outliers using Grubbs' test (criterion $p<0.05$). Any outliers detected were removed from the dataset. GraphPad Prism software was used for all analyses.

3. *Lymnaea stagnalis* as a novel behavioural model for Amyloid β research

The pond snail *Lymnaea stagnalis* is a well-defined and tractable animal model used for the investigation of the cellular and molecular mechanisms of learning and memory. Behaviourally, *Lymnaea* has been used to investigate many different forms of associative memory (see 1.2; for review, see Benjamin and Kemenes, 2009); however, the single-trial food-reward classical-conditioning paradigm has been most successful in connecting cellular and molecular mechanisms to animal behaviour. This paradigm is based on the early discovery that it is possible to pair non-food chemicals with food, which results in a conditioned feeding response that can persist for up to 19 days (Alexander et al., 1984). The paradigm further developed when the optimal conditioned stimulus, amyl acetate solution, and unconditioned stimulus, sucrose solution, were successfully paired to train *Lymnaea* (Alexander et al., 1984). Today, the single-trial food-reward classical-conditioning paradigm is used to link behavioural findings to molecular, cellular, and network changes, and has revealed highly evolutionarily conserved memory mechanisms in the *Lymnaea* nervous system (for review, see Kemenes, 2013; Feng et al., 2009).

The conventional animal models to examine the effects of Aβ on behaviour include transgenic mice and Aβ-injected rodents. Multiple transgenic mouse lines exist to study Aβ's effect on the brain and behaviour, and show a correlation between increased Aβ production in the brain and decreased performance in numerous memory tasks (PDAPP, Tg2576, APP23, TgCRND8, J20, APP+PS1, Tg2576+PS1, APP+ PS1 KI, 5xFAD, and 3xTg-AD, Appendix I.1) (for review, see Webster et al., 2014). Injection of Aβ has also been implicated in impairing complex learned behaviour in live rodents (Cleary et al., 2005; Shankar et al., 2008; Lesne et al., 2006). While Aβ behavioural studies are mostly reserved to rats and mice, invertebrates have also made a large impact on the field. *Drosophila*, a well-developed genetic model, now has many AD transgenic tools available to investigate Aβ's neurotoxic influence and negative effect on memory (for review, see Prussing et al., 2013). *C. elegans*, another well-developed invertebrate model, is currently used for screening *in vivo* AD drugs targeting Aβ-induced toxicity; researchers argue that this allows for a greater study of therapeutics, as *C. elegans* offer more complexity than the current mammalian cell culture model (for review, see Lublin and Link, 2013). However, molluscan models have not been used for Aβ study, even though they offer a wealth of learning and memory information and

unique approaches to the field. Only one group has successfully used a molluscan system to observe the peptide's effect on behaviour. *Helix lucorum* were unable to learn a conditioned food aversion reflex when repeatedly injected with high concentrations of Aβ 25-35, 24 hours before and 72 hours after training, in conjunction with a 5-day multi-trial training protocol (Samarova et al., 2005). However, the effect of Aβ treatment on consolidated memory was not investigated in *Helix* and has been a relatively unexplored form of memory throughout the literature.

The wealth of already existing knowledge on the cellular and molecular mechanisms of associative memory made *Lymnaea* an ideal model system to test the behavioural, cellular, and molecular effects of Aβ peptides using a top-down approach. In the experiments described in this chapter, *Lymnaea stagnalis* were subjected to a pre-neuronal loss Aβ incubation time point paired with the single-trial food-reward classical conditioning paradigm to investigate the effects of Aβ on associative LTM. Snails were treated with either a short amyloidogenic fragment (Aβ 25-35) or full-length Aβ 1-42 and tested to measure impairment of memory 24 hours after treatment. Aβ induced changes in behaviour were measured for both consolidated memory and memory acquisition.

3.1 Aβ 1-42 and Aβ 25-35 disrupts long term memory after 24 hour *in vivo* incubation

The short fragment peptide Aβ 25-35 has been shown to have neurotoxic properties, to affect cognitive processes (for review, see Millucci et al., 2010), and has been used successfully in another molluscan model (Samarova et al., 2005). The fragment represents the core functional domain of the full length Aβ peptide and is able to self-assemble to form a predominantly β-sheet structure. For this reason, it has been used throughout the literature to test the effects of Aβ exposure (for review, see Millucci et al., 2010). The concentration of Aβ 25-35 used in these experiments was 0.1 mM, a concentration used successfully in *Helix* (Samarova et al., 2005). A 24 hour post-training time point for injection of Aβ has been chosen because memory in *Lymnaea* is considered to be fully consolidated (i.e., resistant to treatment with amnesic agents, such as Anisomycin and Actinomycin-D) by this time (Fulton et al., 2005; Marra et al., 2015) and the primary goal was to investigate the disruption of consolidated memory by Aβ. A pilot experiment was run to establish a testing time

point where Aβ-induced memory loss was observed, ranging from 48 hours post-training to 9 days post-training (Appendix II.1). Animals were starved for 2 days, trained at time point 0 hours (the day after starvation completed), injected with 0.1 mM Aβ 25-35 at time point 24 hours, and tested for the conditioned feeding response every day for up to 9 days post-training. The results of this pilot experiment, along with general incubation time points used in the literature, established the testing time point as 24 hours post-injection and 48 hours post-training.

Once a suitable experimental timeline had been established, animals were classically conditioned using the single-trial food-reward training paradigm. Treatment with 0.1 mM Aβ 25-35 at 24 hours after training significantly reduced the animals' feeding response to the CS 24 hours after injection and 48 hours after training (Figure 3.1A and B). However, 0.1 mM Aβ 25-35 is considered to be a rather high concentration, so a more commonly used concentration of 1 μM Aβ 25-35 was administered for comparison. The data showed a trend for decreased memory but no significant memory impairment (Figure 3.1B), so all subsequent experiments used 0.1 mM Aβ 25-35.

While Aβ 25-35 (racemised at D-Ser^{26}) has been immunohistochemically detected in plaques of AD brains (Kubo et al., 2002), the peptide is not actively cleaved from APP. Therefore, the effect of Aβ 1-42, the most toxic of the Aβ peptides with a widely accepted physiological and pathological relevance, was also examined. At 1 μM, Aβ 1-42 significantly reduced the animals' feeding response to the conditioned stimulus (Figure 3.1B). For a treatment control, trained animals were injected with either vehicle or an Aβ 1-42 variant (further referred to as peptide control), and no memory impairment was observed. Therefore, the behavioural effect observed is not a result of either the buffer the Aβ is solubilised in, the injection itself, or a general effect of additional peptide being administered. Both 1 μM Aβ 1-42 and 0.1 mM Aβ 25-35 decreased the animals' response rates to baseline, naive levels. Importantly, neither peptide affected the unconditioned feeding response to sucrose when tested 24 hours after systemic injection (Figure 3.1C). The lack of feeding response to the CS therefore was not due to an impairment of the animals' ability to generate the feeding motor pattern.

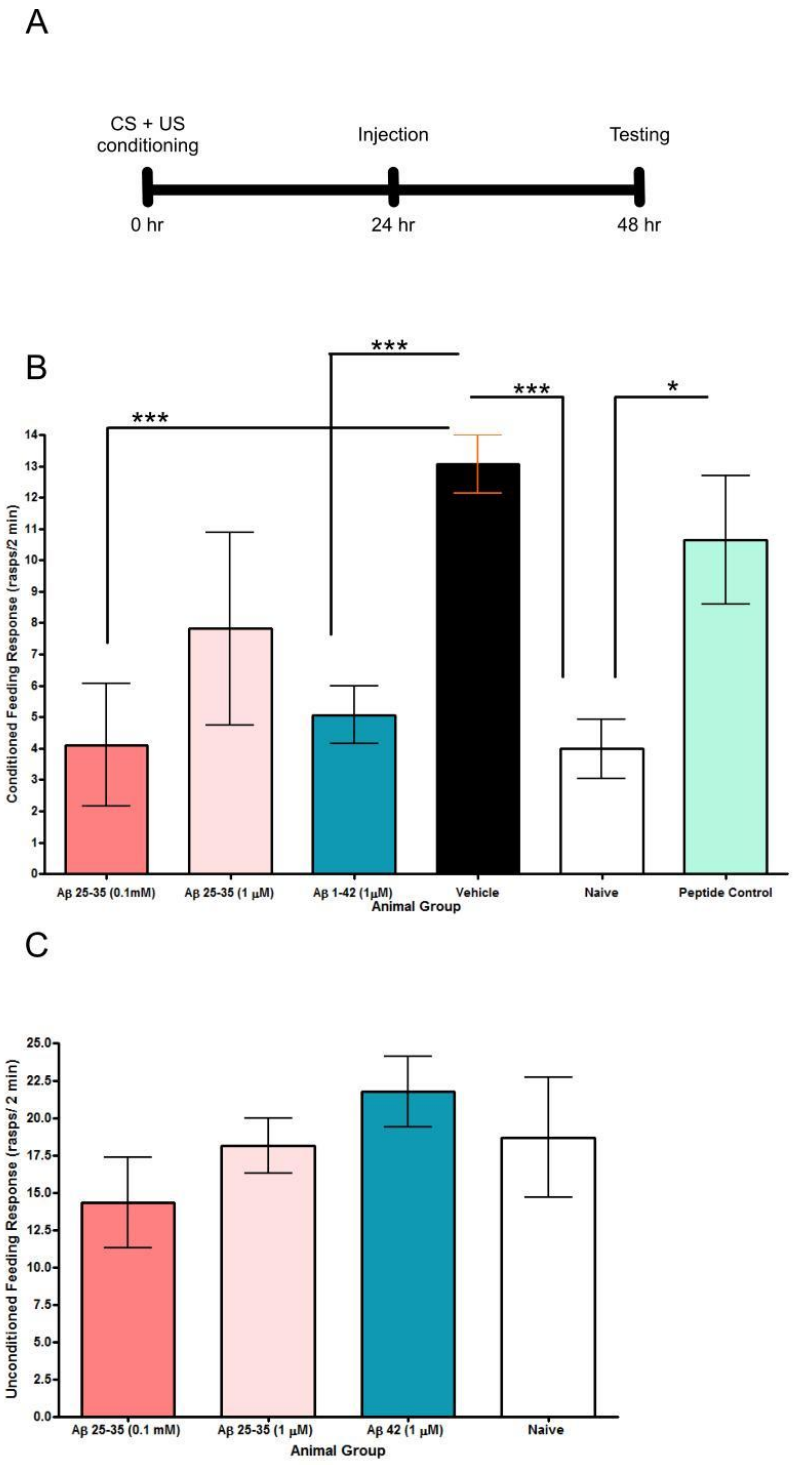

Figure 3.1 Aβ 1-42 and Aβ 25-35 disrupt long term memory after 24 hour *in vivo* incubation. (**A**) Timeline of the experiment. (**B**) Six starved animal groups (0.1 mM Aβ 25-35 [n=18], 1 μM Aβ 25-35 [n=24], 1 μM Aβ 1-42 [n=55], vehicle [n=96], naive [n=55], peptide control [n=20]) were tested for rasp rate to amyl acetate, a measure of the feeding response to the CS. Means ± standard error mean (SEM) values are shown. Asterisks indicate behavioural responses that are significantly lower (***= $p<0.0001$, *= $p<0.05$) than those in the vehicle-treated or peptide control groups. One-way ANOVA, $p=0.0001$. Tukey's tests with $p<0.05$: Vehicle vs. Naive, Aβ 1-42 vs. Vehicle, 0.1 mM Aβ 25-35 vs. Vehicle, Peptide Control vs. Naive. (**C**) Four starved animal groups (0.1 mM Aβ 25-35 [n=9], 1 μM Aβ 25-35 [n=15], 1 μM Aβ 1-42 [n=12], naive [n=10]) were tested for rasp rate in response to the US, sucrose. Means ± SEM values are shown. One-way ANOVA, $p=0.3542$. All Tukey's tests: $p>0.05$.

3.2 Animals treated with 1 μM Aβ 1-42 or 0.1 mM Aβ 25-35 do not exhibit neuronal death after 24 hours *in vivo* incubation

Aβ causes neurodegeneration; cell death in the memory-encoding circuitry would completely abolish memory and would manifest as a severe behavioural deficit. The intent of the behavioural work in Figure 3.1 was to observe pre-neuronal death time points and so three indicators to monitor apoptosis or necrosis were used. First, as mentioned previously, sucrose testing was used to monitor circuitry function through behavioural methodology (Figure 3.1C). If Aβ-induced neuronal death was occurring within the memory and feeding network, the animals would not have a response rate to the US as high as the uninjected, naive group since both the conditioned and unconditioned feeding motor programme are controlled by the same neuronal circuit (Straub et al., 2004). No significant difference was found between Aβ-injected groups and naïve animals (Figure 3.1C). Second, TEM was used to examine sections from treated animals' brains and qualitatively scored for evidence of apoptotic morphology within neurons, including: fractionation of the nucleolus, presence of holes in the nuclear envelope, fractionation of chromatin, and blebbing of the cellular membrane. No evidence of apoptosis was observed in 1 μM Aβ 1-42 or 0.1 mM Aβ 25-35 treated animals when compared to vehicle-injected animals and scored for health (Figure 3.2).

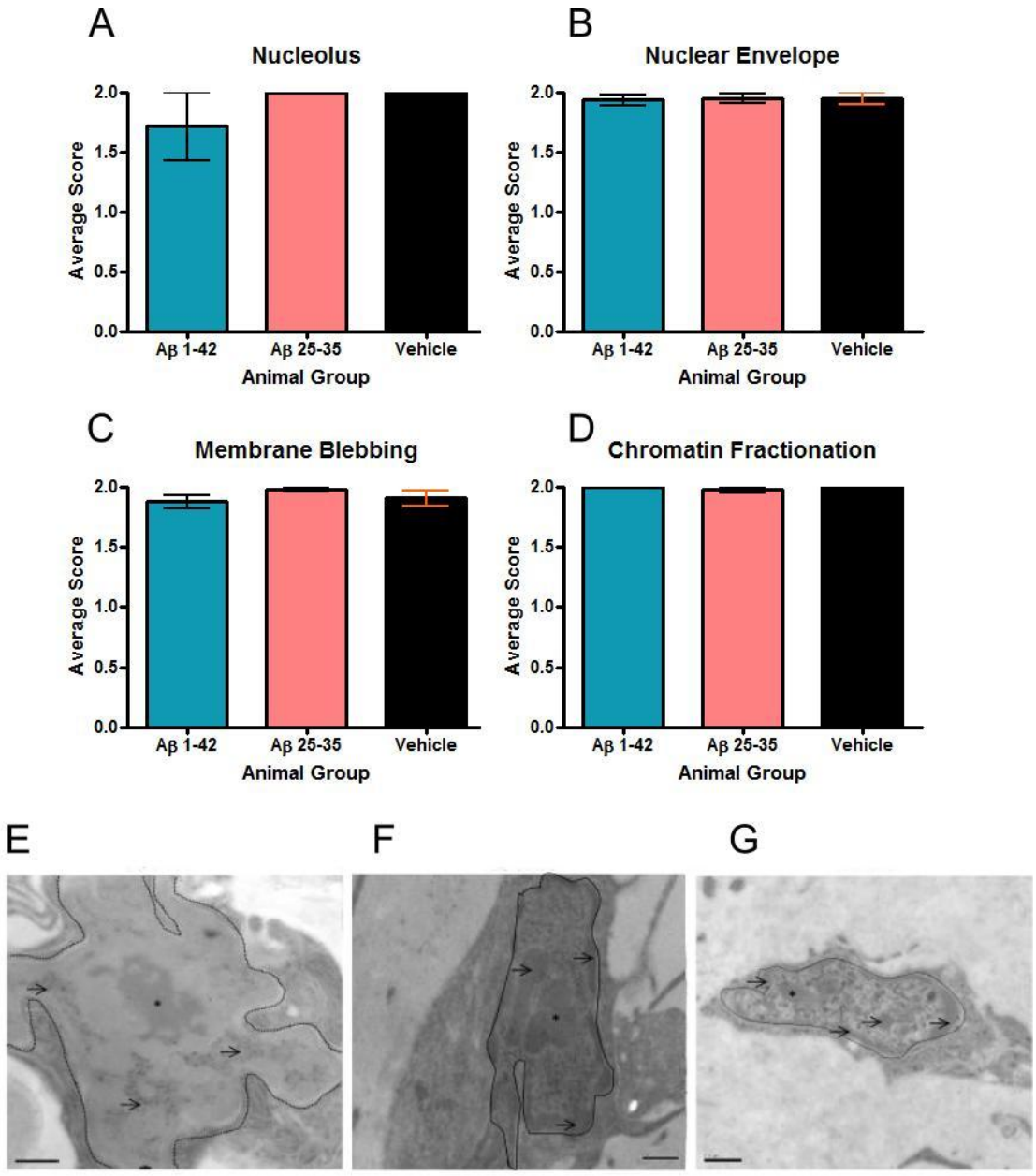

Figure 3.2 Aβ 1-42 and Aβ 25-35 treated animals do not exhibit morphological indicators of cell death after 24 hours *in vivo* incubation. (**A-D**)Three animals groups (Aβ 1-42, Aβ 25-35, Vehicle) were scored for characteristics of health using qualitative scoring (where 0= unhealthy, 1= uncertain, 2= healthy) of TEM images. Means + SEM values are shown. (**A**) Nucleolus. Aβ 1-42 [n=7], Aβ 25-35 [n=8], Vehicle [n=2]. One-way ANOVA, p=0.4895. All Tukey's tests: p>0.05. (**B**) Nuclear envelope. Aβ 1-42 [n=31], Aβ 25-35 [n=38], Vehicle [n=20]. One-way ANOVA, p=0.9688. All Tukey's tests: p>0.05. (**C**) Cellular membrane (lack of membrane blebbing) Aβ 1-42 [n=47], Aβ 25-35 [n=85], Vehicle [n=21]. One-way ANOVA, p=0.1136. All Tukey's tests: p>0.05. (**D**) Absence of chromatin fractionation. Aβ 1-42 [n=29], Aβ 25-35 [n=36], Vehicle [n=20]. One-way ANOVA, p=0.5063. All Tukey's tests: p>0.05. (**E-G**) Representative TEM images of a cell within an Aβ 1-42, Aβ 25-35, or vehicle brain tissue section. The dotted line outlines the nuclear envelope. The asterisk indicates the nucleolus. Arrows indicate areas of heterochromatin. (**E**) Aβ 1-42 image. Scale bar= 0.5 μm. (**F**) Aβ 25-35 image. Scale bar= 0.2 μm. (**G**) Vehicle image. Scale bar= 0.2 μm.

Finally, a TUNEL assay was used on tissue slices from either 0.1 mM Aβ 25-35, 1 μM Aβ 1-42, or vehicle-injected animals and imaged using fluorescence microscopy for signal intensity. The TUNEL assay allows for fragmented DNA to be labelled with marked deoxyuridine triphosphates (dUTPs); this DNA fragmentation is a marker for apoptosis and thus an increased signal indicates increased apoptosis. Signal intensity was not significantly greater in either 0.1 mM Aβ 25-35, 1 μM Aβ 1-42, or vehicle-injected animals when compared to the negative control, but all experimental groups and the negative control showed significantly less signal than the positive control (Figure 3.3). As a negative control, vehicle-injected sections were prepared and imaged without TUNEL reagent (Figure 3.3E). As a positive control, vehicle-injected sections were treated with DNase I, prepared, and imaged (Figure 3.3F). The successful use of the negative control and positive control suggests that the TUNEL assay is binding to apoptotic tissues and that the signal is not a result of tissue autofluorescence. The lack of behavioural, morphological, and DNA indicators of cell death, for both the 1 μM Aβ 1-42 and the 0.1 mM Aβ 25-35, along with the memory impairment observed with both peptides in the previous experiment (Figure 3.1B), justifies the use of these concentrations to investigate pre-neuronal death effects of Aβ 1-42 and Aβ 25-35 in *Lymnaea*.

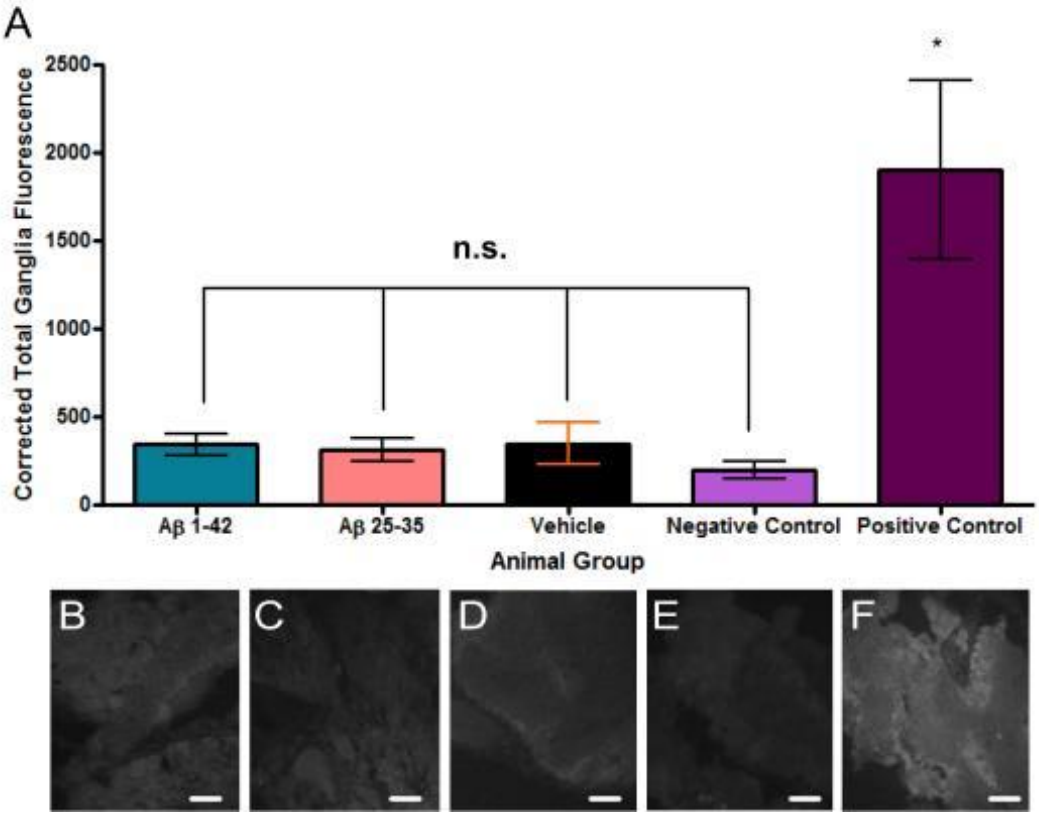

Figure 3.3 Aβ 25-35 and Aβ 1-42 do not cause apoptosis after 24 hour incubation. (**A**) Graphical representation of the amount of dUTP signal in ganglionic sections from five animal groups (Aβ 1-42 [n=12]; Aβ 25-35 [n=7]; Vehicle [n=7]; negative control [n=6]; and positive control [n=3]). Means ± SEM values are shown. Asterisks indicate significantly higher signal intensity in the positive control group compared against each of the other groups. n.s. represents not significantly different groups. One-way ANOVA, $p<0.0001$. Tukey's tests $p<0.05$: Vehicle vs. Positive Control, Aβ 1-42 vs. Positive Control, 0.1 mM Aβ 25-35 vs. Positive Control, Negative Control vs. Positive Control. (**B-F**) Representative fluorescence images of ganglia. (**B**) Aβ 1-42 treated, labelled with TUNEL. (**C**) Aβ 25-35 treated, labelled with TUNEL. (**D**) Vehicle-treated, labelled with TUNEL. (**E**) Negative control, labelled with Labelling Solution only (**F**) Positive control, labelled with TUNEL. Scale bars represent 50 μm.

3.3 Animals treated with 1 μM Aβ 1-42 and 0.1 mM Aβ 25-35 have significantly decreased levels of PSD-95 in comparison to trained and vehicle-injected animals after 24 hours *in vivo* incubation

The previous section indicated that the "learning ganglia" (buccal+cerebral) which contain the circuitry where memory is encoded, do not exhibit cell death after 24 hours *in vivo* incubation of Aβ 1-42 or Aβ 25-35. Importantly for Aβ studies, neurodegeneration starts at the synapse (for review, see Mucke and Selkoe, 2012) and Aβ exposure can reduce spine density and alter synaptic morphology after as little as 24 hours of exposure (Smith et al., 2009). This synaptic deterioration can cause a loss of LTM before any measureable cell death. In fact, the synapse is the suggested target of toxic, oligomeric Aβ in AD (for review, see Wilcox et al., 2011; Mucke and Selkoe, 2012). Postsynaptic density (PSD)-95 is the predominant member of the PSD-membrane-associated guanylate kinase (MAGUK) family of proteins, which act as scaffolding for the postsynapse and helps to stabilise and traffic postsynaptic receptors (Kim and Sheng, 2004). This protein is an established, definitive marker for postsynaptic terminals (Rao et al., 1998) and is critical for LTP and plasticity (Schlueter, et al., 2006; Ehrlich and Malinow, 2004). A reduced PSD-95 protein expression has been found in AD brain (Proctor et al., 2010) and Tg2576 mice (Almeida et al., 2005). A mammalian PSD-95 antibody has been used successfully in *Lymnaea* (Naskar et al., 2014), and the brains' degenerative state was further assessed by quantifying the levels of total PSD-95 using western blotting. It was found that animals injected with either 1 μM Aβ 1-42 or 0.1 mM Aβ 25-35 express significantly decreased levels of PSD-95 when allowed to incubate *in vivo* for 24 hours, in comparison to vehicle-injected animals (Figure 3.4). Naïve animals also had significantly decreased levels of PSD-95 compared to trained and vehicle-injected animals, indicating an increase in PSD-95 levels after training. These findings, along with those in Figures 3.1C, 3.2, and 3.3, suggest that the behavioural deficits observed in Figure 3.1B are not due to neuronal death, but may be due to the decrease in postsynaptic structure after Aβ treatment.

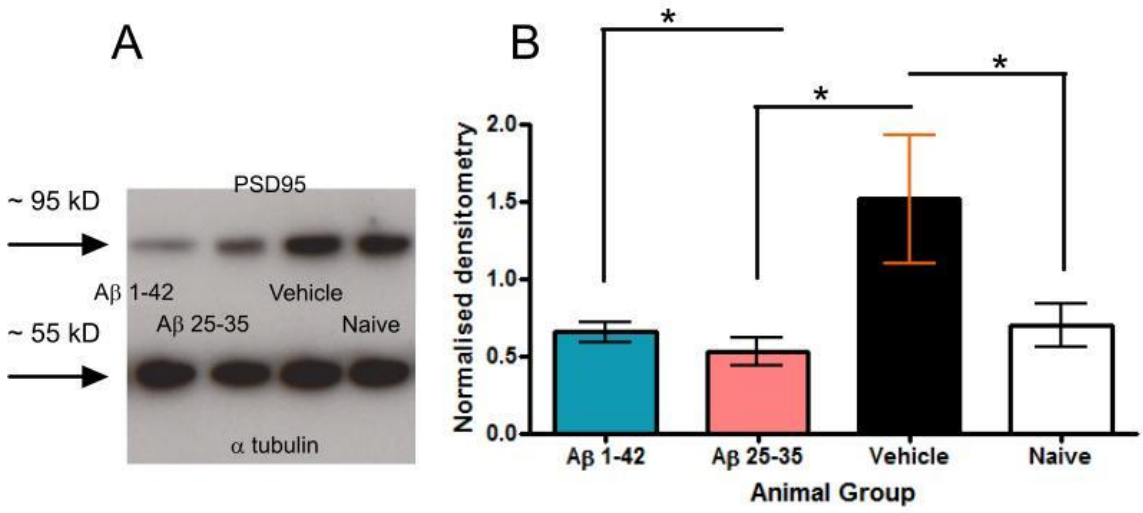

Figure 3.4 PSD-95 levels significantly decrease in animals treated with 1 μM Aβ 1-42 or 0.1 mM Aβ 25-35 for 24 hours *in vivo*. A) Representative western blot for PSD-95 and the accompanying α tubulin loading control blot. **B)** Four animal groups (Aβ 1-42 [n=5], Aβ 25-35 [n=3], Vehicle [n=4], Naïve [n=5]) were compared for intensity of PSD-95 labelling using western blotting. For each group 5 Buccal+Cerebral ganglia were pooled together, western blotted, and labelled with a PSD-95 antibody. Data represents PSD-95 band densitometry/ loading control densitometry. Means ± SEM values are shown. One-way ANOVA, p=0.0318. Tukey's tests p<0.05: Vehicle vs. Aβ 1-42, Vehicle vs. Aβ 25-35, Vehicle vs. Naive

3.4 1 μM Aβ 1-42 or 0.1 mM Aβ 25-35 does not affect memory acquisition or early consolidation

While the primary focus of this body of work is on consolidated LTM, the bulk of experiments throughout the literature have focused on memory acquisition. Various labs have found that memory is impaired following multiple applications of Aβ (Nitta et al., 1997; Chen et al., 1996) or in APP-over expressing transgenic animals (Arendash et al., 2001; Chapman et al., 1999). However, these impairments arise from prolonged exposure to significant amounts of Aβ. Others have also looked at single injections of Aβ, but paired with multiple training trials (McDonald et al., 1996; Stepanichev et al., 2005). This alters the time point being viewed and thus makes the ability to distinguish between memory acquisition and other stages, such as late stage consolidation, very difficult if not impossible. The single-trial conditioning and pre-training single Aβ injection paradigm (Figure 3.5A) shows that treatment does not hinder memory acquisition at 1 μM Aβ 1-42 or 0.1 mM Aβ 25-35 concentrations when these peptides were applied immediately before training and allowed to incubate 24 hours *in vivo* (Figure 3.5B).

Experiments also tested the same effect of Aβ on early memory consolidation, with the peptide injections administered immediately after training (Figure 3.5C), and still no effect on behaviour was observed (Figure 3.5D). In both cases, Aβ 1-42 and Aβ 25-35 groups showed similarities to the vehicle group in that animals produced a significantly increased feeding response to the CS in comparison to naive animals.

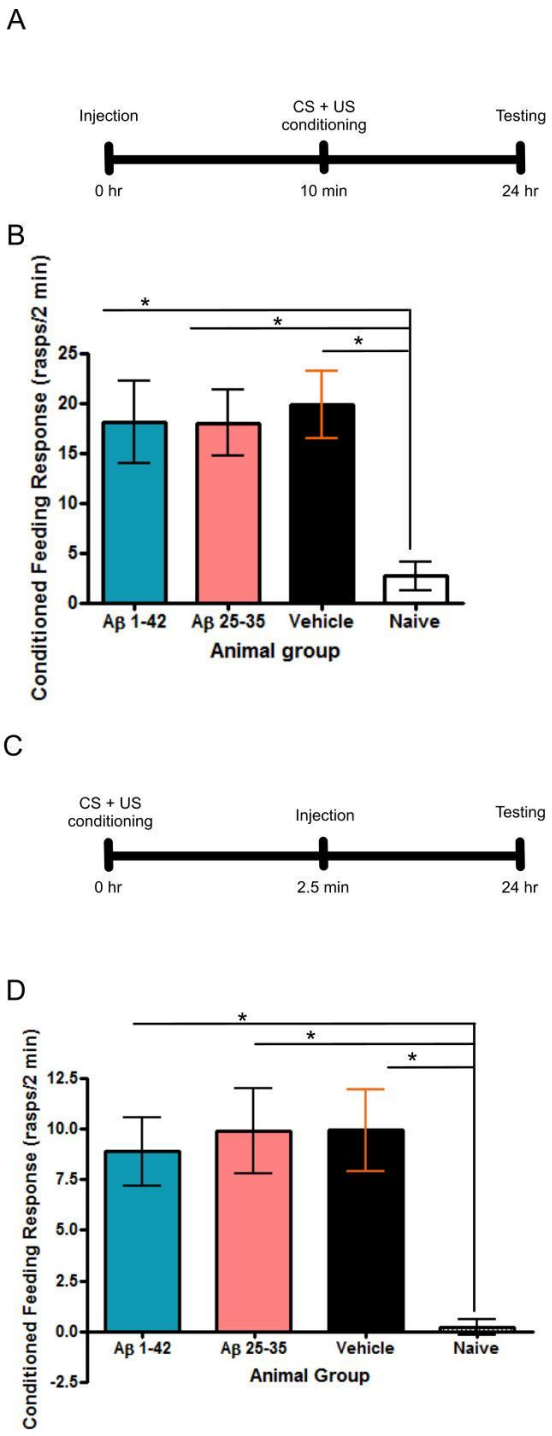

Figure 3.5 Aβ 1-42 and Aβ 25-35 do not disrupt memory acquisition or early consolidation when measured 24 hours post-training. (**A**) Timeline of experiment. (**B**) Four starved animal groups (1 μM Aβ 1-42 [n=27], 0.1 mM Aβ 25-35 [n=30], vehicle [n=16], naive [n=16]) were tested for rasp rate to amyl acetate, a measure of the feeding response to the CS. Means ± SEM values are shown. Asterisks indicate behavioural responses that are significantly higher than those in the naive group. One-way ANOVA, p=0.0039. Tukey's tests with p<0.05: Vehicle vs. Naive, Aβ 1-42 vs. Naive, Aβ 25-35 vs. Naive. (**C**) Timeline of experiment. (**D**) Four starved animal groups (1 μM Aβ 1-42 [n=14], 0.1 mM Aβ 25-35 [n=10], vehicle [n=15], naive [n=9]) were tested for rasp rate to amyl acetate, a measure of the feeding response to the CS. Means ± SEM values are shown. Asterisks indicate behavioural responses that are significantly higher than those in the naive group. One-way ANOVA, p=0.0102. Tukey's tests with p<0.05: Vehicle vs. Naive, Aβ 1-42 vs. Naive, Aβ 25-35 vs. Naive.

The study was then extended to a 48 hour post-treatment testing time point. In this experiment, 1 μM Aβ 1-42 or 0.1 mM Aβ 25-35 injections were applied immediately before training and allowed to incubate 48 hours *in vivo* (Figure 3.6A). By 48 hours, both Aβ 1-42- and Aβ 25-35-treated animals respond to the CS in a significantly decreased manner, when compared to vehicle-injected animals (Figure 3.6B). These three experiments clarify the importance of the incubation time point used and necessitates the distinction of a healthy circuitry at the testing time point. The behavioural disruption observed in Figure 3.6B is likely due to the amount of time that Aβ is allowed to incubate *in vivo*. As circuitry health at 48 hours incubation has not been tested, the health of the network which encodes this memory trace is unknown at this time. However, Aβ does not affect memory acquisition, as any disturbances to acquisition would have affected the 24 hour behavioural response. Another possibility is that memory development between 0 to 24 hour post-training is impervious to Aβ treatment, but that further memory processing between 24 to 48 hour post-training is vulnerable to Aβ treatment.

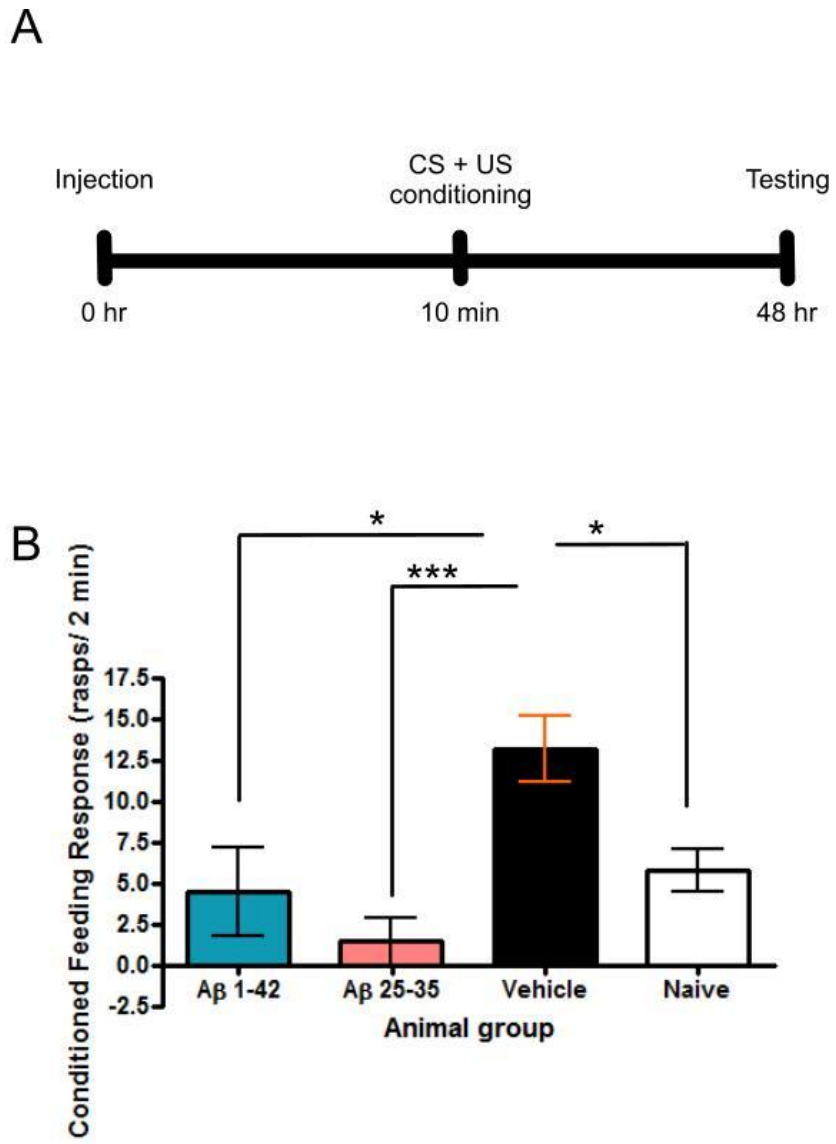

Figure 3.6 Aβ 1-42 and Aβ 25-35 disrupt memory measured 48 hours post-injection. (**A**) Timeline of experiment. (**B**) Four starved animal groups (1 μM Aβ 1-42 [n=18], 0.1 mM Aβ 25-35 [n=16], vehicle [n=32], naive [n=36]) were tested for rasp rate to amyl acetate, a measure of the feeding response to the CS. Means ± SEM values are shown. Asterisks indicate behavioural responses that are significantly lower (***= $p<0.001$, *= $p<0.05$) than those in the vehicle-treated group. One-way ANOVA, $p=0.0002$. Tukey's tests with $p<0.05$: Vehicle vs. Naive, Aβ 1-42 vs. Vehicle, Aβ 25-35 vs. Vehicle.

3.5 Discussion

Lymnaea stagnalis, a well-established animal model for learning and memory research (for review, see Kemenes, 2013), is a prime candidate for investigations of memory dysfunction. Here, *Lymnaea* is established as a highly suitable behavioural model for Aβ research. The experimental evidence indicates that Aβ disrupts consolidated long term memory, but not the acquisition or early consolidation of memory, when allowed to incubate *in vivo* for 24 hours. This combination of the 24 hour incubation time point and the 1 μM Aβ 1-42 and 0.1 mM Aβ 25-35 injected concentrations are very important to this body of work; no cell death is observed, but Aβ treatment clearly decreases postsynapses to naïve levels. The distinction of a healthy circuitry is crucial for future Aβ work, as neuronal death is clearly not involved in early Aβ-induced memory impairment. For example, these experiments suggest that acquisition is not disrupted by Aβ. However, once the peptide is allowed to incubate beyond this "healthy" 24 hour time point, acquisition appears to be disrupted. Clearly, any disrupted acquisition would have been measurable at the 24 hour time point, so the health of the circuitry must instead be considered as the culprit to this contradiction. Other labs have found similar behavioural discrepancies between 24 and 48 hour *in vivo* incubation time points in rats (Freir et al., 2011; Borlikova et al., 2013). Another equally plausible explanation for the finding that Aβ injected around the time of training impairs memory measured at 48 hours (Figure 3.6A) is of course that Aβ incubation overlaps with the 24 hours post-training and 48 hour post-injection experimental time line (Figure 3.1A). This suggests that the 24-48 hour post-training memory is vulnerable to Aβ treatment, likely affecting synaptic and dendritic alterations (Freir et al., 2011).

Lack of neuronal death is an important property of Aβ-treated brains, as shown by the synapse degeneration memory deficit observed in this chapter. Memory may be disrupted by structural alterations of synapses or memory signalling cascades at these early, synapse degeneration-only time points. The experiments suggest a reversal or inhibition of synaptic structures that grow or alter due to training. These possibilities are further supported by the work of Borlikova et al., 2013, where they show that 48 hour *in vivo* incubation of Aβ causes decreased synapse numbers and decreased diameter of the postsynaptic terminal of CA1 hippocampal slices, as measured using TEM (Borlikova et al., 2013). A decrease in the number of synapses at this same 48 hour *in vivo* incubation time point has also been found in Freir et al., 2011. When Aβ was allowed to incubate *in vivo* for 1 hour, there was no measureable change in the

synaptic proteins synaptophysin, PSD-95, or synaptopodin, as measured using western blot (Borlikova et al., 2013).

Contradictions fill the Aβ field. The use of *Lymnaea* will help to clarify some of these problems, which often arise from minor experimental differences. Over-production of Aβ in a transgenic mouse model, single-injections of Aβ, or multiple-injections of Aβ in animals should not be considered as interchangeable methods; the concentrations and structure of the peptides are not comparable. For example, Brouillette et al. 2012, examined the effect of synthetic Aβ 1-42 on passive avoidance task-based memory. In this experiment, animals were injected 6 times over 6 days with Aβ before any training or testing; the Aβ-injected animals expressed significantly less step through latency than the control group (Brouillette et al., 2012). However, as previously stated in this thesis, when synthetically prepared Aβ 1-42 was injected into *Lymnaea* only once before training and tested at the same time point as those used in Brouillette et al., 2012, no behavioural deficits were found. It is worth noting that in the Brouillette et al., 2012 study, clear signs of neuronal death were measured by the testing time point; however in this thesis' study, no neuronal death was observed. Beside comparisons between injected Aβ, animals which naturally over express Aβ are often compared within the literature as well. Transgenic mice are well known to display age-related memory deficits when compared to their wild-type litter mates; an example of a study examining such deficits in Tg2576 mice can be found in Lesne et al., 2006. However, the use of transgenic mice has the similar problem of large amounts of peptide affecting brain tissue, similar to multi-injection designs. Chapman et al., 1999 found that APPswe transgenic mice were unable to improve behavioural performance over time in a T-maze, whereas litter mate controls would improve, and by day 12 only 33% of transgenic mice would learn the behaviour (Chapman et al.,1999). This study also suggests a disruption to memory acquisition, similar to the multi-injection Aβ studies but different from this thesis' single-injection Aβ studies. Notably, neither the Chapman et al., 1999 nor the Brouillette et al., 2012 studies are able to show memory disruption within a healthy brain. All three of these models should be used within the Aβ field, yet comparisons can only be made if neuronal degeneration has first been removed as a possible obscuring factor for behavioural studies. Even then comparisons between the three models must be made carefully; it is important to remember that results obtained from different models may not completely complement each other.

Another difference is found when multiple- versus single-trial training is compared, as Aβ affects memory stages differently. Some forms of memory, such as acquisition, are not precisely measurable using a multi-trial approach, as training requires multiple days and memory will be acquired over this extended time course. The research presented in this chapter suggests that consolidated memory is vulnerable to Aβ, but acquisition of memory is not. Both the acquisition and consolidation results have also been found by Ozdemir et al., 2013, although their experimental procedure was drastically different. Importantly, there were no apoptotic cells observed in the CA1 or CA3 regions at these measured time points (Ozdemir et al., 2013). Another group, which used differing methods, came to the same conclusion as well for Aβ-disrupted consolidated memory, which can be more reliably measured with a multi-training approach than acquisition. Lesne et al., 2006 used a multi-training, multi-injection approach to measure the effects of Aβ*56, an Aβ dodecamer extracted from transgenic Tg2576 mice, on wild-type rats' spatial memory. By 24 hour post-training, Aβ-injected animals showed a significant behavioural deficit (Lesne et al., 2006) compaired to controls. The experiments in this chapter agree with those in Ozdemir et al., 2013 and Lesne et al., 2006, suggesting consolidated memory is vulnerable to Aβ and that this memory process is measurable over single- and multi-training trials. However, memory acquisition, which is much more dependent on training time points, has been found to be affected by Aβ by other groups, as described above in the Chapman et al. 1999 and Brouillette et al. 2012 discussion. Similarly, Samarova et al., 2005 has shown that *Helix lucorum* expressed disrupted memory acquisition when trained multiple times and injected multiple times with Aβ 25-35 before training. These three acquisition studies involve a multi-training approach and the method used is not a reliable measurement of memory acquisition.

For the studies referenced in this chapter, Aβ's effect on memory acquisition may be a false result arising instead from dead or dying circuitry and general unhealthiness of the brain in the animals tested, or as a measurement of memory processes that are not purely acquisition. Similar to the previous discussion of different models being used for Aβ studies, the ability for degeneration to obscure behavioural results is too great not to be considered. However, when neuronal health remains intact, multi- and single-trial training may be comparable, as seen with the Lesne et al. 2006 and Ozdemir et al. 2013 studies, if the form of memory being compared is in fact the same between the two experiments.

Even differences in peptide preparation and the type of fragment administered gives contradictory results; this chapter supports this view through the examination of behavioural deficits arising from Aβ 1-42 compared to Aβ 25-35. The experiment in this thesis suggest that 100-fold more Aβ 25-35 is needed to cause similar behavioural disruption as Aβ 1-42 (Figure 3.1). Similarly, a comparison between Freir et al., 2011 and Borlikova et al., 2013 supports these claims. In Freir et al., 2011, Aβ-containing medium from the 7PA2 cell line was used to consider 0, 3, 6, 9, and 12 hour post-training injection time points with 24 and 48 hour testing time points. They found behavioural deficits only arising in the 6 and 9 hour post-training injection, 48 hour testing time points (Freir et al., 2011). A similar study was conducted by Borlikova et al., 2013, except this study injected Aβ-extracts from AD brain samples and considered 1, 6, and 9 hour post-training injection time points with 24 and 48 hour testing time points. They found behavioural deficits only at the 1 hour post-training injection, 48 hour testing time point (Borlikova et al., 2013). Considering these two very similar experiments, the results differ greatly due to the methodological discrepancy of different forms of injected Aβ being used (Freir et al., 2011; Borlikova et al., 2013). For this reason and those mentioned previously in the discussion, a highly tractable animal model was used in this thesis with very tightly controlled methodology to establish how Aβ disrupts LTM. All proceeding experiments in this thesis used animals or tissue from animals which underwent the same precise training, injection, and testing as mentioned in this chapter, unless otherwise noted.

Chapter 4. Aβ structure and location can be monitored and quantified in *Lymnaea stagnalis*

As established in Chapter 3, *Lymnaea* offers a unique model system to investigate Aβ-induced memory impairment. While the behaviour has been well investigated, a further investigation is needed into the peptides causing this effect. As raised within the previous discussion, contradictions exist throughout the Aβ field. An in-depth study of Aβ peptides, using this now established behavioural model, will help resolve these contradictions.

Aβ peptides are cleaved from the type-1 transmembrane protein APP, the function of which is still unknown. This protein is highly evolutionarily conserved throughout the animal kingdom, with orthologues found in *Drosophila melanogaster* (Luo et al., 1990), *Caenorhabditis elegans* (Daigle and Li, 1993), and *Aplysia californica* (Moroz and Kohn, 2010). Two aspartyl proteases cleave APP, β-secretase followed by γ-secretase, to create Aβ peptides. However, it is only vertebrates which contain the sequence coding pathological Aβ (Tharp and Sarkar, 2013) and no invertebrates have been seen to produce Aβ plaques naturally (Tharp and Sarkar, 2013). It is worth noting, however, that most rodents do not form Aβ deposits either (Link, 2005) and only *O. degus* (Tarragon et al., 2013) and non-human primates appear to model AD-like symptoms caused by endogenous APP proteins (Price and Sisodia, 1994). Interestingly, when *Drosophila* over express APP and β-secretase, Aβ deposits can develop and neurodegeneration and behavioural deficits arise (Carmine-Simmen et al., 2009). These studies in the fruit fly indicate that, while invertebrates do not contain a conserved Aβ sequence, an Aβ-like peptide may be able to be processed.

Aβ 1-42 and Aβ 1-40 are the only naturally cleaved Aβ peptides following normal APP processing. Aβ 25-35 is not produced through APP processing, but may arise through proteolytic degrading enzymes or caspases, as many other fragments have been found in AD CSF (Maddalena et al., 2004) and Aβ 25-35 racemised at D-Ser^{26} has been detected in plaques of AD brain (Kubo et al., 2002). This fragment peptide is known to be neurotoxic and to take on β-sheet structure (for review, see Millucci et al., 2010) which makes Aβ 25-35 an interesting peptide to use in experimentation. However, there are some differing structural characteristics to consider. Pike et al., 1993 observed Aβ 25-35 aggregation over time, initially finding

fine particulate and large sheet-like precipitates and only observing aggregates after 7 days. This is very unlike typical amyloid fibrils formed by Aβ 1-42 (for review, see Serpell, 2014). However, a second lab looked at Aβ 22-35 morphology and found aggregation into straight fibrils (Takadera et al., 1993), which is much more similar to Aβ 1-42 (for review, see Serpell, 2014). The two labs solubilised their fragment peptides using different methods.

Here, systemically applied Aβ is monitored for localisation within the brain, to ensure that Aβ is penetrating the "learning" ganglia. Once Aβ brain penetration was established, different structures and morphologies of the peptides present were investigated in the snails' body fluids and "learning" ganglia after the 24 hour *in vivo* incubation time point. This sheds light on how peptide structure may be linked to the previously established behavioural deficits. Importantly, through this structural study a close comparison between Aβ 25-35 and Aβ 1-42 was possible.

4.1 Aβ antibodies label untreated snail brain

An important factor in developing a model for Aβ research is the ability to track peptide expression in brain tissue. Antibodies are widely used to conduct this type of experimentation and since *Lymnaea* has not yet been subjected to these studies, an initial examination of antibody binding in untreated, naïve brains was necessary. Oligomeric Aβ expression was observed in untreated, naïve ultra thin brain sections using three monoclonal conformational epitope antibodies: Nu1, Nu2, and Nu4 (Lambert et al., 2007). These antibodies were created from three distinct culture colonies grown from the spleen of the same Aβ 1-42 ADDL-treated mouse (Lambert et al., 2007). Nu1 and Nu4 discriminate between AD and control tissues, while Nu2 only recognises synthetic peptide, and all three antibodies show minimal detection of synthetic Aβ 1-42 monomer (Lambert et al., 2007). These antibodies have been used successfully to measure oligomeric Aβ in multiple labs, using different models (Lambert et al., 2007; Velasco et al., 2012; Soura et al., 2012). Labelled brain sections were imaged using a TEM and gold immuno-labelling. Nu1 labelled buccal ganglia sections modestly (Figure 4.1A), while Nu2 expressed higher labelling (Figure 4.1B) and Nu4 exhibited the highest degree of labelling (Figure 4.1C). It is unclear as to why some antibodies labelled more than others.

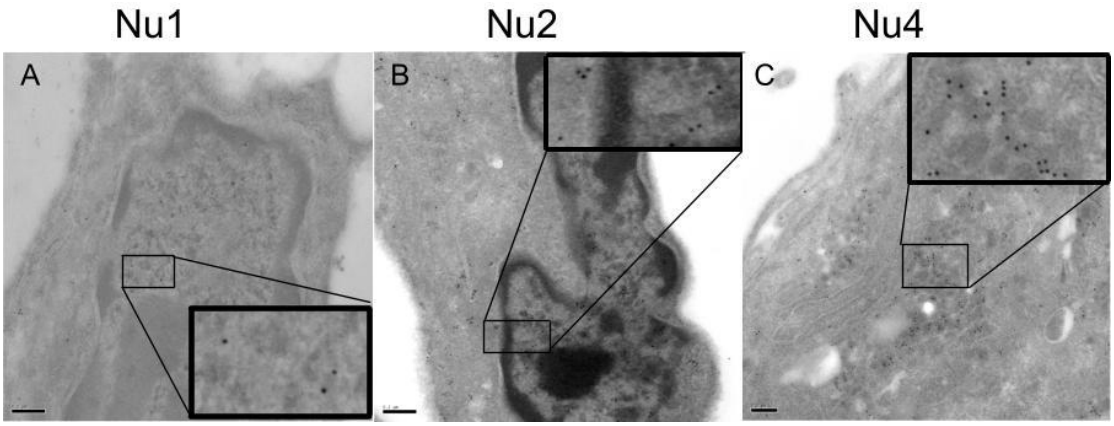

Figure 4.1 Antibodies which label Aβ oligomers bind to naïve snail brains. Representative TEM images of untreated, untrained snail buccal ganglia labelled with (**A**) Nu1 antibody, (**B**) Nu2 antibody, or (**C**) Nu4 antibody. All sections were then labelled with a gold-conjugated secondary antibody. Magnified views of areas of interest are found within boxes in each image. All scale bars represent 0.2 μm.

This study indicates possible antibody distinction for endogenous versus exogenous Aβ signalling; the high Nu4 signal indicates that it could be good for endogenous labelling and the low Nu1 signal indicates that it could be good for exogenous labelling. However, it must be considered that *Lymnaea stagnalis* does not have an APP-like gene sequenced. For the closest possible comparison, *Aplysia californica* will be considered. An *Aplysia* APP has been sequenced as well as PSEN1 and PSEN2 which are proteins involved in the proteolytic cleavage of APP to produce Aβ (Moroz and Kohn, 2010). *Aplysia* APP shares 29% identity with human APP and the Aβ peptide region expresses about 50% higher homology to humans than either *Drosophila* or *C. elegans* (Moroz and Kohn, 2010). *Aplysia* has also been found to contain a short region with probable amyloid forming potential, far more likely than either *Drosophila* or *C. elegans* (Tharp and Sarkar, 2013). Therefore, it is possible that *Aplysia* is capable of producing Aβ fibrils *in vivo*. If *Lymnaea* APP is assumed to be similar to *Aplysia* APP, then it is possible that the Nu4 antibody is labelling endogenous Aβ signal. However, this is speculative; the signal may just be antibody cross-reactivity.

While there is some information on both the amino acid sequence of *Aplysia* Aβ region, as well as amyloid forming potential of this region, it is not sufficient to indicate what antibodies may be used to completely differentiate between endogenous and exogenous Aβ signal. For this reason, a purely immuno-labelling approach to distinguish between endogenous and exogenous Aβ signal was no longer considered.

4.2 A unique combination of peptide-tagging and antibodies distinguishes exogenous from endogenous signal

As section 4.1 suggests, distinguishing between exogenous and endogenous Aβ signal requires more than just antibody comparison. The applied Aβ must be modified in such a way as to not alter its effect on the tissue, while offering an identifiable component; this component should not exist naturally in tissues. For this reason, an AlexaFluor 488 Protein Labelling Kit was used to tag freshly prepared Aβ 1-42, as described in the Methods. The kit has previously been used successfully to label Aβ 1-42 and effects on cell lines have been observed (Soura et al., 2012), with the only identifiable difference being that tagged peptide fibrillisation occurs faster than untagged peptide (Soura et al., 2012). Animals were injected with freshly tagged Aβ 1-42 at concentrations of 1 μM, 25 μM, or 50 μM and brains were viewed using a

fluorescence microscope. Systemically injected Aβ entry into the buccal and cerebral ganglia was monitored. While non-specific tissue autofluorescence does exist in snail neurons, possibly masking the fluorescence of the 1 μM Aβ 1-42, samples from animals treated with 50 μM of the peptide clearly exhibited bright fluorescent punctae surrounding the ganglia (Figure 4.2).

The areas with the highest level of labelling appear to be where perineurium remained around the ganglia. These results indicated that Aβ 1-42 reaches the snail brain within 24 hours after systemic injection. To confirm that Aβ 1-42 actually penetrated the ganglia and neurons, the same AlexaFluor 488-tagged Aβ 1-42 treated ganglia were used for the viewing of immunogold labelled AlexaFluor 488 under the TEM. Using a primary antibody specific for the AlexaFluor 488 tag and a 10 nm gold-conjugated secondary antibody, visualisation of the location of Aβ 1-42 at a high magnification level was possible. Figure 4.3 reveals AlexaFluor 488-tagged Aβ within the ganglia and these can be tracked throughout the brain tissue and inside of cells. Upon determining that Aβ 1-42 does enter ganglia and cells, focus was placed on organelles with a high degree of labelling. Aβ 1-42 labelling was found within the nucleus, mitochondria, and dense-core granules/ vesicles (Figure 4.4). As the concentration of applied Aβ 1-42 increased from 1 μM to 25 μM, so did the qualitative observation of labelling in granules/vesicles (Figure 4.4G-I). There were also areas of highly labelled perineurium (Figure 4.4D-F), suggesting that much of the systemically applied Aβ 1-42 gets caught in the protective tissue surrounding the brain.

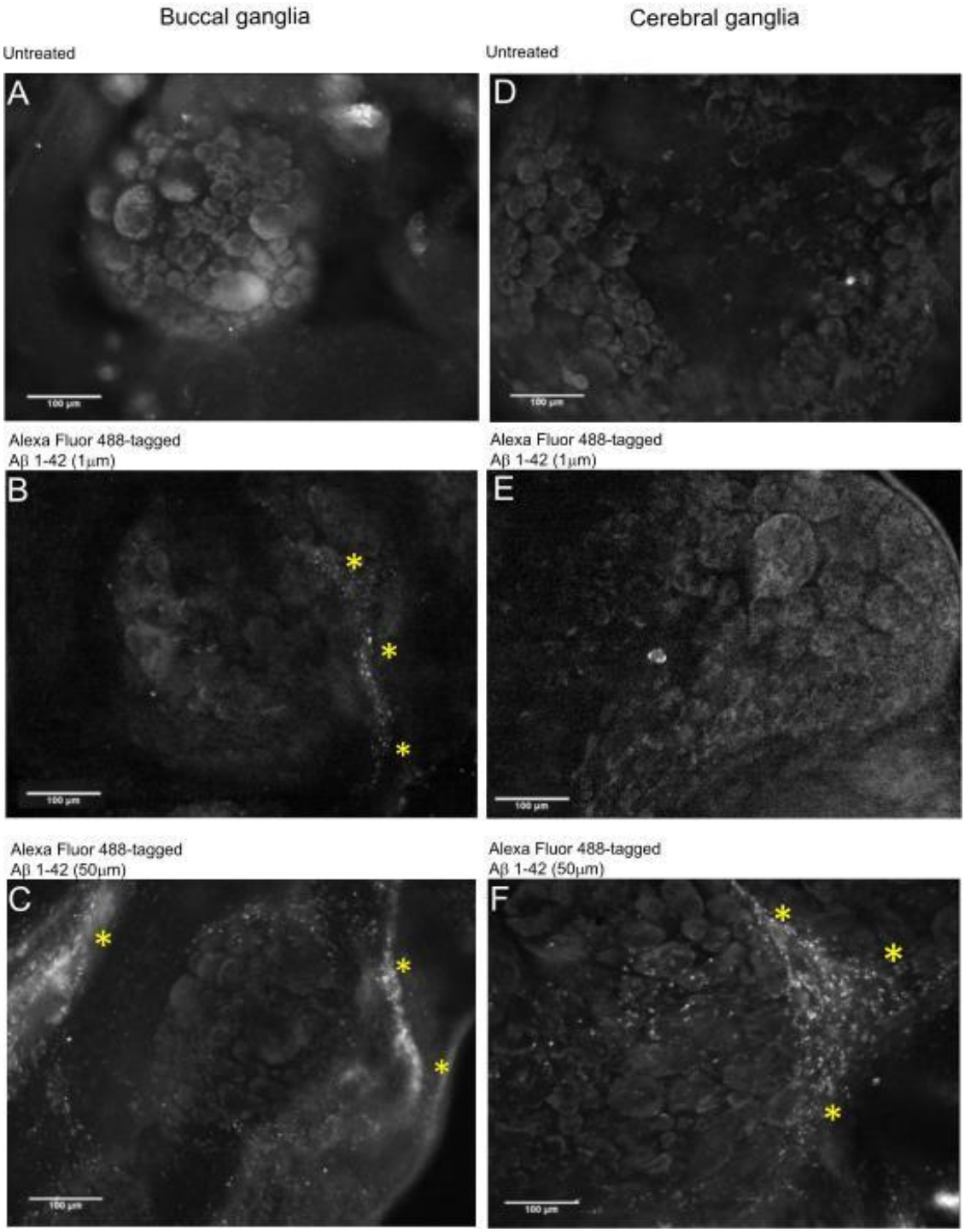

Figure 4.2 AlexaFluor 488-tagged Aβ 1-42 (1μM and 50 μM) reaches the snail brain within 24 hours of *in vivo* incubation. (**A-F**) Whole mount fluorescent images of 1 μM or 50 μM AlexaFluor-Aβ, or untreated brains after 24 hour *in vivo* incubation. (**A and D**) Representative fluorescent images of untreated, desheathed buccal and cerebral ganglia. (**B and E**) Representative fluorescent images of 1 μM treated, desheathed buccal and cerebral ganglia. High levels of fluorescence are indicated with yellow asterisks. (**C and F**) Representative fluorescent images of 50 μM treated, desheathed buccal and cerebral ganglia. High levels of fluorescence are indicated with yellow asterisks.

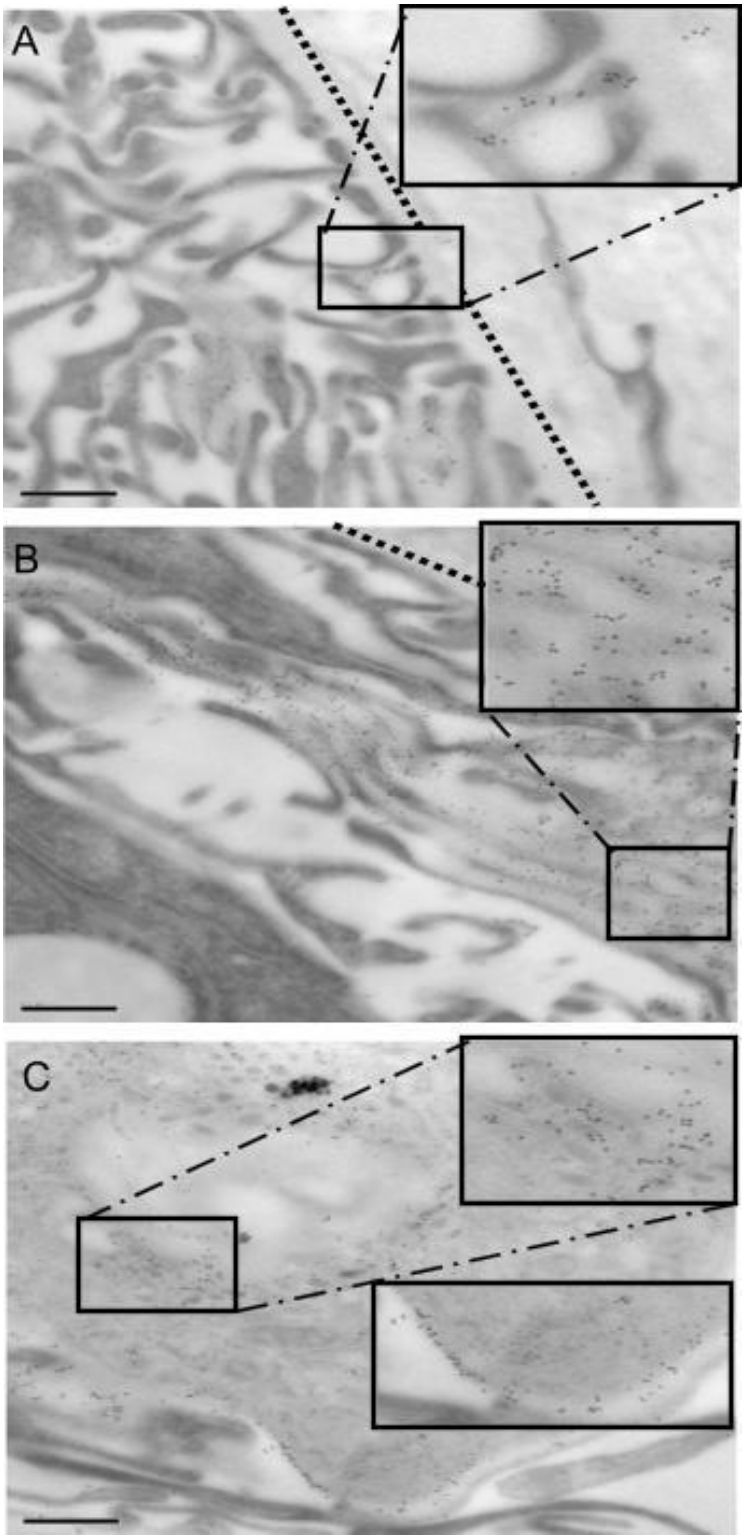

Figure 4.3 AlexaFluor 488-tagged Aβ 1-42 reaches the snail brain within 24 hours of *in vivo* incubation. (**A-C**) Immunogold labelled transmission electron micrographs of 1 μM AlexaFluor-Aβ, 24 hours *in vivo* incubation cerebral ganglia sections. (**A**) 10 nm gold labels that detect the AlexaFluor-Aβ outside of the ganglia, as well as inside the cellular projections near the ganglion edge. (**B**) An accumulation of gold labelled Aβ within cellular projections, well within the ganglia. (**C**) Gold labels within cells indicating that Aβ enters cells. Aβ also localises outside of the cell membrane. Scale bars represent 0.5 μm. Box inserts represent high areas of immunogold label. Dotted line represents ganglia edge.

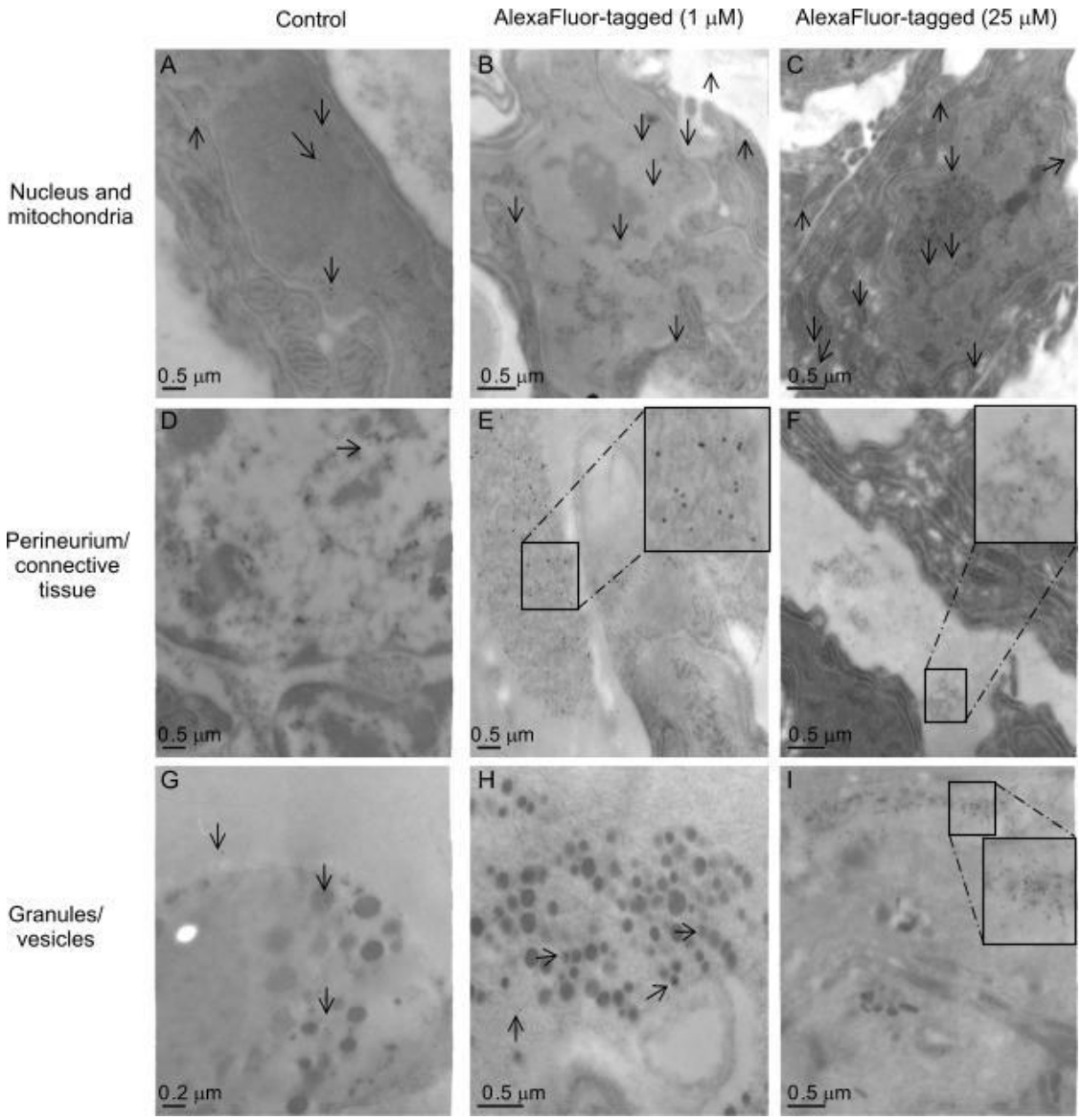

Figure 4.4 AlexaFluor 488-tagged Aβ 1-42 enters the snail brain by 24 hour *in vivo* incubation at 1 μM and 25 μM concentrations. Sections of treated buccal ganglia were labelled with an anti-AlexaFluor 488 primary antibody and a 10 nm gold-conjugated secondary antibody, and imaged using TEM. (**A-C**) Areas of gold labelling within the nucleus and mitochondria are indicated with arrows. (**D-F**) High labelling occurs within the perineurium/connective tissue of Aβ injected animals only. Inserts are added to show areas of high labelling. (**G-I**) There is a qualitative increase in labelling of dense core granules/vesicles with an increase in Aβ accumulation. Arrows indicate labelling and inserts are used to magnify highly labelled areas.

4.3 Aβ can be extracted from animals, imaged, and quantified, indicating structural forms that exist after 24 hours *in vivo* incubation

As the oligomeric forms of Aβ peptides are widely regarded as the toxic structure (for review, see Wilcox et al., 2011), an experiment was conducted in which animals were injected with either 1 μM Aβ 1-42, 0.1 mM Aβ 25-35, or vehicle, and allowed to incubate for 24 hours before their haemolymph, body fluid, was extracted and subjected to formic acid extraction. The haemolymph extracts were added to TEM grids, negative stained, and labelled with the oligomer-specific Nu1 antibody. The Nu1 antibody was specifically used for its lower binding to endogenous proteins (Figure 4.1A). Immunogold particles were observed in both peptide-treated haemolymph samples, but were negligibly detected in vehicle-treated controls (Figure 4.5). Interestingly, Aβ 1-42 has significantly more Nu1-labelling than Aβ 25-35 regardless of the 100-fold higher injected concentration of Aβ 25-35. There is a possibility that Nu1 has a higher affinity for Aβ 1-42, however, the presence of these immunogold particles in the haemolymph extracts indicate that even at 24 hours after systemic administration, soluble and oligomeric Aβ 1-42 and Aβ 25-35 are still available for uptake by the nervous system and that Aβ 1-42 remains in a more oligomeric form than Aβ 25-35 after 24 hours *in vivo*.

To assess whether the formic acid extraction truly separated soluble from insoluble proteins, Aβ 25-35 fraction samples were run on a gel and silver stained to visualise proteins. SDS-PAGE will only allow SDS-soluble proteins to be separated and run correctly; SDS-insoluble proteins will remain stuck in the well. The insoluble fractions (lanes 8-10) did not run on the gel correctly, as seen by the very dark smears located toward the top of the gel in each lane (Figure 4.6); this is expected of insoluble proteins. The soluble fraction (lanes 4-7) did not smear or remain stuck in the wells (Figure 4.6), indicating that the soluble and insoluble proteins were appropriately separated using the formic acid extraction. Lane 6 exhibits a clear protein band at 15-20 kD (Figure 4.6). The lack of banding in lanes 4, 5, and 7 does not necessarily indicate that there is no protein in these fractions, instead this was likely a method problem due to varying concentrations of protein loaded. There was much less protein loaded in all of the soluble fractions than the protein marker lanes and thus the silver stain procedure was stopped for the colour marker over expression and not left to develop long enough for the other soluble fractions.

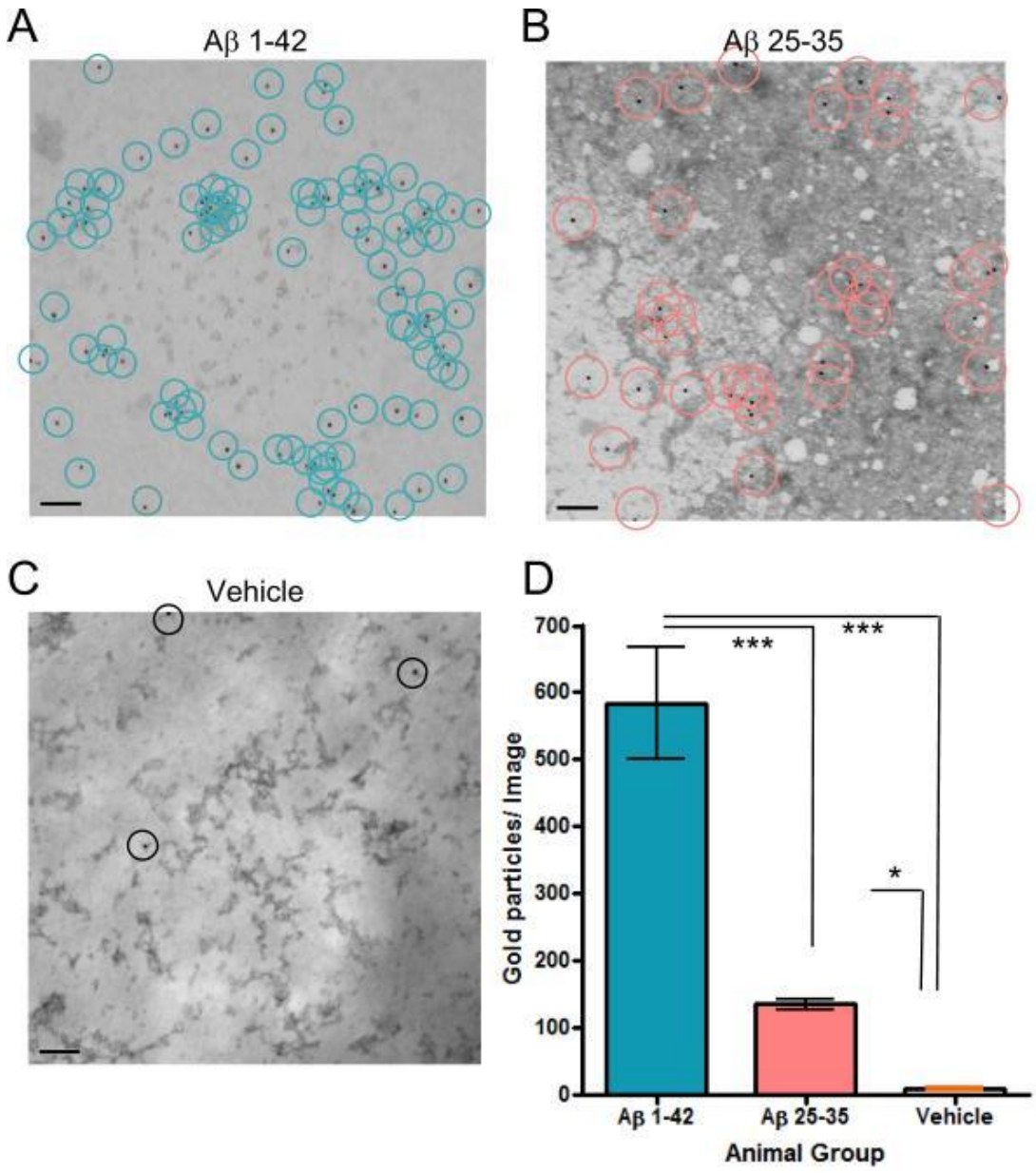

Figure 4.5 Oligomeric Aβ is found in the haemolymph after 24 hour *in vivo* incubation. (**A-C**) Micrographs of negative stained and Nu1 immunogold labelled, formic acid extracted haemolymph from animals treated with either 1 μM Aβ 1-42, 0.1 mM Aβ 25-35, or vehicle after 24 hour *in vivo* incubation. Grids were immunogold labelled for oligomeric Aβ. Circles represent immunogold labels counted. Scale bars represent 100 nm. (**A**) Aβ 1-42 (**B**) Aβ 25-35 (**C**) Vehicle (**D**) Graphical representation of immunogold labels present in 20k magnification micrographs, normalised to protein concentrations measured by BCA. Aβ 1-42 n=14, Aβ 25-35 n=24, Vehicle n=13. Means ± SEM values are shown. Asterisks indicate significant differences in gold particles per image between groups. One-way ANOVA, $p<0.0001$. ***= Tukey's tests with $p<0.0001$: Aβ 1-42 vs. Aβ 25-35 and Aβ 1-42 vs. Vehicle. *= Tukey's tests with $p<0.05$: Aβ 25-35 vs. Vehicle.

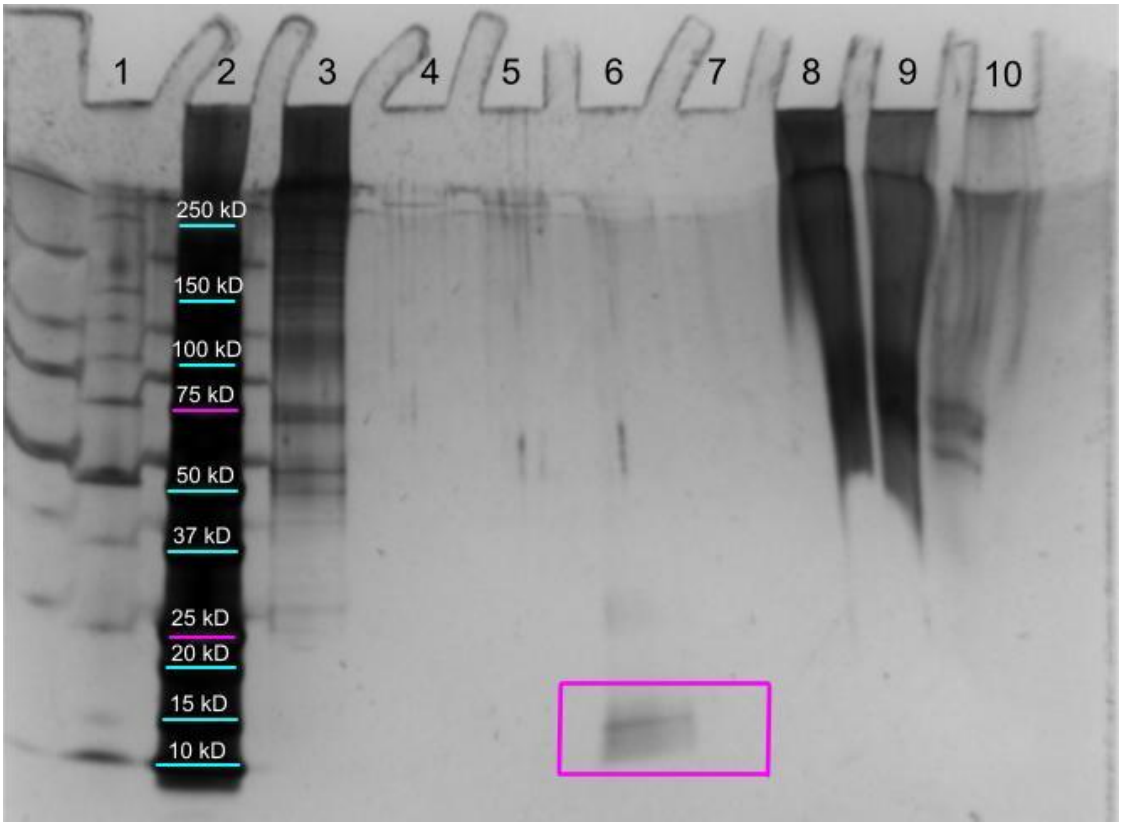

Figure 4.6 Representative silver stained gels of formic acid extraction fractions. Protein markers and Aβ 25-35 fractions were loaded on to an SDS-PAGE as follows: 1) Biotinylated protein marker 2) Dual Colour Marker [molecular weights defined with blue and pink lines, measured in kD] 3) Initial non-amyloid supernatant 4-7) Soluble fraction 8-10) Insoluble fraction; and silver stained for visualisation. The pink box in lane 6 indicates soluble proteins.

The difference in oligomeric expression between Aβ 1-42 and Aβ 25-35 may arise from differences in how the synthetic peptide was prepared. Aβ 25-35 was prepared in the same manner as used in Samarova et al., 2005; it was allowed to solubilise at room temperature for two hours in normal saline solution. The Aβ 1-42 was prepared with a specific effort put into retaining the oligomeric form for as long as possible (Soura et al., 2012). The peptide is first solubilised in HFIP, which keeps Aβ in an α-helical structure (Brooks and Nilsson, 1993). The solvent used to dissolve synthetic Aβ is believed to determine not only initial conformation, but also the aggregation kinetic behaviour that will follow (Williams and Serpell, 2011). The two preparation processes are drastically different and so are likely different structurally from the point of injection. For this reason, Dr. Tom Williams allowed both peptides to incubate at room temperature and imaged at varying *in vitro* time points for morphological differences (Figure 4.7). Electron micrographs showed that Aβ 25-35 forms small crystalline structures that develop into larger elongated crystalline structures after 24 hours (Figure 4.7A-C). In contrast, Aβ 1-42 formed small, spherical oligomeric species that developed into protofibrils and then mature fibrils after 24 hours (Figure 4.7D-F) (Ford et al., 2015). The difference in morphology may account for the observed differences in the behavioural experiments (Figure 3.1B).

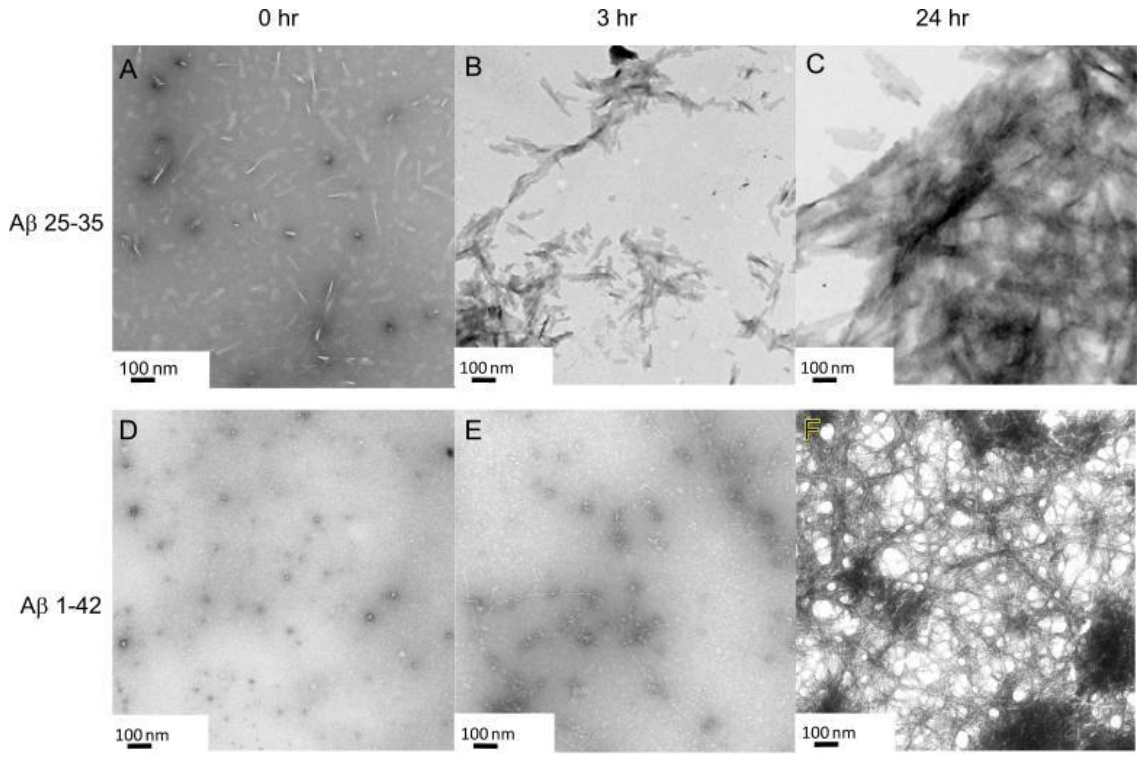

Figure 4.7 Aβ 1-42 and Aβ 25-35 aggregates differently when allowed to incubate in normal saline solution for 24 hours, conducted by Dr. Tom Williams. 94 μM Aβ 25-35 and 100 μM Aβ 1-42 were prepared as described in Methods and allowed to aggregate in normal saline solution over a 24 hour period. Samples were taken at 0, 3, and 24 hours, negative stained, and imaged using TEM. Both Aβ 1-42 and Aβ 25-35 self-assemble over the 24 hour period. **A-C**) Aβ 25-35 forms small, wide crystalline structures. **D-F**) Aβ 1-42 forms small spherical oligomers, protofibrils and finally, mature amyloid fibrils.

4.4 Aβ can be measured in snail brain tissue

While measuring oligomeric Aβ in the haemolymph is interesting for monitoring changes in the structural state of the peptides after 24 hour *in vivo* incubation, there is also interest in what forms of Aβ are in the brain at this time point. Animals were trained, injected, and tested as mentioned in Figure 3.1A and tissue samples were subjected to western blot. The membrane was probed with Nu4, the oligomeric Aβ antibody, which was previously determined to indicate predominantly endogenous Aβ signal (Figure 4.1C). The membrane was then stripped and relabelled for Nu1, the oligomeric Aβ antibody which was previously found to minimally label endogenous signal (Figure 4.1A). As shown in Figure 2.6, Nu4 labels at multiple molecular weights throughout the membrane, but importantly has no distinction between Aβ-treated (1-42 and 25-35) and untreated (Veh and Naïve) lanes. This suggests that the assumption of Nu4 largely labelling endogenous signal is valid. Nu1, however, labels only at three points throughout the membrane and only labels Aβ-treated lanes at the 15-20 kD weight, whereas untreated lanes exhibit no banding or ghost-banding (Figure 4.8). This 15-20 kD banding possibly represents an Aβ tetramer.

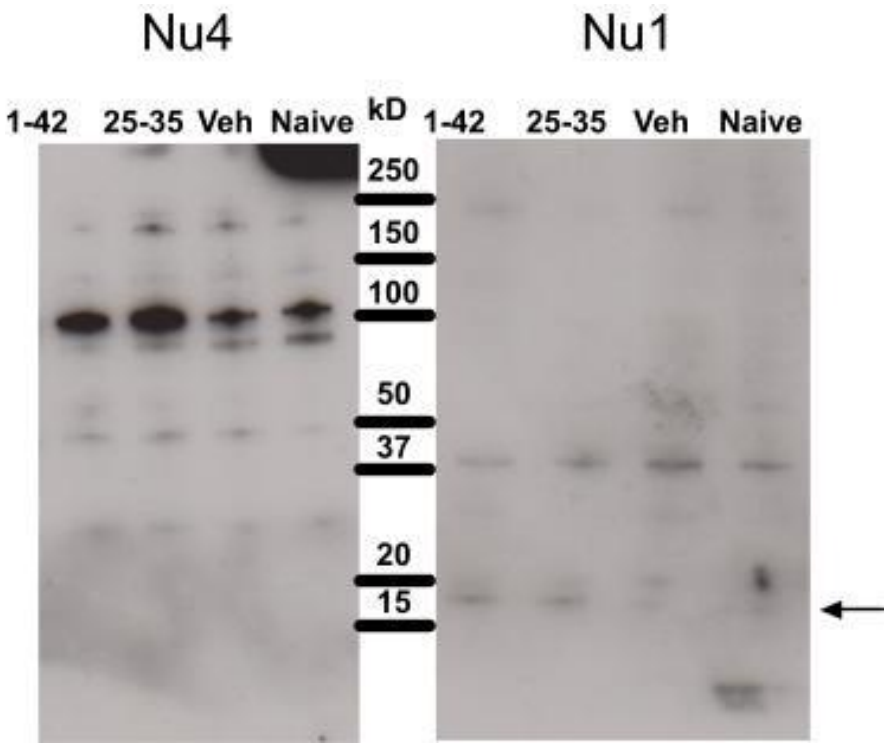

Figure 4.8 Nu4 and Nu1 label Aβ in the snail brain. The left panel represents membrane labelled with the Nu4 antibody. The right panel represents membrane labelled with the Nu1 antibody. The ladder between the two panels indicates molecular weight of proteins, as measured in kD. Lanes are labelled with what protein sample group were loaded (Aβ 1-42, Aβ 25-35, Vehicle, Naïve). Banding indicates labelling of proteins with the given antibody. The arrow in Nu1 indicates a band at 15-20 kD which labels in the 1-42 and 25-35 groups, but not in the Veh or Naïve groups.

4.5 Behavioural and structural studies of an oligomerically-produced Aβ 25-35

The experiments presented in this body of work so far consider behavioural deficits, oligomeric Aβ concentration in body fluids and tissue, and TEM morphology differences between two peptides. Aβ 25-35 only contains 11 amino acids, requires 100-fold greater concentration to elicit behavioural deficits, exhibits approximately 100-fold more oligomeric species in bodily fluids than vehicle-injected animals after 24 hours *in vivo*, and is predominantly crystalline in its morphology for the first 24 hours. However, Aβ 1-42 contains 42 amino acids, elicits behavioural deficits at only 1 μM concentration, exhibits approximately 700-fold more oligomeric species in bodily fluids than vehicle-injected animals after 24 hours *in vivo*, and morphologically evolves from an oligomeric, to protofibrillar, and finally fibrillar state within 24 hours. With Aβ 25-35 being considered an alternative to Aβ 1-42 in systemic studies, it is clear that the two cannot be used as if they are the same peptide. To be certain of this bold statement, Aβ 25-35 was prepared as Aβ 1-42 was prepared, and injected at 1 μM concentration. This controlled preparation and concentration use should resolve any discrepancies between the two peptides if they in fact can be used interchangeably.

Animals were trained, injected with 1 μM oligomerically prepared Aβ 25-35, and tested within the same timeline as used for Figure 3.1A. This timeline is again presented here as Figure 4.9A. Previously shown data is again represented here, to provide a comparison between all 1 μM-injected groups. Oligomerically produced Aβ 1-42, generically produced (solubilised in saline) Aβ 25-35, oligomerically produced Aβ 25-35, vehicle-injected, and naïve animals were compared. Interestingly, oligomerically produced Aβ 25-35 did not cause the same behavioural deficit as those observed in oligomerically produced Aβ 1-42. Oligomeric Aβ 25-35 and vehicle-treated animals had significantly greater behavioural response than both Aβ1-42 and naïve animals (Figure 4.9B).

Like the morphological TEM studies above, oligomerically prepared Aβ 25-35 was allowed to incubate up to 24 hours *in vitro*, added to a TEM grid, negative stained, and imaged using TEM. Devkee Vadukul prepared and imaged these grids, which exhibited some oligomeric species at 0 hours, but these were no longer seen at the 3 hour incubation time (Figure 4.10). By 24 hours, the peptide appeared fibrillar in structure (Figure 4.10C), similar to the 24 hour *in vitro* time point for Aβ 1-42 (Figure 4.7F).

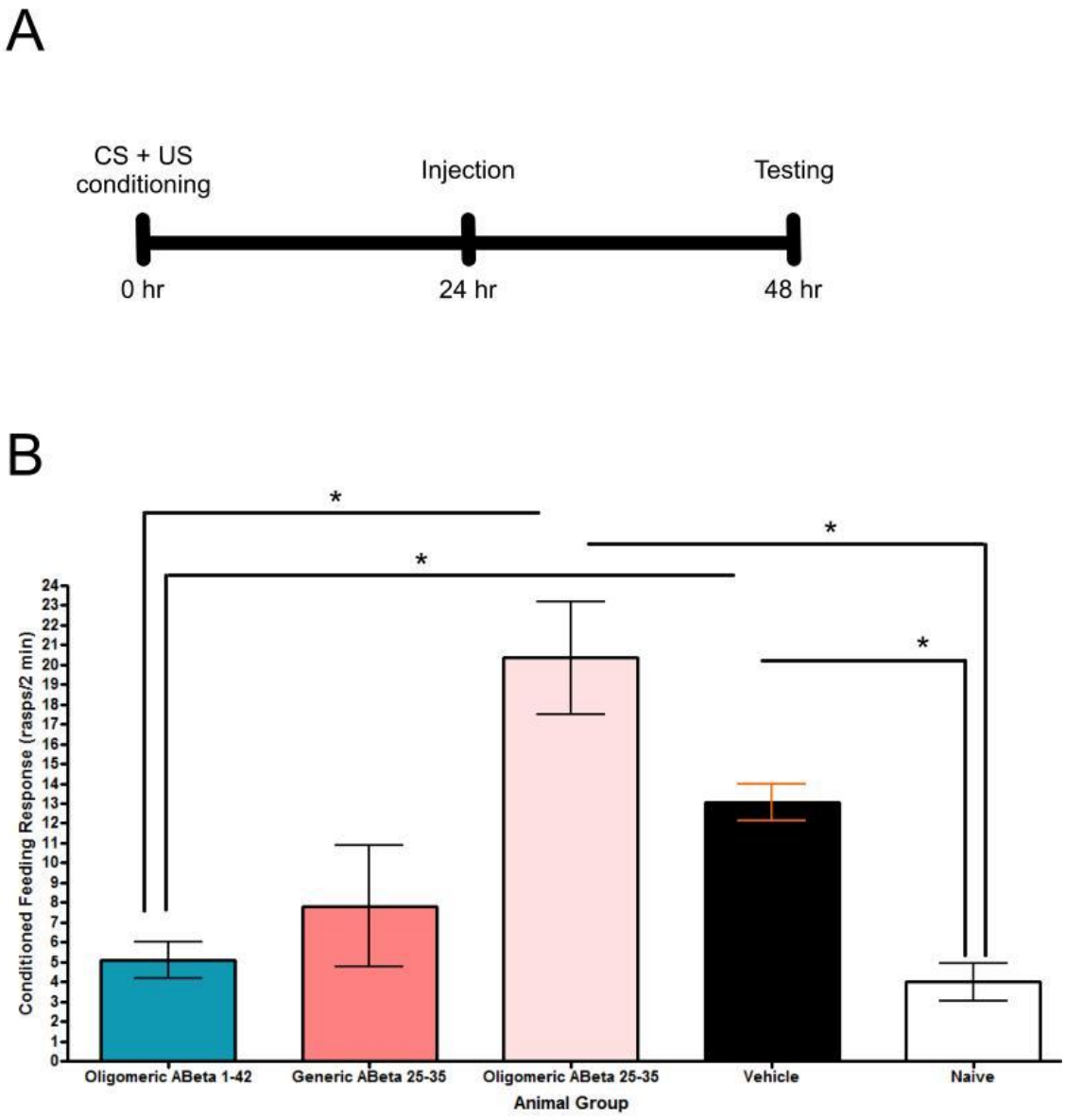

Figure 4.9 Oligomeric Aβ 25-35 does not cause behavioural deficits when 1 μM is allowed to incubate *in vivo* for 24 hours. (**A**) Timeline of the experiment. (**B**) Five starved animal groups (oligomeric 1 μM Aβ 1-42 [n=55], 1 μM Aβ 25-35 [n=24], oligomeric 1 μM Aβ 25-35 [n=23], vehicle [n=96], naive [n=55]) were tested for rasp rate to amyl acetate, a measure of the feeding response to the CS. Means ± SEM values are shown. Asterisks indicate behavioural responses that are significantly different between groups. One-way ANOVA, $p<0.0001$. Tukey's tests with $p<0.05$: Aβ 1-42 vs. Oligomeric Aβ 25-35, Aβ 1-42 vs. Vehicle, Oligomeric Aβ 25-35 vs. Naïve, Vehicle vs. Naïve.

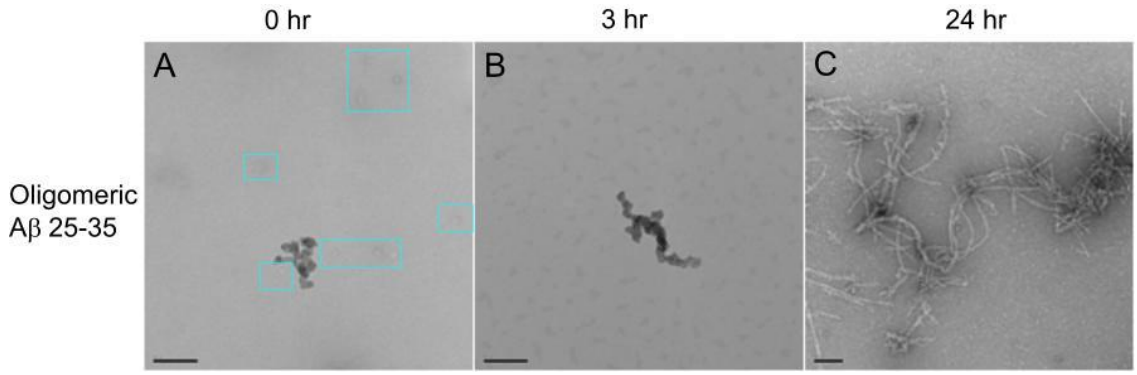

Figure 4.10 Oligomerically prepared Aβ 25-35 fibrillises when allowed to incubate in normal saline solution for 24 hours, microscopy conducted by Devkee Vadukul. 100 μM oligomerically prepared Aβ 25-35 was prepared as described in Methods and allowed to aggregate in normal saline solution over a 24 hour period. Samples were taken at 0, 3, and 24 hours, negative stained, and imaged using the TEM. The peptide self-assembles over the 24 hour period. **A**) Aβ 25-35 has few oligomeric species at the 0 hr time point. Blue boxes indicate oligomers. **B**) No observable morphological Aβ 25-35 species are found at the 3 hr time point. **C**) Aβ 25-35 has fibrillised by the 24 hour time point. Scale bars represent 100 nm.

Finally, as previously described for Figure 4.5, haemolymph was extracted from animals which had 1 μM oligomerically prepared Aβ 25-35 incubating *in vivo* for 24 hours and subjected to formic acid extraction. Soluble fractions were then added to a TEM grid, negative stained, and immuno-labelled for Nu1. Devkee Vadukul imaged these grids. Gold labels were counted and normalised to BCA protein concentration measurements. They were then compared to the other formic acid extracted samples (Figure 4.11; some data in Figure 4.11B has been previously shown in Figure 4.5). Oligomerically prepared Aβ 25-35 had significantly less oligomer labelling compared to Aβ 1-42 and Aβ 25-35; these low levels where similar to the vehicle-injected group.

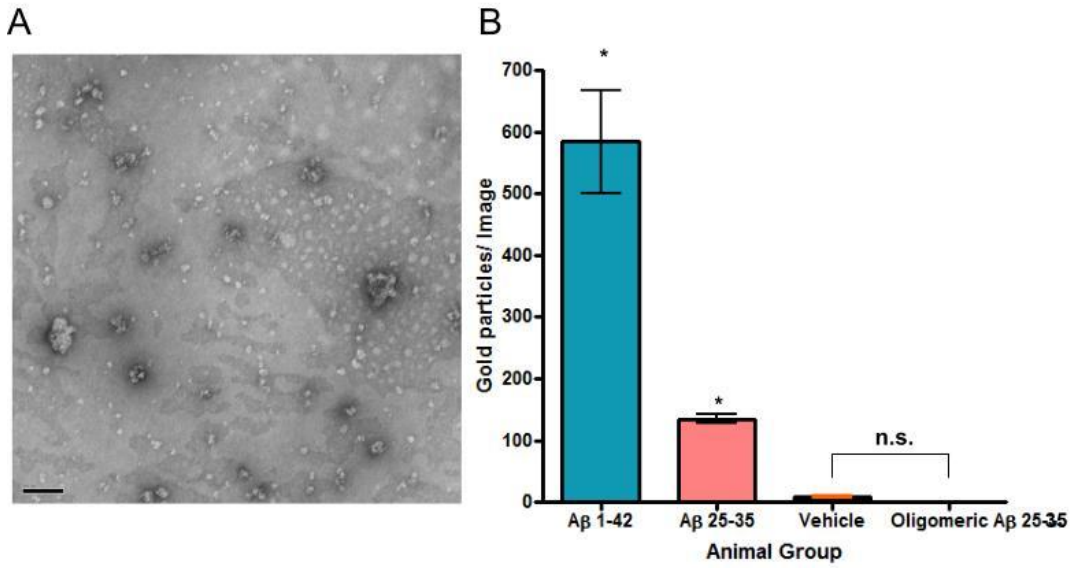

Figure 4.11 Oligomeric Aβ is not found in the haemolymph of oligomerically prepared Aβ 25-35-treated animals after 24 hour *in vivo* incubation, microscopy conducted by Devkee Vadukul. (**A**) Micrograph of negative stained and Nu1 immunogold labelled, formic acid extracted haemolymph from animals treated with 1 μM oligomerically prepared Aβ 25-35 after 24 hour *in vivo* incubation. Grids were immunogold labelled for oligomeric Aβ. Scale bar represents 100 nm. (**B**) Graphical representation of immunogold labels present in 20k magnification micrographs, normalised to protein concentration measured by BCA. Aβ 1-42 n=14, Aβ 25-35 n=24, Vehicle n=13, Oligomeric Aβ 25-35 n=19. Means ± SEM values are shown. Asterisks indicate significant differences in gold particles per image between groups, n.s. represents non-significance. One-way ANOVA, $p<0.0001$. *= Tukey's tests with $p<0.05$: Aβ 1-42 vs. Aβ 25-35, Aβ 1-42 vs. Vehicle, Aβ 1-42 vs. oligomeric Aβ 25-35, Aβ 25-35 vs. Vehicle, Aβ 25-35 vs. oligomeric Aβ 25-35.

4.6 Discussion

The experiments in this chapter show Aβ penetration into snail ganglia and localisation within the brain, followed by structural analysis of both Aβ 1-42 and Aβ 25-35 at the 24 hour *in vivo* incubation time point. To begin, the use of mammalian monoclonal antibodies Nu1, Nu2, and Nu4 were verified within *Lymnaea,* suggesting that Nu2 and Nu4 have high endogenous signalling. To completely distinguish exogenous from endogenous signal, a unique combination of AlexaFluor 488 peptide-tagging with TEM immuno-labelling was successful in showing Aβ brain penetration and localisation to specific organelles within neurons. Experiments then focused on structure and morphologies these peptides had by the 24 hour *in vivo* incubation time point; this was investigated through the use of formic acid extraction and TEM immuno-labelling of haemolymph, TEM negative staining of *in vitro* incubated peptides, and western blotting of brain samples. Importantly, these studies made clear a distinction between the Aβ 1-42 and Aβ 25-35 used in these studies. For consistency, Aβ 25-35 was prepared as Aβ 1-42 was prepared and its effects on behaviour, structure, and morphology were investigated. Behaviourally, Aβ 1-42 causes a significantly decreased conditioned response 24 hours after injection and 48 hours after testing. This same deficit is observed in Aβ 25-35 animals only when injected at 100-fold higher concentrations, and oligomerically prepared Aβ 25-35 has a trend to have greater conditioned response than even the vehicle-injected control. Structurally, Aβ 1-42 has 600-fold more oligomeric species available in the haemolymph 24 hours after injection than Aβ 25-35, and Aβ 25-35 has 100-fold more oligomeric species than oligomerically produced Aβ 25-35. Morphologically, Aβ 1-42 assembles *in vitro* from oligomers, to protofibrils, and finally fibrils by 24 hours. Aβ 25-35 forms crystalline structures, which eventually elongate and aggregate, and oligomerically prepared Aβ 25-35 displays relatively few intermediate species until complete fibrilisation at 24 hours. These discrepancies all suggest one thing, the two peptides cannot be used interchangeably.

The differences between Aβ 1-42, Aβ 25-35, and oligomeric Aβ 25-35 highlight a few very important points. First, that the initial substance that a synthetic peptide is prepared in will drastically alter its structure and aggregation kinetics (Williams and Serpell, 2011). This alteration of structure can cause drastically different effects on the system (i.e., observed memory deficit, no observable effect on memory, or even a trend for increased memory). Secondly, that the presence of the oligomeric species during the 24-48 hour post-training time point correlates to conditioned behavioural response deficits. Aβ 1-42, at the low 1 μM injected concentration, expresses

oligomeric or intermediate species morphology at the 0 and 3 hour time point when allowed to aggregate *in vitro*. Morphologically the Aβ 1-42 sample appears to have fibrillised by 24 hours, but oligomers are still present in high quantities in the animals' haemolymph. However, Aβ 25-35 needs 100-fold greater concentration to induce the same behavioural response and only displays intermediate species morphology immediately after preparation. Like Aβ 1-42, while oligomers could not be readily identified at later time points using TEM negative stain oligomers were found in the haemolymph at 24 hours. This suggests that while oligomers in Aβ 25-35 animals are much less abundant, perhaps why 100-fold more peptide is needed to induced behavioural deficits, they likely exist between the 24-48 hour post-training time point in treated animals. The oligomerically prepared Aβ 25-35, however, fail to remain in an oligomeric state much longer than immediately after preparation. Only a few oligomers were observed immediately after peptide preparation using TEM negative staining. No oligomers were observed at 3 or 24 hours and very few (>1 per image) were able to be extracted from the haemolymph. This animal group was also the only Aβ-treated group to show a trend for increased conditioned behavioural response compared to vehicle-injected controls. These experiments suggest a correlation between oligomeric Aβ presence throughout the *in vivo* incubation time line and the observed behavioural deficits.

Interestingly, this results chapter links both formic acid extracted haemolymph samples with Nu1 antibody labelled brain tissue samples; they both suggest that the Aβ tetramer is the dominant oligomer observed at the 24-48 hour *in vivo* incubation time point. Some methodology used may be falsely creating these tetramers. For example, formic acid extraction subjects the proteins to acid and pH changes, which are known to alter peptide characteristics (Brooks and Nilsson, 1993). It also is assumed that formic acid extraction separates the Aβ peptides from other proteins, but Aβ purity of the sample has not been investigated in this study. Any soluble impurities would run on the gel (Figure 4.6) from which was found a possible tetramer band by silver staining. Another potential methodological issue arises with SDS-PAGE. When samples are created for SDS-PAGE, they are treated with the detergent SDS and other denaturing procedures; this treatment may be causing the peptides to oligomerise or create a prominent trimer/ tetramer band by dissociating higher order aggregates (Bitan et al., 2005). However, many labs trust SDS-PAGE results to be a true representation of low n-oligomers within samples (e.g. Lesne et al., 2006; Shankar et al., 2008). This considered, it is still interesting that the tetramer appears with both the formic acid extraction and SDS-PAGE methods.

5. Aβ 1-42 and 25-35 disrupts CREB in trained *Lymnaea stagnalis*.

The previous two chapters established that systemically injected Aβ enters the ganglionic tissue of *Lymnaea* and causes inhibition of LTM recall, likely through the constant levels of oligomeric Aβ species during incubation. While the memory studied in this thesis is known to be consolidated by 24 hours in *Lymnaea*, the engram can be disrupted by inhibiting specific proteins within the first few days after conditioning (for review, see Alberini, 2011). Therefore, the important, novel findings from the first two chapters laid down a foundation for the analysis of the molecular signalling cascades affected by Aβ.

The key excitatory neurons within the brain are glutamatergic (Molnar and Isaac, 2002), which synapse on to neurons that express glutamate receptors on the postsynaptic terminal and recognise the neurotransmitter glutamate. Glutamate receptors are divided into two groups; ligand-gated (ionotropic) ion channels or G-protein-coupled receptors (GPCRs) (metabotropic). Ionotropic receptors include NMDARs, AMPARs, and nAChRs; metabotropic receptors were not investigated in this thesis. NMDARs can induce either LTP or LTD, depending on the rise in Ca^{2+} at the synapse and the downstream activation of intracellular cascades (for review, see Alberini, 2009). Once LTP is induced, AMPARs are inserted into postsynapses, a process termed “AMPA-fication”, and new dendritic spines grow. However, if LTD is induced, spines shrink and some synapses are actively dismantled (for review, see Alberini, 2009). Both NMDAR and AMPAR activation cause an influx of Ca^{2+} into the cell, which is required for LTP formation. α7-nAChRs also increase Ca^{2+} influx and are particularly Ca^{2+} permeable (Buccafusco et al., 2005; Castro and Albuquerque, 1995). LTP is largely NMDAR-dependent; however, NMDAR-independent forms of LTP exist and rely upon VDCCs for Ca^{2+} influx (Grover and Teyler, 1990; Freir and Herron, 2003). This Ca^{2+} influx activates Ca^{2+}-sensitive proteins which in turn activate downstream elements of signalling cascades. Importantly, many of these signalling cascades result in protein synthesis, which is necessary for LTP and LTM formation (for review, see Alberini, 2009). A crucial transcription factor involved in protein synthesis underlying LTP and LTM is CREB (Impey et al., 1996; Schulz et al., 1999; Bourtchuladze et al., 1994; Barco et al., 2002; Impey et al., 1998b; Taubenfeld et al., 1999; Bito et al., 1996; Deisseroth et al., 1996; Countryman et al., 2005; Pittenger et al., 2002; Yuan et al., 2003; Dash et al., 1990; Kida et al., 2002; Ribeiro et al., 2003).

CREB can be phosphorylated either directly or indirectly by downstream kinases of both ionotropic and metabotropic receptors (for review, see Alberini, 2009). These CREB-activating kinases are varied and include PKA (Abel et al., 1997; Huang et al., 2000; Brindle et al., 1995; Michel et al., 2008), the MAPK family (Huang et al., 2000; English and Sweatt, 1996; Ribeiro et al., 2005; Atkins et al., 1998; Kelly et al., 2003), the CaMK family (Silva et al., 1992 a, b; Wan et al., 2010), PKC (Sacktor et al., 1988; Sossin et al., 1994), and many others. Activation of CREB occurs by phosphorylation of the Ser133 site. While pCREB Ser133 is critical to induce LTP, it is not sufficient (Brindle et al., 1995; Impey et al., 1996); CREB-2 must also be released (Bartsch et al., 1995). Known *Aplysia* CREB-2 substrates exist for PKC, MAPK, PKA, and CAMK (Bartsch et al., 1995). These kinases have the capability to both activate CREB and release CREB-2.

Not only does this chapter and the next chapter, for the first time, explore Aβ-induced disruption of CREB-signalling pathways in *Lymnaea stagnalis*, it is also one of very few studies (e.g. Vitolo et al., 2002) that encompass multiple CREB-signalling factors using the same experimental procedure. In addition, this chapter considers differences in CREB-signalling pathways between trained and untrained animals at a novel time point for *Lymnaea stagnalis*. All experiments have been built on the behavioural deficits described in Chapter 3, in order to directly link molecular disruption to behavioural memory loss. A combination of molecular, pharmacological, and biochemical techniques have been used to test Aβ-induced disruption to protein synthesis and CREB in this chapter, and multiple CREB-signalling cascades in the next chapter. This approach offers an informative picture of how Aβ is affecting memory 48 hours after conditioning and 24 hours after injection in *Lymnaea stagnalis*.

5.1 Training and Aβ treatment does not alter total protein levels at 48 hours post-training

The first approach taken was to test whether training induces changes in general protein levels over time within the consolidated LTM experimental protocol (Figure 3.1A) and if Aβ treatment would alter this. For invertebrate single-trial training, the transcription- dependent and translation- dependent LTM emerges as early as 5 hour after training (Fulton et al., 2005) and memory is thought to be fully consolidated in mammals by 10 to 10.5 hours post-conditioning (Sutherland and Lehmann, 2011). To address whether Aβ disrupts protein levels at the time points used in this thesis, animals were trained, injected, and tested as described in the previous two chapters. The buccal and cerebral ganglia were dissected immediately after testing and protein concentration was measured using BCA. No significant change was found between Aβ-treated, trained, or naive groups at the testing time point (Figure 5.1).

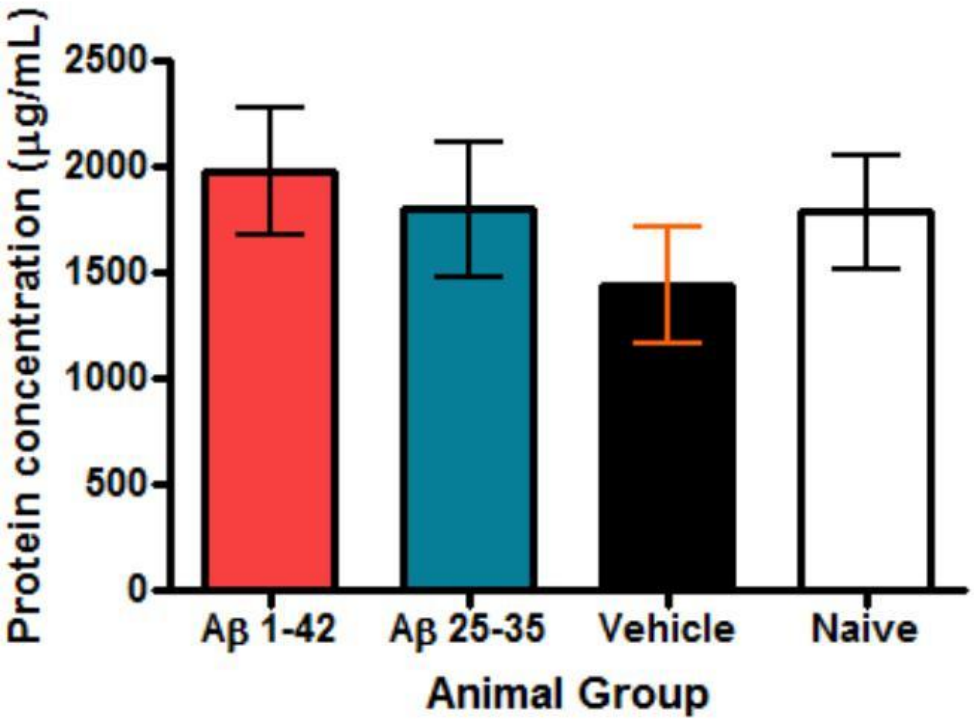

Figure 5.1 Total protein levels do not change 48 hours after training or 24 hours after Aβ injection. BCA was used to measure protein concentration in pooled samples of 5 buccal + cerebral ganglia across four animal groups; Aβ 1-42 n=6, Aβ 25-35 n=6, Vehicle n=11, Naïve n=16. Kruskal Wallis, p=0.2855. Dunn's Multiple Comparison Test, all p>0.05.

The lack of change between groups suggests that there is no significant increase in protein degradation or protein synthesis in any of the groups at this time point. More importantly, these results indicate that a general approach such as this is not sensitive enough to discriminate between protein level changes occurring on a smaller scale. For this reason, requirement for new protein synthesis was investigated, as opposed to general protein level change, at the time points used in this study. Between the 24 hour injection time point and the 48 hour testing time point, memory is being further developed through lingering consolidation, retention, maintenance, and/or storage processes. Once the animal has been tested, the memory will be recalled. Each of these memory processes have distinct biological characteristics and, with an exception for memory recall, likely overlap throughout the Aβ *in vivo* incubation time point. Many labs have focused on exactly what is changing throughout these memory processes, with a strong emphasis on protein synthesis. Importantly, protein synthesis is needed for memory acquisition 0-1 hour after conditioning in *Lymnaea* (Fulton et al., 2005) and many other animal models suggest this early acquisition time point is protein synthesis-dependent, as well as at a later stage during consolidation (for review, see Alberini, 2009). The Kemenes group have previously published data on memory retention at 24 hours being resistant to amnesic agents (G. Kemenes et al., 2006) and so those experiments were not repeated. However, memory recall has not yet been examined in *Lymnaea stagnalis*. There is a consensus, across studies that used vertebrate (e.g. Kida et al., 2002) and invertebrate (e.g. Pedreira et al., 2002) animals, that protein synthesis is not necessary for memory recall. However, this has not been investigated in *Lymnaea* and so to assess the need for protein synthesis at the 48 hour post-injection time point, a behavioural pharmacology approach was utilised. Many labs have used a similar approach to determine a necessity for protein synthesis, whereby the protein synthesis blocker anisomycin is injected directly into the animal (e.g. Fulton et al., 2005). Any protein synthesis will be disrupted by the blocker through inhibition of the peptidyl transferase reaction on ribosomes (Alberts et al., 2004) and should manifest as a behavioural disruption. Initially, an anisomycin incubation time point was determined for optimal blocker strength and minimal disturbance. All animals were injected with 10^{-4} M anisomycin (as used in G. Kemenes et al., 2006) and tested for their response to the US at either 30, 60, or 90 minutes post-anisomycin injection. All three groups responded in a healthy manner to the US (30 minute group [mean 20.00, ±SEM 2.881, n=5], 60 minute group [mean 15.20, ±SEM 4.152, n=5], 90 minute group [mean 17.20, ±SEM 1.934, n=5], One-way ANOVA p= 0.5667), and so the 30 minute incubation time point was used. Once the anisomycin incubation time point was established, it was investigated if protein synthesis was necessary for 48 hour post-

training memory recall. Animals were trained at time point 0, injected with either anisomycin or vehicle at 48 hours, and tested at 48.5 hours. There was no significant difference between the anisomycin group and the vehicle group (Figure 5.2), suggesting that ongoing protein synthesis is not necessary for 48 hour memory recall.

To be certain of the lack of protein synthesis occurring at the 24 hour retention and 48 hour recall time points, the protein synthesis study was extended by utilising radiolabelling. ^{35}S-methionine is a radioactive amino acid that will be incorporated into newly synthesised proteins, which can then be precipitated from brain samples with TCA and quantitatively measured. This labelling procedure is a well-established method for measuring protein synthesis and has been used successfully in *Lymnaea* previously (Fulton et al., 2005). To assess Aβ's impact on protein synthesis occurring from the 24 hour injection to the 48 hour testing time point, animals were trained, injected, and tested as previously shown in Figure 3.1A. However, animals were injected with ^{35}S-methionine along with 1 μM Aβ 1-42, 0.1 mM Aβ 25-35, or vehicle. After testing, buccal+cerebral ganglia were immediately dissected. ^{35}S-methionine measurements for each group were normalised to appropriate BCA measurements to give final results. There was no significant change between the Aβ 1-42, Aβ 25-35, vehicle, or naïve groups (Figure 5.3). These results suggest that Aβ is not affecting protein synthesis between the 24 hour injection and 48 hour testing time point.

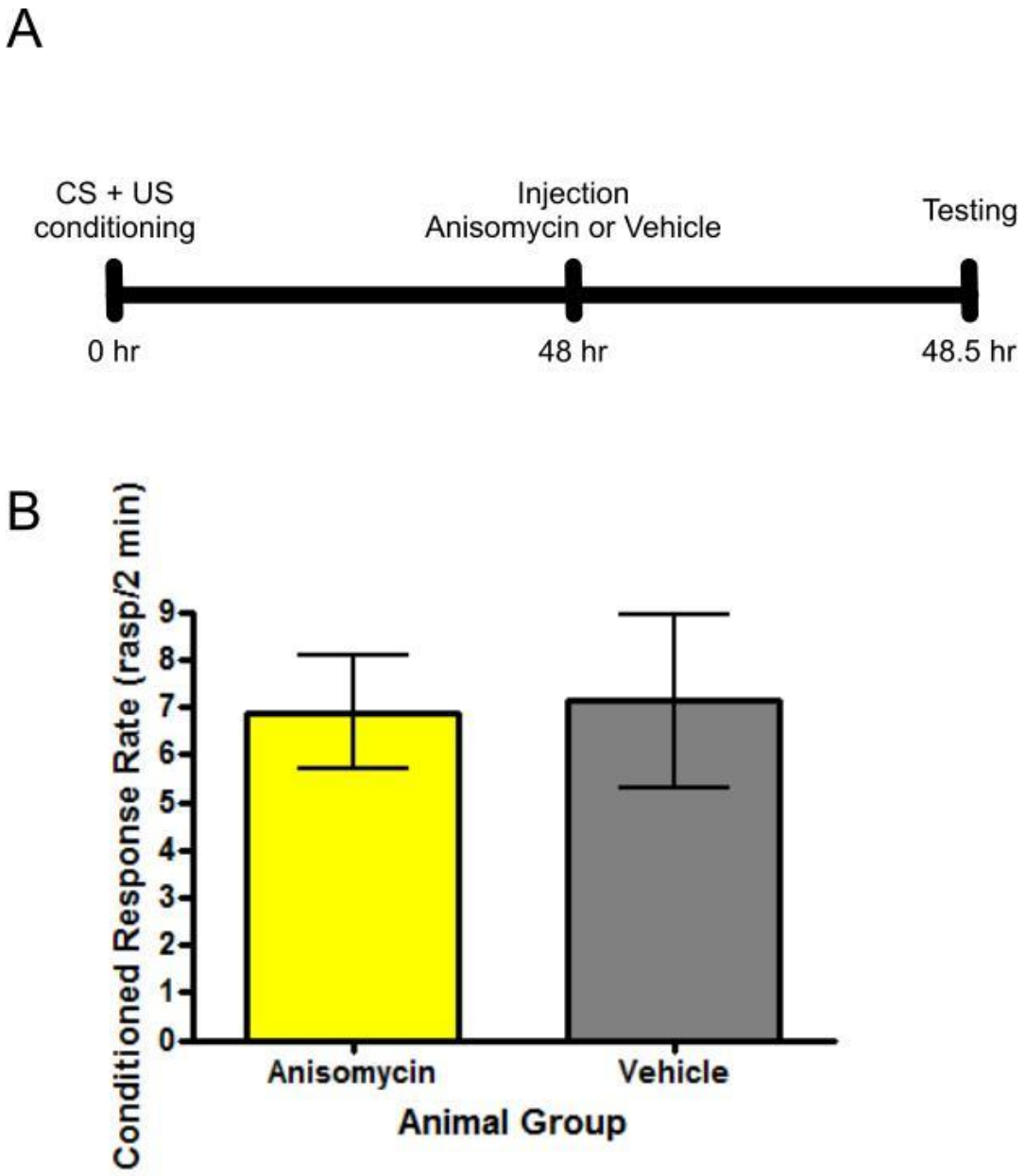

Figure 5.2 Anisomycin does not disrupt 48 hour memory recall. (**A**) Timeline of experiment. (**B**) Two starved animal groups (Anisomycin [n=34], vehicle [n=24]) were tested for rasp rate to amyl acetate, a measure of the feeding response to the CS. Means ± SEM values are shown. Mann Whitney, p=0.7044.

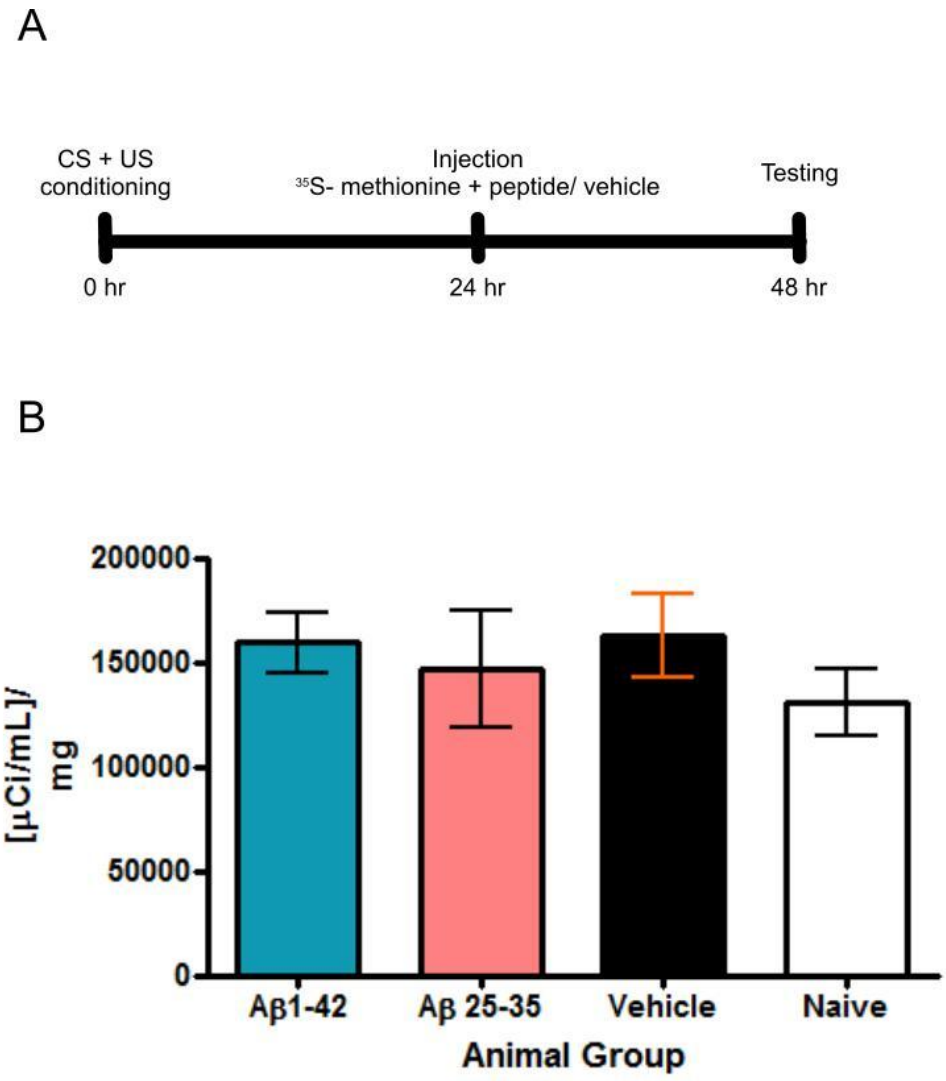

Figure 5.3 Aβ and training do not affect protein synthesis between the 24 hour injection and 48 hour testing time point of the behavioural protocol. (**A**) Timeline of experiment. (**B**) Three animal groups were trained, injected with ^{35}S-methionine/Aβ 1-42 [n=4], ^{35}S-methionine/ Aβ 25-35 [n=4], or ^{35}S-methionine/vehicle [n=4], and tested. A fourth naïve group was injected with ^{35}S-methionine and vehicle [n=4], and tested. The graph represents [µCi/mL]/µg, normalised to the protein concentration of the animal group measured. Means ± SEM values are shown. One-way ANOVA, p=0.6848. All Tukey's tests p>0.05.

5.2 CREB is modified by treatment with Aβ at the 24 hour post-injection/ 48 hour post-training time point

While there is neither a great increase nor decrease in protein synthesis at the 24 hour post-injection/ 48 hour post-training time point observed throughout this body of work (Figures 5.1, 5.2, 5.3), localised protein synthesis is known to occur at the synapse after cell-wide protein synthesis is no longer necessary (Casadio et al., 1999) and it is known that protein turnover occurs on a scale of hours to days naturally in cells (Pratt et al., 2002), demanding protein synthesis to maintain normal protein levels in trained cultures and animals. It is also worth noting that specific proteins are phosphorylated at the time of memory recall, including ERK and AMPA, which results in increased transcription of key immediate early genes, such as JunB (Szapiro et al., 2000; Szapiro, 2002; Strekalova et al., 2003). Although there was no change in or requirement for general protein synthesis, perhaps there is a need for even greater sensitivity to observe any Aβ-induced change. Focusing on one transcription factor, in this case CREB, offers the specificity needed to uncover the Aβ-induced disruption of memory. Increased CREB phosphorylation is sufficient to switch memory from short- to long-term (Impey et al., 1996; Schulz et al., 1999; Bourtchuladze et al., 1994; Barco et al., 2002; Impey et al., 1998b; Taubenfeld et al., 1999; Bito et al., 1996; Deisseroth et al., 1996; Countryman et al., 2005; Pittenger et al., 2002; Yuan et al., 2003; Dash et al., 1990; Kida et al., 2002) and has been implicated in AD (Yamamoto-Sasaki et al., 1999). However, it is important to note that with some experiments (Balschun et al., 2003; Pittenger et al., 2002), when all isoforms of CREB are knocked out in mice undergoing hippocampal LTP-training, protein compensation can overcome the requirement for CREB in certain forms of LTP. So while CREB is critical for memory formation, it is not necessary and sufficient. That being said, CREB and its cAMP/PKA signalling cascade are considered one of the main molecular processes involved in LTM with evolutionary conservation spanning much of the animal kingdom (for review, see Alberini, 2009), including *Lymnaea* (Ribeiro et al., 2003; Michel et al., 2008; Sadamoto et al., 2004).

CREB is a transcription factor that, when phosphorylated at Ser133 and repressors are removed, will recognise and bind as dimers to CRE regions on deoxyribonucleic acid (DNA) and lead to transcription and up-regulation of IEGs. Its structural motif helps CREB transcribe; the C-terminus binds to regulatory sequences via the basic leucine zipper (bZIP) domain and the N-terminus contains the transcriptional activation domain (for review, see Alberini, 2009). In between the C-

terminal and N-terminal is the kinase inducible domain (KID), where Ser133 is located, and this region is where kinases activate CREB and where recruitment of transcriptional co-activators occur (for review, see Alberini, 2009). Besides its importance in synaptic plasticity, CREB also plays a key role in nonsynaptic plasticity. Dominant negative CREB mice had a reduced ability to generate action potentials, reduced membrane resistance due to increased M-K+ currents, and reduced intrinsic excitability (Jancic et al., 2009; Dong et al., 2006). Expression of constitutively active CREB increases firing frequency, reduces resting membrane potential, and increases intrinsic excitability via a reduction of slow and medium AHPs (Han et al., 2006).

CREB-signalling pathways are known to be disrupted in AD, resulting in a decrease in phosphorylated CREB in AD brain (Yamamoto-Sasaki et al., 1999). In spatial-trained $APP_{swe,ind}$ mice, 45 CREB target genes were down-regulated and 4 were up regulated in comparison to wild type trained controls (Parra-Damas et al., 2014), with a large number of down-regulated genes being important IEGs involved in LTP and LTM. Unsurprisingly, activating CREB-signalling pathways in AD transgenic mice has been shown to reverse learning and memory deficits (Gong et al., 2004; Caccamo et al., 2010; Yiu et al., 2011). Injection of Aβ also results in CREB-signalling deregulation. At non-degenerative doses, oligomeric Aβ inhibits CREB-signalling (Tong et al., 2004), especially impacting the cAMP/PKA pathway (Vitolo et al., 2002). For these reasons, the CREB-signalling pathway was selected as the main focus in this chapter to investigate how Aβ is disrupting consolidated memory on a molecular level.

CREB, as well as CREB-2 and CBP, have been cloned in *Lymnaea* (Sadamoto et al., 2004; Hatakeyama and Kemenes, 2005) and CREB has been examined using western blot, immunohistochemistry (Ribeiro et al., 2003), and has been found in the CGC, a neuron involved in memory at the time points examined in this thesis (Ribeiro et al., 2003; Sadamoto et al., 2004). Importantly as well, both forskolin-induced and learning-induced CREB phosphorylation has been demonstrated after the single-trial food-reward classical-conditioning paradigm used in this thesis (Fulton et al., 2005; Ribeiro et al., 2003; Michel et al., 2008). To begin, an approach was used that combines basic sample preparation with western blotting to determine if there was any change in total CREB levels in the buccal+cerebral ganglia between these animal groups (Figure 5.4). This antibody and procedure has been used previously in *Lymnaea* (Ribeiro et al., 2003). There was no significant difference between any of the groups.

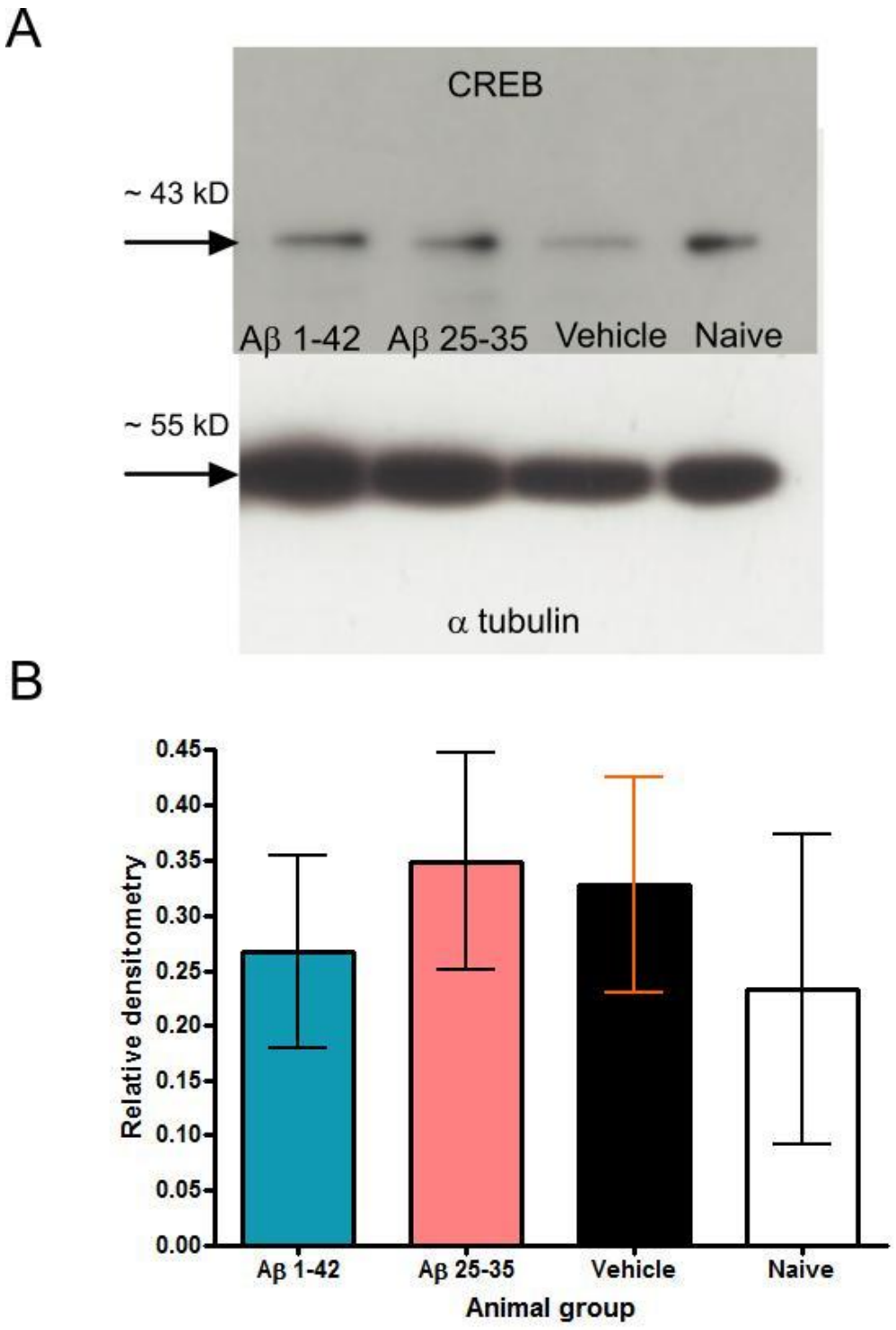

Figure 5.4 Basic sample preparation and western blotting indicate no change in total CREB levels across groups. Four animal groups (Aβ 1-42 [n=9], Aβ 25-35 [n=8], Vehicle [n=9], Naïve [n=3]) were compared for intensity of total CREB labelling using western blotting. For each group 5 buccal+cerebral ganglia were pooled together, run on a gel, and western blotted with a CREB antibody. (**A**) Representative CREB and α tubulin loading control bands. (**B**) Data represents CREB band densitometry/ loading control densitometry. Means ± SEM values are shown. Kruskal-Wallis, p=0.9060. Dunn's Multiple Comparison all p>0.05.

However, CREB can only act as a transcription factor when it is within the nucleus and basic sample preparation includes all proteins within the tissue, including proteins found in the cytosol. Since proteins, including CREB, are processed in the endoplasmic reticulum (ER) and Golgi apparatus, it is important to measure CREB specifically within the nucleus. Phosphorylated CREB must also be measured within the nuclear extract, for similar reasons. To do this, an extraction of nuclear proteins from the tissue samples was needed and so an Episeeker Chromatin Extraction Kit was used to separate the samples into cytosolic and chromatin fractions. To assess if the extraction was successful, cytosolic fractions were detected using western blotting with an antibody raised against H3 and nuclear fractions were detected using anti-α tubulin (Figure 5.5), commonly used markers for nuclear (H3) or cytosolic (α tubulin) proteins (Shaiken and Opekum, 2014). A lack of label will indicate proper separation of the two fractions. Both the H3 antibody (Souvik Naskar, personal communication) and the α tubulin antibody (Figure 3.4) have been shown to label appropriately in *Lymnaea*. No H3 signal was found in the cytosolic fraction and no α tubulin signal was found in the nuclear fraction (Figure 5.5). Thus, all samples had been appropriately separated. It is worth noting that the nuclear Aβ 1-42 fraction exhibits banding that does not exist in any of the other nuclear samples. This is likely due to sample purification error; however, it is important to note that there is no banding at the 55 kD weight and so α tubulin does not exist in the nuclear Aβ 1-42 sample.

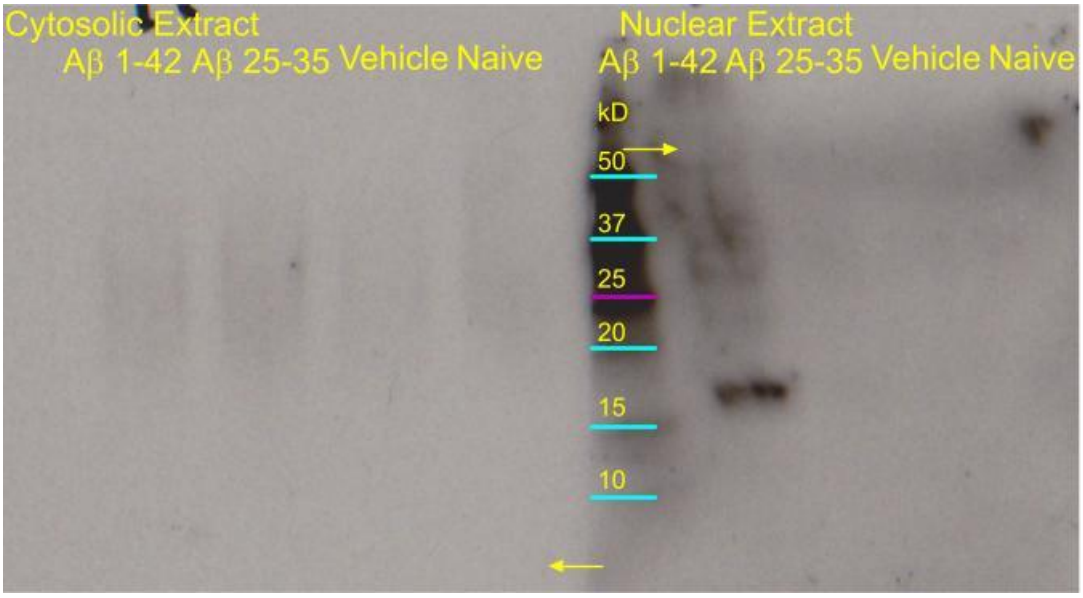

Figure 5.5 Lack of H3 labelling in the cytosolic fraction and lack of α tubulin labelling in the nuclear fraction show that the chromatin extraction procedure was successful. Four animal groups (Aβ 1-42, Aβ 25-35, Vehicle, Naïve) were subjected to chromatin extraction, giving two fractions: cytosolic (left) and nuclear (right). For each group 5 buccal+cerebral ganglia were pooled together, run on a gel, and western blotted with either an anti- H3 (left) or anti- α tubulin (right) antibody. A protein ladder is indicated with bands (blue and pink) of different sizes and yellow arrows indicate areas of predicted molecular weights of H3 and α tubulin, respectively.

Once separated, nuclear fractions did not have enough protein available for western blot detection and so a sandwich ELISA was considered for its increased quantitative properties. However, the use of a sandwich ELISA demands verification of the antibodies used to measure total CREB and phosphorylated CREB since an ELISA will measure all signal, including any non-specific labelling. There is a problem, however, with verification. The protein concentration in nuclear extracts, and the dilution that occurs from the chromatin extraction procedure, makes the use of western blotting not possible. Nuclear fractions were run on an SDS-PAGE and silver stained to determine weights of proteins within each fraction. It was then compared to a western blot of basic, predominantly cytosolic sample preparation of *Lymnaea* brain and labelled with CREB or pCREB Ser133 (Figure 5.6). These results suggest that most of the non-specifically labelled proteins found in the basic, cytosolic sample preparations are removed with the fractionation process. Unfortunately, this combination of SDS-PAGE and silver staining still does not verify if the sandwich ELISA signal is only specifically labelling for CREB or phosphorylated CREB. After many attempts, only one very background-heavy blot produced possible banding signal and this band was found at the appropriate molecular weight for pCREB (Figure 5.6). A clean, clear blot could not be produced for pCREB or CREB labelling with nuclear extracted samples.

Since the extraction was successful and nuclear extracts have low non-specific labelling with CREB and pCREB antibodies, a sandwich ELISA was used to measure the amount of total CREB in the nuclear fractions (Figure 5.7). The sandwich ELISA of the nuclear extracts indicated that nuclear CREB levels are significantly decreased in Aβ 25-35 animals compared to vehicle-injected animals and naïve animals. This is interesting, as other labs have found that steady state CREB levels do not change in Aβ-over expressing transgenic mice (Dineley et al., 2001) or in neuronal cultures treated with Aβ 1-42 (Tong et al., 2004). However, the lack of steady state CREB change in the Aβ 1-42 group is in agreement with the background literature (Dineley et al., 2001; Tong et al., 2004).

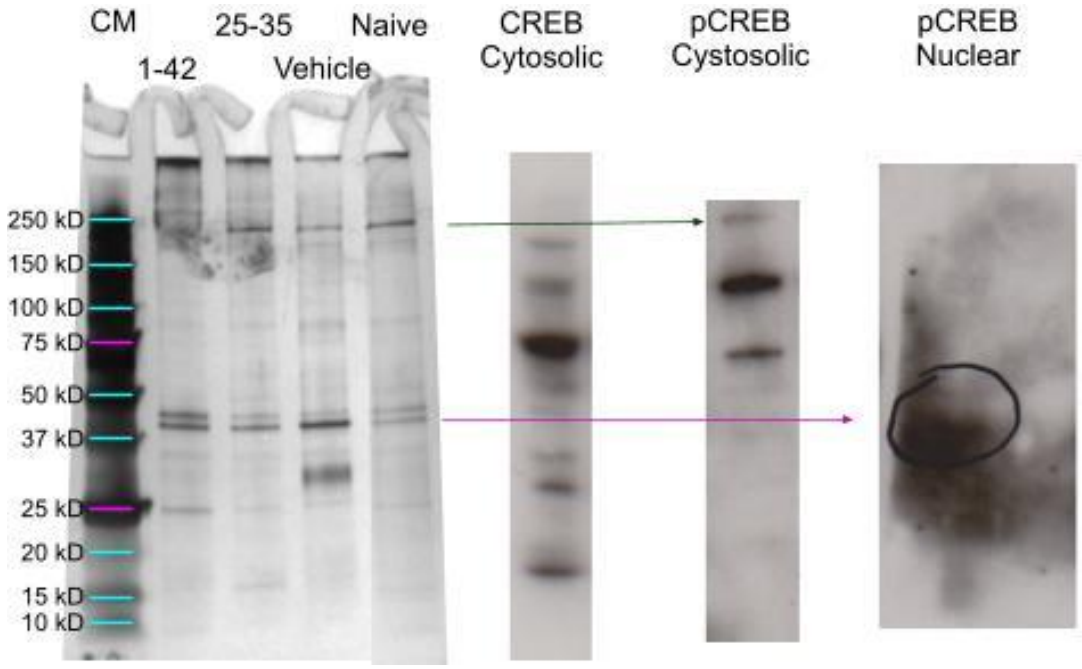

Figure 5.6 Nuclear protein extraction removes non-specific signal from CREB and pCREB antibodies in *Lymnaea* brain tissue samples. From left to right, inserts of silver stained gels with nuclear extract samples from each experimental animal group (CM= colour marker); western blot of CREB-labelled cytosolic sample; western blot of pCREB-labelled cytosolic sample; and western blot of pCREB-labelled nuclear extracted sample. Green arrow indicates non-CREB/non-pCREB proteins in nuclear extract samples, which are at the same molecular weight as non-pCREB signal in cytosolic fractions. Purple arrow indicates proteins at the correct, 43 kD weight, in nuclear extract samples as well as in pCREB-labelled western blotted nuclear extract samples. Black circle indicates possible banding in pCREB-labelled western blotted nuclear extract samples at the correct 43 kD weight.

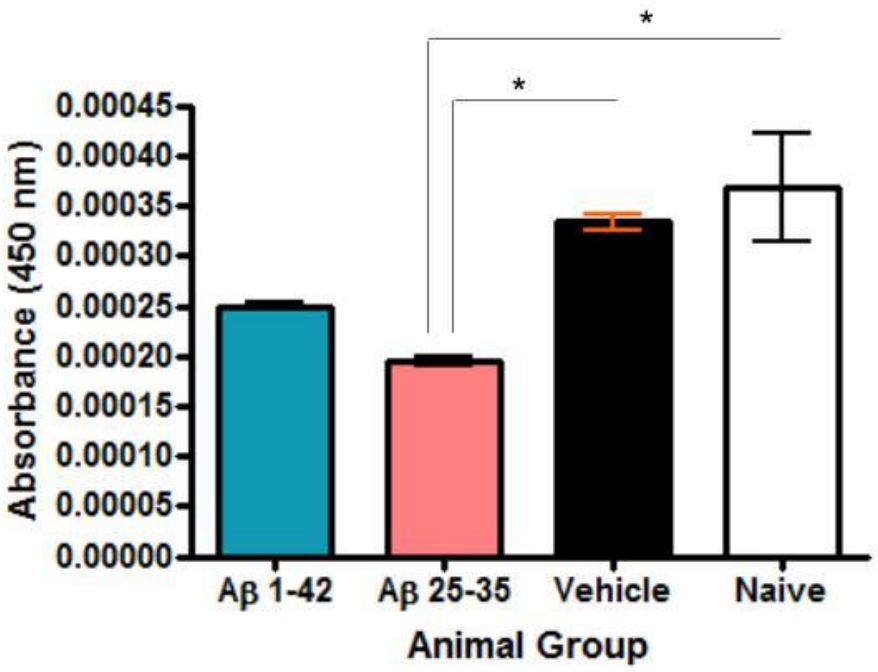

Figure 5.7 Aβ 25-35 decreases total CREB labelling in nuclear fractions. 5 buccal+cerebral ganglia from four animal groups (Aβ 1-42 [n=3], Aβ 25-35 [n=3], Vehicle [n=3], Naïve [n=3]) were subjected to chromatin extraction and nuclear fractions were retained. Each group was added to a sandwich ELISA with total CREB antibody, and measured for absorbance at 450 nm. Means ± SEM values are shown. Asterisks indicate significant difference between groups. One-way ANOVA, $p=0.0076$. Tukey's tests with $p<0.05$: Aβ 25-35 vs. Vehicle, Aβ 25-35 vs. Naïve.

The investigation continued to CREB phosphorylated at Ser133. pCREB is the activated form of CREB critical for LTP and LTM formation (for review, see Alberini, 2009). The natural regulation of pCREB occurs through phosphorylation by several protein kinases and phosphatase activity of PP1 and PP2A (Wadzinski et al., 1993; Hagiwara et al., 1992). It is important to note that CREB can be activated independently of phosphorylation of Ser133 (Bittinger et al., 2004); however, Ser133-independent CREB activation was not explored in this thesis. Many studies have looked at timing of pCREB appearance after training; in mouse IA (inhibitory avoidance) tasks, increased pCREB was measured immediately after training and again at 3 to 6 hours post-training (Bernabeu et al., 1997), coinciding with the protein synthesis time window for memory formation. Another IA training paradigm found additional waves of pCREB at 9 and 20 hours post-training as well, which were found to last for 28 to 48 hours (Taubenfeld et al., 1999; Taubenfeld et al., 2001). This increased pCREB was from increased phosphorylation and not increased steady state CREB levels (Taubenfeld et al., 1999; Taubenfeld et al., 2001). Finally, in *Lymnaea* single-trial food-reward classical-conditioning, pCREB was found to be elevated at 6 hours post-training (Ribeiro et al., 2003).

Studying change in pCREB levels is not only relevant for memory studies, but has also been implicated in AD. Reduced phosphorylation of CREB Ser133 has been observed in post-mortem AD brains (Yamamoto-Sasaki et al., 1999), Tg2576 mice (Dineley et al., 2001), and Aβ oligomers have been shown to inhibit glutamate-stimulated phosphorylated CREB in cortical cultures (Tong et al., 2004). For this reason, phosphorylation of CREB at Ser133 was further investigated. Similar to total CREB measurements, a nuclear extract and sandwich ELISA was necessary to measure pCREB. An antibody for pCREB Ser133 that has previously been used in *Lymnaea* was used again for this study (Ribeiro et al., 2003) and it was found that both Aβ 1-42 and Aβ 25-35 groups have significantly decreased levels of pCREB Ser133 compared to vehicle and naïve groups (Figure 5.8). Aβ 1-42 and Aβ 25-35 are also significantly different from each other, with pCREB significantly decreased in Aβ 1-42 treated animals. These results coincide with the down regulation of pCREB Ser133 found in other models (Yamamoto-Sasaki et al., 1999; Dineley et al., 2001; Tong et al., 2004).

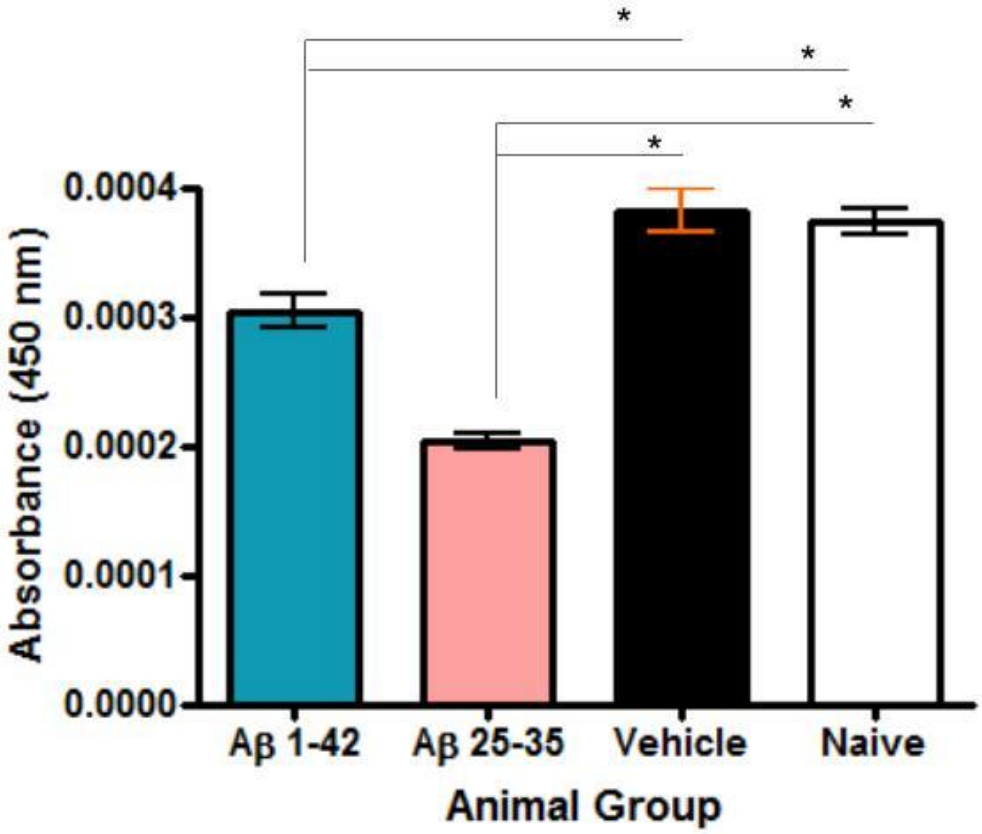

Figure 5.8 pCREB Ser133 labelling is decreased in Aβ 1-42 and Aβ 25-35 nuclear fractions. 5 buccal+cerebral ganglia from four animal groups (Aβ 1-42 [n=5], Aβ 25-35 [n=5], Vehicle [n=5], Naïve [n=5]) were subjected to chromatin extraction and nuclear fractions were retained. Each group were added to a sandwich ELISA with pCREB Ser133 antibody, and measured for absorbance at 450 nm. Means ± SEM values are shown. Asterisks indicate significant difference between groups. One-way ANOVA, $p<0.0001$. Tukey's tests with $p<0.05$: Aβ 1-42 vs. Aβ 25-35, Aβ 1-42 vs. Vehicle, Aβ 1-42 vs. Naïve, Aβ 25-35 vs. Vehicle, Aβ 25-35 vs. Naïve.

5.3 Discussion

In this chapter, studies focused on differences in protein synthesis, CREB, and pCREB Ser133 levels in trained and Aβ- treated animals. No change was found in total protein levels or protein synthesis levels between Aβ-treated, trained, and naïve animals. Animals' brains were dissected directly after testing, suggesting that memory is most likely in the retrieval process during this time. It is well known that protein synthesis is not involved in memory retrieval (Kida et al., 2002; Pedreira et al., 1996), which was confirmed in this chapter. Total CREB levels were measured and compared between animal groups and found that total nuclear CREB is significantly decreased in Aβ 25-35 injected animals, compared to vehicle and naïve animals. CREB and pCREB have not been directly quantified in Aβ 25-35-injected animals previously; however, the decrease in CREB levels of Aβ 25-35-treated *Lymnaea* does not coincide with the Aβ-treated or AD models in the literature, which suggests that total CREB levels do not change (Dineley et al., 2001; Tong et al., 2004). However, *Lymnaea* treated with the full length, physiologically relevant form of the Aβ peptide did not exhibit any difference in total CREB. It is possible that the difference in the two peptides is due to different concentrations applied or that the two peptides act on CREB differently.

Finally, pCREB Ser133 was measured and compared between animal groups. Aβ 25-35- and Aβ 1-42-injected animals showed significantly decreased pCREB compared to vehicle and naïve groups. The decrease of pCREB in the Aβ-treated groups has also been found by other labs using different models (Yamamoto-Sasaki et al., 1999; Dineley et al., 2001; Tong et al., 2004). Since pCREB is necessary for memory retrieval (Szapiro et al., 2002), decreased pCREB level in trained/Aβ-injected animals may be inhibiting memory retrieval. This could be the molecular disruption mechanism that causes the observed behavioural deficit previously found in these Aβ-treated animals. However, the vehicle-injected and naïve pCREB Ser133 levels are not significantly different and pCREB is likely important, but not sufficient, for the Aβ-induced LTM loss. Importantly, there is probably a baseline of pCREB necessary for this memory and the Aβ levels are below this threshold, combining with other unidentified factors to cause the LTM inhibition observed in Aβ-treated animals.

An interesting, and possibly confusing, aspect of the literature becomes apparent at this point in the discussion. How can CREB activation be necessary for memory retrieval, but not protein synthesis? There are two possible answers. First, CREB plays a key role in both synaptic and nonsynaptic plasticity, helping the neurons

to generate action potentials and to regulate membrane resistance, intrinsic excitability (Jancic et al., 2009; Dong et al., 2006), firing frequency, and resting membrane potential (Han et al., 2006). Aβ may widely disrupt nonsynaptic plasticity in this system through altering CREB function without drastically altering protein synthesis. Secondly, while protein synthesis is not required for memory retrieval, it is required for memory reconsolidation (for review, see Alberini and LeDoux, 2013). Reconsolidation is the strengthening of memory after retrieval and requires similar molecular signalling cascades as memory consolidation (for review, see Alberini and LeDoux, 2013). Although brains were dissected as soon as possible in these experiments, cascades were already shifting to reconsolidate the memory trace. It is impossible to distinctly pinpoint one memory process at this time point, as there are likely multiple memory processes undergoing change when the brain is removed. If the animals' brains had not been removed, the decrease in pCREB of Aβ-treated animals would have required a large amount of stimulus and significant overcompensation of the cascades to enable the protein synthesis necessary for memory reconsolidation. It is also worth noting that the decreased pCREB levels in affected neurons are also disadvantageous for any new memory formation within the circuitry as, similar to reconsolidation, it is dependent upon pCREB and protein synthesis. Considering the above, it is clear that decreased pCREB in Aβ-treated animals may not only inhibit the animals' ability to retrieve memory, but would also likely disrupt future memory processes such as reconsolidation or new memory formation within the diseased circuitry. This disruption would manifest as the observed behavioural memory deficits previously discussed in Chapter 3.

6. Aβ 1-42 and 25-35 disrupts CREB-signalling cascades in trained *Lymnaea stagnalis*.

The previous chapter indicated that protein synthesis is not necessary for 48 hour memory recall in *Lymnaea* and that Aβ injection does not disrupt protein synthesis when injected at 24 hours and measured at 48 hours post-conditioning. However, total CREB and pCREB Ser133 is disrupted by Aβ 25-35 and pCREB Ser133 is disrupted by Aβ 1-42 at these time points. This information may provide a direct link to Aβ-induced LTM deficits. However, CREB activation is a downstream element of many signalling cascades involved in LTM and synaptic plasticity (Figure 6.1) and any Aβ-induced disruption to an upstream element could manifest as changes in pCREB. Therefore, upstream disruptions to CREB-signalling cascades were measured in order to pinpoint where Aβ is disrupting the pathway, starting with the most upstream element of CREB-signalling cascades: receptors in the postsynaptic membrane. Much of Aβ's influence on plasticity is believed to occur at the synapse at early time points before any synaptic loss is observed. For example, Aβ treatment causes NMDARs (Lacor et al., 2007; Snyder et al., 2005) and AMPARs (Hsieh et al., 2006) to be internalised from the postsynaptic membrane. This is believed to mimic the loss of synaptic plasticity before synaptic structural changes are observed in early-stage AD (Klein et al., 2007; Lambert et al., 1998).

Different forms of memory require different molecular cascade components. For example, LTM formation requires NMDARs (Steele and Morris, 1999), AMPARs, mGluRs (Schulz et al., 2001), CaMKII (Otmakhov et al., 1997; Giese et al., 1998; Wan et al., 2010; Naskar et al., 2014), PKA (Huang et al., 2000; Michel et al., 2008), MAPK (Huang et al., 2000; Ribeiro et al., 2005), PKC (Paratcha et al., 2000; Weeber et al., 2000), transcription (Fulton et al., 2005; Pedreira et al., 1996), translation (Fulton et al., 2005; Brink et al., 1966; Pedreira et al., 1996), and CREB activation (Impey et al., 1996; Schulz et al., 1999; Bourtchuladze et al., 1994; Barco et al., 2002; Taubenfeld et al., 1999; Bito et al., 1996; Deisseroth et al., 1996; Countryman et al., 2005; Pittenger et al., 2002; Dash et al., 1990; Kida et al., 2002; Ribeiro et al., 2003). However, the behavioural time point investigated in this thesis is focused on consolidated memory, not memory formation or acquisition. As described in Chapter 3, Aβ injection occurs at the 24 hour post-conditioning time point, when memory is known to be fully consolidated in *Lymnaea* (Fulton et al., 2005). Memory is tested and brain samples are collected 48 hours post-conditioning. The term "testing" can be considered memory retrieval (recall). Thus, the forms of memory that the Aβ injection could be disrupting

include: memory retrieval, early memory reconsolidation, memory maintenance (retention), memory storage, or lingering memory consolidation (Dudai and Eisenberg, 2004). Retrieval of LTM involves AMPARs (Hong et al., 2013), mGluRs (Szapiro et al., 2000), VGCCs, PKA (Szapiro et al., 2000), MAPK (Szapiro et al., 2000), PKC, and calcineurin (Mayford and Kandel, 1999) but not CaMKII (Szapiro et al., 2000) or protein synthesis (Szaprio et al., 2002; Kida et al., 2002; Pedreira et al., 1996). The involvement of CREB activation (Szapiro et al., 2002; Kida et al., 2002) and NDMARs (Szapiro et al., 2000; Steele and Morris, 1999; Przybyslawski and Sara, 1997) in memory recall is controversial.

Many of the above mentioned molecular contributors to LTM are disrupted in AD. Memory loss is the predominant symptom of AD and many studies have shown that Aβ inhibits LTP and enhances LTD (Shankar et al. 2008; Li et al., 2009). It is widely accepted that Aβ influences synaptic plasticity by structural and functional interaction with several membrane proteins, including: α7-nAChRs (Wang et al., 2000), NMDARs (Snyder et al., 2005), AMPARs (Parameshwaran et al., 2007; Alberdi et al., 2010), and several others (for review, see Mucke and Selkoe, 2012), and, partially through these interactions, causes neurotoxicity by increasing intracellular Ca^{2+} levels (for review, see LaFerla, 2002). Interestingly, receptor antibody treatment (including NMDARs, insulin receptors, PrP receptor, mGluR5, AMPARs) decreases Aβ oligomer binding to synapses (De Felice et al., 2009; Lauren et al., 2009; Renner et al., 2010; Zhao et al., 2010). It is important to keep in mind that the Aβ-induced LTP deficits are thought to arise from Aβ-induced LTD-like processes. Aβ-induced synaptic depression has an initial increase in synaptic activation of NMDARs by glutamate, followed by synaptic NMDAR desensitization, NMDAR/AMPAR internalization, and activation of extrasynaptic NMDARs and mGluRs; all of these events are involved in the induction of LTD (for review, see Mucke and Selkoe, 2012). The inhibition of LTP can be abolished in Aβ-treated tissues by applying blockers of LTD-related signalling cascades, such as mGluR or p38 MAPK (Wang et al., 2004c).

Receptor dysfunction will lead to aberrant Ca^{2+} influx into the neurons and thus deregulate protein signalling cascades (Figure 6.2). Specifically, CREB-signalling has been found to be inhibited by non-degenerative doses of oligomeric Aβ 1-42 (Tong et al., 2004). The main CREB-signalling cascade, cAMP/PKA, is inhibited by synthetic Aβ oligomers in culture, slice, and *in vivo* Tg2576 mice (for review, see Benilova et al., 2012). Unsurprisingly, CREB-signalling activation reverses learning and memory

deficits in APP+PS1, 3xTg, and TgCRND8 mice (Gong et al., 2004; Caccamo et al., 2010; Yiu et al., 2011).

All experiments in this thesis thus far have been built on the behavioural deficits described in Chapter 3 and this chapter continues to investigate CREB-signalling cascades upstream of the transcription factor. Chapter 5 previously demonstrated that pCREB Ser133 levels are decreased in Aβ-treated animals, indicating the possibility that this molecular disruption leads to LTM loss. Any protein change examined in this chapter may provide a stronger correlative link to memory loss. A combination of molecular, pharmacological, and biochemical techniques have been used to test Aβ-induced disruption to CREB-signalling cascades. This approach offers a comprehensive picture of how Aβ is affecting memory 48 hours after conditioning and 24 hours after injection in *Lymnaea stagnalis*.

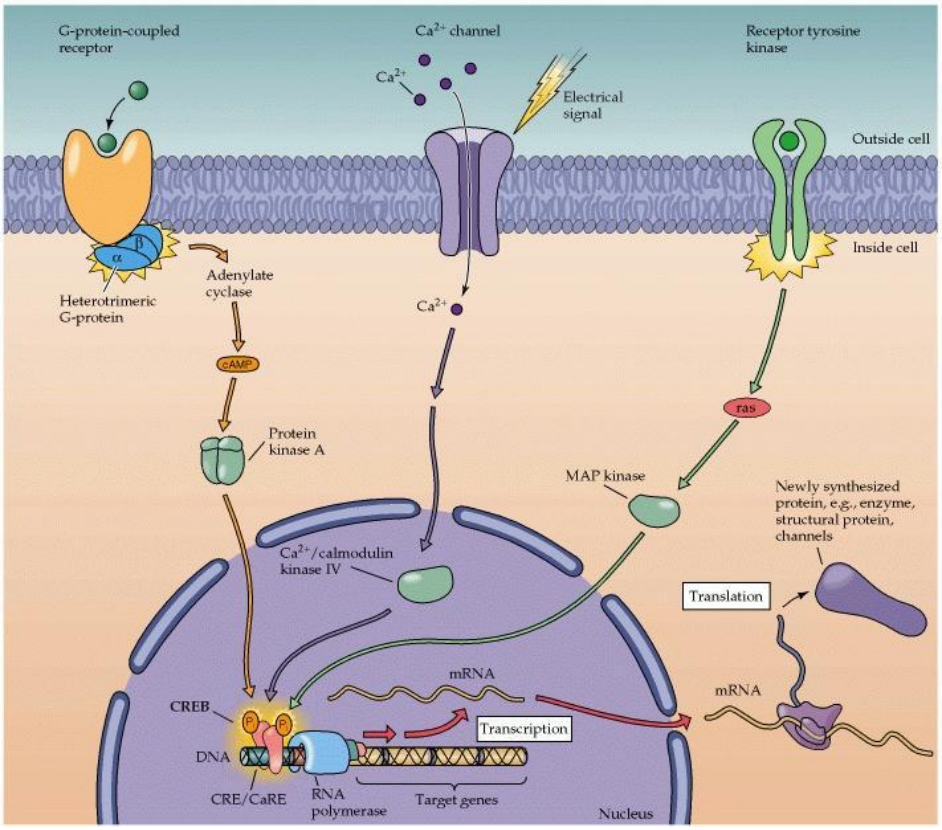

Figure 6.1 CREB-signalling cascades involved in LTP. Schematic of key proteins and events involved in CREB-signalling pathways of LTP (reproduced from Purves et al., 2008).

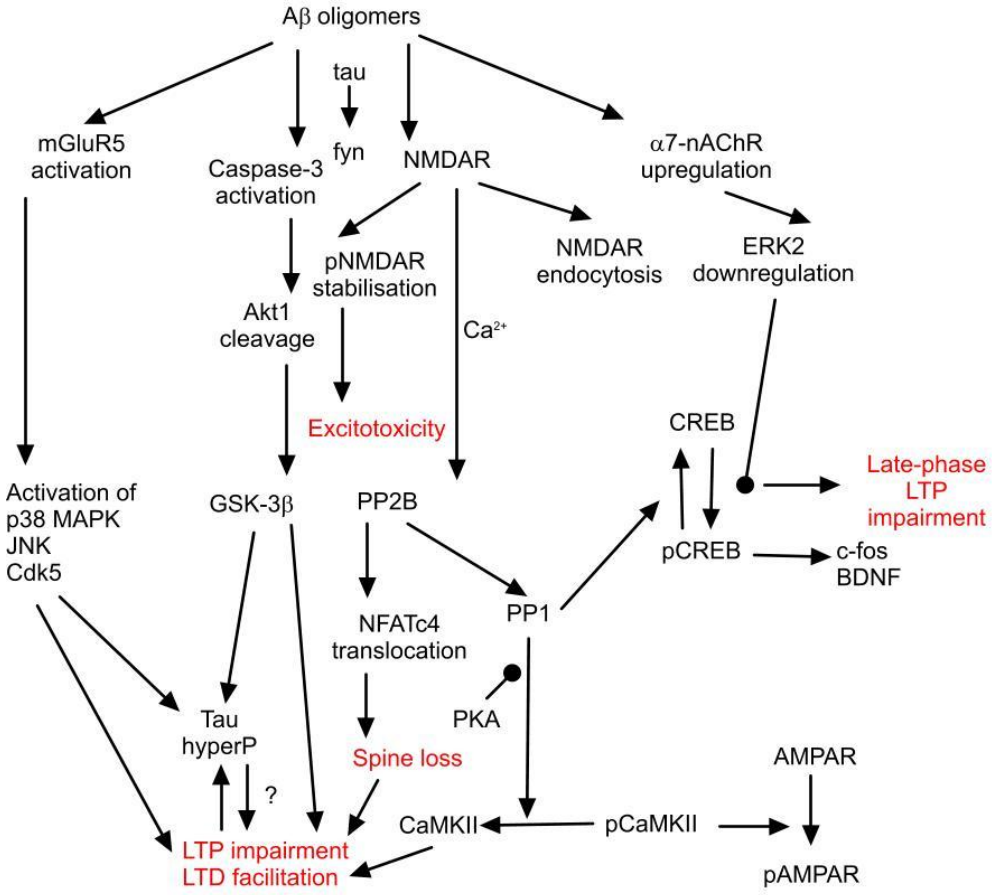

Figure 6.2 Aβ's effect on signalling cascades. Schematic of protein signalling cascades disrupted by Aβ oligomers (adapted from Benilova et al., 2012).

6.1 Receptors involved in memory and/or CREB-signalling pathways may be disrupted by treatment with Aβ at the 24 hour post-injection/ 48 hour post-training time point.

Three different families of receptors have been selected for this study due to their known importance for LTM, involvement in CREB-signalling pathways, and/or because they are known to be disrupted by Aβ. The first family of receptors considered was AMPA. AMPARs are ionotropic, tetrameric complex receptors assembled from a mixture of the subunits: GluA1, GluA2, GluA3, and GluA4, which express fast gating kinetics and rapid desensitisation (for review, see Dingledine et al., 1999). The incorporation of these receptors into and internalisation from postsynaptic sites is one of the main molecular mechanisms underlying LTP and LTD (for review, see Man et al., 2000; Sheng and Lee, 2001). Specifically, the GluA1 subunit mediates NMDAR-dependent AMPAR insertion during LTP (Shi et al., 1999; Hayashi et al., 2000; Lu et al., 2001; Meng et al., 2003).

APP knockout mice have aberrant AMPAR-mediated excitatory synaptic transmission and express reduced GluA1, GluA2, and GluA2/3 in Aβ vulnerable regions of the AD brain (Armstrong et al.,1994; Carter et al., 2004; Thorns et al., 1997; Wakabayashi et al., 1994). Aβ oligomer-induced removal of AMPARs from the post synapse has also been found in aberrant-APP transfected, APP transgenic mice, and Aβ 1-42-treated animals (Gu et al., 2009; Hsieh et al., 2006). Interestingly, the AMPAR inhibitor DNQX (6,7-dinitroquinoxaline-2,3-dione) only slightly inhibits Aβ-induced ROS generation and does not affect Aβ binding to the synapse (De Felice et al., 2007). Taken together, the background indicates that Aβ alters AMPAR distribution and function in an exposure-dependent manner, but that AMPARs are not a direct Aβ target.

Importantly for work in *Lymnaea*, an AMPA GluA1 orthologue exists (Darlison et al., 1993) and mammalian GluA1 antibodies have been used in *Lymnaea* successfully (Naskar et al., 2014). Western blotting was therefore used to measure total GluA1 in buccal+cerebral ganglia and no significant difference between any of the treated or control groups was observed (Figure 6.3).

From Figure 6.3, it is clear that GluA1 is not being markedly produced or degraded from either the Aβ treatment or conditioning at this time point. However, alterations in the form of post-translational modifications can affect receptor function

without changing total GluA1 levels. GluA1 Ser831 and Ser845 mutated knock-in mice are unable to have AMPARs properly trafficked into the postsynapse, suggesting a need for phosphorylation regulation at these amino acid residues for normal synapse AMPA-fication (Lee et al., 2003). These mutant mice are able to acquire memory, but are unable to recall memory when tested 8-24 hours after training, suggesting a role for pGluA1 at Ser831, Ser845, and a role for AMPAR trafficking in consolidated memory (Lee et al., 2003). Often, phosphorylation of Ser845 and Ser831 is rapid and transient, as seen by a lack of phosphorylation change in mice when measured multiple hours after undergoing contextual foot shock (Shukla et al., 2007). As part of the LTP sequence of events, CaMKII phosphorylates AMPARs at Ser831 in a rapid and transient manner which increases the single channel conductance of phosphorylated AMPARs (Barria et al., 1997; Benke et al., 1998). However, LTP can still occur in the absence of increased phosphorylation of Ser831 (Benke et al., 1998; Hayashi et al., 2000; Lee et al. 2003). PKA phosphorylates GluA1 at Ser845, which is necessary but not sufficient to drive GluA1 into the synapse during AMPA-fication (Esteban et al., 2003). When LTD is induced, the PKA-phosphorylated GluA1 Ser845 site becomes dephosphorylated (Montgomery and Madison, 2002). For these reasons, the phosphorylated state of GluA1 at Ser831 and Ser845 were also considered.

Mammalian antibodies against GluA1 Ser831 and GluA1 Ser845 have been successfully used in *Lymnaea* (Souvik Naskar, personal communication). Neither Ser831 (Figure 6.4A, B) nor Ser845 (Figure 6.4C, D) phosphorylation levels differ significantly between any of the animal groups when quantified using western blot.

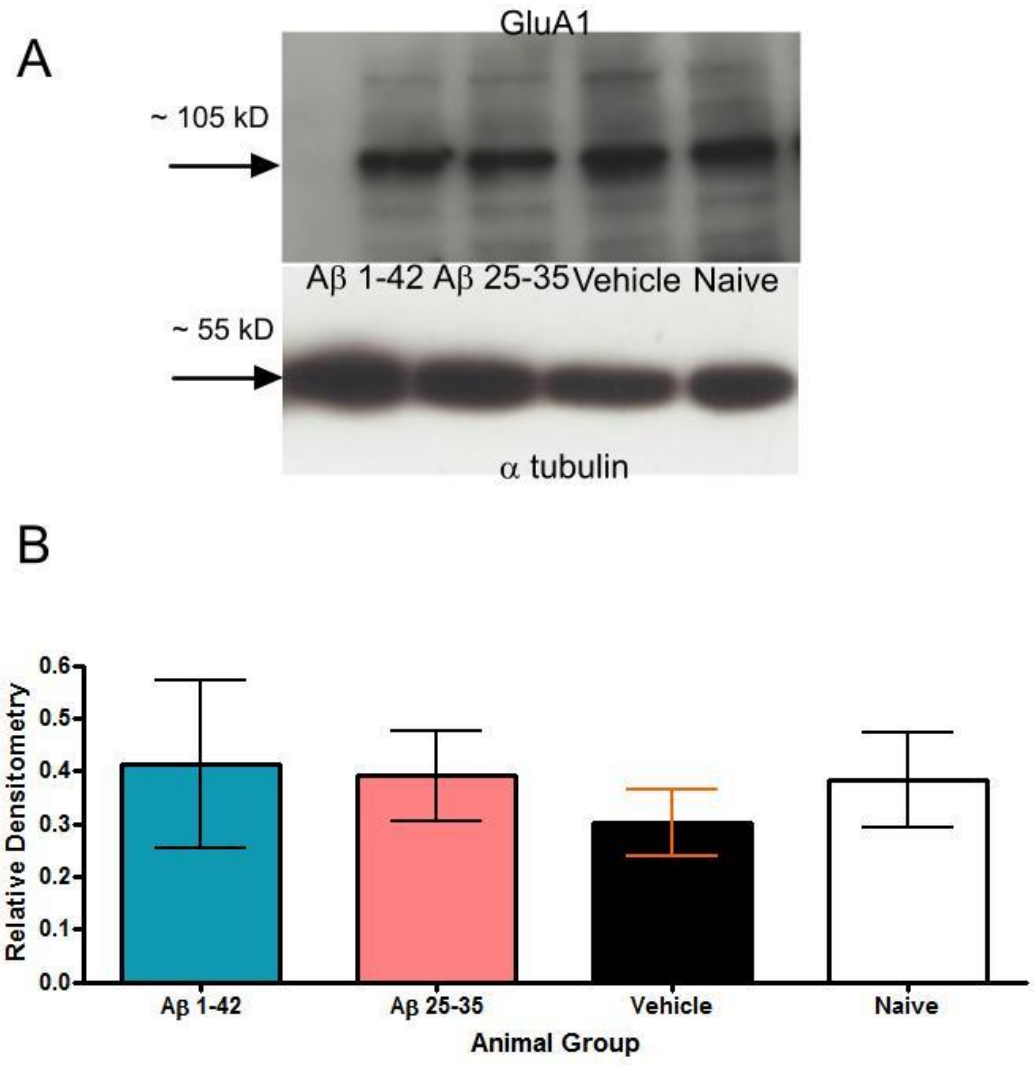

Figure 6.3 Total GluA1 levels are the same across treatment and control groups. Four animal groups (Aβ 1-42 [n=15], Aβ 25-35 [n=15], vehicle [n=15], naïve [n=9]) were compared for intensity of total GluA1 labelling using western blot. For each group 5 buccal+cerebral ganglia were pooled together, run on a gel, and western blotted with a GluA1 antibody. (**A**) Representative GluA1 and α tubulin loading control bands. (**B**) Data represents GluA1 band densitometry/ loading control densitometry. Means ± SEM values are shown. Kruskal-Wallis, p=0.8647. Dunn's Multiple Comparison all p>0.05.

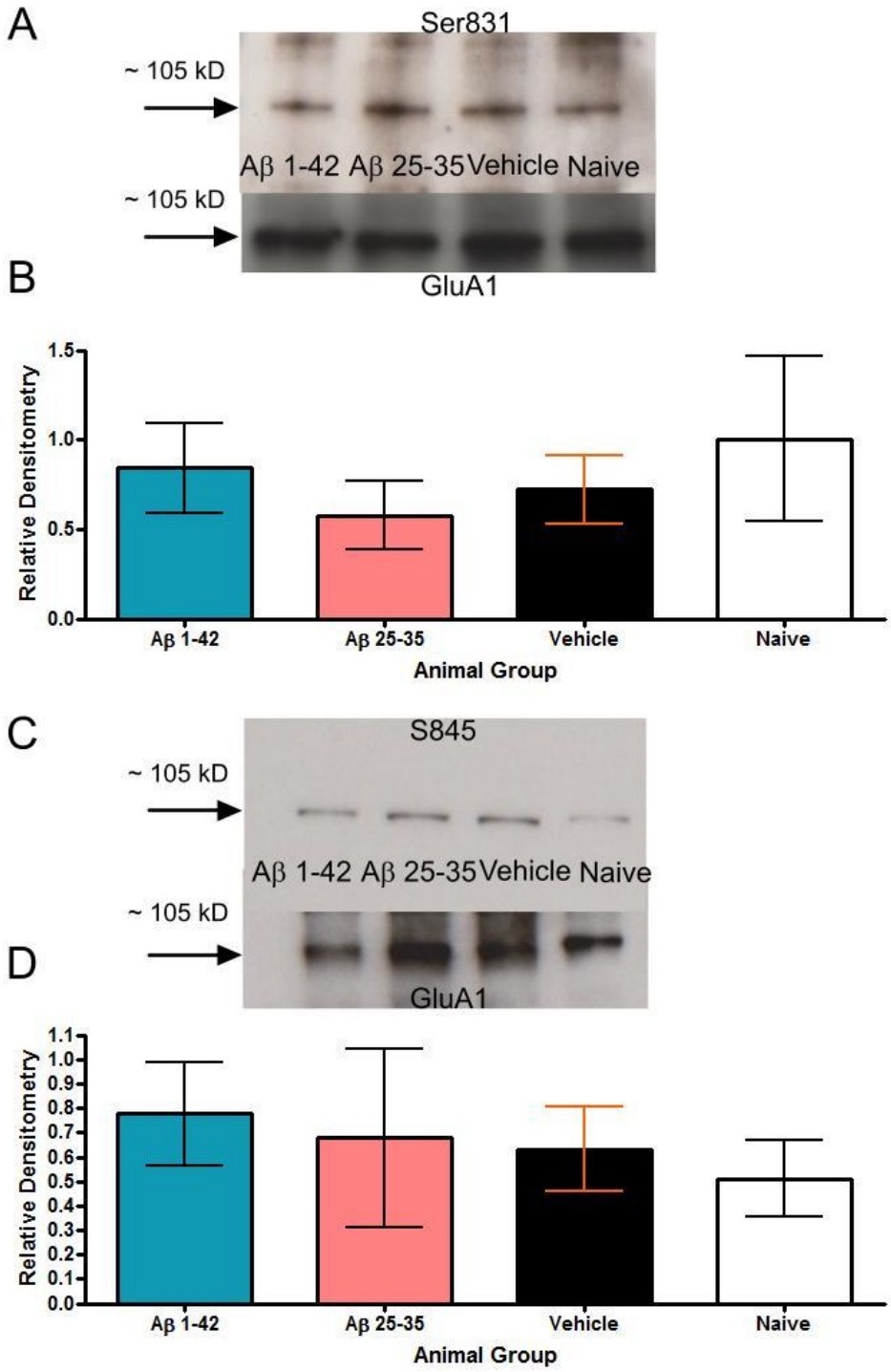

Figure 6.4 Levels of pGluA1 Ser831 and pGluA1 Ser845 are not different between Aβ-treated or trained animal groups. For each group 5 buccal+cerebral ganglia were pooled together, run on a gel, and western blotted with either a pGluA1 Ser831 or pGluA1 Ser845 antibody. (**A-B**) Four animal groups (Aβ 1-42 [n=8], Aβ 25-35 [n=5], Vehicle [n=7], Naïve [n=4]) were compared for intensity of pGluA1 Ser831 labelling using western blot. (**A**) Representative pGluA1 S831 bands and GluA1 bands. (**B**) Data represents pGluA Ser831 band densitometry/ steady state protein densitometry. Means ± SEM values are shown. Kruskal-Wallis, p=0.9220. Dunn's Multiple Comparison all p>0.05. (**C-D**) Four animal groups (Aβ 1-42 [n=8], Aβ 25-35 [n=7], Vehicle [n=9], Naïve [n=6]) were compared for intensity of pGluA1 Ser845 labelling using western blot. (**C**) Representative pGluA1 S845 bands and GluA1 bands. (**D**) Data represents pGluA Ser845 band densitometry/ steady state protein densitometry. Means ± SEM values are shown. Kruskal-Wallis, p=0.5999. Dunn's Multiple Comparison all p>0.05.

The second family of receptors considered is NMDA. NMDARs act as a coincidence detector, allowing Ca^{2+} entry to the postsynapse only when presynaptic and postsynaptic activity coincides. At this time, a voltage-dependent release of the Mg^{2+} ion from the NMDAR pore must also occur to unblock the channel and glycine or D-serine must bind as a cofactor for NMDAR to allow Ca^{2+} influx (Mayer et al., 1984; Nowak et al., 1984; Fadda et al., 1988). NMDAR's role as a coincidence detector, along with the Ca^{2+} entry into the postsynapse, is necessary for certain forms of LTP (Bliss and Collingridge, 1993). Besides its requirement in memory acquisition and consolidation, NMDARs have been shown to be important in memory storage as well, through the use of inducible and reversible NMDAR knockout mice (Cui et al., 2004). In fact, persistent NMDAR activity is believed to be necessary for the first several days after training to ensure proper LTM maintenance and storage (Frankland et al., 2001). One way in which NMDARs are regulated is by a redox modulatory site in the hydrophobic pore of the receptor complex, which allows retrograde messengers like NO and ROS to directly down-regulate gating frequency and open-time of the receptor (Aizenman et al., 1990; Lei et al., 1992). NMDARs also seem to be involved in their own downstream up-regulation; Ca^{2+} influx through these receptors can lead to CREB activation, which acts as a transcription factor for the NMDAR1 gene (Lau et al., 2004).

The link between AD and NMDAR dysfunction is so great that Memantine, a non-selective NMDAR antagonist, is currently used for the treatment of moderate to severe AD (De Felice et al., 2007) due to its ability to slow cognitive decline (Fastbom et al.,1998; Winbald and Poritis, 1999). A significant loss of NMDARs occurs in AD brains (Sze et al., 2001; Mishizen-Eberz et al., 2004) and reduction of surface NMDARs is found in Aβ-treated tissues (Brouillette et al., 2012; Roselli et al., 2005; Snyder et al., 2005; Lacor et al., 2007). However, how Aβ effects NMDARs is not completely clear. Aβ is known to bind to NR1 and NR2B subunits in hippocampal neurons (Lacor et al., 2004; Lacor et al., 2007) and will immunoprecipitate with NMDAR subunits in synaptosomes (De Felice et al., 2007; Renner et al., 2010; Roenicke et al., 2011). Application of an NR1 antibody or the NMDA inhibitor APV ((2R)-amino-5-phosphonovaleric acid) to cultured neurons results in a 50% decrease in Aβ oligomer-synapse binding (De Felice et al., 2007; Lacor et al., 2007). For this reason, some reports suggest that Aβ directly affects important functions of the receptors and inhibits induction of NMDAR-dependent LTP (Snyder et al., 2005; Shankar et al., 2007; Lambert et al., 1998; Wang et al., 2002), specifically NR2B subunit-containing receptors (Li et al., 2009; Rammes et al., 2011; Roenicke et al., 2011). *In vitro* studies have shown that NMDAR-independent LTP is not inhibited by Aβ

1-42 (Wang et al., 2004b) and both these NMDAR-dependent and NMDAR-independent results have been replicated *in vivo* (Hu et al., 2009). NR1 antibodies, MK-801, APV, or Memantine, eliminate the Ca^{2+} influx that otherwise results in oligomer-induced ROS (De Felice et al., 2007; Lacor et al., 2007), decreasing the neurotoxicity within the cell and the amount of ROS able to act on the NMDAR redox modulatory site (Mattson, 1995).

However, it is important to note that these findings are not simple; not all NMDAR-dependent LTP is vulnerable to Aβ and Aβ is able to facilitate NMDAR-independent LTD (Hu et al., 2009; Li et al., 2009; Shankar et al., 2008). Extra- or perisynaptic NMDARs, which are often rich in the NR2B subunit, are known to induce LTD when activated and have been shown to mediate the inhibition of LTP/induction of LTD in the presence of Aβ oligomers (Li et al., 2011; Hsieh et al., 2006; Li et al., 2009). The disruption to LTP is believed to be mediated by Aβ-disrupted α7-nAChRs, causing NMDARs to be endocytosed (Snyder et al., 2005) and causing further deregulation of NMDAR signaling (Shankar et al., 2007). This Aβ-induced disruption of α7-nAChRs may be the most upstream element of a cascade of deregulation, causing NMDARs to induce neurotoxicity and the dependence of α7-nAChR disruption may be why Aβ's effect on NMDAR function is complicated (for review, see Mucke and Selkoe, 2012).

Importantly for this work in *Lymnaea*, 80% of central nervous system (CNS) neurons express the two NMDA NR1 isoforms (Ha et al., 2006), which have similar structure to mammalian NR1. Both NR1s have three transmembrane regions and a hydrophobic domain that forms a pore structure (Ha et al., 2006). *Lymnaea* NR1 also appear to have conserved redox modulation capabilities and sites for post-translational modifications (in the form of phosphorylation or N-glycosylation) mediated by PKC, casein kinase II, and PKA (Ha et al., 2006). Unfortunately, there are differences between NR1 function in *Lymnaea* and mammals. APV does not block *Lymnaea*'s NMDA receptors and the voltage-dependent Mg^{2+} block does not exist in *Lymnaea* (Moroz et al., 1993). Limitations considered, the basic NMDAR functions, such as permeability to Ca^{2+} ions and receptiveness to glutamate signal, are retained in *Lymnaea* NR1s and thus are very likely to play an important role in LTP in this model system (Moroz et al., 1993; Ha et al., 2006). Importantly as well, the inhibitor MK-801 has been used successfully in *Lymnaea* (Wan et al., 2010). Because MK-801 can be used successfully in this model, NR1 inhibition at the 24 hour post-training time point was first investigated to determine if it was sufficient to inhibit LTM at 48 hour post-training. Importantly, naïve animals injected with either vehicle or MK-801 had similar

behavioural responses, indicating that treatment does not drastically interfere with the animals' motor abilities. Both naïve groups had significantly less behavioural response than trained, vehicle-injected animals. Trained and MK-801 injected animals showed neither significantly greater response from untrained animals nor decreased response from trained animals, instead exhibiting a decreasing trend (Figure 6.5).

NR1 was further investigated, but before any immuno-labelling could be performed, the use of a mammalian NR1 antibody needed to be verified for use in *Lymnaea*. To do this, a sequence alignment was compared between *Lymnaea* and rat NR1 to find sites of homology. Unfortunately, none of the homologous sites were matches to the antigens of commercially available antibodies. Still, two antibodies were considered. *Lymnaea* and rat brain tissue were run side-by-side and western blotted to compare banding patterns. The two antibodies were tested and both expressed low banding pattern between *Lymnaea* and rat, and did not exhibit banding at the appropriate molecular weight in the *Lymnaea* sample (Appendix III.1). These antibodies were deemed unsuitable for further use in *Lymnaea*.

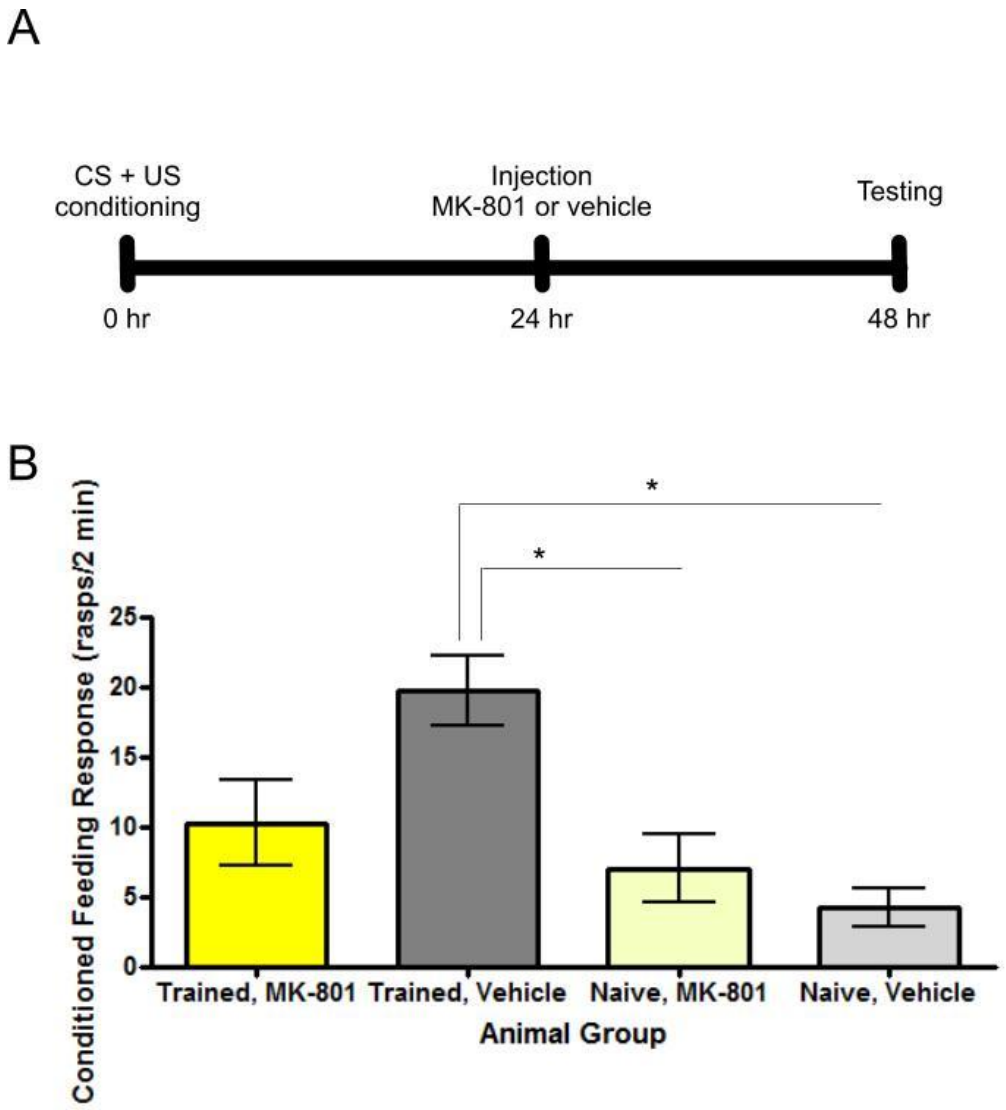

Figure 6.5 MK-801 injection results in a trend for decreased LTM in trained animals. (**A**) Timeline of experiment. (**B**) Four starved animal groups (Trained, MK-801 [n=15]; Trained, Vehicle [n=15]; Naïve, MK-801 [n=15]; Naïve, Vehicle [n=14]) were tested for rasp rate to amyl acetate, a measure of the feeding response to the CS. Means ± SEM values are shown. Asterisks indicate significantly increased feeding response from naïve animals. Kruskal-Wallis, p=0.0011. Dunn's Multiple Comparison with p<0.05= Trained, Vehicle vs. Naïve, MK-801; Trained, Vehicle vs. Naïve, Vehicle.

The final family of receptors studied in this body of work are nicotinic acetylcholine receptors. nAChRs belong to the Cys loop family of pentameric ionotropic channels (Alkondon et al., 1998). These receptors can be homomeric or heteromeric and are composed of a mixture of the 8 α subunits or 3 β subunits (for review, see Dani and Bertrand, 2007), which are highly permeable to Na^+, K^+, and Ca^{2+} (for review, see Lendvai and Vizi, 2008). nAChRs pass current at highly negative membrane potentials and make only a small contribution to ion influx at very active synapses (for review, see Dani and Bertrand, 2007). In mammalian synaptic transmission, nAChRs predominantly mediate presynaptic modulation of neurotransmitter release, although are also located at many nonsynaptic sites (for review, see Lendvai and Vizi, 2008) and in the postsynapse, and are generally not involved in fast synaptic transmission (for review, see Dani and Bertrand, 2007). This is due to their predominant role in nonsynaptic transmission; nAChR-mediated effect on neurons is slow because neurotransmitter signal is received after long-lasting diffusion. However, once the receptors are activated, ion influx is rapid (for review, see Lendvai and Vizi, 2008). So while these receptors are not involved in fast synaptic transmission, they are considered to be involved in fast nonsynaptic transmission, especially in comparison to the other nonsynaptic metabotropic receptors (for review, see Lendvai and Vizi, 2008). Stimulation of excitatory synaptic transmission paired with release of acetylcholine results in induced LTP in the Schaffer-collateral/commissural pathway, which is mediated through either muscarinic or nicotinic receptors (Gu et al., 2011). Nicotinic receptor-dependent LTP is mediated predominantly by α7-nAChR facilitation of Ca^{2+} entry through NMDARs (Gu et al., 2011). This is done after a nAChR-induced enhancement of presynaptic neurotransmitter, especially the neurotransmitter glutamate, is released from the presynaptic terminal (for review, see Dani and Bertrand, 2007). α7-nAChR's role as a presynaptic glutamate enhancer also increases AMPAR-mediated excitatory postsynaptic current (Mansvelder and McGehee, 2000). When α7-nAChRs are blocked pharmacologically, working memory is impaired in rats (Levin et al., 1996) and when nicotinic agonists are administered to human and non-human primates, learning and memory is improved (Levin et al., 2006).

As mentioned above, nAChRs play their major role in nonsynaptic plasticity. 86-93% of cholinergic boutons in the CNS of mammals do not make synaptic connections but are still functionally active in releasing ACh into the extracellular space, contributing to diffuse volume transmission (Descarries et al., 1997; Kasa et al., 1995). Interestingly, the majority of these nAChR-containing hippocampal neurons are glutamatergic or GABAergic, not cholinergic (Fabian-Fine et al., 2001). Only 12% of

these are GABAergic, with the predominant nAChR-containing neuronal type being glutamatergic (Kawai et al., 2002). Therefore, in order for ACh to activate nAChRs in these neurons, it must diffuse into the synaptic cleft from the extracellular space in a nonsynaptic manner while glutamate or GABA signals synaptically (for review, see Lendvai and Vizi, 2008). Excess ACh in the synaptic cleft is hydrolysed by the enzyme acetycholinesterase (AChE), creating choline as one of its products (for review, see Dani and Bertrand, 2007). This choline is also able to activate and desensitise nAChRs (Alkondon and Albuquerque, 2006).

The AChE inhibitor Donepezil is given to those with AD following the early studies which discovered a decrease in number of cholinergic neurons (Davies and Maloney 1976; Whitehouse et al., 1982), a decrease in acetylcholine synthesis (Sims et al., 1983), reduced number of cholinergic receptors in the cortex (White et al., 1977; Kellar et al., 1987), and reduced AChE activity (Perry et al., 1978a,b) in disease patients. AD brains also exhibit an increased proportion of α7-nAChR-expressing astrocytes (Jones and Wonnacott, 2004), which may contribute to the Ca^{2+} dyshomeostasis and aberrant inflammation found in the disease (Xiu et al., 2005). While nAChRs seem like a useful therapeutic target, these drugs only very modestly alleviate the cognitive deficits of AD (for review, see Dani and Bertrand, 2007). While pre-treatment with anticholinesterases can prevent Aβ-induced inhibition of LTP, treatment no longer inhibits Aβ's effect when applied after the peptide (Klyubin et al., 2014). Aβ 1-42 has high affinity for α7-nAChRs (Wang et al., 2000) and when bound, causes inhibition of nicotine-evoked currents (Liu et al., 2001; Pettit et al., 2001). An interesting study suggests that Aβ's effect on α7-nAChR function is complex; Kroker et al., 2013 used oligomeric Aβ 1-42 in combination with multiple receptor blockers to determine which receptors were most highly disrupted by Aβ during LTP. They found that only one α7-nAChR drug, SSR180711, out of three nAChR drugs including Donepezil, was successful in rescuing oligomeric Aβ 1-42 impairment of LTP (Kroker et al., 2013).

Importantly for work in *Lymnaea*, 12 nAChR transcripts exist and are expressed exclusively on many of the CNS neurons (Zeimal and Vulfius, 1967; Vulfius et al., 1967). Specifically, subunit B is predominantly found in the buccal ganglia and subunit A is predominantly found in the cerebral ganglia (van Nierop et al., 2006). The structure of *Lymnaea* nAChRs are similar to mammalian Cys loop family ionotropic channels with highest homology to mammalian nAChR and express 35-84% sequence homology to human nAChRs (van Nierop et al., 2006). In fact, experiments using

Lymnaea and the Ach binding protein offered a breakthrough in the structural and functional understanding of nAChRs (Smit et al., 2001). Importantly, nAChRs appear to function differently in *Lymnaea* than in mammals; in the molluscan CNS, cholinergic synaptic transmission is predominantly fast (van Nierop et al., 2006) as opposed to the slow synaptic, but fast nonsynaptic transmission observed in mammals. An nAChR mammalian antibody also has not yet been used successfully in *Lymnaea* so, similarly to the NR1 studies, before immuno-labelling could be performed an appropriate sequence alignment was done to find a mammalian nAChR antibody that may be used in this model. A rat α7-nAChR was aligned to nAChR subunit A in *Lymnaea* (Appendix III.2). *Lymnaea* nAChR A is one of the cation-selective nAChR receptors that display a particularly high contribution to the nAChRs in the cerebral ganglia (van Nierop et al., 2006). With the alignment, an antibody was selected with highest sequence homology to the antigen. Similar to NR1, there were discrepancies between the *Lymnaea* sequence and the antigen and so samples were run on a gel and western blotted with α7-nAChR to determine correct banding at the 56 kD weight (Figure 6.6). While there was smudging in the sample, likely due to low homology between *Lymnaea* and antigen, there is one distinct band at the predicted 56 kD weight in the *Lymnaea* sample. As there is non-specific signal in the *Lymnaea* sample, it would be best to use pre-absorption to ensure appropriate use of the antibody and this should be considered for future research. However, the single band appearing at the predicted weight in the *Lymnaea* sample makes it very likely that this antibody is useful. This antibody was used with western blotting to measure total α7-nAChR levels in the experimental and control samples (Figure 6.6). No significant difference was found between any of the animal groups.

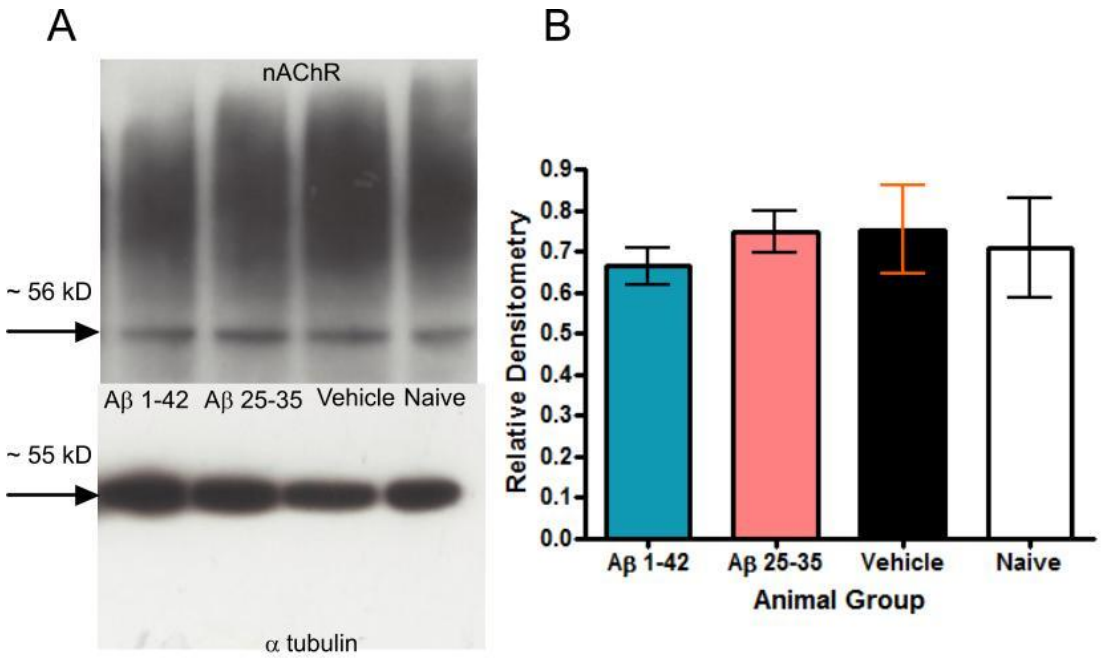

Figure 6.6 α7-nAChR-like subunit does not change in *Lymnaea* between Aβ-treated and conditioned animal groups. (**A**) Representative nAChR bands and α tubulin loading control bands (**B**) Four animal groups (Aβ 1-42 [n=6], Aβ 25-35 [n=6], Vehicle [n=6], Naïve [n=6]) were compared for intensity of α7-nAChR labelling using western blot. Data represents α7-nAChR band densitometry/ loading control densitometry. Means ± SEM values are shown. One-way ANOVA, p=0.8841. Tukey's tests all p>0.05.

6.2 Second messengers involved in CREB-signalling pathways are not disrupted by treatment with Aβ at the 24 hour post-injection/ 48 hour post-training time point.

Adenylyl cyclase is a second messenger associated with GPCRs and is involved in the cAMP/PKA CREB-signalling pathway. When monoamine neurotransmitters such as dopamine (Self et al., 1998), octopamine, or serotonin (Levitan and Barondes, 1974) arrive at their appropriate GPCR, adenylyl cyclase will then be activated. This initiates the cAMP/PKA pathway by converting ATP into cAMP. Adenylyl cyclase is also known to be involved in LTP by acting as a Ca^{2+} sensor (Chetkovich and Sweatt et al., 1993; Wong et al., 1999). Besides direct GPCR activation, adenylyl cyclase is also sensitive to calmodulin in the presence of Ca^{2+} and thus can be stimulated by other receptors, such as NMDARs, that allow large amounts of Ca^{2+} into the cell (Eliot et al., 1989; Chetkovich et al., 1991). Therefore, adenylyl cyclase (and its downstream pathway) and CaMKII act together to potentiate signal; cAMP inhibits PP1, which allows CaMKII to autophosphorylate itself more easily and thus makes its signal persistent (Brown et al., 2000; Genoux et al., 2002). Besides adenylyl cyclases involvement in LTP, it is also involved in leading to the phosphorylation of Ca^{2+} channels in neuronal intrinsic plasticity (Zhang and Linden, 2003).

Adenylyl cyclase's importance in LTM was brought to light by the genetic mutation of its orthologue, *rutabaga*, in *Drosophila* (Dudai et al., 1983; Levin et al., 1992). *Rutabaga* mutation studies implicate adenylyl cyclase and the cAMP/PKA pathway in controlling neuronal firing patterns and synaptic efficacy (Zhao and Wu, 1997; Renger et al., 2000). The need for adenylyl cyclase in spatial memory and LTP has also been found in rodents using both mutant mice and adenylyl cylcase antagonists (Wu et al., 1995; Huang et al., 1994; Frey et al., 1993; Wang et al., 2004a). Knockdown of adenylyl cyclase in mice results in the down-regulation of the expression of many genes in the hippocampus; interestingly, most of these genes are up-regulated at memory storage time points in wild type, trained mice (Wieczorek et al., 2010). This coincides with the knowledge that adenylyl cyclase is required for memory maintenance and retention (Wong et al., 1999; Shan et al. 2008; Wieczorek et al. 2010), suggesting that this second messenger plays an important role in activating the long-lasting transcriptional change necessary for LTM persistence. Considering how integral a role this second messenger plays in memory, it is unsurprising that adenylyl cylcase dysfunction has been directly linked to AD (Terry et al., 1994)

Importantly for work in *Lymnaea*, an adenylyl cyclase orthologue exists (de Jong-Brink et al., 1986). However, an adenylyl cyclase mammalian antibody has not yet been used successfully in *Lymnaea*. Similarly to the NR1 and nAChR studies, before immuno-labelling could be performed, an appropriate sequence alignment was completed to find a mammalian adenylyl cyclase antibody that may be used (Appendix III.3). However, the sequences had low alignment. Still, a mammalian antibody was selected and used to label western blots of *Lymnaea* and rat samples. Banding patterns did not align and so the antibody was deemed unsuccessful in *Lymnaea* (Appendix III.3).

When adenylyl cyclase is up regulated, it increases the amount of intracellular cAMP, another second messenger involved in the cAMP/PKA CREB-signalling pathway. However, the cAMP increase is only believed to last for 2 hours after stimulus exposure (Bacskai et al., 1993). During this time, cAMP will bind to the regulatory subunits of PKA, causing them to dissociate from the catalytic subunits and allowing the kinase to phosphorylate its downstream targets. The cAMP/PKA pathway has been implicated in Aβ-induced memory dysfunction (Vitolo et al., 2002; Tong et al., 2004) and addition of the cAMP-phosphatase inhibitor rolipram has been found to rescue Aβ-induced memory deficits (Vitolo et al., 2002). In experiments where cAMP was already increased, treatment with the adenylyl cyclase activator forskolin did not rescue Aβ-diminished LTP (Grammas et al., 1994). Increased levels of cAMP have been measured in AD fibroblasts (Martinez et al., 1999) and this agrees with cAMP measurements from AD patient microvessels (Grammas et al., 1994).

Experiments in *Lymnaea* examined the effect of injecting cAMP into the CGC soma and found an enhancement of the neuron's output, similarly to artificial depolarisation (Nikitin et al., 2006); this suggests a direct link between the cAMP/PKA pathway and a key intrinsic function sufficient in influencing *Lymnaea* behaviour. As cAMP is not a protein, a cAMP antibody will label appropriately across all species. Instead of western blotting, a dot blot approach was taken to measure total cAMP levels within these samples (Figure 6.7A). No significant difference between any of the experimental or control groups was found (Figure 6.7B). However, the dot blot method is only semi-quantitative. To ensure the results, a direct ELISA was used to compare total cAMP levels between samples (Figure 6.7C-D). Again, no significant difference between groups was found.

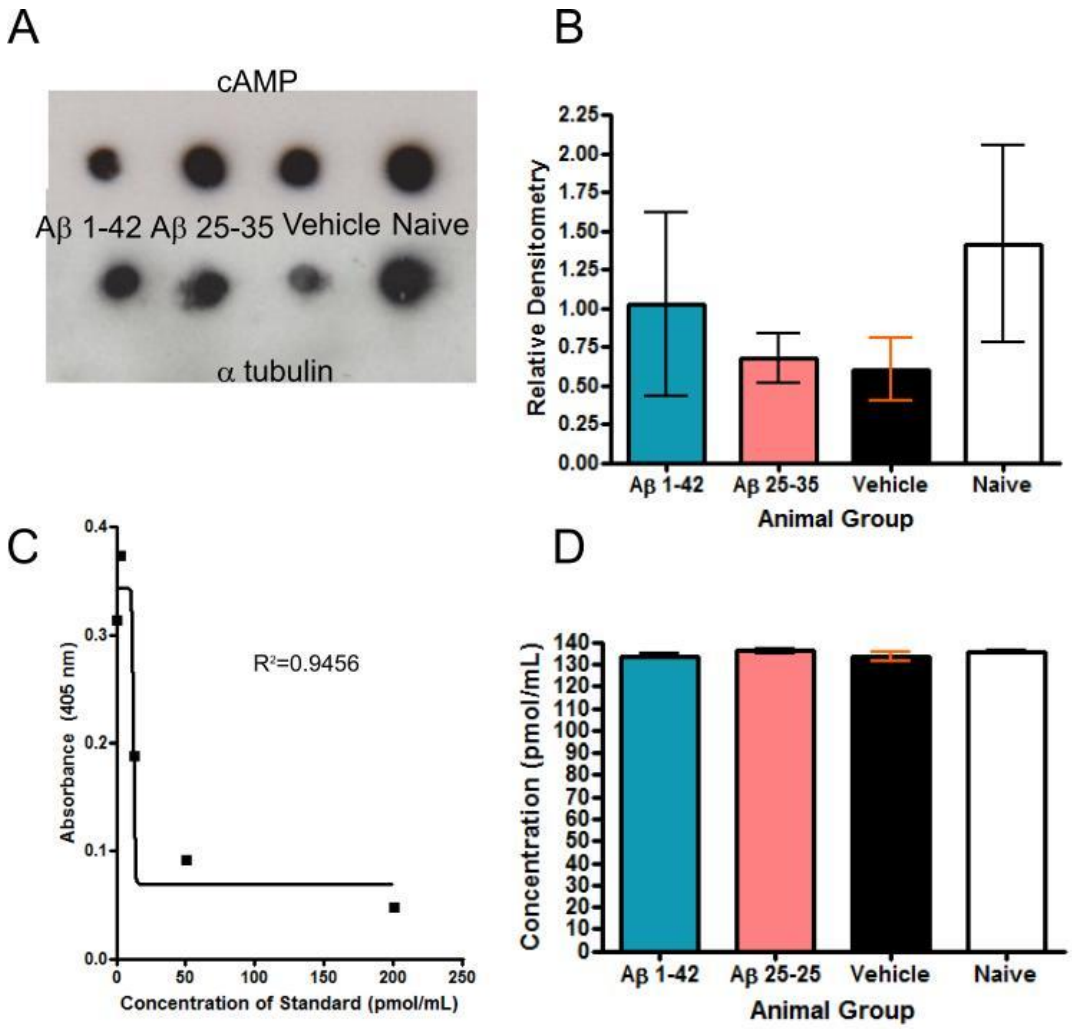

Figure 6.7 cAMP levels do not change with Aβ treatment or training. (**A**) Representative cAMP dot blot and α tubulin loading control dot blot. (**B**) Results from dot blot experiments. Four animal groups (Aβ 1-42 [n=9], Aβ 25-35 [n=9], Vehicle [n=8], Naïve [n=8]) were compared for intensity of cAMP labelling using dot blot. Data represents cAMP dot densitometry/ loading control densitometry. Means ± SEM values are shown. Kruskal-Wallis, p=0.7998. Dunn's Multiple Comparison all p>0.05. (**C**) Graph of standards' concentration vs. absorbance at 450 nm, which allowed for values in **D** to be calculated. Best-fit line is shown, using a Boltzmann sigmoidal equation. R^2=0.9456 (**D**) Four animal groups (Aβ 1-42 [n=2], Aβ 25-35 [n=2], Vehicle [n=2], Naïve [n=2]) were added to a cAMP direct ELISA kit, and measured for absorbance at 450 nm. Means ± SEM values are shown. One-way ANOVA, p=0.4227. Tukey's tests all p>0.05.

6.3 Kinases involved in CREB-signalling pathways are disrupted by treatment with Aβ at the 24 hour post-injection/ 48 hour post-training time point.

Kinases are important components of signalling cascades in that they activate the most downstream proteins involved. This section will describe experiments to examine three key kinases involved in CREB-related cascades; however, it is important to note that these are only three kinases out of over 300 different kinase-activating stimuli that are known to be capable of phosphorylating CREB at Ser133 (Johannessen et al., 2004). Initially, changes in PKC levels were investigated. PKC is a multigene family, consisting of at least 10 isoforms, 9 of which are found in neurons (Naik et al., 2000; Sossin, 2007; Steinberg, 2008). A conventional metabotropic signalling pathway, through mGluR1/5s, yields inositol triphosphate (IP3) and diacyl-glycerol (DAG). IP3 stimulates the release of intracellular Ca^{2+} and DAG activates the Ca^{2+}-sensitive kinase PKC. This signalling allows the Ca^{2+}-sensitive PKC to act out its role as a regulator in cell metabolism, neuronal function (Nishizuka, 1986; Hama et al., 1986), and LTP/LTM (Anwyl, 1989; Linden and Routtenberg, 1989; Michel et al., 2011) (Figure 6.8), and allows for release of Ca^{2+} from intracellular stores. PKC activation has been implicated in the early phase of LTP, but not memory acquisition (Sweatt, 1999; Ren et al., 2013; Zhang et al., 2009), and the kinase was found to be autophosphorylated on Thr634 and Thr641 at this early LTP time point (Sweatt et al., 1998). PKC may play its role in LTM through its necessity to maximally activate adenylyl cyclase, which in turn allows PKA to activate CREB (Sibley et al. 1986; Yoshimasa et al., 1987; Pieroni and Byrne, 1993; Cooper et al., 1995; Lorenzetti et al., 2008). Multiple labs (Roberson et al., 1999; Stratton et al., 1989) have also provided a critical link between upstream PKC to MAPK, further suggesting PKC involvement in downstream CREB activation. This occurs by PKC activating Ras or Raf-1, both of which are part of the MAPK cascade (for review, see Sweatt, 2001). However, it is believed that MAPK-independent and PKA-independent PKC can phosphorylate CREB directly (Xie and Rothstein, 1995), as well as *Aplysia* CREB2 (for review, see Bailey et al., 2004).

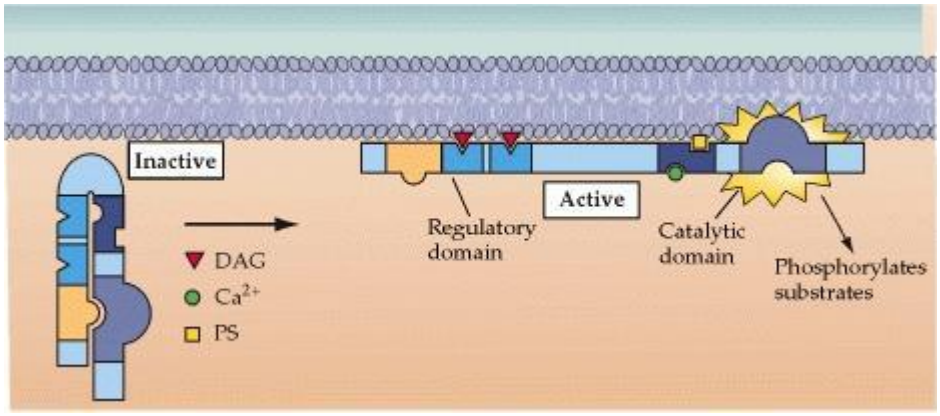

Figure 6.8 Mechanism of activation of PKC. Binding of the second messenger, DAG, to PKC allows a conformational change of the kinase to expose the catalytic site. Once exposed, the catalytic domain can then be activated (reproduced from Purves et al., 2008).

A Ca^{2+}-independent form of PKC, PKMζ, exists as well and it is this form that is necessary and sufficient for the maintenance phase of LTP (Klann et al., 1991; Sacktor et al., 1993) and LTM (Jerusalinsky et al., 1994; Shema et al., 2007; Serrano et al., 2008), as well as being required for the storage of spatial memory (Ling et al., 2002; Pastalkova et al., 2006; Yao et al., 2008; Migues et al., 2010). In *Aplysia*, PKC is a calpain substrate (Inoue et al., 1977; Klann et al., 1991) which allows Ca^{2+}-dependent protease to cleave PKC and yields the constitutively active form PKMζ (Bougie et al., 2009; Villareal et al., 2009). This activation of PKMζ is dependent upon increased Ca^{2+} influx through NMDARs. When inhibited, loss of PKMζ results in the reversal of *in vivo* LTP and loss of fully consolidated behavioural memory (Ling et al., 2002; Serrano et al., 2005; Shema et al., 2007; Shema et al., 2011).

PKC is also involved in intrinsic plasticity; it receives signals from VDCCs, activating PKC to phosphorylate ion channels and increasing neuronal intrinsic plasticity (for review, see Zhang and Linden, 2003) by increasing ion channel conductance (DeRemeir et al., 1985; Alkon et al., 1986; Madison et al., 1986; Malenka et al., 1986), changing rates of neurotransmitter synthesis or release (Berry, 1986; Wang et al., 1986; Zurgil and Zispel, 1985; Nichols et al., 1987; Shapira et al., 1987), changing cytoskeletal function (Litchfield and Bell, 1986), and regulating the sensitivity of neurotransmitter receptors (Kelleher et al., 1984; Sibley et al., 1984). Action potential height is also increased when PKC is activated (Sugita et al., 1992), but no change is observed in action potential width, amplitude of AHP, or input resistance (DeRiemer et al., 1985).

Decreased levels of PKC have been found in AD tissues (Masliah et al., 1990; Matsushima et al., 1996; Favit et al., 1998; Battaini and Pascale, 2005); specifically, PKCγ activity is decreased in AD patient fibroblasts (Favit et al., 1998). Aβ treatment studies have also found decreased steady state and active PKC levels in comparison to control groups (Chauhan et al., 1991; Favit et al., 1998; Lee et al., 2004). Aβ-induced reduction of PKC phosphorylation is likely due to the pseudo-substrate site on which Aβ can directly bind to the kinase; this direct binding has been seen with Aβ 1-42 using pull-down assays (Lee et al., 2004). Aβ 25-35 also appears to directly bind PKC through the pseudo-substrate site; when the site is mutated, peptide-induced reduction of kinase phosphorylation is no longer observed (Lee et al., 2004). When transgenic Tg2576 mice are treated over a 12 week period with the PKCε and α activator Bryostatin 1, mice which usually exhibit behavioural deficits instead have enhanced learning abilities and memory performance (Hongpaisan et al., 2011). These Bryostatin

1-treated Tg2576 mice also exhibited decreased soluble Aβ 1-42 in hippocampal CA1 pyramidal neurons, and increased dendritic spines and total number of synapses compared to age-matched Tg2576 mice without treatment (Hongpaisan et al., 2011). Similar results were observed when Aβ 25-35 and the PKC agonist phorbal 12-myristate 13-acetate (PMA) were co-applied to cells. When cells would usually exhibit repressed late-LTP (L-LTP) signs with application of Aβ 25-35 alone, addition of the agonist rescued L-LTP signal (Zhang et al., 2009). Interestingly, PKC is thought to directly influence Aβ production in healthy neurons by increasing degradation of Aβ via the endothelin converting enzyme (Choi et al., 2006) and inhibiting the Aβ forming β–secretase (Wang et al., 2009).

Importantly for work in *Lymnaea*, a PKC orthologue exists (Dictus et al., 1998). However, a PKC mammalian antibody has not yet been used successfully in *Lymnaea*. Similar to other studies mentioned previously in this chapter, before any immuno-work could be performed, an appropriate sequence alignment was completed to find a mammalian PKC antibody that may be used in *Lymnaea* (Appendix III.4A). An α, β, γ PKC antibody with perfect sequence alignment to *Lymnaea* was selected and used successfully in western blotting. Only one single band appears in the *Lymnaea* sample and it occurs at the predicted 80 kD weight. However, to be certain that the band in *Lymnaea* is the same as the band found in mammalian animals, samples from both animals were run side-by-side on a gel and western blotted with the PKC antibody (Appendix III.4B). The bands match up exactly at 80 kD, with very strong signal in both. While a pre-absorption study should be conducted in the future for complete certainty, this antibody can be used successfully in *Lymnaea*. Therefore, this antibody was used to measure total α, β, γ PKC in experimental and control groups. Using western blot, it was determined that there was no significant difference between animal groups (Figure 6.9).

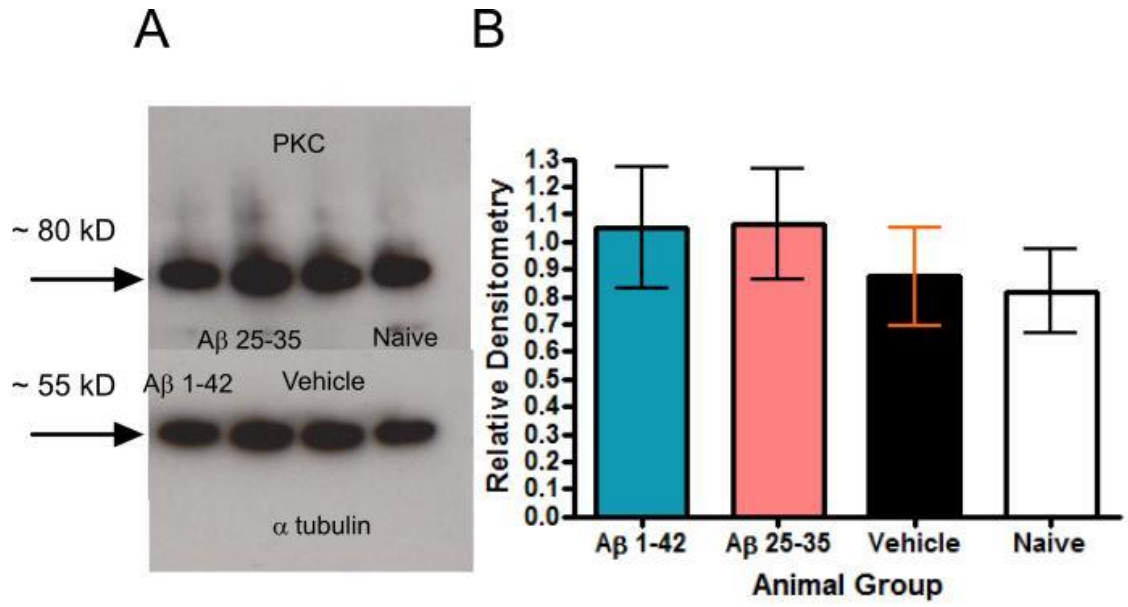

Figure 6.9 Total PKC is not affected by Aβ treatment or training at the 24 hour post-injection, 48 hour post-training time point. (**A**) Representative PKC bands and α tubulin loading control bands. (**B**) Four animal groups (Aβ 1-42 [n=8], Aβ 25-35 [n=8], Vehicle [n=8], Naïve [n=8]) were compared for intensity of PKC labelling using western blot. Data represents PKC band densitometry/ loading control densitometry. Means ± SEM values are shown. One-way ANOVA, p=0.7383. Tukey's tests all p>0.05.

Although there was no change in total PKC levels, it was important to assess whether active PKC was involved in the behavioural time points used throughout this thesis. Thus, the next experiment investigated if PKC inhibition is sufficient to remove LTM when injected 24 hours after training and tested 48 hours after training. Bisindolylmaleimide I (Bis), a PKC inhibitor which acts at the ATP binding site (Toullec et al., 1991), has previously been used successfully in *Lymnaea* (Rosenegger and Lukowiak, 2013) and similar concentrations and incubation time points were used in these behavioural pharmacology studies. PKC inhibition was sufficient to disrupt LTM (Figure 6.10), similar to Aβ 1-42 and 25-35 disrupted LTM. Specifically, this behavioural pharmacology indicates a need for either classical or novel PKC at the 24 hour post-training time point, as Bis inhibits these forms of the kinase, but not the atypical form (Sossin, 2007; Villareal et al., 2009). These experiments also suggest that although total PKC levels do not change with Aβ treatment, active PKC may be affected by Aβ. However, it is also possible that Aβ does not target PKC and the kinase is simply important for memory at this time point. Aβ's effect on active PKC will need to be considered in future research.

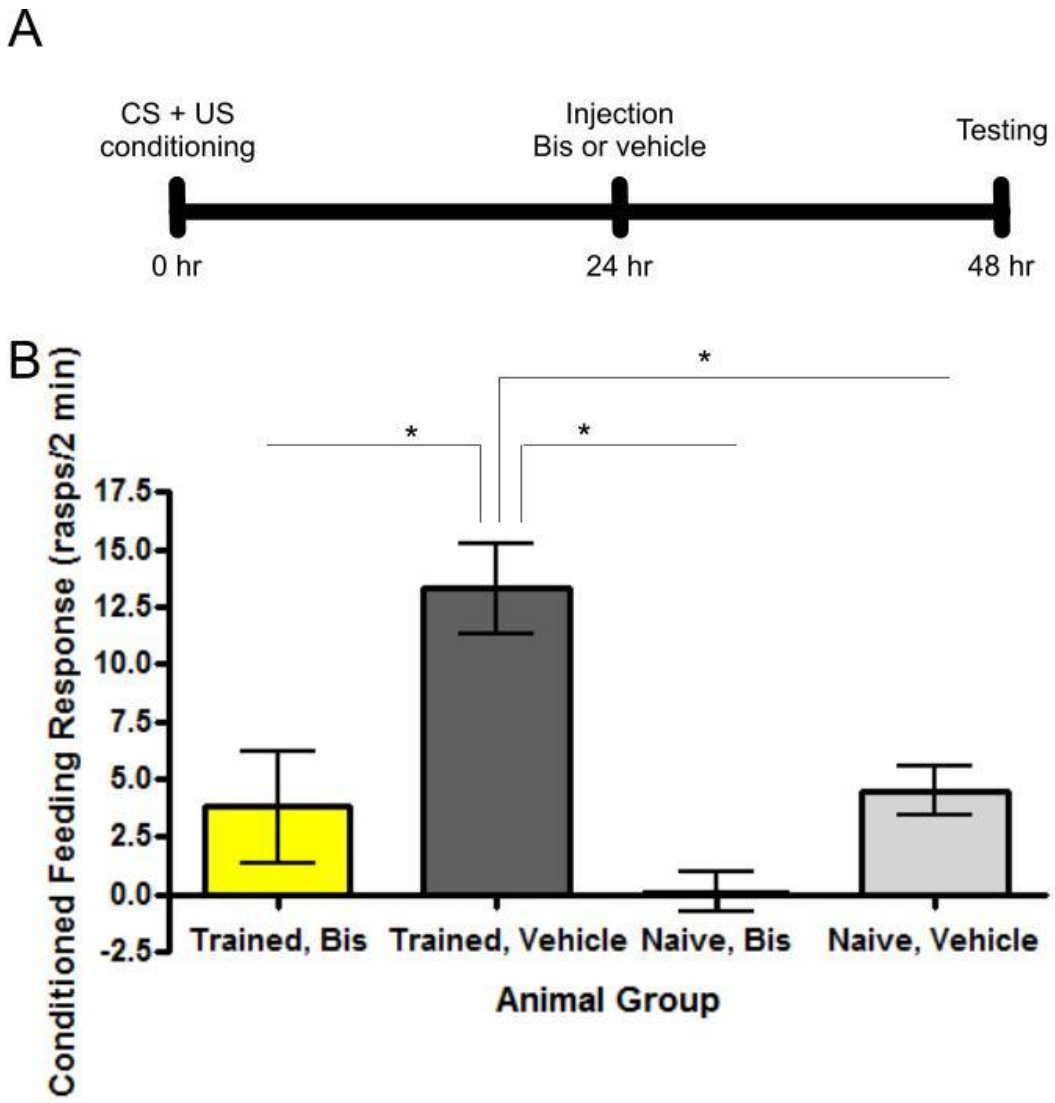

Figure 6.10 PKC inhibition is sufficient to disrupt LTM. (**A**) Timeline of experiment. (**B**) Four starved animal groups (Trained, Bis [n=19]; Trained, Vehicle [n=37]; Naïve, Bis [n=18]; Naïve, Vehicle [n=34]) were tested for rasp rate to amyl acetate, a measure of the feeding response to the CS. Means ± SEM values are shown. Asterisks indicate significantly decreased feeding response from trained, vehicle-injected animals. Kruskal-Wallis, $p<0.0001$. Dunn's Multiple Comparison with $p<0.05$= Trained, Vehicle vs. Naïve, Vehicle; Trained, Vehicle vs. Naïve, Bis; Trained, Vehicle vs. Trained, Bis.

The second kinase investigated was PKA, well-known for directly phosphorylating CREB at Ser133. PKA is composed of two catalytic subunits and two regulatory subunits. Each regulatory subunit contains two cAMP binding sites (Taylor et al., 1990); when cAMP binds these two sites, the catalytic subunits will dissociate (Figure 6.11). Once dissociated, catalytic subunits will translocate to the nucleus to phosphorylate CREB and regulatory subunits will be degraded by ubiquitin-mediated proteolysis. Injection of the catalytic subunits alone is sufficient to elicit STF (Castellucci et al., 1980). PKA is also critical for multiple types of LTM, including: sensitisation, classical conditioning, and operant conditioning (Baxter and Byrne, 2006). PKA is implicated at the time of training and at an intermediate phase of LTP, for maintaining the potentiation past the first 3 hours after training (Abel et al., 1997; Hayashi et al., 2004; Bourtchouladze et al., 1998; Michel et al., 2008). This biphasic profile of PKA activation coincides with CREB phosphorylation at Ser133 (Bernabeu et al., 1997; Roberson et al., 1999). In *Aplysia*, a third wave of PKA activation occurs around 20 hours post-sensitisation (Sutton et al., 2001) and a late phase persistent activation of PKA has been found in other LTF studies as well (Greenberg et al., 1987; Sweatt and Kandel, 1989; Muller and Carew, 1998). Besides its role in LTP, PKA also phosphorylates ion channels when activated by 5-HTRs, leading to increased neuronal intrinsic plasticity (Zhang and Linden, 2009). One of these channels is NMDAR; PKA phosphorylation has been found to both increase the amplitude and increase Ca^{2+}-dependent desensitisation of NMDAR-elicited currents in hippocampal neurons (Skeberdis et al., 2006). PKA application mimics effects of 5-HT and is the responsible component of increased neuronal excitability, spike broadening, neurotransmitter release, and S-K^+ channel closure (Sugita et al., 1992; Baxter and Byrne, 1990; Goldsmith and Abrams, 1992; Siegelbaum et al., 1982).

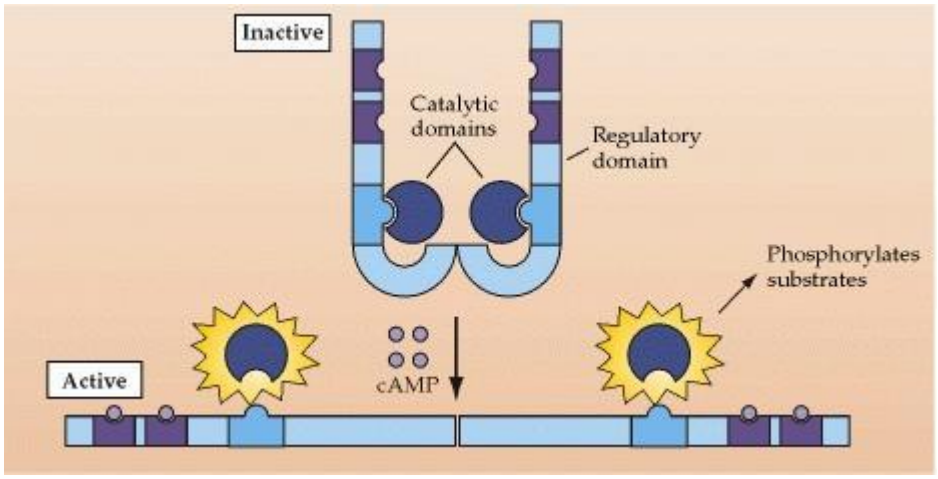

Figure 6.11 Mechanism of activation of PKA. The second messenger, cAMP, will bind twice to each regulatory subunit of PKA. Once bound, the catalytic subunits will dissociate from the regulatory subunits, allowing the catalytic subunits to phosphorylate substrates (reproduced from Purves et al., 2008).

Along with all of the previously noted disruption of cAMP and adenylyl cyclase in AD or Aβ-treated tissues, activation of PKA has been found to prevent Aβ-mediated inhibition of NMDAR-dependent LTP (Vitolo et al., 2002; Wang et al., 2009). This suggests that the PKA pathway, and especially the kinase which activates CREB, is a potential target for Aβ's effect on memory. This cAMP/PKA CREB-signalling occurs similarly in molluscs as in mammals. Much of this molecular cascade work was first discovered in the sea slug *Aplysia* and has been replicated in rodents. Importantly for work in *Lymnaea*, a PKA orthologue exists and a mammalian PKA antibody has been used successfully (Michel et al., 2008). Michel and colleagues also found that injecting a PKA inhibitor into trained animals when pCREB levels are increased will cause pCREB levels to immediately decrease (Michel et al., 2008). These studies suggest a specific link between PKA activity and pCREB levels in *Lymnaea*. The same antibody used by Michel and colleagues was used in the experiments presented in this thesis, to label western blots of experimental and control groups (Figure 6.12), and found no significant difference between any of the samples.

Further PKA studies were conducted to investigate if the inhibition of PKA is sufficient to disrupt LTM at the 24 hour post-injection, 48 hour post-training time point. The PKA inhibitor, H-89, has been used successfully in *Lymnaea* previously (Marra et al., 2013) and similar concentrations and incubation time points were used for the drug. H-89 will competitively inhibit PKA activity with very little inhibition of other kinases (Chijiwa et al., 1990). PKA inhibition neither significantly decreased the conditioned response from trained levels nor increased it from naïve levels (Figure 6.13). These results suggest that PKA is likely involved in memory at this time point, but is not sufficient.

The inconclusive behavioural pharmacology results lead us to further investigate Aβ's effect on active PKA by using an ELISA to measure PKA activity between animal groups (Figure 6.14). All trained groups had significantly decreased active PKA levels at this time point and both Aβ groups had significantly less active PKA than vehicle-injected animals as well.

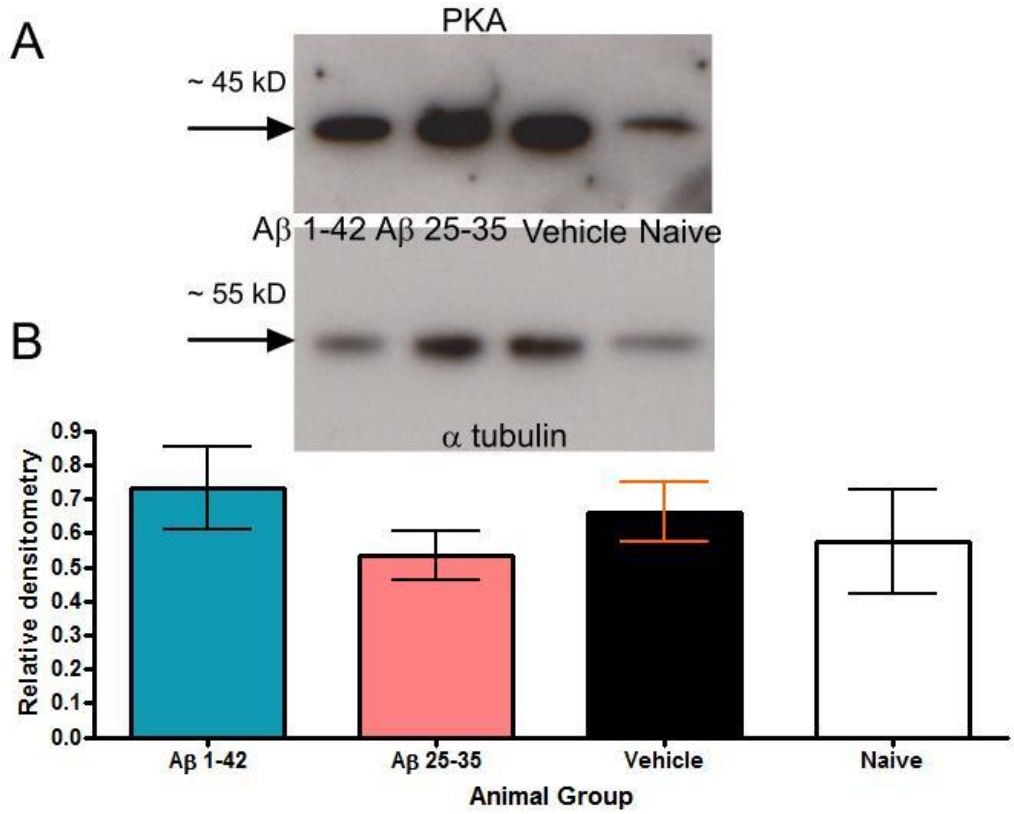

Figure 6.12 Total PKA levels are not affected by Aβ-treatment or training at the 24 hour post-injection, 48 hour post-training time point. (**A**) Representative catalytic PKA bands and α tubulin loading control bands (**B**) Four animal groups (Aβ 1-42 [n=16], Aβ 25-35 [n=15], Vehicle [n=15], Naïve [n=13]) were compared for intensity of total PKA labelling using western blot. Data represents PKA band densitometry/ loading control densitometry. Means ± SEM values are shown. Kruskal-Wallis, p=0.5242. Dunn's Multiple Comparison all p>0.05.

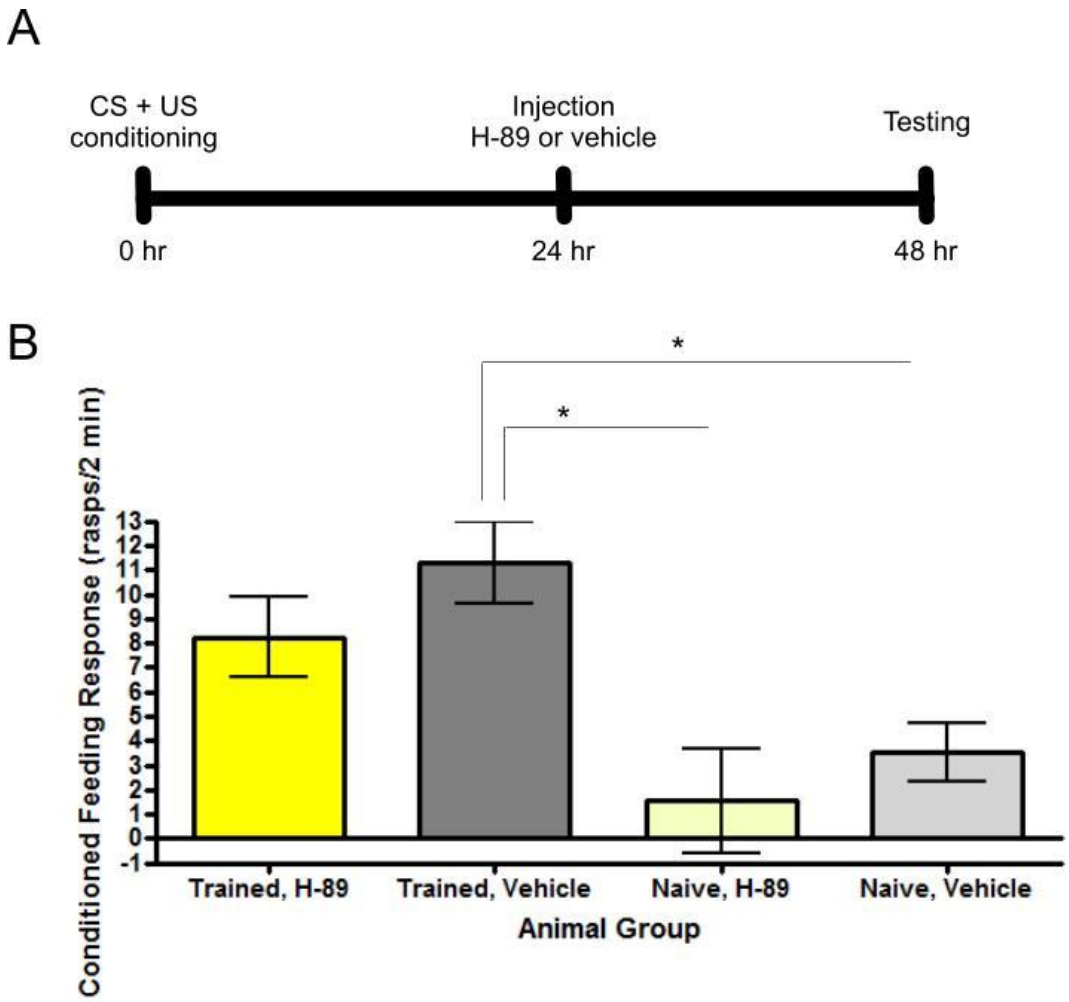

Figure 6.13 PKA inhibition leads to a behavioural response that is neither significantly decreased from trained levels nor significantly increased from naïve levels. (**A**) Timeline of experiment. (**B**) Four starved animal groups (Trained, H-89 [n=32]; Trained, Vehicle [n=33]; Naïve, H-89 [n=13]; Naïve, Vehicle [n=33]) were tested for rasp rate to amyl acetate, a measure of the feeding response to the CS. Means ± SEM values are shown. Asterisks indicate significantly decreased feeding response from trained, vehicle-injected animals. Kruskal-Wallis, p=0.0019. Dunn's Multiple Comparison with $p<0.05$= Trained, Vehicle vs. Naïve, Vehicle; Trained, Vehicle vs. Naïve, H-89.

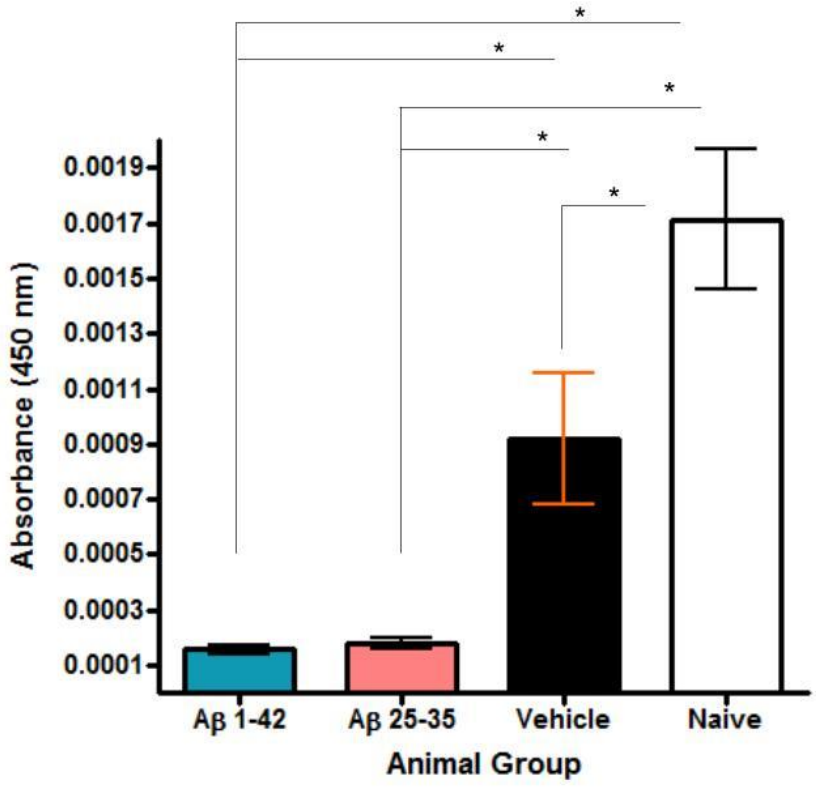

Figure 6.14 Active PKA is significantly decreased in trained animals, and further decreased by Aβ injection. Four animal groups (Aβ 1-42 [n=9]; Aβ 25-35 [n=9]; Vehicle [n=8]; Naïve [n=8]) buccal+cerebral ganglia were subjected to an active PKA sandwich ELISA. Means ± SEM values are shown. Asterisks indicate significantly decreased feeding response from trained, vehicle-injected animals or naïve animals. One-way ANOVA, $p<0.0001$. Tukey's tests with $p<0.05$= Aβ 1-42 vs. Vehicle, Aβ 1-42 vs. Naïve, Aβ 25-35 vs. Vehicle, Aβ 25-35 vs. Naïve, Vehicle vs. Naïve.

The final kinase investigated was ERK1/2. ERK1/2 is a member of the MAPK family, which consists of serine/threonine protein kinases and is involved in multiple signalling cascades, including cell growth and survival (Volmat and Pouyssegur, 2001). ERK has also been implicated in both the early phase and maintenance phase of LTP (Sweatt, 1999). This thesis only considers ERK, which will be further referred to as MAPK unless otherwise noted, as it is the only MAPK currently sequenced in *Lymnaea*. All three ionotropic receptors, as well as some of the metabotropic receptors, are able to modulate MAPK activity (for review, see Wang et al., 2007). Once stimulated, the MAPK cascade involves sequential signalling of four proteins, including small GTPases (such as Ras and Rac), MAPK kinase kinase (such as Raf and MEKK), MAPK kinase (such as MEK), and MAPK. Active pMAPKs, dual phosphorylated at Thr202 and Tyr204, translocate to the nucleus and phosphorylate target transcription factors. Specifically, MAPK indirectly phosphorylates CREB through RSK2 (for review, see Sweatt, 2001) at Ser133 and inhibition of MAPK results in reduced CREB phosphorylation (Mao et al., 2004; Xing et al., 1998). It has also been found that MAPK is responsible for phosphorylating CBP at Ser301, which is critical for activating transcription (Impey et al., 2002), and removes CREB-2, which has two MAPK consensus sites (Gonzalez et al., 1991; Michael et al., 1998).

When synaptic NMDARs are pharmacologically activated in the rodent hippocampus, MAPK phosphorylation is found to increase (Wang et al., 2004b; English and Sweatt, 1996) and applying NMDAR antagonists during classical conditioning will block MAPK phosphorylation (Atkins et al., 1998). This increase in MAPK phosphorylation comes from Ca^{2+} influx through synaptic NMDARs which activates Ca^{2+}-sensitive kinases, such as CaMKII and PKC (Thandi et al., 2002; English and Sweatt, 1996); these Ca^{2+}-sensitive kinases, along with NMDAR-mediated generation of action potential, activate MAPK (Zhao et al., 2005). The synaptic NMDAR-mediated increase in MAPK phosphorylation is found specifically in neurons, not glia, and this increase is rapid and transient (for review, see Wang et al., 2007). AMPARs and mGluRs are believed to positively regulate MAPK phosphorylation as well (Wang et al., 2004c; Choe and Wang, 2001) and this allows MAPK to activate other signalling cascades, like the protein-synthesising mTOR pathway (for review, see Giovannini et al., 2015), which will not be further considered in this thesis. Receptors can inhibit MAPK activity as well, as seen with extrasynaptic NMDARs (Ivanov et al., 2006).

The cAMP-PKA pathway is a well-known activator of the MAPK cascade (Impey et al., 1998a; Yao et al., 1998; Ambrosini et al., 2000; Vossler et al., 1997); even in *Aplysia*, MAPK and PKA appear to translocate to the nucleus together to

activate CREB and remove CREB-2 (for review, see Bailey et al., 2004). The adenylyl cyclase activator forskolin has also been shown to increase MAPK phosphorylation and nuclear translocation (Martin et al., 1997), suggesting cross-talk between the two pathways. MAPK's phosphorylation of CREB at Ser133 thus makes it an important component of LTP and LTM (Thomas and Huganir, 2004; English and Sweatt, 1996; Ribeiro et al., 2005; Atkins et al., 1998; Selcher et al., 1999; Schafe et al., 2000). MAPK activation is thought to have two phases after training; one rapid and transient, where phosphorylation at Thr42 significantly increases at one hour and two hours after conditioning (Atkins et al., 1998) and a second that is delayed and persistent, which has been found to last at least 24 hours in rodent CA3 (Trifilieff et al., 2007; Trifilieff et al., 2006). MAPK is also believed to be involved at later memory storage time points (Eckel-Mahan et al., 2008) as well as having a known role in increasing neuronal intrinsic plasticity by phosphorylating ion channels when an appropriate signal is received by 5-HTRs (Zhang and Linden, 2003). MAPK's phosphorylation of VDCCs attenuates the voltage-dependency of the channels and helps the cell more easily reach a depolarised state (Roberson et al., 1999).

Through α7-nAChRs, ERK2 has been shown to be activated by Aβ treatment (Wang et al., 2003a; Schliebs and Arendt, 2011). In Aβ 25-35 injected animals, ERK protein level expression increased compared to uninjected animals (Ghasemi et al., 2014). Increased phosphorylation of ERK protein has also been found in $APP_{swe,ind}$ mice, AD, and Down's Syndrome post-mortem brains (Echeverria et al., 2004); however, other studies indicate that pERK is decreased in Tg2576 mice (Ma et al., 2007).

Importantly for work in *Lymnaea*, a MAPK orthologue exists (Ribeiro et al., 2005) and there has been additional characterisation of *Lymnaea* MAPK. The MAPK inhibitor U0126 does not affect LTM when injected 24 hours after conditioning and tested either 30 minutes after injection or 24 hours after injection in *Lymnaea* (Ribeiro et al., 2005). Although there was no memory loss by inhibition of MAPK at the time points investigated in this thesis, it was important to test whether Aβ affects MAPK in *Lymnaea*. The antibody previously found to appropriately label MAPK in *Lymnaea* was used (Ribeiro et al., 2005) to label western blots of the experimental and control groups (Figure 6.15A-B), and no significant difference was found between any of the samples. This agrees with a previous study looking at steady state MAPK levels in *Lymnaea* after conditioning (Ribeiro et al., 2005) and in tau over-expressing transgenic mouse hippocampus (Echeverria et al., 2004). However, considering the previous two kinases investigated in this chapter, it seems that the activated kinase is most important at this

testing time point and may be a target for Aβ. A dual phosphorylated Thr202/Tyr204 MAPK antibody has been successfully used in *Lymnaea* as well (Ribeiro et al., 2005), and this same antibody was used to measure activated MAPK levels (Figure 6.15C-D). No significant difference in any of the experimental or control groups was observed.

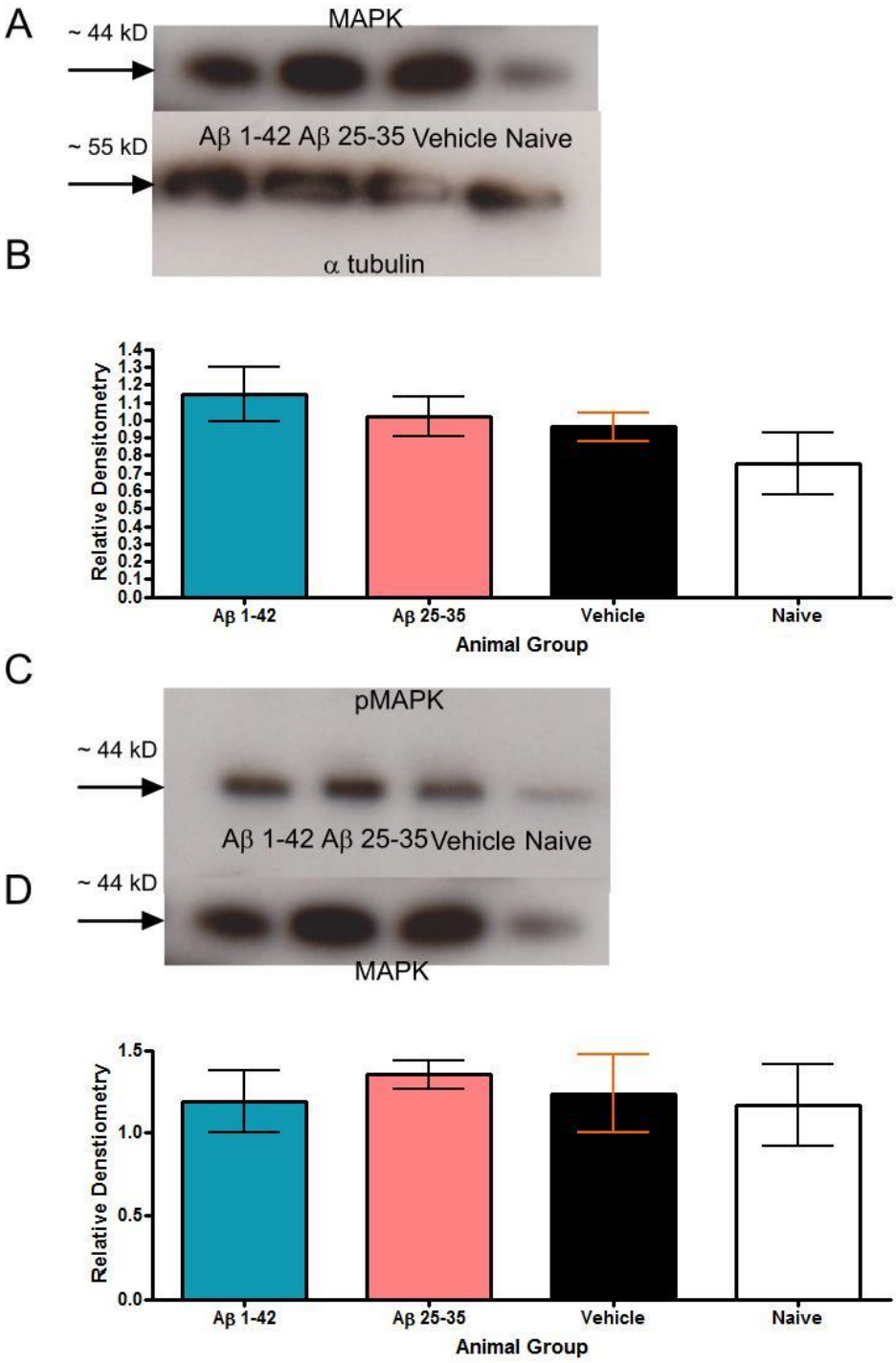

Figure 6.15 MAPK and dual pMAPK levels do not change with either Aβ treatment or training at the observed time point. (**A**) Representative bands of total MAPK and α tubulin loading control (**B**) Four animal groups (Aβ 1-42 [n=9], Aβ 25-35 [n=8], Vehicle [n=10], Naïve [n=8]) were compared for intensity of total MAPK labelling using western blot. Data represents MAPK band densitometry/ loading control densitometry. Means ± SEM values are shown. Kruskal-Wallis, p=0.1868. Dunn's Multiple Comparison all p>0.05. (**C**) Representative bands of dual pMAPK and total MAPK (**D**) Four animal groups (Aβ 1-42 [n=9], Aβ 25-35 [n=7], Vehicle [n=9], Naïve [n=7]) were compared for intensity of dual pMAPK labelling using western blot. Data represents dual pMAPK band densitometry/ total MAPK band densitometry. Means ± SEM values are shown. Kruskal-Wallis, p=0.6488. Dunn's Multiple Comparison all p>0.05.

6.4 Discussion

The background literature considered, Aβ's effect on consolidated memory is very difficult to unravel. There are synaptic and nonsynaptic components, many cases of correlation but very little of causation, and a large number of proteins that appear to be influenced by the peptide, many of which have not been considered in this thesis. Of course, many molecular signalling cascades overlap and influence other pathways, as well as play a role in both synaptic and nonsynaptic plasticity, making the task even trickier. However, *Lymnaea* may offer two unique perspectives in clarifying Aβ's effect on consolidated memory and, perhaps, offering fresh ideas for therapeutic targets. Firstly, many proteins possibly influenced by Aβ treatment were examined here and these experiments were run using very tightly controlled procedures. Very few labs have looked at such an extensive list of proteins under the same experimental design (e.g. Vitolo et al., 2002). Secondly, *Lymnaea* offers a unique approach to understanding synaptic vs. nonsynaptic plasticity by measuring intrinsic neuronal properties of the key modulatory neuron, the CGC. As CGC depolarisation is sufficient to induce conditioned behavioural responses (I. Kemenes et al., 2006), it is an excellent model for studying nonsynaptic plasticity. Synaptic components have also been identified within the feeding and memory circuitry, offering points of synaptic measurement within the engram as well (for review, see Kemenes, 2013).

The experiments described in this results chapter verify the usefulness of *Lymnaea* as a model system for screening Aβ targets. Both Aβ 1-42 and Aβ 25-35 were shown to lead to decreased phosphorylation of nuclear CREB at Ser133 and Aβ 25-35 caused decreased steady state levels of nuclear CREB as well. This all occurs in animals that exhibit memory deficits, have no neuronal death, and have decreased postsynaptic scaffolding proteins, at a time point which is not dependent upon protein synthesis. In order to tackle the question of "How does Aβ influence behaviour specifically by decreasing pCREB?" upstream elements of CREB signalling pathways were considered. Experimentation began at the receptor level, measuring changes in total receptor proteins as well as measuring changes in phosphorylation at key sites and inhibiting receptor function at the 24 hour time point. Total GluA1 and nAChR do not change after training or Aβ treatment, the phospho-sites Ser831 and Ser845 on GluA1 do not change after training or Aβ treatment, and NMDAR possibly plays a role in memory recall but its inhibition is not sufficient to fully disrupt memory. Much of the work at the receptor level still needs confirmation in order to draw a final conclusion. Firstly, it is believed that receptors at synaptic or perisynaptic sites are changing based

on both Aβ treatment and training. Measuring total levels of receptors or subunits will likely mask any of these changes taking place, so a fractionation technique combined with protein quantification is needed. Secondly, localisation of these receptors is key to their function, especially for nAChRs and NMDARs. It will be important to visualise any change in receptor localisation on dendritic spines between Aβ-treated and untreated groups. Finally, an NMDAR1 antibody needs to be successfully optimised for use in *Lymnaea stagnalis* to fully determine any changes occurring from Aβ treatment. Only after these experiments are successful will it be possible to study Aβ-induced deregulation of receptors and the correlative links to pCREB change and behavioural modification.

Next, second messenger levels in the buccal+cerebral ganglia were considered and found that cAMP levels do not change after Aβ treatment or training. A total measurement of adenylyl cyclase was not possible due to antigen inaccuracies between the mammalian antibody and this molluscan model, but an appropriate antibody will need to be optimised for use in *Lymnaea* to consider Aβ's effect on second messengers of the cAMP/PKA pathway. As adenylyl cyclase is suggested to have an important role in memory maintenance (Wong et al., 1999; Shan et al. 2008; Wieczorek et al. 2010), it would be interesting to see if blocking adenylyl cyclase function at the 24 hour injection time point would result in a memory deficit at the 48 hour testing time point. If so, an adenylyl cyclase activator could be injected alongside the Aβ peptides and an observation could be made as to whether these animals express healthy behaviour 24 hours post-injection. This behavioural pharmacological approach may help uncover the role of second messengers in Aβ-induced memory loss, which so far remains elusive.

Finally, three key kinases involved in CREB-signalling and memory were considered. No change was found in total kinase levels after training or Aβ treatment, but active sites differed and inhibitors of some of these kinases disrupted memory in a similar manner as Aβ treatment. First PKC was considered and found to be necessary for proper behavioural response at these time points, but exhibited no significant change in the steady state α, β, γ PKC isoforms after training or Aβ treatment. Unfortunately, an active PKC experiment has not yet been completed due to lack of time. This experiment is crucial to determine if Aβ is affecting PKC; only when this experiment is completed can investigations be continued into Aβ-induced change in PKC as a direct link to memory dysfunction. What must also be considered for future experiments are the isoforms being affected or measured in *Lymnaea*. PKMζ is the

suggested isoform necessary and sufficient for memory maintenance (Jerusalinsky et al., 1994; Shema et al., 2007; Serrano et al., 2008), but so far only α, β, γ isoforms have been measured using western blot and Bis, an inhibitor for novel and classic isoforms, has been injected into the animal. None of the studies so far have considered PKMζ or atypical PKC. However, there may be overlap between the mammalian antibody and PKMζ signal in *Lymnaea*, and it is very likely that the Bis inhibitor is affecting atypical PKC as well. Inhibitor studies are done in mammals, but PKMζ is created in *Aplysia* and *Lymnaea* in a very different manner than in mammals (Michel et al., 2012), so it cannot be assumed that this atypical *Lymnaea* PKC is safe from Bis inhibition based on mammalian pharmacological studies alone. More experiments into PKMζ may help to reveal Aβ-induced dysfunction of these pathways.

The second kinase considered in this results chapter was PKA and it was found that, similar to NMDAR inhibition, inhibiting PKA caused a decrease in behavioural response, but no significant effect on memory. This suggests that perhaps PKA plays a role in memory at this time point, but it is certainly not sufficient. Investigations were continued to include active PKA and found that all trained groups expressed decreased active PKA in comparison to naïve animals, and that both Aβ treated groups had significantly less active PKA than vehicle-injected groups. Interestingly, the active PKA levels are similar to those seen in pCREB. And similarly to pCREB Ser133, the vehicle-injected animals do not have significantly increased active PKA levels compared to naïve animals. Therefore, it is likely that the low PKA activity in Aβ-treated group is leading to low phosphorylation of CREB in these animals. The active PKA results also bring up other interesting points. cAMP is known to activate PKA and a decrease in activated PKA in the Aβ treated samples was observed, but no decrease in cAMP was seen. This suggests that perhaps the kinase is being degraded, abolishing active signal of the catalytic subunit since there is enough second messenger in the neurons to activate this kinase. However, there was no change in total catalytic PKA. In fact, there was no change in steady state measurements of any protein measured in this chapter, suggesting that there is not an aberrant increase in proteasomal degradation of these proteins. Instead, perhaps the target is not catalytic PKA, but is regulatory PKA. Only catalytic PKA was measured, and not the regulatory subunits which should detach and be degraded after animals are trained. It would be very interesting to measure regulatory PKA levels in Aβ treated animals using western blot to determine if 1) the PKA subunits are detaching appropriately and 2) if the proteasome pathway is appropriately degrading detached regulatory subunits. Another very interesting avenue to consider is measuring cAMP-bound proteins using western blot; quantifying bound

cAMP to regulatory PKA compared to bound cAMP to regulatory/catalytic PKA will show if cAMP is still capable of binding the regulatory subunit and if the regulatory subunit is capable of detaching from the catalytic subunit. Taken together with the regulatory PKA western blot measurements, these experiments will give further insight into the deregulation of active PKA in Aβ treated animals.

The last kinase considered in this results chapter was ERK1/2. No change was found in steady state levels between Aβ treated, trained, or naïve levels, or any change in dual phosphorylation sites Thr202/Tyr204. These experiments are a clear indication that, in the experimental timeline used in this thesis, Aβ does not affect ERK1/2 protein level or function and is one of the proteins considered in this thesis that does not need further experimental work. Further experiments are needed to completely link Aβ-induced CREB pathway deregulation to the observed behavioural deficits in a causative, as opposed to correlative, way.

7. General Discussion

The experiments presented in this thesis study the effects of Aβ 25-35 and Aβ 1-42 on *Lymnaea* LTM, with particular emphasis on peptide structure and change in molecular signalling cascades. To begin, a behavioural timeline was established. Animals were starved, trained, injected with Aβ 25-35 or Aβ 1-42 24 hours after training, and tested 24 hours after injection. This time line and the food-reward classical-conditioning paradigm were used to prepare animals and brain samples used in experiments mentioned throughout this entire thesis, to maintain consistency. Importantly, 0.1 mM Aβ 25-35 and 1 μM Aβ 1-42 disrupts LTM recall when applied to this combination of time line and paradigm (Figure 7.1A). No cell death was found in the buccal and cerebral ganglia in these animals, but the postsynaptic terminal protein marker, PSD-95, levels were significantly decreased in the Aβ-treated groups. Since LTM recall was inhibited by both Aβ 25-35 and Aβ 1-42, memory acquisition and consolidation were also considered. Neither of these stages of memory formation were compromised after 24 hour *in vivo* Aβ incubation (Figure 7.1B-C). However, when Aβ peptides were injected before training, allowed to incubate 48 hours, and then tested, animals exhibited decreased behavioural conditioned response rates (Figure 7.1D). These experiments together brought to light the importance of the duration of the incubation with the Aβ peptides relative to memory phases. In *Lymnaea*, LTM is fully consolidated by 24 hours post-training and conditioned responses can be maintained for up to 14 days post-training (Alexander et al., 1984), so the difference in the effects of Aβ injection before training on 24 hour vs. 48 hour memory is not due to testing different forms of memory at these two differing time points. Instead, the difference observed here is likely due to the amount of time that Aβ is allowed to incubate *in vivo*. As a test for neuronal death after 48 hours of incubation was not performed, it cannot be ruled out that death had occurred by this later post-injection time point in the feeding and memory network. Although it is shown that Aβ does not affect the acquisition of 24 hour memory, it is possible that if the peptide is allowed to incubate long enough to disrupt the network, then appropriate memory retrieval is not possible. However, the most parsimonious explanation for the deleterious effects of both Aβ peptides on memory at 48 hours is that at 24 hours post-training and post-injection there are still sufficient amounts of oligomeric Aβ available to interfere with the consolidated memory trace, as was also indicated by measurements of oligomeric Aβ levels in the haemolymph (Figure 4.4).

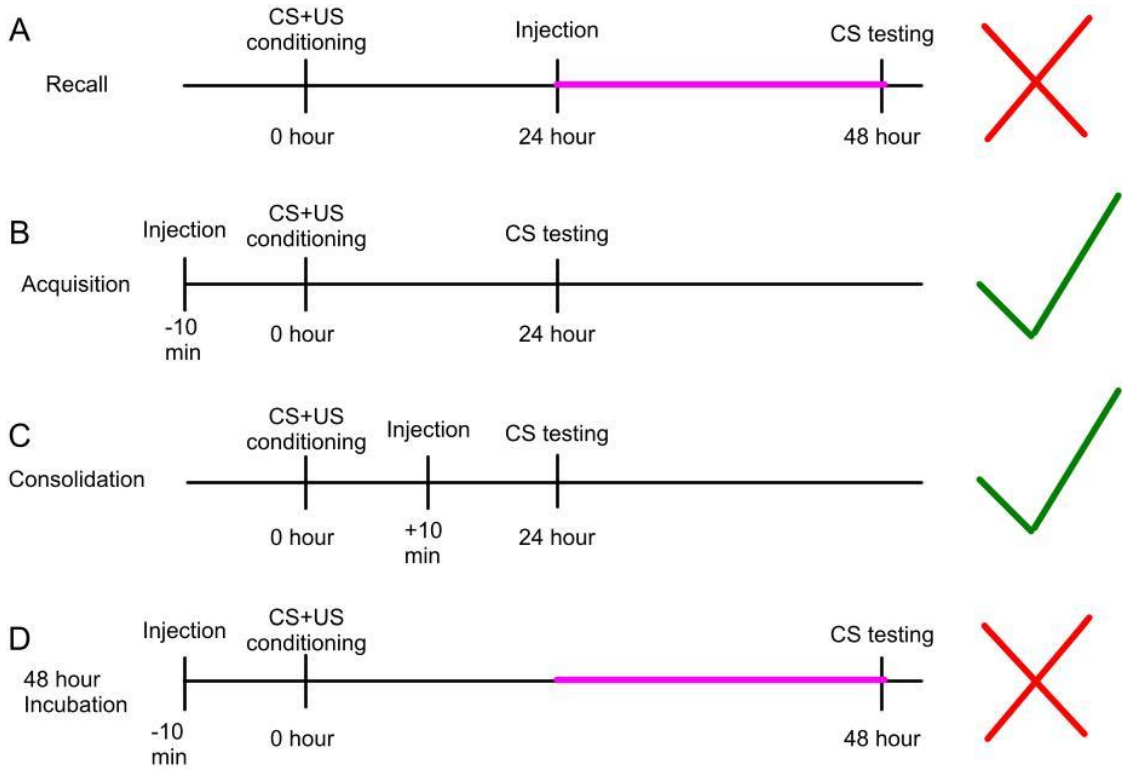

Figure 7.1 Behavioural memory timelines. (**A**) 24 hour *in vivo* incubation, memory recall time point. Memory is inhibited. (**B**) 24 hour *in vivo* incubation, memory acquisition time point. Memory functions correctly. (**C**) 24 hour *in vivo* incubation, memory consolidation time point. Memory functions correctly. (**D**) 48 hour *in vivo* incubation, memory acquisition time point. Memory is inhibited. The red "x" indicates experiments where memory is inhibited. The green "check" indicates experiments where memory functions correctly. The pink line indicates the 24-48 hour post-conditioning time point that may be vulnerable to Aβ treatment.

After establishing Aβ-induced behavioural memory disruption, experimental focus shifted to the differences between Aβ 25-35 and Aβ 1-42 to determine why 100-fold more Aβ 25-35 is necessary to induce the same behavioural deficits as those observed with Aβ 1-42. These investigations used peptide-tagging, conformational epitope antibodies, and TEM-observed morphology to compare structural differences between the two peptides. First, peptide localisation was observed on a ganglionic and ultrastructural level, showing ganglia penetration by the peptide and peptide localisation in the nucleus, mitochondria, and dense core granules. Once ganglia penetration was confirmed, the structural state of both Aβ peptides was investigated. In Aβ extracts from the haemolymph, significantly more Aβ 1-42 oligomeric species were detected compared to Aβ 25-35 and both Aβ-treated extracts had more oligomeric species than the vehicle-treated group. In brain extracts, both Aβ 1-42 and Aβ 25-35 treated groups exhibited bands at the molecular weight of Aβ tetramers whereas vehicle-treated and naïve groups exhibited no bands. To complement immuno-labelling of oligomers in haemolymph extracts and brain samples, Aβ morphology was also monitored *in vitro* using negative stain TEM. Aβ 1-42 was found to assemble from an oligomeric, to protofibrillar, and finally into fibrils over a 24 hour period while Aβ 25-35 assembled from small crystalline structures into larger, aggregated crystalline structures. These experiments indicated that Aβ 1-42 and Aβ 25-35 are not interchangeable peptides since they appear to differ in their assembly process and eventual aggregated morphologies. To confirm, Aβ 25-35 was prepared in the same manner as Aβ 1-42 and injected at Aβ 1-42 concentrations. Oligomeric Aβ 25-35 did not disrupt LTM recall and structurally, Aβ extracts from haemolymph had virtually no oligomeric species after 24 hours of incubation. This oligomerically prepared Aβ 25-35 also assembled *in vitro* differently than Aβ 25-35 or Aβ 1-42, by exhibiting a small amount of oligomers immediately after preparation and eventually fibrillising by 24 hours. These experiments together confirm that Aβ 1-42 and Aβ 25-35 cannot be treated as the same peptide, do not act in the same manner, and thus cannot be used interchangeably. The comparison of different preparations of Aβ 25-35 also places an importance upon peptide preparation and the starting structural state of the peptide. Aβ treated with HFIP and further processing to remain in an oligomeric form will initially exhibit oligomeric structure immediately after preparation and will be fibrillar by 24 hours, as seen with both Aβ 1-42 and Aβ 25-35. However, when Aβ 25-35 is simply solubilised in buffer it takes on a crystalline structure immediately after preparation and this structure elongates and aggregates by 24 hours. This is very important, as only

certain Aβ structures are considered neurotoxic (for review, see Wilcox et al., 2011). Perhaps most excitingly, these experiments suggest that consistent levels of Aβ oligomeric species from 24-48 hours post-training are necessary for the observed behavioural deficits to occur. Aβ 1-42 and Aβ 25-35 exhibit morphological intermediate species immediately after preparation and high levels of oligomeric Aβ can be extracted from the animals' haemolymph after 24 hour incubation; treatment with either peptide results in memory dysfunction. However, oligomerically prepared Aβ 25-35 exhibits small quantities of oligomers immediately after preparation, but no oligomers exist in the haemolymph after 24 hour incubation; animals treated with this peptide exhibit a trend for increased behavioural response. Finally, the tetrameric species appear to be the dominant oligomer in both the Aβ 1-42 and Aβ 25-35 treated samples after 24 hours *in vivo*; this was observed both when Aβ-treated samples are run on a western blot and labelled with an Aβ oligomer-detecting primary antibody and also when Aβ-extracted haemolymph samples from Aβ 25-35 treated animals were run on an SDS-PAGE and silver stained for protein content. While dimers and dodecamers are the current focus for identifying toxic Aβ oligomers (Lesne et al., 2006; Shankar et al., 2008), many authors suggest that several soluble Aβ species ranging from 10 to 100 kD are toxic (McLean et al., 1999; Hepler et al., 2006). The tetramer falls within this molecular weight. In fact, structural studies on Aβ suggest that the Aβ 1-42 dimer is suited to form an open tetramer structure, which is believed to be crucial for the formation of hexamer paranuclei which will then stack to form dodecamers (Bernstein et al., 2010). Aβ 1-40, the much less toxic Aβ peptide, forms dimers which give rise to a closed tetramer structure, which does not allow the same paranuclei formation (Bernstein et al., 2010). Seemingly. this tetrameric Aβ structure and the presence of oligomers over the 24-48 hour post-training time line are the only similarities between Aβ 1-42 and Aβ 25-35, which both cause behavioural disruption. Therefore, it is possible that the tetramer observed in this thesis is the toxic Aβ structure that is disrupting memory.

The study of how Aβ affects LTM in *Lymnaea* continued with experiments focusing on molecular signalling cascades leading to learning-induced protein synthesis. A general approach was taken first, viewing change in general protein synthesis after Aβ injection or training. No gross increase or decrease in protein concentration between groups was observed. Protein synthesis was more specifically tested, using anisomycin and behavioural pharmacology with S^{35}-methionine labelling; both experiments confirmed that there is no change in protein synthesis at the 48 hour

testing time point in either Aβ-treated or trained animals. The experiments then became much more specific, focusing on the transcription factor CREB and its signalling cascades. In chromatin-extracted brain tissues, only the Aβ 25-35 treated group showed significantly decreased levels of total CREB protein compared to all other animal groups. pCREB Ser133 levels were then measured using the same chromatin-extracted samples; all trained groups expressed significantly decreased pCREB levels, with both Aβ-treated groups expressing significantly less pCREB Ser133 than vehicle-injected groups, and Aβ 1-42 had even less signal than Aβ 25-35. Experiments then focused on what up-stream elements of CREB signalling may be causing the pCREB changes. Many elements expressed no significant increase or decrease from either training or Aβ-injection; however, some proteins were identified as points of interest (see Table 7.1). NMDARs were considered, using behavioural pharmacology instead of western blotting. MK-801 was injected instead of Aβ into trained animals, causing the animals to display a decreased trend for memory, but no significant difference between either trained animals or untrained animals. PKA was also considered. While there was no change in steady state catalytic PKA, behavioural pharmacology experiments using H-89 suggest that PKA may be important in the time points used, although is not sufficient for memory recall. ELISA experiments also suggest that activated PKA levels are significantly decreased in all trained groups, and are significantly decreased in Aβ–treated groups in comparison to vehicle-treated groups. Finally, while PKC α, β, γ steady state levels did not change from training or Aβ treatment, when Bis was injected in place of Aβ the animals were unable to express a behavioural response. This suggests that PKC is necessary at the memory time points considered in this thesis, making PKC a potential Aβ target.

Protein	**Trained, Aβ 1-42 injected**	**Trained, Aβ 25-35 injected**
GluA1	No change	No change
pGluA1 Ser831	No change	No change
pGluA1 Ser845	No change	No change
α7-nAChR	No change	No change
cAMP	No change	No change
PKA	No change	No change
pPKA	Decreased	Decreased
MAPK	No change	No change
pMAPK	No change	No change
PKC	No change	No change
CREB	No change	Decreased
pCREB Ser133	Decreased, Aβ 1-42< Aβ 25-35	Decreased

Table 7.1 Summary of steady state and phosphorylation changes in CREB-signalling pathways. List of proteins studied in this thesis with their corresponding increased, decreased, or no change levels from trained and vehicle-injected animals. Animal groups compared to trained and vehicle-injected animals included in columns: trained, Aβ 1-42 injected and trained, Aβ 25-35 injected.

Collaborative experiments with Dr. Michael Crossley, which were not detailed in this thesis but are detailed in Ford et al. (2015), also provide insight into how Aβ may be producing its effect on LTM. Using a two electrode current-clamp-based electrophysiological method, we found that CGCs in preparations from Aβ 1-42-injected animals had similar intrinsic properties as CGCs in preparations from vehicle-injected animals. However, CGCs in preparations from Aβ 25-35-treated animals displayed a repolarised membrane potential and a decreased membrane resistance compared to trained and vehicle-treated controls. Interestingly, the Aβ 25-35-induced changes only occurred in animals that had been trained prior to injection. Animals injected without conditioning showed no Aβ-induced change (Ford et al., 2015). This idea of a "training-induced vulnerability" of neurons to Aβ is not novel; other labs have used different techniques to arrive at a similar conclusion (e.g. Deshpande et al., 2009). For example, Deshpande and colleagues noted that the affinity of Aβ oligomers to bind synaptic markers will increase after neuronal activation (Deshpande et al., 2009). The electrophysiology studies presented here again discriminate Aβ 1-42 and Aβ 25-35, suggesting that Aβ 25-35 has an added nonsynaptic effect on neurons which Aβ 1-42 does not. This is important considering the integral role of nonsynaptic plasticity in learning and memory (for review, see Disterhof and Oh, 2006; Zhang and Linden, 2003), specifically in *Lymnaea* (for review, see Kemenes, 2013). However, the electrophysiological results of the Aβ 25-35 treated animals is not congruent with the nonsynaptic plasticity changes observed throughout the literature in AD models. For example, the critical changes found in 5xFAD mice indicate decreased neuronal excitability and increased mean AHP peak (Kaczorowski et al., 2011), which were not affected in Aβ 25-35 treated *Lymnaea*. Of course, transgenic mice are exposed to Aβ much longer than the *Lymnaea* used in these studies, but current literature on intrinsic effects of Aβ all suggest that excitability is disrupted (Kaczorowski et al., 2011; Minkeviciene et al., 2009; Driver et al., 2007; Kerrigan et al., 2014). Instead of a directly nonsynaptic disruption, the neuronal property changes measured in *Lymnaea* after 24 hours of Aβ 25-35 *in vivo* incubation is possibly a result of the decreased CREB and pCREB Ser133 found in these animals. CREB is known to play an important role in nonsynaptic plasticity, by helping to generate action potentials and to regulate membrane resistance, intrinsic excitability (Jancic et al., 2009; Dong et al., 2006), firing frequency, and resting membrane potential (Han et al., 2006). Importantly, a change in membrane potential and membrane resistance have been found in Aβ 25-35 injected *Lymnaea*, properties directly influenced by CREB, but the typical nonsynaptic plasticity changes observed in other AD models are not found in Aβ 25-35 treated *Lymnaea*.

Since both CREB and pCREB Ser133 are decreased after Aβ 25-35 treatment, the link to intrinsic neuronal property changes observed in these animals, but not observed in Aβ 1-42 which only display decreased pCREB Ser133, is most plausible. These experiments further suggest that Aβ 25-35 is acting in a neurotoxic manner, but differently from how Aβ 1-42 peptides act. Therefore, it must be reiterated that synthetically produced Aβ 25-35 is not an appropriate substitute for Aβ 1-42.

The results thus far help develop hypotheses concerning Aβ's effect on LTM. These combined experiments indicate three major disruptions that could directly impair LTM in *Lymnaea* (Figure 7.2). First, the decrease in PSD-95 suggests degeneration of the synapses which would remove memory traces via structural abnormalities. Second, pCREB Ser133 is necessary for memory recall (for review, see Alberini, 2009) and is shown to be significantly decreased in Aβ-treated animals compared to vehicle-treated animals (Yamamoto-Sasaki et al., 1999; Dineley et al., 2001; Tong et al., 2004), suggesting that low pCREB levels may be an important factor disrupting memory recall via biochemical abnormalities. Finally, work done in collaboration with Dr. Michael Crossley showed a repolarisation of CGC membrane potential and decrease of CGC membrane resistance in Aβ 25-35 treated animals (Ford et al., 2015). This change in CGC membrane potential is known to be sufficient to inhibit memory function in *Lymnaea* (I. Kemenes et al., 2006) and so would be sufficient to disrupt memory recall via nonsynaptic cell properties. The structural and nonsynaptic properties have not been further investigated; however, it is interesting to consider the case of synaptic degeneration. As previously mentioned, it appears that Aβ oligomers must be present during the 24-48 hour post-training time line to cause behavioural deficits. This 24-48 hour post-training time line was also observed in the behavioural studies, where peptides allowed to incubate 0-24 hours post-training had no effect on behavioural responses but peptides allowed to incubate 0-48 and 24-48 hours post-training did cause memory deficits. As *Lymnaea* memory is known to be resistant to amnesic agents by the 24 hour injection time point, it can be assumed that memory is consolidated and is being maintained and stored between 24-48 hours post-training (for reviews, see Kemenes, 2013; Alberini, 2009). Storage and maintenance are heavily dependent on synaptic rearrangement, growth, and alterations within the dendritic tree (for review, see Alberini, 2009); avoidance conditioning studies suggest that this increase in synaptic remodelling lasts from 6 hours to 72 hours post-training before returning to basal levels (O'Malley et al., 1998). Thus, it is fully possible that the 24-48 hour post-training time point of Aβ vulnerability contains either memory lapses similar to those found at earlier time points in *Lymnaea* (Marra et al., 2013) or that Aβ

is only able to have an effect on memory during time points dependent on dendritic/ synaptic growth and restructuring (Freir et al., 2011). This exciting hypothesis is further supported by the finding that PSD-95 levels are decreased in both Aβ-treated groups compared to vehicle-treated groups, and is increased in vehicle-treated groups compared to naïve groups. This training-induced increase in PSD-95 from naïve levels is the only protein found to be increased at the time points used in this thesis, making it a very exciting target for future research.

While only hypotheses can made about the structural and nonsynaptic influence of Aβ on *Lymnaea* LTM, biochemical abnormalities have been extensively considered in this thesis (Figure 7.2). These experiments suggest that Aβ's effect on pCREB Ser133 may be one molecular disruption leading to the observed deficits in LTM recall. However, vehicle-injected animals and naïve animals had similar pCREB levels after recall, suggesting that pCREB is likely necessary for memory at this time point, but not sufficient. It also suggests that there is likely a pCREB baseline level necessary for appropriate CREB activity and that Aβ-injected groups are below this baseline, which would ultimately lead to disrupted memory. The experiments of this thesis also suggest that Aβ's effect on pCREB levels is likely indirect, altering upstream signalling elements. One component directly upstream of CREB is PKA. Importantly, active PKA levels between experimental groups mimic levels observed in pCREB in the same groups. Behavioural pharmacology experiments also suggest that PKA may be involved in memory at this time point, but is not sufficient. This coincides with the active PKA and pCREB findings in vehicle-injected and naïve animals. Specifically, vehicle-injected groups do not have increased active PKA or pCREB, suggesting that neither component of the cascade is sufficient for the observed LTM deficits, but that there may be a baseline level of active PKA and pCREB needed for healthy function which the Aβ-treated groups do not meet.

The NMDAR behavioural pharmacology results suggest that these receptors may be the direct Aβ target and upstream component of PKA, as both NMDAR inhibition and PKA inhibition express a similar decreased trend in behavioural response. The importance of NMDARs in Aβ-treated animals and AD is overwhelming in the literature (De Felice et al., 2007; Sze et al., 2001; Mishizen-Eberz et al., 2004; Brouillette et al., 2012; Almeida et al., 2005; Roselli et al., 2005; Snyder et al., 2005; Lacor et al., 2007; Lacor et al., 2004; Renner et al., 2010; Roenicke et al., 2011). NMDAR's involvement in recall is undecided; some labs have shown importance of NMDARs for recall at least two hours after reactivation (Przybyslawski and Sara, 1997)

while others claim NMDARs are not necessary for recall (Szapiro et al., 2000; Steele and Morris, 1999). This bolsters the claims of NMDAR's importance suggested in this thesis. Aβ direct targeting of NMDAR causing downstream disruption of phosphorylated CREB has also been suggested elsewhere (Snyder et al., 2005). Another very important component of these cascades is PKC. The behavioural pharmacology results suggest that PKC may be a target of Aβ, considering that PKC is necessary for LTM recall at these time points, and both Aβ 1-42 and 25-35 have been shown to directly bind to PKC (Lee et al., 2004), making PKC a possible direct target of Aβ. Investigation into active PKC is a very exciting avenue for future research. Both PKA and PKC provide interesting insight into what may be occurring in the neurons after Aβ treatment.

The active PKA link to the Aβ-induced pCREB disruption observed in this thesis gives rise to speculation about how Aβ disrupts LTM recall. The upstream receptors of PKA in *Lymnaea* are GPCRs (for review, see Kemenes, 2013) (Figure 7.2), which have not been considered in this thesis. When these receptors are activated then adenylyl cyclase will be activated, increasing cAMP in the cell and thus allowing catalytic PKA to detach from its regulatory subunits. Since active PKA is decreased in Aβ treated animals, this suggests that these GPCRs may be direct targets of Aβ. However, the parallel behavioural pharmacology studies of NMDARs and PKA suggest that the Aβ-induced NMDAR disruption, which is known to exist (De Felice et al., 2007; Sze et al., 2001; Mishizen-Eberz et al., 2004; Brouillette et al., 2012; Almeida et al., 2005; Roselli et al., 2005; Snyder et al., 2005; Lacor et al., 2007; Lacor et al., 2004; Renner et al., 2010; Roenicke et al., 2011), could directly influence PKA activity. This second possibility would arise from the known Aβ-induced aberrant increase in intracellular Ca^{2+} through multiple receptors, such as NMDAR; Ca^{2+} was not directly measured in this thesis, so it is assumed that the experimental groups have increased intracellular Ca^{2+} (Figure 7.2). An increased influx of Ca^{2+} could deregulate adenylyl cyclase, which can act as a Ca^{2+}-sensor, leading to a change in downstream targets such as PKA (Figure 7.2). This aberrant Ca^{2+} influx also explains potential effects on PKC, which also acts as a Ca^{2+}-sensor (Figure 7.2). Of course, this speculation assumes that changes at the receptor level alter ion influx, which alters PKA and PKC activation, inhibiting the kinases' ability to phosphorylate CREB at Ser133 (Figure 7.2). However, alteration of PKA and PKC will change much more than CREB's phosphorylation state. The two kinases also play important roles in nonsynaptic plasticity. Many K^+ and Ca^{2+} channels are post-translationally modified by PKA and some Ca^{2+} channels are known

to be modified by PKC (for review, see Levitan, 1985). CREB also plays an important role in nonsynaptic plasticity, as mentioned previously.

These initial experiments introduce *Lymnaea stagnalis* to the Aβ field. With this animal model, Aβ-induced memory disruption can be examined on a behavioural, network, cellular, and molecular level; these experiments can often be done in the same animal and often *in vivo*. Biophysical tools can also be used in *Lymnaea* for studying Aβ peptide structural changes. This level of specificity and tight control over experimental design can and should be used to help further develop the Aβ field. Besides introducing a new invertebrate model to Aβ research, this thesis also disproves the interchangeable use of synthetically prepared Aβ 25-35 in place of Aβ 1-42 and has built exciting ground-work for future CREB-signalling cascade studies.

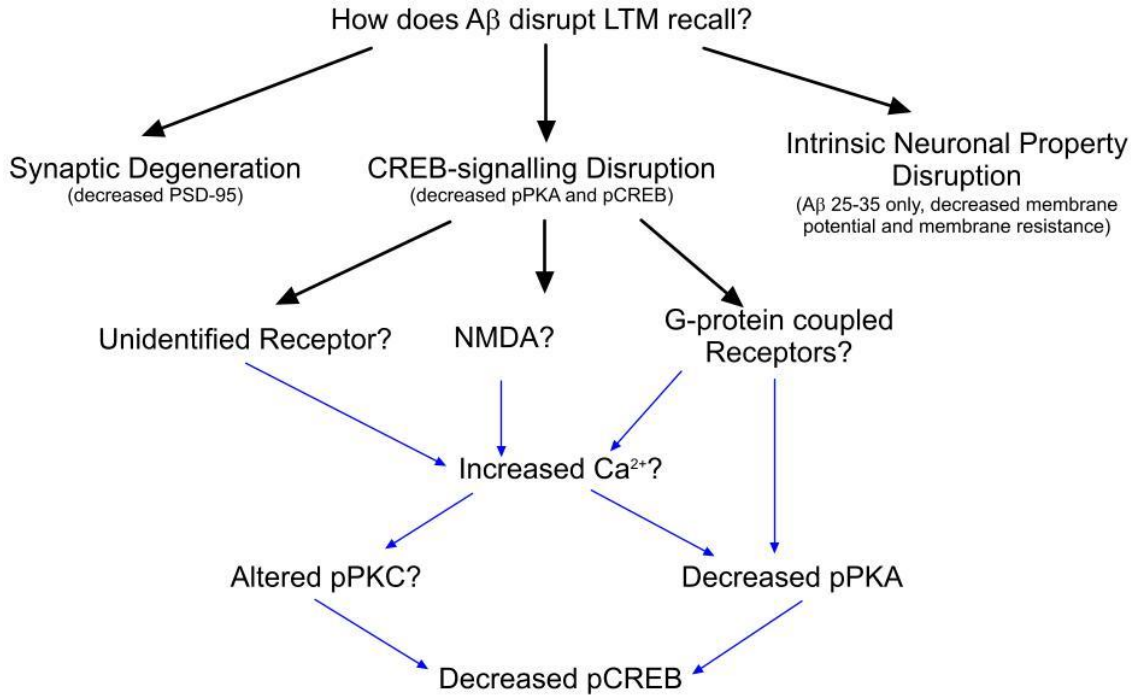

Figure 7.2 Schematic of results found in this thesis. The dominant question of this thesis can possibly be answered by three important results- synaptic degeneration, CREB-signalling disruption, and intrinsic neuronal property disruption. CREB-signalling may further be disrupted directly at the receptor level, which alters downstream components and eventually decreasing pCREB levels. "?" indicate suggested Aβ-induced alterations. Blue, thin arrows indicate suggested signalling pathways.

7.1 Future experiments

There are many additional studies that could take forward the experiments detailed in this thesis. First, understanding the interactions between Aβ and CREB molecular signalling pathways will require further analysis. For example, NMDAR subunit NR1, adenylyl cyclase, and active PKC should be quantified. An appropriate NR1 antibody will need to be optimised for use in *Lymnaea*, as will an appropriate adenylyl cyclase antibody. This investigation into adenylyl cyclase has high potential to prove fruitful, as adenylyl cyclase is suggested to have an important role in memory maintenance (Wong et al., 1999; Shan et al. 2008; Wieczorek et al. 2010). To determine if adenylyl cyclase optimisation is worthwhile, it would be interesting to see if blocking adenylyl cyclase function at the 24 hour injection time point would result in a memory deficit at the 48 hour testing time point. If so, it would then be interesting to inject an adenylyl cyclase activator, such as forskolin, alongside the Aβ peptides and observe if these animals express healthy behaviour. These experiments will further narrow the potential targets of Aβ involved in CREB signalling. From the results displayed in this thesis, some very exciting and unique experiments will bolster the findings and further the understanding of how Aβ disrupts CREB-signalling proteins.

Interestingly, this thesis suggests that the decreased active PKA and pCREB observed in both Aβ-treated groups may link the two cascade components. This hypothesis requires testing. Behavioural pharmacology would prove the hypothesis; animals would be trained, injected, and tested under the same protocol as has been used throughout this entire thesis. Importantly, a PKA activator, such as forskolin (Ribeiro et al., 2003) or PACAP (Pirger et al., 2010), would be injected alongside the Aβ. If PKA is a target of Aβ, then the Aβ-treated animals would exhibit behavioural responses at similar levels as those measured in vehicle-treated animals. Assuming this experiment would be successful, another interesting PKA experiment would benefit these studies. This thesis has shown that the catalytic subunit of PKA does not change and thus the amount of protein capable of phosphorylation is the same across experimental groups. Therefore, for Aβ to cause a decrease in active PKA, something must be disrupted in the normal PKA process. Normally, cAMP will bind to the regulatory subunits, causing them to detach from the catalytic subunits, exposing PKA phosphorylation sites. Does Aβ inhibit regulatory subunit detachment, cAMP binding, or regulatory subunit degradation? Simple western blotting can answer each question. A cAMP antibody has already been used successfully in this thesis and should be used in a western blot of all experimental animal groups. The signal on these western blots

will indicate cAMP-bound proteins; specifically, bands for cAMP-bound regulatory PKA and cAMP-bound regulatory/catalytic PKA will indicate cAMP binding (regulatory PKA levels) and subunit detachment disruptions in Aβ-treated animals (regulatory/catalytic PKA levels). The next western blotting experiment would be more difficult; a regulatory PKA antibody, for a subunit which has not been sequenced in *Lymnaea*, could be used to label a western blot to indicate levels of regulatory PKA in all experimental groups to determine if regulatory subunits are properly being degraded in Aβ-treated and trained animals. Regulatory subunit degradation is crucial for conditioning (for review, see Hedge and DiAntonio, 2002) and an increase in rolipram, a cAMP enhancer, or an increase in Uch hydrolase, known to target regulatory PKA for degradation (for review, see Hedge and DiAntonio, 2002), will alleviate LTP and behavioural deficits in APP transgenic mice (Shirwany et al., 2007). Thus, inhibited degradation of regulatory PKA could inhibit catalytic PKA activation while allowing the steady state catalytic PKA levels to remain unchanged.

The first experiment to further PKC investigation will have to be quantification of its activation. If PKC activation is disrupted by Aβ, then there are a few very interesting experiments which can continue the investigation of Aβ's effect on PKC. Importantly, PKMζ, an atypical isoform of PKC involved in memory maintenance (Jerusalinsky et al., 1994; Shema et al., 2007; Serrano et al., 2008), should be tested. First, a behavioural pharmacology test using the PKMζ inhibitor chelerythrine in place of Aβ should be conducted to determine if PKMζ is important at the time points used in this thesis. The use of chelerythrine to block PKMζ has already been used successfully in *Lymnaea* (Marra et al., 2013). A western blot of PKMζ levels should also be quantified, to determine if Aβ alters levels of this potentially important kinase.

Another very important study concerns all of the receptors examined in this thesis. No change in total receptor level or in specific phosphorylation states was found. However, total receptor quantification will likely mask any differences occurring at synaptic or perisynaptic locations. For synaptic studies, the sample will need to undergo a synaptic fractionation and then run on a western blot for proper quantification. Perhaps an even better method, considering that perisynaptic or presynaptic sites are important for many of the receptors considered, would be immunohistochemical quantification. Co-labelling would be used; the antibody for the receptor in question and an appropriate control label to verify dendritic localisation should be paired and any areas of co-labelling can be quantified and compared across experimental groups. NMDARs are of particular interest, considering their potential

influence on memory as indicated by previously mentioned behavioural pharmacology studies and the background literature indicating direct Aβ binding and disruption of NMDARs (De Felice et al., 2007; Sze et al., 2001; Mishizen-Eberz et al., 2004; Brouillette et al., 2012; Almeida et al., 2005; Roselli et al., 2005; Snyder et al., 2005; Lacor et al., 2007; Lacor et al., 2004; Renner et al., 2010; Roenicke et al., 2011). Both NR1 and NR2B subunits should be considered, NR1 in the synaptic area and NR2B in the perisynaptic area of postsynapses. However, a decent NR1 antibody will need to be found for use in *Lymnaea* and an NR2B antibody will need more work for finding an appropriate use in *Lymnaea*, as NR2B has not yet been sequenced in this animal model. α7-nAChRs are similar for their importance in Aβ-related studies and are importantly located in extrasynaptic areas of the postsynapse and on the presynapse. The antibodies used in this thesis, although sufficient for western blotting, will need to be further optimised for immunohistochemistry. The GluA1 antibodies used in this thesis have already been used successfully in immunohistochemistry experiments using *Lymnaea* (Naskar et al., 2014).

The suggested future experiments thus far have only considered CREB-signalling pathways examined in this thesis. However, there are many other proteins believed to be involved in Aβ-induced memory disruption. There are more direct targets of Aβ, including but not limited to: NR2B, PrP receptors, insulin receptors, and mGluR5 (De Felice et al., 2007; Lauren et al., 2009; Renner et al., 2010; Shankar et al., 2008; Lacor et al., 2007). There are also many more indirect targets of Aβ, including but not limited to: PP1, PP2A, calcineurin, p38 MAPK, Wnt, and glycogen synthase kinase 3 (GSK-3) (Knobloch et al., 2007; Snyder et al., 2005; Chen et al., 2002; Shankar et al., 2007; Wang et al., 2004c; Anderton et al., 2000; Ma, 2014). However, studies of these additional proteins are limited in *Lymnaea* as the animal has not been fully sequenced and many of these proteins have not been identified. The lab of Ildiko Kemenes is currently developing *Lymnaea* for use as a genetic model (Ildiko Kemenes, personal communication), which when completed, may allow for further investigations into the above mentioned proteins. Luckily, Aβ studies using *Lymnaea* do not have to stop while the model is being further developed. There are three more important and well-documented *Lymnaea* proteins/ pathways that can and should be considered for how Aβ disrupts LTM recall: CaMKII, PACAP and its receptors, and the NO/cGMP pathway. CaMKII is an essential kinase for LTM formation and maintenance in *Lymnaea*, as well as mammals (Wan et al., 2010; Frankland et al., 2001), and has been studied in *Lymnaea* using western blotting, immunohistochemistry, and behavioural pharmacology (Wan et al., 2010; Naskar et al., 2014). CaMKII is directly implicated in

the synaptic loss observed in Aβ treatment and AD (for review, see Ly and Song, 2011), possibly through its acting as a Ca^{2+} sensor. Another option is the PACAP receptor, which is upstream of PKA and is known to detect the conditioned stimulus after single-trial food-reward classical-conditioning (Pirger et al., 2010). Importantly, addition of PACAP successfully reversed age-related memory loss in *Lymnaea* (Pirger et al., 2014). Its connection to PKA and use in memory deficit reversal suggests it may be an interesting avenue to pursue. Finally, the NO/cGMP pathway should be considered in investigating how Aβ disrupts LTM recall. NO is important for memory consolidation in *Lymnaea*, producing downstream effects that specifically influence the CGC (Ribeiro et al., 2008; Korneev et al., 2005; Nikitin et al., 2008) and has been implicated in causing increased neurotoxicity in Aβ 25-35 treated rats (Limon et al., 2009).

These future experiments may help unlock important therapeutic targets for Aβ-induced disruption of memory in AD. It is highly believed, in the learning and memory field, that the invertebrate model is a fantastic representation of the more complex mammalian model. Therefore, this model should be used to research Aβ-induced memory deficits and well as other memory-related diseases. The simplicity of the model may offer an important tool in finding disease targets, which can then be further developed in a more complex mammalian model. However, the initial investigation into what specifically is being targeted, and not what is just an unimportant downstream effect, is difficult to dissociate. *Lymnaea* can help with that dissociation. This humble snail may provide therapeutic insight, by demanding a narrowed and precise approach to be taken by the field.

References

Abel, T., Nguyen, P. V., Barad, M., Deuel, T. A. S. & Kandel, E. R. Genetic demonstration of a role for PKA in the late phase of LTP and in hippocampus-based long-term memory. *Cell* **88**, 615-626 (1997).

Abraham, W. C. & Williams, J. M. Properties and mechanisms of LTP maintenance. *Neuroscientist* **9**, 463-474, (2003).

Aizenman, E., Hartnett, K. A. & Reynolds, I. J. Oxygen free-radicals regulated NMDA receptor function via a redox modulatory site. *Neuron* **5**, 841-846 (1990).

Alberdi, E. *et al.* Amyloid beta oligomers induce Ca2+ dysregulation and neuronal death through activation of ionotropic glutamate receptors. *Cell Calcium* **47**, 264-272 (2010).

Alberini, C. M. Transcription Factors in Long-Term Memory and Synaptic Plasticity. *Physiological Reviews* **89**, 121-145 (2009).

Alberini, C. M. The role of reconsolidation and the dynamic process of long-term memory formation and storage. *Frontiers in Behavioral Neuroscience* **5**, (2011).

Alberini, C. M. & LeDoux, J. E. Memory reconsolidation. *Current Biology* **23**, R746-R750 (2013).

Alberts, B. *et al.* Molecular biology of the cell. Fifth edition. *Molecular biology of the cell. Fifth edition.*, 1-1392 (2008).

Alexander, J., Audesirk, T. E. & Audesirk, G. J. One-Trial Reward Learning In The Snail Lymnaea-Stagnalis. *Journal of Neurobiology* **15**, 67-72, (1984).

Alkon, D. L. *et al.* C-kinase activation prolongs Ca2+-dependent inactivation of K+-currents. *Biochemical and Biophysical Research Communications* **134**, 1245-1253 (1986).

Alkondon, M., Pereira, E. F. R. & Albuquerque, E. X. alpha-Bungarotoxin- and methyllycaconitine-sensitive nicotinic receptors mediate fast synaptic

transmission in interneurons of rat hippocampal slices. *Brain Research* **810**, 257-263 (1998).

Alkondon, M. & Albuquerque, E. X. Subtype-specific inhibition of nicotinic acetylcholine receptors by choline: A regulatory pathway. *Journal of Pharmacology and Experimental Therapeutics* **318**, 268-275 (2006).

Allinson, T. M. J., Parkin, E. T., Turner, A. J. & Hooper, N. M. ADAMs family members as amyloid precursor protein alpha-secretases. *Journal of Neuroscience Research* **74**, 342-352, (2003).

Almeida, C. G. *et al.* Beta-amyloid accumulation in APP mutant neurons reduces PSD-95 and GluR1 in synapses. *Neurobiology of Disease* **20**, 187-198 (2005).

Alzheimers, A. 2012 Alzheimer's disease facts and figures. *Alzheimers & Dementia* **8**, 131-168, (2012).

Ambrosini, A. *et al.* cAMP cascade leads to Ras activation in cortical neurons. *Molecular Brain Research* **75**, 54-60 (2000).

Anagnostaras, S. G., Maren, S. & Fanselow, M. S. Temporally graded retrograde amnesia of contextual fear after hippocampal damage in rats: Within-subjects examination. *Journal of Neuroscience* **19**, 1106-1114 (1999).

Anderton, B. H., Dayanandan, R., Killick, R. & Lovestone, S. Does dysregulation of the Notch and wingless/Wnt pathways underlie the pathogenesis of Alzheimer's disease? *Molecular Medicine Today* **6**, 54-59, (2000).

Andrew, R.J & Savage, H. Appetitive learning using visual conditioned stimuli in the pond snail, Lymnaea. *Neurobiology of Learning and Memory* **3**, 258-273 (2000).

Antonov, I., Antonova, I., Kandel, E. R. & Hawkins, R. D. Activity-dependent presynaptic facilitation and Hebbian LTP are both required and interact during classical conditioning in Aplysia. *Neuron* **37**, 135-147 (2003).

Anwyl, R. Protein kinase-C and long-term potentiation in the hippocampus. *Trends in Pharmacological Sciences* **10**, 236-239 (1989).

Arendash, G. W. *et al.* Progressive, age-related behavioral impairments in transgenic mice carrying both mutant amyloid precursor protein and presenilin-1 transgenes. *Brain Research* **891**, 42-53, (2001).

Armstrong, D. M., Ikonomovic, M. D., Sheffield, R. & Wenthold, R. J. AMPA-selective glutamate-receptor subtype immunoreactivity in the entorhinal cortex of nondemented elderly and patients with Alzheimers-disease. *Brain Research* **639**, 207-216 (1994).

Atkins, C. M., Selcher, J. C., Petraitis, J. J., Trzaskos, J. M. & Sweatt, J. D. The MAPK cascade is required for mammalian associative learning. *Nature Neuroscience* **1**, 602-609 (1998).

Atwood, C. S., Martins, R. N., Smith, M. A. & Perry, G. Senile plaque composition and posttranslational modification of amyloid-beta peptide and associated proteins. *Peptides* **23**, 1343-1350, (2002).

Bacskai, B. J. *et al.* Spatially resolved dynamics of camp and protein kinase a subunits in aplysia sensory neurons. *Science* **260**, 222-226, (1993).

Bailey, C. H. & Chen, M. Long-term-memory in Aplysia modulated the total number of varicosities of single identified sensory neurons. *Proceedings of the National Academy of Sciences of the United States of America* **85**, 2373-2377, (1988).

Bailey, C. H., Kandel, E. R. & Si, K. S. The persistence of long-term memory: A molecular approach to self-sustaining changes in learning-induced synaptic growth. *Neuron* **44**, 49-57 (2004).

Balschun, D. *et al.* Does cAMP response element-binding protein have a pivotal role in hippocampal synaptic plasticity and hippocampus-dependent memory? *Journal of Neuroscience* **23**, 6304-6314 (2003).

Bao, J. X., Kandel, E. R. & Hawkins, R. D. Involvement of presynaptic and postsynaptic mechanisms in a cellular analog of classical conditioning at Aplysia sensory-motor neuron synapses in isolated cell culture. *Journal of Neuroscience* **18**, 458-466 (1998).

Barco, A., Alarcon, J. M. & Kandel, E. R. Expression of constitutively active CREB protein facilitates the late phase of long-term potentiation by enhancing synaptic capture. *Cell* **108**, 689-703 (2002).

Barnes, P. & Good, M. Impaired Pavlovian cued fear conditioning in Tg2576 mice expressing a human mutant amyloid precursor protein gene. *Behavioural Brain Research* **157**, 107-117, (2005).

Barria, A., Derkach, V. & Soderling, T. Identification of the Ca2+/calmodulin-dependent protein kinase II regulatory phosphorylation site in the alpha-amino-3-hydroxyl-5-methyl-4-isoxazole-propionate-type glutamate receptor. *Journal of Biological Chemistry* **272**, 32727-32730 (1997).

Bartsch, D. *et al.* Aplysia CREB2 represses long-term facilitation- relief of repression converts transient facilitation into long-term functional and structural-change. *Cell* **83**, 979-992 (1995).

Barzilai, A., Kennedy, T. E., Sweatt, J. D. & Kandel, E. R. 5-HT modulates protein-synthesis and the expression of specific proteins during long-term facilitation in Aplysia sensory neurons. *Neuron* **2**, 1577-1586, (1989).

Battaini, F. & Pascale, A. Protein kinase C signal transduction regulation in physiological and pathological aging. *Reversal of Aging: Resetting the Pineal Clock* **1057**, 177-192 (2005).

Baumketner, A. *et al.* Amyloid beta-protein monomer structure: A computational and experimental study. *Protein Science* **15**, 420-428, (2006).

Baxter, D. A. & Byrne, J. H. Differential-effects of cAMP and serotonin on membrane current, action-potential duration, and excitability in somata of pleural sensory neurons in Aplysia. *Journal of Neurophysiology* **64**, 978-990 (1990).

Baxter, D. A. & Byrne, J. H. Feeding behavior of Aplysia: A model system for comparing cellular mechanisms of classical and operant conditioning. *Learning & Memory* **13**, 669-680 (2006).

Bellen, H. J., Gregory, B. K., Olsson, C. L. & Kiger, J. A. 2 Drosophila learning mutants, dunce and rutabaga, provide evidence of a maternal role for cAMP on embryogenesis. *Developmental Biology* **121**, 432-444, (1987).

Benilova, I., Karran, E. & De Strooper, B. The toxic A beta oligomer and Alzheimer's disease: an emperor in need of clothes. *Nature Neuroscience* **15**, 349-357 (2012).

Benjamin, P. R. & Rose, R. M. Central generation of bursting in the feeding system of the snail, Lymnaea-stagnalis. *Journal of Experimental Biology* **80**, 93-118 (1979).

Benjamin, P.R., & Winlow, W. The distribution of three wide-acting synaptic inputs to identified neurons in the isolated brain of Lymnaea. Comparative *Biochemial Physiology* **70**, 293-307 (1981).

Benjamin, P.R. & Kemenes, G. Lymnaea. *Current Biology* **1**, R9-11 (2009).

Benjamin, P.R. & Kemenes, G. Lymnaea learning and memory. *Scholarpedia* **5**, 4247 (2010).

Benjamin, P. R. Distributed network organization underlying feeding behavior in the mollusk Lymnaea. *Neural systems & circuits* **2**, 4-4, (2012).

Benke, T. A., Luthi, A., Isaac, J. T. R. & Collingridge, G. L. Modulation of AMPA receptor unitary conductance by synaptic activity. *Nature* **393**, 793-797 (1998).

Bernabeu, R. *et al.* Involvement of hippocampal cAMP/cAMP-dependent protein kinase signaling pathways in a late memory consolidation phase of aversively motivated learning in rats. *Proceedings of the National Academy of Sciences of the United States of America* **94**, 7041-7046 (1997).

Bernstein, S. L. *et al.* Amyloid-beta protein oligomerization and the importance of tetramers and dodecamers in the aetiology of Alzheimer's disease. *Nature Chemistry* **1**, 326-331, (2009).

Berry, R. W. Calcium and protein-kinase-C inhibit biosynthesis of Aplysia egg-laying hormone. *Molecular Brain Research* **1**, 185-187 (1986).

Bitan, G., Lomakin, A. & Teplow, D. B. Amyloid beta-protein oligomerization - Prenucleation interactions revealed by photo-induced cross-linking of unmodified proteins. *Journal of Biological Chemistry* **276**, 35176-35184, (2001).

Bitan, G., Fradinger, E. A., Spring, S. M. & Teplow, D. B. Neurotoxic protein oligomers - what you see is not always what you get. *Amyloid-Journal of Protein Folding Disorders* **12**, 88-95 (2005).

Bito, H., Deisseroth, K. & Tsien, R. W. CREB phosphorylation and dephosphorylation: A Ca2(+)- and stimulus duration-dependent switch for hippocampal gene expression. *Cell* **87**, 1203-1214 (1996).

Bittinger, M.A, et al.. Activation of cAMP response element-mediated gene expression by regulated nuclear transport of TORC proteins. *Current Biology* **14**, 2156-2161 (2004).

Bliss, T. V. P. & Collingridge, G. L. A Synaptic model of memory- long-term potentiation in the hippocampus. *Nature* **361**, 31-39 (1993).

Blum, S., Moore, A. N., Adams, F. & Dash, P. K. A mitogen-activated protein kinase cascade in the CA1/CA2 subfield of the dorsal hippocampus is essential for long-term spatial memory. *Journal of Neuroscience* **19**, 3535-3544 (1999).

Boehm, J. *et al.* Synaptic incorporation of AMPA receptors during LTP is controlled by a PKC phosphorylation site on GluR1. *Neuron* **51**, 213-225 (2006).

Borlikova, G. G. *et al.* Alzheimer brain-derived amyloid beta-protein impairs synaptic remodeling and memory consolidation. *Neurobiology of Aging* **34**, 1315-1327, (2013).

Bosch, M. & Hayashi, Y. Structural plasticity of dendritic spines. *Current Opinion in Neurobiology* **22**, 383-388, (2012).

Bougie, J. K. *et al.* The atypical protein kinase C in Aplysia can form a protein kinase M by cleavage. *Journal of Neurochemistry* **109**, 1129-1143 (2009).

Boulianne, G. L. *et al.* Cloning and characterization of the Drosophila presenilin homologue. *Neuroreport* **8**, 1025-1029, (1997).

Bourtchuladze, R. *et al.* Deficient long-term-memory in mice with a targeted mutation of the cAMP-responsive element-binding protein. *Cell* **79**, 59-68 (1994).

Bourtchouladze, R. *et al.* Different training procedures recruit either one or two critical periods for contextual memory consolidation, each of which requires protein synthesis and PKA. *Learning & Memory* **5**, 365-374 (1998).

Braak, H. & Braak, E. Neuropathological staging of Alzheimer-related changes. *Acta Neuropathologica* **82**, 239-259 (1991).

Brierley, M. J., Yeoman, M. S. & Benjamin, P. R. Glutamate is the transmitter for N2v retraction phase interneurons of the Lymnaea feeding system. *Journal of Neurophysiology* **78**, 3408-3414 (1997).

Brindle, P., Nakajima, T. & Montminy, M. Multiple protein-kinase A-regulated events are required for transcriptional induction by cAMP. *Proceedings of the National Academy of Sciences of the United States of America* **92**, 10521-10525 (1995).

Brink, J. J., Davis, R. E. & Agranoff, B. W. Effects of puromycin acetoxycycloheximide and actinomycin D on protein synthesis in goldfish brain. *Journal of Neurochemistry* **13**, 889(1966).

Brooks, C. L. & Nilsson, L. Promotion of helix formation in peptides dissolved in alcohol and water-alcohol mixtures. *Journal of the American Chemical Society* **115**, 11034-11035 (1993).

Brouillette, J. *et al.* Neurotoxicity and Memory Deficits Induced by Soluble Low-Molecular-Weight Amyloid-beta(1-42) Oligomers Are Revealed In Vivo by Using a Novel Animal Model. *Journal of Neuroscience* **32**, 7852-7861, (2012).

Brown, G. P. *et al.* Long-term potentiation induced by theta frequency stimulation is regulated by a protein phosphatase-1-operated gate. *Journal of Neuroscience* **20**, 7880-7887 (2000).

Brunelli, M., Castellucci, V. & Kandel, E. R. Synaptic facilitation and behavioral sensitization in Aplysia- possible role of serotonin and cyclic-AMP. *Science* **194**, 1178-1181, (1976).

Buccafusco, J. J., Letchworth, S. R., Bencherif, M. & Lippiello, P. M. Long-lasting cognitive improvement with nicotinic receptor agonists: mechanisms of pharmacokinetic-pharmacodynamic discordance. *Trends in Pharmacological Sciences* **26**, 352-360 (2005).

Burrell, B. D. & Sahley, C. L. Learning in simple systems. *Current Opinion in Neurobiology* **11**, 757-764, (2001).

Busciglio, J., Gabuzda, D. H., Matsudaira, P. & Yankner, B. A. Generation of beta-amyloid in the secretory pathway in neuronal and nonneuronal cells. *Proceedings of the National Academy of Sciences of the United States of America* **90**, 2092-2096, (1993).

Caccamo, A., Maldonado, M. A., Bokov, A. F., Majumder, S. & Oddo, S. CBP gene transfer increases BDNF levels and ameliorates learning and memory deficits in a mouse model of Alzheimer's disease. *Proceedings of the National Academy of Sciences of the United States of America* **107**, 22687-22692 (2010).

Carmine-Simmen, K. *et al.* Neurotoxic effects induced by the Drosophila amyloid-beta peptide suggest a conserved toxic function. *Neurobiology of Disease* **33**, 274-281 (2009).

Carter, T. L. *et al.* Differential preservation of AMPA receptor subunits in the hippocampi of Alzheimer's disease patients according to Braak stage. *Experimental Neurology* **187**, 299-309 (2004).

Casadio, A. *et al.* A transient, neuron-wide form of CREB-mediated long-term facilitation can be stabilized at specific synapses by local protein synthesis. *Cell* **99**, 221-237 (1999).

Cashman, R. E. & Grammas, P. cAMP-dependent protein kinase in cerebral microvessels in aging and Alzheimer disease. *Molecular and Chemical Neuropathology* **26**, 247-258 (1995).

Castellucci, V. F. *et al.* Intracellular injection of the catalytic subunit of cyclic AMP-dependent protein-kinase simulates facilitation of transmitter release underlying behavioral sensitization in Aplysia. *Proceedings of the National Academy of Sciences of the United States of America-Biological Sciences* **77**, 7492-7496 (1980).

Castro, N. G. & Albuquerque, E. X. Alpha-bungarotoxin-sensitive hippocampal nicotinic receptor-channel has a high-calcium permeability. *Biophysical Journal* **68**, 516-524 (1995).

Cedar, H., Schwartz, J. H. & Kandel, E. R. Cyclic adenosine-monophosphate in nervous-system of Aplysia-californica. 1. Increased synthesis in response to synaptic stimulation. *Journal of General Physiology* **60**, 558-&, (1972).

Chapman, P. F. *et al.* Impaired synaptic plasticity and learning in aged amyloid precursor protein transgenic mice. *Nature Neuroscience* **2**, 271-276 (1999).

Chauhan, A., Chauhan, V. P. S., Brockerhoff, H. & Wisniewski, H. M. Action of amyloid beta-protein on protein-kinase-C activity. *Life Sciences* **49**, 1555-1562 (1991).

Chen, S. Y., Wright, J. W. & Barnes, C. D. The neurochemical and behavioral effects of beta-amyloid peptide(25-35). *Brain Research* **720**, 54-60, (1996).

Chen, Q. S., Wei, W. Z., Shimahara, T. & Xie, C. W. Alzheimer amyloid beta-peptide inhibits the late phase of long-term potentiation through calcineurin-dependent mechanisms in the hippocampal dentate gyrus. *Neurobiology of Learning and Memory* **77**, 354-371, (2002).

Chetkovich, D. M., Gray, R., Johnston, D. & Sweatt, J. D. N-Methyl-D-Aspartate receptor activation increases cAMP levels and voltage-gated Ca2+ channel activity in area CA1 of hippocampus. *Proceedings of the National Academy of Sciences of the United States of America* **88**, 6467-6471 (1991).

Chetkovich, D. M. & Sweatt, J. D. NMDA receptor activation increases cyclic-AMP in area CA1 of the hippocampus via calcium-calmodulin stimulation of adenylyl-cyclase. *Journal of Neurochemistry* **61**, 1933-1942 (1993).

Chijiwa, T. *et al.* Inhibition of forskolin-induced neurite outgrowth and protein-phosphorylation by a newly synthesized selective inhibitor of cyclic AMP-dependent protein-kinase, N-2-(P-Bromocinnamylamino)Ethyl-5-Isoquinolinesulfonamide (H-89), of PC12D Pheochromocytoma cells. *Journal of Biological Chemistry* **265**, 5267-5272 (1990).

Chiti, F. & Dobson, C. M. Protein misfolding, functional amyloid, and human disease. *Annual Review of Biochemistry* **75**, 333-366, (2006).

Chitwood, R. A., Li, Q. & Glanzman, D. L. Serotonin facilitates AMPA-type responses in isolated siphon motor neurons of Aplysia in culture. *Journal of Physiology-London* **534**, 501-510, (2001).

Choe, E. S. & Wang, J. Q. Group I metabotropic glutamate receptor activation increases phosphorylation of cAMP response element-binding protein, Elk-1, and extracellular signal-regulated kinases in rat dorsal striatum. *Molecular Brain Research* **94**, 75-84 (2001).

Choi, D. S. *et al.* PKC epsilon increases endothelin converting enzyme activity and reduces amyloid plaque pathology in transgenic mice. *Proceedings of the National Academy of Sciences of the United States of America* **103**, 8215-8220 (2006).

Cleary, J. P. *et al.* Natural oligomers of the amyloid-protein specifically disrupt cognitive function. *Nature Neuroscience* **8**, 79-84, (2005).

Conrad, P., Wu, F. & Schacher, S. Changes in functional glutamate receptors on a postsynaptic neuron accompany formation and maturation of an identified synapse. *Journal of Neurobiology* **39**, 237-248, (1999).

Cooper, D. M. F., Mons, N. & Karpen, J. W. Adenylyl cyclases and the interaction between calcium and cAMP signaling. *Nature* **374**, 421-424 (1995).

Countryman, R. A., Orlowski, J. D., Brightwell, J. J., Oskowitz, A. Z. & Colombo, P. T. CREB phosphorylation and c-Fos expression in the hippocampus of rats during

acquisition and recall of a socially transmitted food preference. *Hippocampus* **15**, 56-67 (2005).

Crow, T. J. & Alkon, D. L. Associative behavioral-modification in Hermissenda- cellular correlates. *Science* **209**, 412-414, (1980).

Crow, T., Forrester, H., Williams, M., Waxham, M.N., & Neary, J.T. Down-regulation of preotin kinase C blocks 5-HT-induced enhancement in *Hermissenda* B photoreceptors. *Neuroscience Letters* **121**, 107-110 (1991).

Crow, T., Xue-Bian, J.J., Siddiqi, V., Kang, Y., & Neary, J.T. Phosphorylation of mitogen-activated protein kinase by one-trial and multi-trial classical conditioning. *Journal of Neuroscience* **18**, 3480-3487 (1998).

Crow, T., & Xue-Bian, J.J. One-trial in vitro conditioning regulates a cytoskeletal-related protein (CSP24) in the conditioned stimulus pathway of *Hermissenda*. *Journal of Neuroscience* **22**, 10514-10518 (2002).

Crow, T.J. Pavlovian conditioning of *Hermissenda*: Current cellular, molecular, and circuit perspectives. *Learning and Memory* **11**, 229-238 (2004).

Cui, Z. Z. *et al.* Inducible and reversible NR1 knockout reveals crucial role of the NMDA receptor in preserving remote memories in the brain. *Neuron* **41**, 781-793 (2004).

Daigle, I. & Li, C. APL-1, a Caenorhabditis-elegans gene encoding a protein related to the human beta-amyloid protein-precursor. *Proceedings of the National Academy of Sciences of the United States of America* **90**, 12045-12049 (1993).

Dale, H. Chemical transmission of the effects of nerve impulses. *British medical journal* **1**, 835-841 (1934).

Dale, N. & Kandel, E. R. L-glutamate may be the fast excitatory transmitter of Aplysia sensory neurons. *Proceedings of the National Academy of Sciences of the United States of America* **90**, 7163-7167, (1993).

Dani, J. A. & Bertrand, D. Nicotinic acetylcholine receptors and nicotinic cholinergic mechanisms of the central nervous system. *Annual Review of Pharmacology and Toxicology* **47**, 699-729 (2007).

Darlison, M. G., Hutton, M. L. & Harvey, R. J. Molluscan ligand-gated ion channel receptors.*Experientia Supplementum (Basel)* **63**, 48-64 (1993).

Dash, P. K., Hochner, B. & Kandel, E. R. Injection of the cAMP-responsive element into the nucleus of Aplysia sensory neurons blocks long-term facilitation. *Nature* **345**, 718-721 (1990).

Davies, P. & Maloney, A. J. F. Selective loss of central cholinergic neurons in Alzheimers-disease. *Lancet* **2**, 1403-1403 (1976).

De Felice, F. G. *et al.* A beta oligomers induce neuronal oxidative stress through an N-methyl-D-aspartate receptor-dependent mechanism that is blocked by the Alzheimer drug memantine. *Journal of Biological Chemistry* **282**, 11590-11601 (2007).

De Felice, F. G. *et al.* Protection of synapses against Alzheimer's-linked toxins: Insulin signaling prevents the pathogenic binding of A beta oligomers. *Proceedings of the National Academy of Sciences of the United States of America* **106**, 1971-1976 (2009).

de Jong-Brink, M., Bergamin-Sassen, M.J., Kuyt, J.R., & Tewari-Kanhai, AL. Enzyme cytochemical evidence for the activation of adenylate cyclase in the follicle cells of vitellogenic oocytes by the dorsal body hormone in the snail Lymnaea stagnalis. *General and Comparative Endocrinology* **63**, 212-219 (1986).

Degroot, R. P., Denhertog, J., Vandenheede, J. R., Goris, J. & Sassonecorsi, P. Multiple and cooperative phosphorylation events regulate the CREM activator function. *Embo Journal* **12**, 3903-3911 (1993).

Deisseroth, K., Bito, H. & Tsien, R. W. Signaling from synapse to nucleus: Postsynaptic CREB phosphorylation during multiple forms of hippocampal synaptic plasticity. *Neuron* **16**, 89-101 (1996).

Delobette, S., Privat, A. & Maurice, T. In vitro aggregation facilitates beta-amyloid peptide-(25-35)-induced amnesia in the rat. *European Journal of Pharmacology* **319**, 1-4, (1997).

Deriemer, S. A., Strong, J. A., Albert, K. A., Greengard, P. & Kaczmarek, L. K. Enhancement of calcium current in Aplysia neurons by phorbol ester and protekin kinase-C. *Nature* **313**, 313-316 (1985).

Descarries, L., Gisiger, V. & Steriade, M. Diffuse transmission by acetylcholine in the CNS. *Progress in Neurobiology* **53**, 603-625 (1997).

Dictus, W., Broersvendrig, C. M. & Dejongbrink, M. The role of IP3, PKC, and PHI in the stimulus-response coupling of calfluxin-stimulated albumin glands of the fresh-water snail Lymnaea-stagnalis. *General and Comparative Endocrinology* **70**, 206-215 (1988).

Dineley, K. T. *et al.* beta-amyloid activates the mitogen-activated protein kinase cascade via hippocampal alpha 7 nicotinic acetylcholine receptors: In vitro and in vivo mechanisms related to Alzheimer's disease. *Journal of Neuroscience* **21**, 4125-4133 (2001).

Dingledine, R., Borges, K., Bowie, D. & Traynelis, S. F. The glutamate receptor ion channels. *Pharmacological Reviews* **51**, 7-61 (1999).

Dobson, C. M. Protein folding and misfolding. *Nature* **426**, 884-890, (2003).

Dong, Y. *et al.* CREB modulates excitability of nucleus accumbens neurons. *Nature Neuroscience* **9**, 475-477 (2006).

Driver, J. E. *et al.* Impairment of hippocampal gamma (gamma)-frequency oscillations in vitro in mice overexpressing human amyloid precursor protein (APP). *European Journal of Neuroscience* **26**, 1280-1288, (2007).

Dudai, Y., Uzzan, A. & Zvi, S. Abnormal activity of adenylate-cyclase in the Drosophila memory mutant rutabaga. *Neuroscience Letters* **42**, 207-212 (1983).

Dudai, Y. The neurobiology of consolidations, or, how stable is the engram? *Annual Review of Psychology* **55**, 51-86, (2004).

Dudai, Y. & Eisenberg, M. Rites of passage of the engram: Reconsolidation and the lingering consolidation hypothesis. *Neuron* **44**, 93-100 (2004).

Dura, J.M., Preat, T., & Tully, T. Identification of linotte, a new gene affecting learning and memory in Drosophila melanogaster. Journal of Neurogenetics **9**, 1-14 (1993).

Dykens, J.A. Isolated cerebral and cerebellar mitochondria produce free radicals when exposed to elevated Ca2+ and Na+; implications for neurodegeneration. *Journal of Neurochemistry* **63**, 584-591 (1994).

Echeverria, V. *et al.* Altered mitogen-activated protein kinase signaling, tau hyperphosphorylation and mild spatial learning dysfunction in transgenic rats expressing the beta-amyloid peptide intracellularly in hippocampal and cortical neurons. *Neuroscience* **129**, 583-592 (2004).

Eckel-Mahan, K. L. *et al.* Circadian oscillation of hippocampal MAPK activity and cAMP: implications for memory persistence. *Nature Neuroscience* **11**, 1074-1082 (2008).

Eckert, A., Schulz, K. L., Rhein, V. & Goetz, J. Convergence of Amyloid-beta and Tau Pathologies on Mitochondria In Vivo. *Molecular Neurobiology* **41**, 107-114, (2010).

Edelstein, A., Amodaj, N., Hoover, K., Vale, R., & Stuurman, N. Computer controls of microscopes using μManager. *Current protocols in molecular biology/* edited by Frederick M. Ausubel … [et al.] Chapter 14, Unit 14.20 (2010).

Ehrlich, I. & Malinow, R. Postsynaptic density 95 controls AMPA receptor incorporation during long-term potentiation and experience-driven synaptic plasticity. *Journal of Neuroscience* **24**, 916-927, (2004).

Ekinci, F. J., Malik, K. U. & Shea, T. B. Activation of the L voltage-sensitive calcium channel by mitogen-activated protein (MAP) kinase following exposure of

neuronal cells to beta-amyloid - Map kinase mediates beta-amyloid-induced neurodegeneration. *Journal of Biological Chemistry* **274**, 30322-30327, (1999).

Eliot, L. S., Dudai, Y., Kandel, E. R. & Abrams, T. W. Ca2+-calmodulin sensitivity may be common to all forms of neural adenylate-cyclase. *Proceedings of the National Academy of Sciences of the United States of America* **86**, 9564-9568 (1989).

English, J. D. & Sweatt, J. D. Activation of p42 mitogen-activated protein kinase in hippocampal long term potentiation. *Journal of Biological Chemistry* **271**, 24329-24332 (1996).

Esteban, J. A. *et al.* PKA phosphorylation of AMPA receptor subunits controls synaptic trafficking underlying plasticity. *Nature Neuroscience* **6**, 136-143 (2003).

Fabian-Fine, R. et al., Ultrastructural distribution of the alpha7 nicotinic acetylcholine receptor subunit in rat hippocampus. *Journal of Neuroscience* **21**, 7993-8003 (2001).

Fadda, E., Danysz, W., Wroblewski, J. T. & Costa, E. Glycine and D-serine increase the affinity of N-Methyl-D-Aspartate sensitive glutamate binding-sites in rat-brain synaptic-membranes. *Neuropharmacology* **27**, 1183-1185 (1988).

Fastbom, J., Forsell, Y. & Winblad, B. Benzodiazepines may have protective effects against Alzheimer disease. *Alzheimer Disease & Associated Disorders* **12**, 14-17 (1998).

Favit, A., Grimaldi, M., Nelson, T. J. & Alkon, D. L. Alzheimer's-specific effects of soluble beta-amyloid on protein kinase C-alpha and -gamma degradation in human fibroblasts. *Proceedings of the National Academy of Sciences of the United States of America* **95**, 5562-5567 (1998).

Feng, Z. P. *et al.* Transcriptome analysis of the central nervous system of the mollusc Lymnaea stagnalis. *Bmc Genomics* **10**, (2009).

Finch, C. E. & Sapolsky, R. M. The evolution of Alzheimer disease, the reproductive schedule, and apoE isoforms. *Neurobiology of Aging* **20**, 407-428, (1999).

Folkers, E. Visual learning and memory of *Drosophila melanogastar* wild type C-S and the mutants dunce, amnesiac, turnip, and rutabaga. *Journal of Insect Physiology* **28**, 535-539 (1982).

Fossgreen, A. *et al.* Transgenic Drosophila expressing human amyloid precursor protein show gamma-secretase activity and a blistered-wing phenotype. *Proceedings of the National Academy of Sciences of the United States of America* **95**, 13703-13708, (1998).

Francis, R. *et al.* aph-1 and pen-2 are required for notch pathway signaling, gamma-secretase cleavage of beta APP, and presenilin protein accumulation. *Developmental Cell* **3**, 85-97, (2002).

Frankland, P. W., O'Brien, C., Ohno, M., Kirkwood, A. & Silva, A. J. alpha-CaMKII-dependent plasticity in the cortex is required for permanent memory. *Nature* **411**, 309-313 (2001).

Frankland, P. W. & Bontempi, B. The organization of recent and remote memories. *Nature Reviews Neuroscience* **6**, 119-130, (2005).

Freir, D. B., Holscher, C. & Herron, C. E. Blockade of long-term potentiation by beta-amyloid peptides in the CA1 region of the rat hippocampus in vivo. *Journal of Neurophysiology* **85**, 708-713 (2001).

Freir, D. B. & Herron, C. E. Inhibition of L-type voltage dependent calcium channels causes impairment of long-term potentiation in the hippocampal CA1 region in vivo. *Brain Research* **967**, 27-36 (2003).

Freir, D. B. *et al.* A beta oligomers inhibit synapse remodelling necessary for memory consolidation. *Neurobiology of Aging* **32**, 2211-2218 (2011).

Frey, U., Krug, M., Reymann, K. G. & Matthies, H. Anisomycin, an inhibitor of protein-synthesis, blocks late phases of LTP phenomena in the Hippocampal CA1 region in vitro. *Brain Research* **452**, 57-65, (1988).

Frey, U., Huang, Y. Y. & Kandel, E. R. Effects of cAMP stimulate a late-stage of LTP in hippocampal CA1 neurons. *Science* **260**, 1661-1664 (1993).

Frey, U. & Morris, R. G. M. Synaptic tagging and long-term potentiation. *Nature* **385**, 533-536, (1997).

Fulton, D., Kemenes, I., Andrew, R. J. & Benjamin, P. R. A single time-window for protein synthesis-dependent long-term memory formation after one-trial appetitive conditioning. *European Journal of Neuroscience* **21**, 1347-1358 (2005).

Galeazzi, L., Ronchi, P., Franceschi, C. & Giunta, S. In vitro peroxidase oxidation induces stable dimers of beta-amyloid (1-42) through dityrosine bridge formation. *Amyloid-International Journal of Experimental and Clinical Investigation* **6**, 7-13, (1999).

Genoux, D. *et al.* Protein phosphatase 1 is a molecular constraint on learning and memory. *Nature* **418**, 970-975 (2002).

Georganopoulou, D. G. *et al.* Nanoparticle-based detection in cerebral spinal fluid of a soluble pathogenic biomarker for Alzheimer's disease. *Proceedings of the National Academy of Sciences of the United States of America* **102**, 2273-2276, (2005).

Ghasemi, R., Zarifkar, A., Rastegar, K., Maghsoudi, N. & Moosavi, M. Repeated intra-hippocampal injection of beta-amyloid 25-35 induces a reproducible impairment of learning and memory: Considering caspase-3 and MAPKs activity. *European Journal of Pharmacology* **726**, 33-40 (2014).

Giese, K. P., Fedorov, N. B., Filipkowski, R. K. & Silva, A. J. Autophosphorylation at Thr(286) of the alpha calcium-calmodulin kinase II in LTP and learning. *Science* **279**, 870-873 (1998).

Giovannini, M.G., Lana, D., & Pepeu, G. The integrated role of Ach, ERK and mTOR in the mechanisms of hippocampal inhibitory avoidance memory. *Neurobiology of Learning and Memory* **119**, 18-33 (2015).

Glanzman, D. L. Postsynaptic regulation of the development and long-term plasticity of Aplysia sensorimotor synapses in cell-culture. *Journal of Neurobiology* **25**, 666-693, (1994).

Glanzman, D.L. Common mechanisms of synaptic plasticity in vertebrates and invertebrates. *Current Biology* **20**, R31-R36 (2010).

Goldsmith, B. A. & Abrams, T. W. CAMP mediates action potential broadening, as well as increased excitability, produced by 5-HT in Aplysia sensory neurons. *Society for Neuroscience Abstracts* **18**, 16-16 (1992).

Gong, Y. S. *et al.* Alzheimer's disease-affected brain: Presence of oligomeric A beta ligands (ADDLs) suggests a molecular basis for reversible memory loss. *Proceedings of the National Academy of Sciences of the United States of America* **100**, 10417-10422 (2003).

Gong, B. *et al.* Persistent improvement in synaptic and cognitive functions in an Alzheimer mouse model after rolipram treatment. *Journal of Clinical Investigation* **114**, 1624-1634 (2004).

Gonzalez, F. A., Raden, D. L. & Davis, R. J. Identification of substrate recognition determinants for human ERK1 and ERK2 protein-kinase. *Journal of Biological Chemistry* **266**, 22159-22163 (1991).

Gouras, G. K. *et al.* Intraneuronal A beta 42 accumulation in human brain. *American Journal of Pathology* **156**, 15-20 (2000).

Grammas, P., Roher, A. E. & Ball, M. J. Increased accumulation of cAMP in cerebral microvessels in Alzheimer-disease. *Neurobiology of Aging* **15**, 113-116 (1994).

Greenberg, S. M., Castellucci, V. F., Bayley, H. & Schwartz, J. H. A molecular mechanism for long-term sensitization in Aplysia. *Nature* **329**, 62-65 (1987).

Greenfield, J. P. *et al.* Endoplasmic reticulum and trans-Golgi network generate distinct populations of Alzheimer beta-amyloid peptides. *Proceedings of the National Academy of Sciences of the United States of America* **96**, 742-747, (1999).

Greeve, I. *et al.* Age-dependent neurodegeneration and Alzheimer-amyloid plaque formation in transgenic Drosophila. *Journal of Neuroscience* **24**, 3899-3906, (2004).

Grover, L. M. & Teyler, T. J. 2 components of long-term potentiation induced by different patterns of afferent activation. *Nature* **347**, 477-479 (1990).

Grutzendler, J., Kasthuri, N. & Gan, W. B. Long-term dendritic spine stability in the adult cortex. *Nature* **420**, 812-816, (2002).

Gu, Z., Liu, W. & Yan, Z. beta-Amyloid Impairs AMPA Receptor Trafficking and Function by Reducing Ca2+/Calmodulin-dependent Protein Kinase II Synaptic Distribution. *Journal of Biological Chemistry* **284**, 10639-10649 (2009).

Gu, Z. & Yakel, J. L. Timing-Dependent Septal Cholinergic Induction of Dynamic Hippocampal Synaptic Plasticity. *Neuron* **71**, 155-165 (2011).

Ha, T. J., Kohn, A. B., Bobkova, Y. V. & Moroz, L. L. Molecular characterization of NMDA-like receptors in Aplysia and Lymnaea: Relevance to memory mechanisms. *Biological Bulletin* **210**, 255-270 (2006).

Haass, C. *et al.* Amyloid beta-peptide is produced by cultured-cells during normal metabolism. *Nature* **359**, 322-325, (1992).

Hagiwara, M. *et al.* Transcriptional attenuation following cAMP induction requires PP-1-mediated dephosphorylation of CREB. *Cell* **70**, 105-113 (1992).

Hama, T., Huang, K. P. & Guroff, G. Protein-kinase-C as a component of a nerve growth factor-sensitive phosphorylation system in PC12 cells. *Proceedings of the National Academy of Sciences of the United States of America* **83**, 2353-2357 (1986).

Han, M. H. *et al.* Role of cAMP response element-binding protein in the rat locus ceruleus: Regulation of neuronal activity and opiate withdrawal behaviors. *Journal of Neuroscience* **26**, 4624-4629 (2006).

Hardy, J. The amyloid hypothesis for Alzheimer's disease: a critical reappraisal. *Journal of Neurochemistry* **110**, 1129-1134, (2009).

Harper, J. D., Wong, S. S., Lieber, C. M. & Lansbury, P. T. Observation of metastable A beta amyloid protofibrils by atomic force microscopy. *Chemistry & Biology* **4**, 119-125, (1997).

Hartley, D. M. *et al.* Transglutaminase induces protofibril-like amyloid beta-protein assemblies that are protease-resistant and inhibit long-term potentiation. *Journal of Biological Chemistry* **283**, 16790-16800, (2008).

Hatakeyama, D., & Kemenes, G. Molecular cloning of CREB Binding Protein (CBP) of the pond snail *Lymnaea stagnalis*. *British Neuroscience Association Abstracts* **18**. 68 (2005).

Hatakeyama, D., et al.. Requirement of new protein synthesis of a transcription factor for memory consolidation: paradoxical changes in mRNA and protein levels of C/EBP. *Journaly of Molecular Biology* **356**, 569-577 (2006).

Hayashi, Y. *et al.* Driving AMPA receptors into synapses by LTP and CaMKII: Requirement for GluR1 and PDZ domain interaction. *Science* **287**, 2262-2267 (2000).

Hayashi, M. L. *et al.* Altered cortical synaptic morphology and impaired memory consolidation in forebrain-specific dominant- negative PAK transgenic mice. *Neuron* **42**, 773-787 (2004).

Hegde, A. N. & DiAntonio, A. Ubiquitin and the synapse. *Nature Reviews Neuroscience* **3**, 854-861, (2002).

Hepler, R.W., et al.. Solution state characterization of amyloid beta-derived diffusible ligands. *Biochemistry* **45**, 15157-15167 (2006).

Hodgkin, A. L. & Huxley, A. F. A quantitative description of membrane current and its application to conduction and excitation in nerve. *Journal of Physiology-London* **117**, 500-544 (1952).

Hoe, H.-S., Lee, H.-K. & Pak, D. T. S. The Upside of APP at Synapses. *Cns Neuroscience & Therapeutics* **18**, 47-56, (2012).

Holtzman, D.M., Herz, J., & Bu, G. Apolipoprotein E and apolipoprotein E receptors: normal biology and roles in Alzheimer's disease. *Cold Spring Harbor Perspective Medicine* **2**, a006312 (2012).

Hong, C. S. & Koo, E. H. Isolation and characterization of Drosophila presenilin homolog. *Neuroreport* **8**, 665-668, (1997).

Hong, I. *et al.* AMPA receptor exchange underlies transient memory destabilization on retrieval. *Proceedings of the National Academy of Sciences of the United States of America* **110**, 8218-8223 (2013).

Hongpaisan, J., Sun, M.-K. & Alkon, D. L. PKC epsilon Activation Prevents Synaptic Loss, A beta Elevation, and Cognitive Deficits in Alzheimer's Disease Transgenic Mice. *Journal of Neuroscience* **31**, 630-643 (2011).

Horiuchi, J., Yamazaki, D., Naganos, S., Aigaki, T. & Saitoe, M. Protein kinase A inhibits a consolidated form of memory in Drosophilae. *Proceedings of the National Academy of Sciences of the United States of America* **105**, 20976-20981, (2008).

Hsiao, K. *et al.* Correlative memory deficits, A beta elevation, and amyloid plaques in transgenic mice. *Science* **274**, 99-102, (1996).

Hsieh, H. *et al.* AMPAR removal underlies A beta-induced synaptic depression and dendritic spine loss. *Neuron* **52**, 831-843 (2006).

Hu, N.-W., Klyubin, I., Anwy, R. & Rowan, M. J. GluN2B subunit-containing NMDA receptor antagonists prevent A beta-mediated synaptic plasticity disruption in vivo. *Proceedings of the National Academy of Sciences of the United States of America* **106**, 20504-20509 (2009).

Huang, Y. Y., Li, X. C. & Kandel, E. R. cAMP contributes to messy fiber LTP by initiating both a covalently mediated early phase and macromolecular synthesis-dependent late-phase. *Cell* **79**, 69-79 (1994).

Huang, Y. Y., Martin, K. C. & Kandel, E. R. Both protein kinase a and mitogen-activated protein kinase are required in the amygdala for the macromolecular synthesis-dependent late phase of long-term potentiation. *Journal of Neuroscience* **20**, 6317-6325 (2000).

Impey, S. *et al.* Induction of CRE-mediated gene expression by stimuli that generate long-lasting LTP in area CA1 of the hippocampus. *Neuron* **16**, 973-982 (1996).

Impey, S. *et al.* Cross talk between ERK and PKA is required for Ca2+ stimulation of CREB-dependent transcription and ERK nuclear translocation. *Neuron* **21**, 869-883 (1998a).

Impey, S. *et al.* Stimulation of cAMP response element (CRE)-mediated transcription during contextual learning. *Nature Neuroscience* **1**, 595-601 (1998b).

Impey, S. *et al.* Phosphorylation of CBP mediates transcriptional activation by neural activity and CaM kinase IV. *Neuron* **34**, 235-244 (2002).

Inoue, M., Kishimoto, A., Takai, Y. & Nishizuka, Y. Studies on a cyclic nucleotide-independent protein-kinase and its proenzyme in mammalian-tissues. W. Proenzyme and its activation by calcium-dependent protease from rat-brain. *Journal of Biological Chemistry* **252**, 7610-7616 (1977).

Ivanov, A. *et al.* Opposing role of synaptic and extrasynaptic NMDA receptors in regulation of the extracellular signal-regulated kinases (ERK) activity in cultured rat hippocampal neurons. *Journal of Physiology-London* **572**, 789-798 (2006).

Jancic, D., Lopez de Armentia, M., Valor, L. M., Olivares, R. & Barco, A. Inhibition of cAMP Response Element-Binding Protein Reduces Neuronal Excitability and Plasticity, and Triggers Neurodegeneration. *Cerebral Cortex* **19**, 2535-2547 (2009).

Janowitz, M. K. & Van Rossum, M. C. W. Excitability changes that complement Hebbian learning. *Network-Computation in Neural Systems* **17**, 31-41, (2006).

Jerusalinsky, D. *et al.* Post-training intrahippocampal infusion of protein-kinase-C inhibitors causes amnesia in rats. *Behavioral and Neural Biology* **61**, 107-109 (1994).

Jin, M. *et al.* Soluble amyloid beta-protein dimers isolated from Alzheimer cortex directly induce Tau hyperphosphorylation and neuritic degeneration. *Proceedings of the National Academy of Sciences of the United States of America* **108**, 5819-5824 (2011).

Johannessen, M., Delghandi, M. P. & Moens, U. What turns CREB on? *Cellular Signalling* **16**, 1211-1227 (2004).

Jones, I. W. & Wonnacott, S. Precise localization of alpha 7 nicotinic acetylcholine receptors on glutamatergic axon terminals in the rat ventral tegmental area. *Journal of Neuroscience* **24**, 11244 (2004).

Kaczorowski, C. C., Sametsky, E., Shah, S., Vassar, R. & Disterhoft, J. F. Mechanisms underlying basal and learning-related intrinsic excitability in a mouse model of Alzheimer's disease. *Neurobiology of Aging* **32**, 1452-1465, (2011).

Kaminsky, Y. G., Marlatt, M. W., Smith, M. A. & Kosenko, E. A. Subcellular and metabolic examination of amyloid-beta peptides in Alzheimer disease pathogenesis: Evidence for A beta(25-35). *Experimental Neurology* **221**, 26-37, (2010).

Kandel, E. R. & Pittenger, C. The past, the future and the biology of memory storage. *Philosophical Transactions of the Royal Society of London Series B-Biological Sciences* **354**, 2027-2052, (1999).

Kane, N. S., Robichon, A., Dickinson, J. A. & Greenspan, R. J. Learning without performance in PKC-deficient Drosophila. *Neuron* **18**, 307-314, (1997).

Kasa, P. *et al.* Synaptic and nonsynaptic cholinergic innervations of the various types of neurons in the main olfactory-bulb of adult-rat-immunocytochemistry choline-acetyltransferase. *Neuroscience* **67**, 667-677 (1995).

Kawai, H., Zago, W. & Berg, D. K. Nicotinic alpha 7 receptor clusters on hippocampal GABAergic neurons: Regulation by synaptic activity and neurotrophins. *Journal of Neuroscience* **22**, 7903-7912 (2002).

Kawai, R., Yasuoka, T., & Sakakibara, M. Dynamical aspects of in vitro conditioning in *Hermissenda* type B photoreceptor. *Zoological Science* **20**, 1-6 (2003).

Kellar, K. J., Whitehouse, P. J., Martinobarrows, A. M., Marcus, K. & Price, D. L. Muscarinic and nicotinic cholinergic binding-sites in Alzheimers-disease cerebral-cortex. *Brain Research* **436**, 62-68 (1987).

Kelleher, D. J., Pessin, J. E., Ruoho, A. E. & Johnson, G. L. Phorbol ester induces desensitization of adenylate-cyclase and phosphorylation of the beta-adrenergic-receptor in turkey erythrocytes. *Proceedings of the National Academy of Sciences of the United States of America-Biological Sciences* **81**, 4316-4320 (1984).

Kelly, A., Laroche, S. & Davis, S. Activation of mitogen-activated protein kinase/extracellular signal-regulated kinase in hippocampal circuitry is required for consolidation and reconsolidation of recognition memory. *Journal of Neuroscience* **23**, 5354-5360 (2003).

Kemenes, G. & Benjamin, P.R. Appetitive learning in snails shows characteristics of conditioning in vertebrates. *Brain Research* **1**, 163-166 (1989).

Kemenes, G., Elekes, K., Hiripi, L. & Benjamin, P. R. A comparison of four techniques for mapping the distribution of serotonin and serotonin-containing neurons in fixed and living ganglia of the snail Lymnaea. *Journal of Neurocytology* **18**, 193-208 (1989).

Kemenes, G. *et al.* Cellular changes in the feeding system after tactile and chemical appetitive classical conditioning in Lymnaea. *European Journal of Neuroscience* **12**, 93-93 (2000).

Kemenes, I., Kemenes, G., Andrew, R. J., Benjamin, P. R. & O'Shea, M. Critical time-window for NO-cGMP-dependent long-term memory formation after one-trial appetitive conditioning.*Journal of Neuroscience* **22**, 1414-1425 (2002).

Kemenes, G., Kemenes, I., Michel, M., Papp, A. & Muller, U. Phase-dependent molecular requirements for memory reconsolidation: Differential roles for protein synthesis and protein kinase A activity. *Journal of Neuroscience* **26**, 6298-6302 (2006).

Kemenes, I. *et al.* Role of delayed nonsynaptic neuronal plasticity in long-term associative memory. *Current Biology* **16**, 1269-1279, (2006).

Kemenes, G., & Benjamin, P.R. *Lymnaea*. *Current Biology* **19**, R9-R11 (2009).

Kemenes, G. in *Invertebrate Learning and Memory* Vol. 22 *Handbook of Behavioral Neuroscience* (eds R. Menzel & P. R. Benjamin) 251-264 (2013).

Kerrigan, T. L., Brown, J. T. & Randall, A. D. Characterization of altered intrinsic excitability in hippocampal CA1 pyramidal cells of the A beta-overproducing PDAPP mouse. *Neuropharmacology* **79**, 515-524, (2014).

Khodorov, B. *et al.* On the origin of a sustained increase in cytosolic Ca2+ concentration after a toxic glutamate treatment of the nerve-cell culture. *Febs Letters* **324**, 271-273, (1993).

Kida, S. *et al.* CREB required for the stability of new and reactivated fear memories. *Nature Neuroscience* **5**, 348-355 (2002).

Kim, J. J., Clark, R. E. & Thompson, R. F. Hippocampectomy impairs the memory of recently, but not remotely, acquired trace eyeblink conditioning-responses. *Behavioral Neuroscience* **109**, 195-203, (1995).

Kim, J. H., Anwyl, R., Suh, Y. H., Djamgoz, M. B. A. & Rowan, M. J. Use-dependent effects of amyloidogenic fragments of beta-amyloid precursor protein on synaptic plasticity in rat hippocampus in vivo. *Journal of Neuroscience* **21**, 1327-1333 (2001).

Kim, J. H. *et al.* Presynaptic activation of silent synapses and growth of new synapses contribute to intermediate and long-term facilitation in Aplysia. *Neuron* **40**, 151-165, (2003).

Kim, E. J. & Sheng, M. PDZ domain proteins of synapses. *Nature Reviews Neuroscience* **5**, 771-781, (2004).

Klann, E., Chen, S. J. & Sweatt, J. D. Persistent protein-kinase activation in the maintenance phase of long-term potentiation. *Journal of Biological Chemistry* **266**, 24253-24256 (1991).

Klein, M. & Kandel, E. R. Presynaptic modulation of voltage-dependent Ca2+ current-mechanism for behavioral sensitization in Aplysia-californica. *Proceedings of the National Academy of Sciences of the United States of America* **75**, 3512-3516, (1978).

Klein, M. & Kandel, E. R. Mechanisms of calcium current modulation underlying facilitation and behavioral sensitization in Aplysia. *Proceedings of the National Academy of Sciences of the United States of America-Biological Sciences* **77**, 6912-6916, (1980).

Klein, W. L., Lacor, P. N., De Felice, F. G. & Ferreira, S. T. Molecules that disrupt memory circuits in Alzheimer's disease: The attack on synapses by A beta oligomers (ADDLs). *Memories: Molecules and Circuits*, 155-179 (2007).

Klyubin, I. *et al.* Neurotransmitter receptor and time dependence of the synaptic plasticity disrupting actions of Alzheimer's disease A beta in vivo. *Philosophical Transactions of the Royal Society B-Biological Sciences* **369** (2014).

Knobloch, M., Farinelli, M., Konietzko, U., Nitsch, R. M. & Mansuy, I. M. A beta oligomer-mediated long-term potentiation impairment involves protein phosphatase 1-dependent mechanisms. *Journal of Neuroscience* **27**, 7648-7653, (2007).

Kojima, S., Nanakamura, H., Nagayama, S., Fujito, Y. & Ito, E. Enhancement of an inhibitory input to the feeding central pattern generator in Lymnaea stagnalis during conditioned taste-aversion learning. *Neuroscience Letters* **230**, 179-182, (1997).

Korneev, S. A. *et al.* Timed and targeted differential regulation of nitric oxide synthase (NOS) and anti-NOS genes by reward conditioning leading to long-term memory formation. *Journal of Neuroscience* **25**, 1188-1192, (2005).

Kroker, K. S., Moreth, J., Kussmaul, L., Rast, G. & Rosenbrock, H. Restoring long-term potentiation impaired by amyloid-beta oligomers: Comparison of an acetylcholinesterase inhibitior and selective neuronal nicotinic receptor agonists. *Brain Research Bulletin* **96**, 28-38 (2013).

Kubo, T., Nishimura, S., Kumagae, Y. & Kaneko, I. In vivo conversion of racemized beta-amyloid (D-Ser(26) A beta 1-40) to truncated and toxic fragments (D-Ser(26) A beta 25-35/40) and fragment presence in the brains of Alzheimer's patients. *Journal of Neuroscience Research* **70**, 474-483, (2002).

Lacor, P. N. *et al.* Synaptic targeting by Alzheimer's-related amyloid beta oligomers. *Journal of Neuroscience* **24**, 10191-10200 (2004).

Lacor, P. N. *et al.* A beta oligomer-induced aberrations in synapse composition, shape, and density provide a molecular basis for loss of connectivity in Alzheimer's disease. *Journal of Neuroscience* **27**, 796-807 (2007).

LaFerla, F. M. Calcium dyshomeostasis and intracellular signalling in Alzheimer's disease. *Nature Reviews Neuroscience* **3**, 862-872 (2002).

Lambert, M. P. *et al.* Diffusible, nonfibrillar ligands derived from A beta(1-42) are potent central nervous system neurotoxins. *Proceedings of the National Academy of Sciences of the United States of America* **95**, 6448-6453 (1998).

Lambert, M. P. *et al.* Monoclonal antibodies that target pathological assemblies of A beta. *Journal of Neurochemistry* **100**, 23-35 (2007).

Lammich, S. *et al.* Constitutive and regulated alpha-secretase cleavage of Alzheimer's amyloid precursor protein by a disintegrin metalloprotease. *Proceedings of the National Academy of Sciences of the United States of America* **96**, 3922-3927, (1999).

Lau, G. C., Saha, S., Faris, R. & Russek, S. J. Up-regulation of NMDAR1 subunit gene expression in cortical neurons via a PKA-dependent pathway. *Journal of Neurochemistry* **88**, 564-575 (2004).

Lauren, J., Gimbel, D. A., Nygaard, H. B., Gilbert, J. W. & Strittmatter, S. M. Cellular prion protein mediates impairment of synaptic plasticity by amyloid-beta oligomers. *Nature* **457**, 1128-U1184 (2009).

Lee, H. K. *et al.* Phosphorylation of the AMPA receptor GluR1 subunit is required for synaptic plasticity and retention of spatial memory. *Cell* **112**, 631-643 (2003).

Lee, W. *et al.* Amyloid beta peptide directly inhibits PKC activation. *Molecular and Cellular Neuroscience* **26**, 222-231 (2004).

Lee, Y.-S., Bailey, C. H., Kandel, E. R. & Kaang, B.-K. Transcriptional regulation of long-term memory in the marine snail Aplysia. *Molecular Brain* **1**, (2008).

Lei, S. Z. *et al.* Effect of nitric-oxide production on the redox modulatory site of the NMDA receptor channel complex. *Neuron* **8**, 1087-1099 (1992).

Lendvai, B. & Vizi, E. S. Nonsynaptic chemical transmission through nicotinic acetylcholine receptors. *Physiological Reviews* **88**, 333-349 (2008).

Leon, W. C. *et al.* A Novel Transgenic Rat Model with a Full Alzheimer's-Like Amyloid Pathology Displays Pre-Plaque Intracellular Amyloid-beta-Associated Cognitive Impairment. *Journal of Alzheimers Disease* **20**, 113-126 (2010).

Lesne, S. *et al.* A specific amyloid-beta protein assembly in the brain impairs memory. *Nature* **440**, 352-357 (2006).

Levin, E. D., Kim, P. & Meray, R. Chronic nicotine working and reference memory effects in the 16-arm radial maze: Interactions with D-1 agonist and antagonist drugs. *Psychopharmacology* **127**, 25-30 (1996).

Levin, E. D., McClernon, F. J. & Rezvani, A. H. Nicotinic effects on cognitive function: behavioral characterization, pharmacological specification, and anatomic localization. *Psychopharmacology* **184**, 523-539 (2006).

Levitan, I. B. & Barondes, S. H. Octopamine-stimulated and serotonin-stimulated phosphorylation of specific protein in abdominal-ganglion of Aplysia-Californica. *Proceedings of the National Academy of Sciences of the United States of America* **71**, 1145-1148 (1974).

Levitan, I. B. Phosphorylation of ion channels. *Journal of Membrane Biology* **87**, 177-190, (1985).

Li, S. *et al.* Soluble Oligomers of Amyloid beta Protein Facilitate Hippocampal Long-Term Depression by Disrupting Neuronal Glutamate Uptake. *Neuron* **62**, 788-801 (2009).

Li, S. *et al.* Soluble A beta Oligomers Inhibit Long-Term Potentiation through a Mechanism Involving Excessive Activation of Extrasynaptic NR2B-Containing NMDA Receptors.*Journal of Neuroscience* **31**, 6627-6638 (2011).

Limon, I.D., et al.. Amyloid beta (25-35) impairs memory and increases NO in the temporal cortex of rats. *Neuroscience Research* **63**, 129-137 (2009).

Lichtenthaler, S.F. Alpha-secretase cleavage of the amyloid precursor protein: proteolysis regulated by signaling pathways and protein trafficking. *Current Alzheimer's Research* **9**, 165-177 (2012).

Linden, D. J. & Routtenberg, A. The role of protein kinase-C in long-term potentiation a testable model. *Brain Research Reviews* **14**, 279-296 (1989).

Ling, D. S. F. *et al.* Protein kinase M zeta is necessary and sufficient for LTP maintenance. *Nature Neuroscience* **5**, 295-296 (2002).

Link, C. D. Invertebrate models of Alzheimer's disease. *Genes Brain and Behavior* **4**, 147-156 (2005).

Litchfield, D. W. & Ball, E. H. Phosphorylation of the cytoskeletal protein talin by protein-kinase-C. *Biochemical and Biophysical Research Communications* **134**, 1276-1283 (1986).

Liu, Q. S., Kawai, H. & Berg, D. K. beta-Amyloid peptide blocks the response of alpha 7-containing nicotinic receptors on hippocampal neurons. *Proceedings of the National Academy of Sciences of the United States of America* **98**, 4734-4739 (2001).

Loewi, O. The Ferrier lecture on Problems Connected with the Principle of Humoral Transmission of Nervous Impulses. *Proceedings of the Royal Society Series B-Biological Sciences* **118**, 299-316, (1935).

Lorenzetti, F. D., Baxter, D. A. & Byrne, J. H. Molecular mechanisms underlying a cellular analog of operant reward learning. *Neuron* **59**, 815-828 (2008).

Lu, W. Y. *et al.* Activation of synaptic NMDA receptors induces membrane insertion of new AMPA receptors and LTP in cultured hippocampal neurons. *Neuron* **29**, 243-254 (2001).

Lublin, A.L., & Link, C.D. Alzheimer's disease drug discovery: in vivo screening using Caenorhabditis elegans as a model for β-amyloid peptide-induced toxicity. *Drug Discovery Today Technology* **10**, 115-119 (2013).

Lukowiak K., Martens, K. Orr, M., Parvez, K., Rosenegger, D., and Sangha, S. Modulation of aerial respiratory behaviour in a pond snail. *Respiratory Physiology in Neurobiology* **154**, 61-72 (2006).

Luo, L. Q., Martinmorris, L. E. & White, K. Identification, secretion, and neural expression of APPL, a Drosophila protein similar to human amyloid protein-precursor. *Journal of Neuroscience* **10**, 3849-3861 (1990).

Ly, P. T. T. & Song, W. Loss of activated CaMKII at the synapse underlies Alzheimer's disease memory loss. *Journal of Neurochemistry* **119**, 673-675, (2011).

Ma, Q.-L. *et al.* Evidence of A beta- and transgene-dependent defects in ERK-CREB signaling in Alzheimer's models. *Journal of Neurochemistry* **103**, 1594-1607 (2007).

Ma, T. GSK3 in Alzheimer's disease: mind the isoforms. *Journal of Alzheimer's Disease* **4**, 707-710 (2014).

Maddalena, A. S. *et al.* Cerebrospinal Fluid Profile of Amyloid beta Peptides in Patients with Alzheimer's Disease Determined by Protein Biochip Technology. *Neurodegenerative Diseases* **1**, 231-235, (2004).

Madison, D. V., Malenka, R. C. & Nicoll, R. A. Phorbol esters block a voltage-sensitive chloride current in hippocampal pyramidal cells. *Nature* **321**, 695-697 (1986).

Malenka, R. C., Madison, D. V., Andrade, R. & Nicoll, R. A. Phorbol esters mimic some cholinergic actions in hippocampal pyramidal neurons. *Journal of Neuroscience* **6**, 475-480 (1986).

Maletic-Savatic, M., Malinow, R. & Svoboda, K. Rapid dendritic morphogenesis in CA1 hippocampal dendrites induced by synaptic activity. *Science* **283**, 1923-1927, (1999).

Malinow, R. & Malenka, R. C. AMPA receptor trafficking and synaptic plasticity. *Annual Review of Neuroscience* **25**, 103-126, (2002).

Man, H. Y., Ju, W., Ahmadian, G. & Wang, Y. T. Intracellular trafficking of AMPA receptors in synaptic plasticity. *Cellular and Molecular Life Sciences* **57**, 1526-1534 (2000).

Manseau, F., Sossin, W. S. & Castellucci, V. F. Long-term changes in excitability induced by protein kinase C activation in Aplysia sensory neurons. *Journal of Neurophysiology* **79**, 1210-1218 (1998).

Mansvelder, H. D. & McGehee, D. S. Long-term potentiation of excitatory inputs to brain reward areas by nicotine. *Neuron* **27**, 349-357 (2000).

Mao, L. M., Tang, Q. S., Samdani, S., Liu, Z. G. & Wang, J. Q. Regulation of MAPK/ERK phosphorylation via ionotropic glutamate receptors in cultured rat striatal neurons. *European Journal of Neuroscience* **19**, 1207-1216 (2004).

Marra, V., O'Shea, M., Benjamin, P. R. & Kemenes, I. Susceptibility of memory consolidation during lapses in recall. *Nature Communications* **4** (2013).

Martens, K., Amarell, M., Parvez, K., Hittel, K., De Caigny, P., Ito, E., Lukowiak, K. One-trial conditioning of aerial respiratory behaviour in Lymnaea stagnalis. *Neurobiology of Learning and Memory* **88**, 232-242 (2007).

Martin, K. C. *et al.* MAP kinase translocates into the nucleus of the presynaptic cell and is required for long-term facilitation in Aplysia. *Neuron* **18**, 899-912 (1997).

Martinez, M. *et al.* Increased cerebrospinal fluid cAMP levels in Alzheimer's disease. *Brain Research* **846**, 265-267 (1999).

Masliah, E. *et al.* Differential involvement of protein kinase-C isozymes in Alzheimers-disease. *Journal of Neuroscience* **10**, 2113-2124 (1990).

Matsushima, H., Shimohama, S., Chachin, M., Taniguchi, T. & Kimura, J. Ca2+-dependent and Ca2+-independent protein kinase C changes in the brains of patients with Alzheimer's disease. *Journal of Neurochemistry* **67**, 317-323 (1996).

Mattson, M. P. Calcium and neuronal injury in Alzheimers-disease- contribution of beta-amyloid precursor protein mismetabolism, free-radicals, and metabolic compromise. *Calcium Hypothesis of Aging and Dementia* **747**, 50-76 (1994).

Mattson, M. P. Calcium and neurodegeneration. *Aging Cell* **6**, 337-350, (2007).

Mayer, M. L., Westbrook, G. L. & Guthrie, P. B. Voltage-dependent block by Mg2+ of NMDA responses in spinal-cord neurons. *Nature* **309**, 261-263 (1984).

Mayford, M. & Kandel, E. R. Genetic approaches to memory storage. *Trends in Genetics* **15**, 463-470 (1999).

McDonald, M. P., Dahl, E. E., Overmier, J. B., Mantyh, P. & Cleary, J. Effects of an exogenous beta-amyloid peptide on retention for spatial-learning. *Behavioral and Neural Biology* **62**, 60-67, (1994).

McDonald, M. P., Overmier, J. B., Bandyopadhyay, S., Babcock, D. & Cleary, J. Reversal of beta-amyloid-induced retention deficit after exposure to training and state cues. *Neurobiology of Learning and Memory* **65**, 35-47, (1996).

McDonald, J. M. *et al.* The presence of sodium dodecyl sulphate-stable A beta dimers is strongly associated with Alzheimer-type dementia. *Brain* **133**, 1328-1341 (2010).

McDonald, J. M., Cairns, N. J., Taylor-Reinwald, L., Holtzman, D. & Walsh, D. M. The levels of water-soluble and triton-soluble A beta are increased in Alzheimer's disease brain. *Brain Research* **1450**, 138-147 (2012).

McCrohan, C. R. & Benjamin, P. R. Synaptic relationships of the cerebral giant-cells with moto-neurons in the feeding system of Lymnaea-stagnalis. *Journal of Experimental Biology* **85**, 169-186 (1980).

McLean, C.A., et al.. Soluble pool of Abeta amyloid as a determinant of severity of neurodegeneration in Alzheimer's disease. *Annual Neurology* **46**, 860-866 (1999).

Meng, Y. H., Zhang, Y. & Jia, Z. P. Synaptic transmission and plasticity in the absence of AMPA glutamate receptor GluR2 and GluR3. *Neuron* **39**, 163-176 (2003).

Michael, D. *et al.* Repeated pulses of serotonin required for long-term facilitation activate mitogen-activated protein kinase in sensory neurons of Aplysia. *Proceedings of the National Academy of Sciences of the United States of America* **95**, 1864-1869 (1998).

Michel, M., Kemenes, I., Mueller, U. & Kemenes, G. Different phases of long-term memory require distinct temporal patterns of PKA activity after single-trial classical conditioning. *Learning & Memory* **15**, 694-702 (2008).

Michel, M., Green, C. L. & Lyons, L. C. PKA and PKC are required for long-term but not short-term in vivo operant memory in Aplysia. *Learning & Memory* **18**, 19-23 (2011).

Michel, M., Green, C.L., Gardner, J.S., Organ, C.L., and Lyons, L.C. Massed training-induced intermediate-term operant memory in aplysia requires protein synthesis and multiple persistent kinase cascades. *Journal of Neuroscience* **13**, 4581-4591 (2012).

Mietelska-Porowska, A., Wasik, U., Goras, M., Filipek, A., & Niewiadomska, G. Tau protein modifications and interactions: their role in function and dysfunction. *International Journal of Molecular Science* **15**, 4671-4713 (2014).

Migues, P. V. *et al.* PKM zeta maintains memories by regulating GluR2-dependent AMPA receptor trafficking. *Nature Neuroscience* **13**, 630-U147 (2010).

Millucci, L., Raggiaschi, T., Franceschini, D., Terstappen, G., & Santucci, A. Rapid aggregation and assembly in aqueous solution of A beta (25-35) peptide. *Journal of Bioscience* **34**, 293-303 (2009).

Millucci, L., Ghezzi, L., Bernardini, G. & Santucci, A. Conformations and Biological Activities of Amyloid Beta Peptide 25-35. *Current Protein & Peptide Science* **11**, 54-67 (2010).

Minkeviciene, R. *et al.* Amyloid beta-Induced Neuronal Hyperexcitability Triggers Progressive Epilepsy. *Journal of Neuroscience* **29**, 3453-3462, (2009).

Mishizen-Eberz, A. J. *et al.* Biochemical and molecular studies of NMDA receptor subunits NR1/2A/2B in hippocampal subregions throughout progression of Alzheimer's disease pathology. *Neurobiology of Disease* **15**, 80-92 (2004).

Molnar, E. & Isaac, J. T. R. Developmental and activity dependent regulation of ionotropic glutamate receptors at synapses. *TheScientificWorldJournal* **2**, 27-47 (2002).

Montgomery, J. M. & Madison, D. V. State-dependent heterogeneity in synaptic depression between pyramidal cell pairs. *Neuron* **33**, 765-777 (2002).

Moroz, L. L., Gyori, J. & Salanki, J. NMDA-like receptors in the CNS of mollusks. *Neuroreport* **4**, 201-204 (1993).

Moroz, L. L. & Kohn, A. B. Do different neurons age differently? Direct genome-wide analysis of aging in single identified cholinergic neurons. *Frontiers in Aging Neuroscience* **2** (2010).

Morris, K. & Serpell, L. From natural to designer self-assembling biopolymers, the structural characterisation of fibrous proteins & peptides using fibre diffraction. *Chemical Society Reviews* **39**, 3445-3453, (2010).

Mozzachiodi, R. & Byrne, J. H. More than synaptic plasticity: role of nonsynaptic plasticity in learning and memory. *Trends in Neurosciences* **33**, 17-26, \ (2010).

Mucke, L. & Selkoe, D. J. Neurotoxicity of Amyloid beta-Protein: Synaptic and Network Dysfunction. *Cold Spring Harbor Perspectives in Medicine* **2** (2012).

Muller, U. & Carew, T. J. Serotonin induces temporally and mechanistically distinct phases of persistent PKA activity in Aplysia sensory neurons. *Neuron* **21**, 1423-1434 (1998).

Murphy, G. G. & Glanzman, D. L. Mediation of classical conditioning in Aplysia californica by long-term potentiation of sensorimotor synapses. *Science* **278**, 467-471 (1997).

Nagerl, U. V., Eberhorn, N., Cambridge, S. B. & Bonhoeffer, T. Bidirectional activity-dependent morphological plasticity in hippocampal neurons. *Neuron* **44**, 759-767, (2004).

Naik, M. U. *et al.* Distribution of protein kinase M zeta and the complete protein kinase C isoform family in rat brain. *Journal of Comparative Neurology* **426**, 243-258 (2000).

Naskar, S., Wan, H. & Kemenes, G. pT305-CaMKII stabilizes a learning-induced increase in AMPA receptors for ongoing memory consolidation after classical conditioning. *Nature Communications* **5**, (2014).

Naylor, R., Hill, A. F. & Barnham, K. J. Neurotoxicity in Alzheimer's disease: is covalently crosslinked A beta responsible? *European Biophysics Journal with Biophysics Letters* **37**, 265-268, (2008).

Ness, S., Rafili, M., Aisen, P., Krams, M., Silverman, W., & Manji, H. Down's syndrome and Alzheimer's disease: towards secondary prevention. *Nature Review Drug Discovery* **11**, 655-656 (2012).

Nikitin, E.S., Kiss, T., Staras, K., O;shea, M., Benjamin, P.R., & Kemenes, G. Persistent sodium current is a target for cAMP-induced neuronal plasticity in a state-setting modulatory interneuron. *Journal of Neurophysiology* **95**, 453-463 (2006).

Nikitin, E. S. *et al.* Persistent sodium current is a nonsynaptic substrate for long-term associative memory. *Current Biology* **18**, 1221-1226, (2008).

Nilsberth, C. *et al.* The 'Arctic' APP mutation (E693G) causes Alzheimer's disease by enhanced A beta protofibril formation. *Nature Neuroscience* **4**, 887-893, (2001).

Nishizuka, Y. Studies and perspectives of protein-kinase-C. *Science* **233**, 305-312 (1986).

Nitta, A., Fukuta, T., Hasegawa, T. & Nabeshima, T. Continuous infusion of beta-amyloid protein into the rat cerebral ventricle induces learning impairment and neuronal and morphological degeneration. *Japanese Journal of Pharmacology* **73**, 51-57, (1997).

Nowak, L., Bregestovski, P., Ascher, P., Herbet, A. & Prochiantz, A. Magnesium gates glutamate-activated channels in mouse central neurons. *Nature* **307**, 462-465 (1984).

O'Malley, A., O'Connell, A.W., & Regan, C.M. Ultrastructural analysis reveals avoidance conditioning to induce a transient increase in hippocampal dentate spine density in the 6 hour post-training period of consolidation. *Neuroscience* **87**, 607-613 (1998).

O'Nuallain, B. *et al.* Amyloid beta-Protein Dimers Rapidly Form Stable Synaptotoxic Protofibrils. *Journal of Neuroscience* **30**, 14411-14419 (2010).

Oda, T. *et al.* Purification and characterization of brain clusterin. *Biochemical and Biophysical Research Communications* **204**, 1131-1136, (1994).

Oddo, S. *et al.* Triple-transgenic model of Alzheimer's disease with plaques and tangles: Intracellular A beta and synaptic dysfunction. *Neuron* **39**, 409-421, (2003).

Oliet, S. H. R., Malenka, R. C. & Nicoll, R. A. Bidirectional control of quantal size by synaptic activity in the hippocampus. *Science* **271**, 1294-1297, (1996).

Otmakhov, N., Griffith, L. C. & Lisman, J. E. Postsynaptic inhibitors of calcium/calmodulin-dependent protein kinase type II block induction but not maintenance of pairing-induced long-term potentiation. *Journal of Neuroscience* **17**, 5357-5365 (1997).

Ouimet, C. C., Baerwald, K. D., Gandy, S. E. & Greengard, P. Immunocytochemical localization of amyloid precursor protein in rat-brain. *Journal of Comparative Neurology* **348**, 244-260, (1994).

Ozdemir, M. B. *et al.* Injection of specific amyloid-beta oligomers (beta(1-40):beta(1-42)=10:1) into rat medial septum impairs memory retention without inducing hippocampal apoptosis. *Neurological Research* **35**, 798-803, (2013).

Palop, J.J., *et al.*. Aberrant excitatory neuronal activity and compensatory remodelling of inhibitory hippocampal circuits in mouse models of Alzheimer's disease. *Neuron* **55**, 697-711 (2007).

Parameshwaran, K. *et al.* Amyloid beta-peptide A beta(1-42) but not A beta(1-40) attenuates synaptic AMPA receptor function. *Synapse* **61**, 367-374 (2007).

Parameshwaran, K., Dhanasekaran, M. & Suppiramaniam, V. Amyloid beta peptides and glutamatergic synaptic dysregulation. *Experimental Neurology* **210**, 7-13, (2008).

Paratcha, G. *et al.* Involvement of hippocampal PKC beta I isoform in the early phase of memory formation of an inhibitory avoidance learning. *Brain Research* **855**, 199-205 (2000).

Parra-Damas, A. *et al.* Crtc1 Activates a Transcriptional Program Deregulated at Early Alzheimer's Disease-Related Stages. *Journal of Neuroscience* **34**, 5776-5787 (2014).

Pastalkova, E. *et al.* Storage of spatial information by the maintenance mechanism of LTP.*Science* **313**, 1141-1144 (2006).

Pearson, H. A. & Peers, C. Physiological roles for amyloid beta peptides. *Journal of Physiology-London* **575**, 5-10, (2006).

Pedreira, M. E., Dimant, B. & Maldonado, H. Inhibitors of protein and RNA synthesis block context memory and long-term habituation in the crab Chasmagnathus. *Pharmacology Biochemistry and Behavior* **54**, 611-617 (1996).

Penfield, W. Memory mechanisms. *AMA Archives of Neurology and Psychiatry* **67**, 178-198 (1952).

Perry, E. K., Perry, R. H., Blessed, G. & Tomlinson, B. E. Changes in brain cholinesterases in senile dementia of Alzheimer type. *Neuropathology and Applied Neurobiology* **4**, 273-277 (1978a).

Perry, E. K. *et al.* Correlation of cholinergic abnormalities with senile plaques and mental test-scored in senile dementia. *British Medical Journal* **2**, 1457-1459 (1978b).

Pettit, D. L., Shao, Z. & Yakel, J. L. beta-Amyloid(1-42) peptide directly modulates nicotinic receptors in the rat hippocampal slice. *Journal of Neuroscience* **21** (2001).

Pieroni, J. P. & Byrne, J. H. Differential-effects of serotonin, FMRFamide, and small cardioactive peptide on multiple, distributed processes modulating sensorimotor synaptic transmission in Aplysia. *Journal of Neuroscience* **12**, 2633-2647 (1992).

Pike, C. J., Burdick, D., Walencewicz, A. J., Glabe, C. G. & Cotman, C. W. Neurodegeneration induced by beta-amyloid peptides in vitro- the role of peptide assembly state. *Journal of Neuroscience* **13**, 1676-1687 (1993).

Pike, C. J. *et al.* Structure-activity analyses of beta-amyloid peptides- contribution of the beta-25-35 region to aggregation and neurotoxicity. *Journal of Neurochemistry* **64**, 253-265 (1995).

Pirger, Z. *et al.* Pituitary Adenylate Cyclase Activating Polypeptide (PACAP) and Its Receptors Are Present and Biochemically Active in the Central Nervous System of the Pond Snail Lymnaea stagnalis. *Journal of Molecular Neuroscience* **42**, 464-471, (2010a).

Pirger, Z. *et al.* A Homolog of the Vertebrate Pituitary Adenylate Cyclase-Activating Polypeptide Is Both Necessary and Instructive for the Rapid Formation of Associative Memory in an Invertebrate. *Journal of Neuroscience* **30**, 13766-13773, (2010b).

Pittenger, C. *et al.* Reversible inhibition of CREB/ATF transcription factors in region CA1 of the dorsal hippocampus disrupts hippocampus-dependent spatial memory. *Neuron* **34**, 447-462 (2002).

Pratt, J. M. *et al.* Dynamics of protein turnover, a missing dimension in proteomics. *Molecular & Cellular Proteomics* **1**, 579-591 (2002).

Preat, T. Decreased odor avoidance after electric shock in Drosophila mutants biases learning and memory tests. *Journal of Neuroscience* **18**, 8534-8538 (1998).

Price, D. L. & Sisodia, S. S. Cellular and molecular-biology of Alzhiemer's-disease and animal-models. *Annual Review of Medicine* **45**, 435-446 (1994).

Prussing, K., Voigt, A., Schulz, J. Drosophila melanogaster as a model organism for Alzheimer's disease. *Molecular Neurodegeneration* **8**, 35 (2013).

Proctor, D. T., Coulson, E. J. & Dodd, P. R. Reduction in Post-Synaptic Scaffolding PSD-95 and SAP-102 Protein Levels in the Alzheimer Inferior Temporal Cortex

is Correlated with Disease Pathology. *Journal of Alzheimers Disease* **21**, 795-811, (2010).

Przybyslawski, J. & Sara, S. J. Reconsolidation of memory after its reactivation. *Behavioural Brain Research* **84**, 241-246 (1997).

Puolivali, J. *et al.* Hippocampal A beta 42 levels correlate with spatial memory deficit in APP and PS1 double transgenic mice. *Neurobiology of Disease* **9**, 339-347 (2002).

Purves, D., Augustine, G. J., Fitzpatrick, D., Hall, W. C., LaMantia, A., McNamara, J. O., & White, L. E. Neuroscience, fourth edition. *Sinauer Associates, inc.* (2008).

Puzzo, D. *et al.* Picomolar Amyloid-beta Positively Modulates Synaptic Plasticity and Memory in Hippocampus. *Journal of Neuroscience* **28**, 14537-14545 (2008).

Rammes, G., Hasenjaeger, A., Sroka-Saidi, K., Deussing, J. M. & Parsons, C. G. Therapeutic significance of NR2B-containing NMDA receptors and mGluR5 metabotropic glutamate receptors in mediating the synaptotoxic effects of beta-amyloid oligomers on long-term potentiation (LTP) in murine hippocampal slices. *Neuropharmacology* **60**, 982-990 (2011).

Ramsden, M., Henderson, Z. & Pearson, H. A. Modulation of Ca2+ channel currents in primary cultures of rat cortical neurones by amyloid beta protein (1-40) is dependent on solubility status. *Brain Research* **956**, 254-261, (2002).

Randall, A. D., Witton, J., Booth, C., Hynes-Allen, A. & Brown, J. T. The functional neurophysiology of the amyloid precursor protein (APP) processing pathway. *Neuropharmacology* **59**, 243-267, (2010).

Rao, A., Kim, E., Sheng, M. & Craig, A. M. Heterogeneity in the molecular composition of excitatory postsynaptic sites during development of hippocampal neurons in culture. *Journal of Neuroscience* **18**, 1217-1229 (1998).

Reed, M. N. *et al.* Cognitive effects of cell-derived and synthetically derived A beta oligomers. *Neurobiology of Aging* **32**, 1784-1794, (2011).

Reissner, K. J., Shobe, J. L. & Carew, T. J. Memory nodes in memory processing: insights from Aplysia. *Cellular and Molecular Life Sciences* **63**, 963-974, (2006).

Ren, S.-Q. *et al.* PKC lambda is critical in AMPA receptor phosphorylation and synaptic incorporation during LTP. *Embo Journal* **32**, 1365-1380 (2013).

Renger, J. J., Ueda, A., Atwood, H. L., Govind, C. K. & Wu, C. F. Role of cAMP cascade in synaptic stability and plasticity: Ultrastructural and physiological analyses of individual synaptic boutons in Drosophila memory mutants. *Journal of Neuroscience* **20**, 3980-3992 (2000).

Renner, M. *et al.* Deleterious Effects of Amyloid beta Oligomers Acting as an Extracellular Scaffold for mGluR5. *Neuron* **66**, 739-754 (2010).

Ribeiro, M. J. *et al.* Cyclic AMP response element-binding (CREB)-like proteins in a molluscan brain: cellular localization and learning-induced phosphorylation. *European Journal of Neuroscience* **18**, 1223-1234 (2003).

Ribeiro, M. J. *et al.* Activation of MAPK is necessary for long-term memory consolidation following food-reward conditioning. *Learning & Memory* **12**, 538-545 (2005).

Ribeiro, M. *et al.* Characterization of NO-sensitive guanylyl cyclase: expression in an identified interneuron involved in NO-cGMP-dependent memory formation. *European Journal of Neuroscience* **28**, 1157-1165, (2008).

Roberson, E. D. *et al.* The mitogen-activated protein kinase cascade couples PKA and PKC to cAMP response element binding protein phosphorylation in area CA1 of hippocampus.*Journal of Neuroscience* **19**, 4337-4348 (1999).

Roenicke, R. *et al.* Early neuronal dysfunction by amyloid beta oligomers depends on activation of NR2B-containing NMDA receptors. *Neurobiology of Aging* **32**, 2219-2228 (2011).

Rose, R. M. & Benjamin, P. R. Relationship of the central motor pattern to the feeding cycle of Lymnaea-stagnalis. *Journal of Experimental Biology* **80**, 137-163 (1979).

Rose, R. M. & Benjamin, P. R. Interneuronal control of feeding in the pond snail Lymnaea-stagnalis 2. The interneuronal mechanism generating feeding cycles. *Journal of Experimental Biology* **92**, 203-228 (1981).

Roselli, F. et al. Soluble beta amyloid 1-40 induces NMDA-dependent degradation of postsynaptic density-95 at glutamatergic synapses. *Journal of Neuroscience* **25**, 11061-11070 (2005).

Rosen, D. R., Martinmorris, L., Luo, L. Q. & White, K. A Drosophila gene encoding a protein resembling the human beta-amyloid protein-precursor. *Proceedings of the National Academy of Sciences of the United States of America* **86**, 2478-2482, (1989).

Rosenegger, D. & Lukowiak, K. The participation of NMDA receptors, PKC, and MAPK in Lymnaea memory extinction. *Neurobiology of Learning and Memory* **100**, 64-69 (2013).

Roychaudhuri, R., Yang, M., Hoshi, M. M. & Teplow, D. B. Amyloid beta-Protein Assembly and Alzheimer Disease. *Journal of Biological Chemistry* **284**, 4749-4753 (2009).

Russo, C. *et al.* Heterogeneity of water-soluble amyloid beta-peptide in Alzheimer's disease and Down's syndrome brains. *Febs Letters* **409**, 411-416, (1997).

Sacktor, T. C., Kruger, K. E. & Schwartz, J. H. Activation of protein kinase-C by serotonin-biochemical-evidence that it participates in the mechanisms underlying facilitation in Aplysia. *Journal De Physiologie* **83**, 224-231 (1988).

Sacktor, T. C. *et al.* Persistent activation of the zeta-isoform of protein-kinase-C in the maintenance of long-term potentiation. *Proceedings of the National Academy of Sciences of the United States of America* **90**, 8342-8346 (1993).

Sadamoto, H. *et al.* CREB in the pond snail Lymnaea stagnalis: Cloning, gene expression, and function in identifiable neurons of the central nervous system. *Journal of Neurobiology* **58**, 455-466, (2004).

Sakakibara, M. Comparative study of visuo-vestibular conditioning in Lymnaea stagnalis. *Biology Bulletin* **3**, 298-307 (2006).

Samarova, E. I. *et al.* Effect of beta-amyloid peptide on behavior and synaptic plasticity in terrestrial snail. *Brain Research Bulletin* **67**, 40-45 (2005).

Sattelle, D.B. & Lane, N.J. Architecture of gastropod central nervous tissues in relation to ionic movements. *Tissue Cell* **4**, 253-270 (1972).

Schafe, G. E. *et al.* Activation of ERK/MAP kinase in the amygdala is required for memory consolidation of Pavlovian fear conditioning. *Journal of Neuroscience* **20**, 8177-8187 (2000).

Schliebs, R. & Arendt, T. The cholinergic system in aging and neuronal degeneration. *Behavioural Brain Research* **221**, 555-563 (2011).

Schlueter, O. M., Xu, W. & Malenka, R. C. Alternative N-terminal domains of PSD-95 and SAP97 govern activity-dependent regulation of synaptic AMPA receptor function. *Neuron* **51**, 99-111 (2006).

Scholz, K. P. & Byrne, J. H. Long-term sensitization in Aplysia – biophysical correlates in tail sensory neurons. *Science* **235**, 685-687, (1987).

Schulz, S., Siemer, H., Krug, M. & Hollt, V. Direct evidence for biphasic cAMP responsive element-binding protein phosphorylation during long-term potentiation in the rat dentate gyrus in vivo. *Journal of Neuroscience* **19**, 5683-5692 (1999).

Schulz, B. *et al.* The metabotropic glutamate receptor antagonist 2-methyl-6-(phenylethynyl)-pyridine (MPEP) blocks fear conditioning in rats. *Neuropharmacology* **41**, 1-7 (2001).

Scoville, W. B. & Milner, B. Loss of recent memory after bilateral hippocampal lesions. *Journal of Neurology Neurosurgery and Psychiatry* **20**, 11-21, (1957).

Selcher, J. C., Atkins, C. M., Trzaskos, J. M., Paylor, R. & Sweatt, J. D. A necessity for MAP kinase activation in mammalian spatial learning. *Learning & Memory* **6**, 478-490 (1999).

Self, D. W. *et al.* Involvement of cAMP-dependent protein kinase in the nucleus accumbens in cocaine self-administration and relapse of cocaine-seeking behavior. *Journal of Neuroscience* **18**, 1848-1859 (1998).

Selkoe, D. J. Molecular pathology of the aging human-brain. *Trends in Neurosciences* **5**, 332-336 (1982).

Selkoe, D. J. Alzheimer's disease is a synaptic failure. *Science* **298**, 789-791, (2002).

Selkoe, D. J. Soluble oligomers of the amyloid beta-protein impair synaptic plasticity and behavior. *Behavioural Brain Research* **192**, 106-113, (2008).

Selkoe, D. J. SnapShot: Pathobiology of Alzheimer's Disease. *Cell* **154**, 468-+, (2013).

Serpell, L. Amyloid structure. *Amyloids in Health and Disease* **56**, 1-10, (2014).

Serrano, P., Yao, Y. D. & Sacktor, T. C. Persistent phosphorylation by protein kinase M zeta maintains late-phase long-term potentiation. *Journal of Neuroscience* **25**, 1979-1984 (2005).

Serrano, P. *et al.* PKM zeta Maintains Spatial, Instrumental, and Classically Conditioned Long-Term Memories. *Plos Biology* **6**, 2698-2706 (2008).

Seubert, P. *et al.* Secretion of beta-amyloid precursor protein cleaved at the amino terminus of the beta-amyloid peptide. *Nature* **361**, 260-263, (1993).

Shaiken, T. E. & Opekun, A. R. Dissecting the cell to nucleus, perinucleus and cytosol.*Scientific Reports* **4** (2014).

Shan, Q., Chan, G. C. K. & Storm, D. R. Type 1 Adenylyl Cyclase Is Essential for Maintenance of Remote Contextual Fear Memory. *Journal of Neuroscience* **28**, 12864-12867 (2008).

Shankar, G. M. *et al.* Natural oligomers of the Alzheimer amyloid-beta protein induce reversible synapse loss by modulating an NMDA-type glutamate receptor-dependent signaling pathway. *Journal of Neuroscience* **27**, 2866-2875 (2007).

Shankar, G. M. *et al.* Amyloid-beta protein dimers isolated directly from Alzheimer's brains impair synaptic plasticity and memory. *Nature Medicine* **14**, 837-842 (2008).

Shapira, R., Silberberg, S. D., Ginsburg, S. & Rahamimoff, R. Activation of protein-kinase-C augments avoked transmitter release. *Nature* **325**, 58-60 (1987).

Shema, R., Sacktor, T. C. & Dudai, Y. Rapid erasure of long-term memory associations in the cortex by an inhibitor of PKM zeta. *Science* **317**, 951-953 (2007).

Shema, R. *et al.* Enhancement of Consolidated Long-Term Memory by Overexpression of Protein Kinase M zeta in the Neocortex. *Science* **331**, 1207-1210 (2011).

Sheng, M. & Lee, S. H. AMPA receptor trafficking and the control of synaptic transmission.*Cell* **105**, 825-828 (2001).

Shi, S. H. *et al.* Rapid spine delivery and redistribution of AMPA receptors after synaptic NMDA receptor activation. *Science* **284**, 1811-1816 (1999).

Shirwany, N. A., Payette, D., Xie, J. & Guo, Q. The amyloid beta ion channel hypothesis of Alzheimer's disease. *Neuropsychiatric disease and treatment* **3**, 597-612 (2007).

Shukla, K., Kim, J., Blundell, J. & Powell, C. M. Learning-induced glutamate receptor phosphorylation resembles that induced by long term potentiation. *Journal of Biological Chemistry* **282**, 18100-18107 (2007).

Sibley, D. R., Nambi, P., Peters, J. R. & Lefkowitz, R. J. Phorbol diesters promote beta-adrenergic-receptor phosphorylation and adenylate-cyclase desensitization in duck erythrocytes. *Biochemical and Biophysical Research Communications* **121**, 973-979 (1984).

Sibley, D. R., Jeffs, R. A., Daniel, K., Nambi, P. & Lefkowitz, R. J. Phorbol diester treatement promotes enhanced adenylate cyclase activity in frog erythrocytes. *Archives of Biochemistry and Biophysics* **244**, 373-381 (1986).

Siegelbaum, S. A., Camardo, J. S. & Kandel, E. R. Serotonin and cyclic-AMP close single K+- channels in Aplysia sensory neurons. *Nature* **299**, 413-417 (1982).

Silva, A. J., Paylor, R., Wehner, J. M. & Tonegawa, S. Impaired spatial-learning in alpha-calcium-calmoduliun kinase-II mutant mice. *Science* **257**, 206-211 (1992a).

Silva, A. J., Stevens, C. F., Tonegawa, S. & Wang, Y. Y. Deficient hippocampal long-term potentiation in alpha-calcium-calmodulin kinase-II mutant mice. *Science* **257**, 201-206 (1992b).

Sims, N.R., Bowen, D.M., Neary, D., & Davison, A.N. Metabolic processes in Alzheimer's diease: adenine nucleotide content and production of 14CO2 from [U-14C] glucose in vitro in human neocortex. *Journal of Neurochemistry* **41**, 1329-1334 (1983).

Simonian, N. A. & Coyle, J. T. Oxidative stress in neurodegenerative diseases. *Annual Review of Pharmacology and Toxicology* **36**, 83-106, (1996).

Skeberdis, V. A. *et al.* Protein kinase A regulates calcium permeability of NMDA receptors. *Nature Neuroscience* **9**, 501-510 (2006).

Smit, A. B. *et al.* A glia-derived acetylcholine-binding protein that modulates synaptic transmission. *Nature* **411**, 261-268 (2001).

Smith, D. P. *et al.* Copper-mediated amyloid-beta toxicity is associated with an intermolecular histidine bridge. *Journal of Biological Chemistry* **281**, 15145-15154, (2006).

Smith, D. L., Pozueta, J., Gong, B., Arancio, O. & Shelanski, M. Reversal of long-term dendritic spine alterations in Alzheimer disease models. *Proceedings of the National Academy of Sciences of the United States of America* **106**, 16877-16882, (2009).

Snowdon, D. A. Aging and Alzheimer's disease: Lessons from the Nun Study. *Gerontologist* **37**, 150-156 (1997).

Snyder, E. M. *et al.* Regulation of NMDA receptor trafficking by amyloid-beta. *Nature Neuroscience* **8**, 1051-1058 (2005).

Sokolov, Y. *et al.* Soluble amyloid oligomers increase bilayer conductance by altering dielectric structure. *The Journal of general physiology* **128**, 637-647, (2006).

Sossin, W. S., Sacktor, T. C. & Schwartz, J. H. Persistent activation of protein kinase C during the development of long-term facilitation in Aplysia. *Learning & memory (Cold Spring Harbor, N.Y.)* **1**, 189-202 (1994).

Sossin, W. S. Isoform specificity of protein kinase Cs in synaptic plasticity. *Learning & Memory* **14**, 236-246 (2007).

Soura, V. *et al.* Visualization of co-localization in A beta 42-administered neuroblastoma cells reveals lysosome damage and autophagosome accumulation related to cell death. *Biochemical Journal* **441**, 579-590 (2012).

Steele, R. J. & Morris, R. G. M. Delay-dependent impairment of a matching-to-place task with chronic and intrahippocampal infusion of the NMDA-Antagonist D-AP5. *Hippocampus* **9**, 118-136 (1999).

Steinberg, S. F. Structural basis of protein kinase C isoform function. *Physiological Reviews* **88**, 1341-1378 (2008).

Stepanichev, M. Y., Moiseeva, Y. V., Lazareva, N. A. & Gulyaeva, N. V. Studies of the effects of fragment (25-35) of beta-amyloid peptide on the behavior of rats in a radial maze. *Neuroscience and behavioral physiology* **35**, 511-518, (2005).

Stratton, K. R., Worley, P. F., Huganir, R. L. & Baraban, J. M. Muscarinic agonists and phorbol esters increase tyrosine phosphorylation of a 40-kilodalton protein in hippocampal slices. *Proceedings of the National Academy of Sciences of the United States of America* **86**, 2498-2501 (1989).

Straub, V. A., Styles, B. J., Ireland, J. S., O'Shea, M. & Benjamin, P. R. Central localization of plasticity involved in appetitive conditioning in Lymnaea. *Learning & Memory* **11**, 787-793 (2004).

Strekalova, T. *et al.* Memory retrieval after contextual fear conditioning induces c-Fos and JunB expression in CA1 hippocampus. *Genes Brain and Behavior* **2**, 3-10 (2003).

Sugita, S., Goldsmith, J. R., Baxter, D. A. & Byrne, J. H. Involvement of protein-kinase-C in serotonin-induced spike broadening and synaptic facilitation in sensorimotor connections of Aplysia. *Journal of Neurophysiology* **68**, 643-651 (1992).

Sutherland, R. J. & Lehmann, H. Alternative conceptions of memory consolidation and the role of the hippocampus at the systems level in rodents. *Current Opinion in Neurobiology* **21**, 446-451 (2011).

Sutton, M. A., Masters, S. E., Bagnall, M. W. & Carew, T. J. Molecular mechanisms underlying a unique intermediate phase of memory in Aplysia. *Neuron* **31**, 143-154 (2001).

Sweatt, J. D. & Kandel, E. R. Persistent and transcriptionally-dependent increase in protein-phosphorylation in long-term facilitation of Aplysia sensory neurons. *Nature* **339**, 51-54 (1989).

Sweatt, J. D. *et al.* Protected-site phosphorylation of protein kinase C in hippocampal long-term potentiation. *Journal of Neurochemistry* **71**, 1075-1085 (1998).

Sweatt, J. D. Toward a molecular explanation for long-term potentiation. *Learning & Memory* **6**, 399-416 (1999).

Sweatt, J. D. The neuronal MAP kinase cascade: a biochemical signal integration system subserving synaptic plasticity and memory. *Journal of Neurochemistry* **76**, 1-10 (2001).

Szapiro, G. *et al.* Participation of hippocampal metabotropic glutamate receptors, protein kinase A and mitogen-activated protein kinases in memory retrieval. *Neuroscience* **99**, 1-5 (2000).

Szapiro, G. *et al.* Molecular mechanisms of memory retrieval. *Neurochemical Research* **27**, 1491-1498 (2002).

Sze, C. I., Bi, H., Kleinschmidt-DeMasters, B. K., Filley, C. M. & Martin, L. J. N-Methyl-D-aspartate receptor subunit proteins and their phosphorylation status are altered selectively in Alzheimer's disease. *Journal of the Neurological Sciences* **182**, 151-159 (2001).

Takadera, T., Sakura, N., Mohri, T. & Hashimoto, T. Toxic effect of a beta-amyloid peptide (beta-22-35) on the hippocampal neuron and its prevention. *Neuroscience Letters* **161**, 41-44 (1993).

Takahashi, R. H. *et al.* Oligomerization of Alzheimer's beta-amyloid within processes and synapses of cultured neurons and brain. *Journal of Neuroscience* **24**, 3592-3599, (2004).

Tarragon, E. *et al.* Octodon degus: A Model for the Cognitive Impairment Associated with Alzheimer's Disease. *Cns Neuroscience & Therapeutics* **19**, 643-648, doi:10.1111/cns.12125 (2013).

Taubenfeld, S. M., Wiig, K. A., Bear, M. F. & Alberini, C. M. A molecular correlate of memory and amnesia in the hippocampus. *Nature Neuroscience* **2**, 309-310 (1999).

Taubenfeld, S. M. *et al.* Fornix-dependent induction of hippocampal CCAAT enhancer-binding protein beta and delta co-localizes with phosphorylated cAMP response element-binding protein and accompanies long-term memory consolidation. *Journal of Neuroscience* **21**, 84-91 (2001).

Taylor, S. S., Buechler, J. A. & Yonemoto, W. cAMP-dependent protein-kinase-framework for a diverse family of regulatory enzymes. *Annual Review of Biochemistry* **59**, 971-1005 (1990).

Terry, R. D. *et al.* Physical basis of cognitive alteration in Alzheimers-disease 0 synapse loss is the major correlated of cognitive impairment. *Annals of Neurology* **30**, 572-580, (1991).

Terry, R. D., Katzman, R., Bick, K. L. & Sisodia, S. S. Alzheimer disease, Second edition. *Alzheimer disease, Second edition* (1999).

Thandi, S., Blank, J. L. & Challiss, R. A. J. Group-I metabotropic glutamate receptors, mG1u1a and mG1u5a, couple to extracellular signal-regulated kinase (ERK) activation via distinct, but overlapping, signalling pathways. *Journal of Neurochemistry* **83**, 1139-1153 (2002).

Tharp, W. G. & Sarkar, I. N. Origins of amyloid-beta. *Bmc Genomics* **14** (2013).

Thomas, G. M. & Huganir, R. L. Mapk cascade signalling and synaptic plasticity. *Nature Reviews Neuroscience* **5**, 173-183 (2004).

Thorns, V., Mallory, M., Hansen, L. & Masliah, E. Alterations in glutamate receptor 2/3 subunits and amyloid precursor protein expression during the course of Alzheimer's disease and Lewy body variant. *Acta Neuropathologica* **94**, 539-548 (1997).

Thorpe, J. R. The application of LR gold resin for immunogold labeling. *Methods Molecular Biology* **117**, 99-110 (1999).

Tong, L., Balazs, R., Thornton, P.L., & Cotman, C. W. Beta amyloid peptide at sublethal concentrations downregulates BDNF functions in cultured cortical neurons. *Journal of Neuroscience* **24**, 6799-6809 (2004).

Toullec, D. *et al.* The Bisindolylmaleimide GF-109203X is a potent and selective inhibitor of protein-kinase-c. *Journal of Biological Chemistry* **266**, 15771-15781 (1991).

Trifilieff, P. *et al.* Foreground contextual fear memory consolidation requires two independent phases of hippocampal ERK/CREB activation. *Learning & Memory* **13**, 349-358 (2006).

Trifilieff, P., Calandreau, L., Herry, C., Mons, N. & Micheau, J. Biphasic ERK1/2 activation in both the hippocampus and amygdala may reveal a system consolidation of contextual fear memory. *Neurobiology of Learning and Memory* **88**, 424-434 (2007).

Tucci, P. *et al.* Memantine prevents memory consolidation failure induced by soluble beta amyloid in rats. *Frontiers in Behavioral Neuroscience* **8**, (2014).

Tycko, R. Solid-State NMR Studies of Amyloid Fibril Structure. *Annual Review of Physical Chemistry, Vol* **62**, 279-299, (2011).

van Nierop, P. *et al.* Identification and functional expression of a family of nicotinic acetylcholine receptor subunits in the central nervous system of the mollusc Lymnaea stagnalis. *Journal of Biological Chemistry* **281**, 1680-1691 (2006).

Velasco, P. T. *et al.* Synapse-Binding Subpopulations of A beta Oligomers Sensitive to Peptide Assembly Blockers and scFv Antibodies. *Acs Chemical Neuroscience* **3**, 972-981 (2012).

Villareal, G. *et al.* Role of Protein Kinase C in the Induction and Maintenance of Serotonin-Dependent Enhancement of the Glutamate Response in Isolated Siphon Motor Neurons of Aplysia californica. *Journal of Neuroscience* **29**, 5100-5107 (2009).

Vitolo, O. V. *et al.* Amyloid beta-peptide inhibition of the PKA/CREB pathway and long-term potentiation: Reversibility by drugs that enhance cAMP signaling. *Proceedings of the National Academy of Sciences of the United States of America* **99**, 13217-13221 (2002).

Volmat, V. & Pouyssegur, J. Spatiotemporal regulation of the p42/p44 MAPK pathway. *Biology of the Cell* **93**, 71-79 (2001).

Vossler, M. R. *et al.* cAMP activates MAP kinase and Elk-1 through a B-Raf- and Rap1-dependent pathway. *Cell* **89**, 73-82 (1997).

Vulfius, E. A., Veprintz.Bn, Zeimal, E. V. & Michelso.Mj. Arrangement of cholinpreceptors on neuronal membrane of 2 pulmonate gastropods. *Nature* **216**, 400 (1967).

Wadzinski, B. E. *et al.* Nuclear-protein phosphatase-2A dephosphorylates protein-kinase A-phosphorylated CREB and regulates CREB and regulates CREB transctiptional stimulation. *Molecular and Cellular Biology* **13**, 2822-2834 (1993).

Wainwright, M. L., Byrne, J. H. & Cleary, L. J. Dissociation of morphological and physiological changes associated with long-term memory in Aplysia. *Journal of Neurophysiology* **92**, 2628-2632, (2004).

Wakabayashi, K. *et al.* Phenotypic down-regulation of glutamate receptor subunit GluR1 in Alzheimer's diseases. *Neurobiology of Aging* **20**, 287-295 (1999).

Walsh, D. M., Lomakin, A., Benedek, G. B., Condron, M. M. & Teplow, D. B. Amyloid beta-protein fibrillogenesis - Detection of a protofibrillar intermediate. *Journal of Biological Chemistry* **272**, 22364-22372, (1997).

Walsh, D. M., Tseng, B. P., Rydel, R. E., Podlisny, M. B. & Selkoe, D. J. The oligomerization of amyloid beta-protein begins intracellularly in cells derived from human brain. *Biochemistry* **39**, 10831-10839, (2000).

Walsh, D. M. *et al.* Naturally secreted oligomers of amyloid beta protein potently inhibit hippocampal long-term potentiation in vivo. *Nature* **416**, 535-539, (2002).

Walsh, D. M. & Selkoe, D. J. Deciphering the molecular basis of memory failure in Alzheimer's disease. *Neuron* **44**, 181-193, (2004).

Walsh, D. M. & Selkoe, D. J. A beta Oligomers - a decade of discovery. *Journal of Neurochemistry* **101**, 1172-1184, (2007).

Wan, H., Mackay, B., Iqbal, H., Naskar, S. & Kemenes, G. Delayed Intrinsic Activation of an NMDA-Independent CaM-kinase II in a Critical Time Window Is Necessary for Late Consolidation of an Associative Memory. *Journal of Neuroscience* **30**, 56-63 (2010).

Wang, M. Y., Cahill, A. L. & Perlman, R. L. Phorbol 12, 13-dibutyrate increases tyrosine-hydroxylase activity in the superior cervical-ganglion of the rat. *Journal of Neurochemistry* **46**, 388-393 (1986).

Wang, H. Y. *et al.* beta-amyloid(1-42) binds to alpha 7 nicotinic acetylcholine receptor with high affinity - Implications for Alzheimer's disease pathology. *Journal of Biological Chemistry* **275**, 5626-5632 (2000).

Wang, H. W. *et al.* Soluble oligomers of beta amyloid (1-42) inhibit long-term potentiation but not long-term depression in rat dentate gyrus. *Brain Research* **924**, 133-140 (2002).

Wang, H. Y., Li, W. W., Benedetti, N. J. & Lee, D. H. S. alpha(7) nicotinic acetylcholine receptors mediate beta-amyloid peptide-induced tau protein phosphorylation. *Journal of Biological Chemistry* **278**, 31547-31553 (2003a).

Wang, H. *et al.* Inducible protein knockout reveals temporal requirement of CaMKII reactivation for memory consolidation in the brain. *Proceedings of the National Academy of Sciences of the United States of America* **100**, 4287-4292 (2003b).

Wang, H. B., Ferguson, G. D., Pineda, V. V., Cundiff, P. E. & Storm, D. R. Overexpression of type-1 adenylyl cyclase in mouse forebrain enhances recognition memory and LTP. *Nature Neuroscience* **7**, 635-642 (2004a).

Wang, Q. W., Rowan, M. J. & Anwyl, R. beta-amyloid-mediated inhibition of NMDA receptor-dependent long-term potentiation induction involves activation of microglia and stimulation of inducible nitric oxide synthase and superoxide. *Journal of Neuroscience* **24**, 6049-6056 (2004b).

Wang, Q. W., Walsh, D. M., Rowan, M. J., Selkoe, D. J. & Anwyl, R. Block of long-term potentiation by naturally secreted and synthetic amyloid beta-peptide in hippocampal slices is mediated via activation of the kinases c-Jun N-terminal kinase, cyclin-dependent kinase 5, and p38 mitogen-activated protein kinase as well as metabotropic glutamate receptor type 5. *Journal of Neuroscience* **24**, 3370-3378 (2004c).

Wang, J. Q., Fibuch, E. E. & Mao, L. Regulation of mitogen-activated protein kinases by glutamate receptors. *Journal of Neurochemistry* **100**, 1-11 (2007).

Wang, Q.-w., Rowan, M. J. & Anwyl, R. Inhibition of LTP by beta-amyloid is prevented by activation of beta 2 adrenoceptors and stimulation of the cAMP/PKA signalling pathway. *Neurobiology of Aging* **30**, 1608-1613 (2009).

Webster, S. J., Bachstetter, A. D., Nelson, P. T., Schmitt, F. A. & Van Eldik, L. J. Using mice to model Alzheimer's dementia: an overview of the clinical disease and the preclinical behavioral changes in 10 mouse models. *Frontiers in genetics* **5**, 88-88, (2014).

Weeber, E. J. *et al.* A role for the beta isoform of protein kinase C in fear conditioning. *Journal of Neuroscience* **20**, 5906-5914 (2000).

Westerman, M. A. *et al.* The relationship between A beta and memory in the Tg2576 mouse model of Alzheimer's disease. *Journal of Neuroscience* **22**, 1858-1867 (2002).

White, P. *et al.* Neocortical cholinergic neurons in elderly people. *Lancet* **1**, 668-671 (1977).

Whitehouse, P. J. *et al.* Alzheimers-disease and senile dementia- loss of neurons in the basal forebrain. *Science* **215**, 1237-1239 (1982).

Wieczorek, L., Maas, J. W., Jr., Muglia, L. M., Vogt, S. K. & Muglia, L. J. Temporal and Regional Regulation of Gene Expression by Calcium-Stimulated Adenylyl Cyclase Activity during Fear Memory. *Plos One* **5** (2010).

Wilcox, K. C., Lacor, P. N., Pitt, J. & Klein, W. L. A beta Oligomer-Induced Synapse Degeneration in Alzheimer's Disease. *Cellular and Molecular Neurobiology* **31**, 939-948 (2011).

Williams, T. L. & Serpell, L. C. Membrane and surface interactions of Alzheimer's A beta peptide - insights into the mechanism of cytotoxicity. *Febs Journal* **278**, 3905-3917 (2011).

Wilson, C. A., Doms, R. W. & Lee, V. M. Y. Intracellular APP processing and A beta production in Alzheimer disease. *Journal of Neuropathology and Experimental Neurology* **58**, 787-794 (1999).

Winblad, B. & Poritis, N. Memantine in severe dementia: Results of the M-9-BEST study (benefit and efficacy in severly demented patients during treatment with memantine). *International Journal of Geriatric Psychiatry* **14**, 135-146 (1999).

Wong, S. T. *et al.* Calcium-stimulated adenylyl cyclase activity is critical for hippocampus-dependent long-term memory and late phase LTP. *Neuron* **23**, 787-798 (1999).

Wu, Z. L. *et al.* Altered behavior and long-term potentiation in type-1 adenylyl-cyclase mutant mice. *Proceedings of the National Academy of Sciences of the United States of America* **92**, 220-224 (1995).

Xia, W. M. *et al.* Presenilin 1 regulates the processing of beta-amyloid precursor protein C-terminal fragments and the generation of amyloid beta-protein in endoplasmic reticulum and Golgi. *Biochemistry* **37**, 16465-16471, (1998).

Xie, H. J. & Rothstein, T. L. Protein-kinase-c mediates activation of nuclear cAMP response element-binding protein (CREB) in B-lymphocytes stimulated through surface Ig. *Journal of Immunology* **154**, 1717-1723 (1995).

Xing, J., Kornhauser, J. M., Xia, Z. G., Thiele, E. A. & Greenberg, M. E. Nerve growth factor activates extracellular signal-regulated kinase and p38 mitogen-activated protein kinase pathways to stimulate CREB serine 133 phosphorylation. *Molecular and Cellular Biology* **18**, 1946-1955 (1998).

Xiu, J., Nordberg, A., Zhang, J. T. & Guan, Z. Z. Expression of nicotinic receptors on primary cultures of rat astrocytes and up-regulation of the alpha 7, alpha 4 and beta 2 subunits in response to nanomolar concentrations of the beta-amyloid peptide(1-42). *Neurochemistry International* **47**, 281-290 (2005).

Xu, H. X. *et al.* Generation of Alzheimer beta-amyloid protein in the trans-Golgi network in the apparent absence of vesicle formation. *Proceedings of the National Academy of Sciences of the United States of America* **94**, 3748-3752, (1997).

Xu, F., et al.. Protease nexin-2/amyloid beta-protein precursor limits cerebral thrombosis. *Proceedings of the National Academy of Sciences* **102**, 18135-18140 (2005).

Yamamoto-Sasaki, M., Ozawa, H., Saito, T., Rosler, M. & Riederer, P. Impaired phosphorylation of cyclic AMP response element binding protein in the hippocampus of dementia of the Alzheimer type. *Brain Research* **824**, 300-303 (1999).

Yang, A. J., Chandswangbhuvana, D., Margol, L. & Glabe, C. G. Loss of endosomal/lysosomal membrane impermeability is an early event in amyloid A beta 1-42 pathogenesis. *Journal of Neuroscience Research* **52**, 691-698 (1998).

Yao, H., York, R. D., Misra-Press, A., Carr, D. W. & Stork, P. J. S. The cyclic adenosine monophosphate-dependent protein kinase (PKA) is required for the sustained activation of mitogen-activated kinases and gene expression by nerve growth factor. *Journal of Biological Chemistry* **273**, 8240-8247 (1998).

Yao, Y. *et al.* PKM zeta maintains late long-term potentiation by N-ethylmaleimide-sensitive factor/GluR2-dependent trafficking of postsynaptic AMPA receptors. *Journal of Neuroscience* **28**, 7820-7827 (2008).

Yeoman, M. S., Pieneman, A. W., Ferguson, G. P., Termaat, A. & Benjamin, P. R. Modulatory role for the serotonergic cerebral giant-cells in the feeding system of the snail, Lymnaea. 1. Fine wire recording in the intact animal and pharmacology. *Journal of Neurophysiology* **72**, 1357-1371 (1994).

Yeoman, M. S., Vehovszky, A., Kemenes, G., Elliott, C. J. H. & Benjamin, P. R. Novel interneuron having hybrid modulatory-central pattern generator properties in the feeding system of the snail, Lymnaea-stagnalis. *Journal of Neurophysiology* **73**, 112-124 (1995).

Yeoman, M. S., Brierley, M. J. & Benjamin, P. R. Central pattern generator interneurons are targets for the modulatory serotonergic cerebral giant cells in the feeding system of Lymnaea. *Journal of Neurophysiology* **75**, 11-25 (1996).

Yin J.C.P, Wallach, J.S., Del Vecchio, M., Wilder, E.L., Quinn, W.G., & Tully, T. Induction of a dominant negative CREB transgene specifically blocks long-term memory in *Drosophila*. *Cell* **79**, 49-58 (1994).

Yiu, A. P., Rashid, A. J. & Josselyn, S. A. Increasing CREB Function in the CA1 Region of Dorsal Hippocampus Rescues the Spatial Memory Deficits in a Mouse Model of Alzheimer's Disease. *Neuropsychopharmacology* **36**, 2169-2186 (2011).

Yoshimasa, T., Sibley, D. R., Bouvier, M., Lefkowitz, R. J. & Caron, M. G. Cross-talk between cellular signaling pathways suggested by phorbol-ester-induced adenylate-cyclase phosphorylation. *Nature* **327**, 67-70 (1987).

Zakharenko, S. S., Zablow, L. & Siegelbaum, S. A. Visualization of changes in presynaptic function during long-term synaptic plasticity. *Nature Neuroscience* **4**, 711-717, (2001).

Zampagni, M. *et al.* Lipid rafts are primary mediators of amyloid oxidative attack on plasma membrane. *Journal of Molecular Medicine-Jmm* **88**, 597-608, (2010).

Zeimal, E. V. & Vulfius, E. A. The action of cholinomimetics and cholinolytics on the gastropod neurons. *Symposium on neurobiology of invertebrates*, 255-265 (1968).

Zhang, W. & Linden, D. J. The other side of the engram: Experience-driven changes in neuronal intrinsic excitability. *Nature Reviews Neuroscience* **4**, 885-900 (2003).

Zhang, J.-F., Qi, J.-S. & Qiao, J.-T. Protein kinase C mediates amyloid beta-protein fragment 31-35-induced suppression of hippocampal late-phase long-term potentiation in vivo. *Neurobiology of Learning and Memory* **91**, 226-234 (2009).

Zhao, M. L. & Wu, C. F. Alterations in frequency coding and activity dependence of excitability in cultured neurons of Drosophila memory mutants. *Journal of Neuroscience* **17**, 2187-2199 (1997).

Zhao, M. L., Adams, J. P. & Dudek, S. M. Pattern-dependent role of NMDA receptors in action potential generation: Consequences on extracellular signal-regulated kinase activation. *Journal of Neuroscience* **25**, 7032-7039 (2005).

Zhao, W.-Q. *et al.* Inhibition of Calcineurin-mediated Endocytosis and alpha-Amino-3-hydroxy-5-methyl-4-isoxazolepropionic Acid (AMPA) Receptors Prevents Amyloid beta Oligomer-induced Synaptic Disruption. *Journal of Biological Chemistry* **285**, 7619-7632 (2010).

Zolamorgan, S. M. & Squire, L. R. The primate hippocampal-formation – evidence for a time-limited role in memory storage. *Science* **250**, 288-290, (1990).

Zurgil, N. & Zisapel, N. Phorbol ester and calcium act synergistically to enhance neurotransmitter release by brain neurons in culture. *Febs Letters* **185**, 257-261 (1985).

Appendix

I. Throughout the thesis

I.1 Transgenic mouse models of AD

Many transgenic mouse lines are used to study AD. Confusingly, some of the most used lines have multiple names to indicate the same transgenics. Here, those that have multiple names are indicated with either a * or a ^. All transgenic mice mentioned in this thesis are included here, with a short description of their mutations and other relevant transgenics.

Tg(APP$_{swe}$)2576*: In these mice, human APP$_{695}$ contains a double mutation at Lys^{670} → Asn and Met^{671} → Leu. APP$_{swe}$ was then inserted into a hamster prion protein vector with the open reading frame replaced from PrP → APP (Hsiao et al., 1996).

Tg2576*: Also known as APP$_{swe}$. In these mice, human APP$_{695}$ contains a double mutation at Lys^{670} → Asn and Met^{671} → Leu (Westerman et al., 2002).

APP$_{695}$SWE*: Also known as APP$_{swe}$. In these mice, human APP$_{695}$ contains a double mutation at Lys^{670} → Asn and Met^{671} → Leu (Chapman et al., 1999).

APP+PS1: Double transgenic mouse generated by crossing APP$_{swe}$ (see above) mice with a line expressing the PS1 (M146L) mutation in the PSEN1 gene (Arendash et al., 2001).

Arctic APP: A point mutation in APP at E693G (Nilsberth et al., 2001).

APdE9: These transgenic mice are made by co-injecting a vector encoding mutant APP (the APP$_{swe}$ mutation) and mutant PSEN1 (the δE9 mutation) (Minkevicience et al., 2009).

hAPP^: This model over expresses human APP with two mutations; one at the above mentioned APP$_{swe}$ and the other at V717F, often referred to as APP$_{Ind}$ (Palop et al., 2007).

PDAPP: This model is also known as APP$_{ind}$ and contains the mutation V717F (Webster et al., 2014).

APP23: This model has a 7-fold over expression of the APP$_{swe}$ mutation (Webster et al., 2014).

TgCRND8: These transgenic mice over express human APP, with APP_{swe} and APP_{ind} mutations, 5-fold greater than endogenous murine APP (Webster et al., 2014).

J20^: This line is also called hAPP. They over express human APP with the APP_{swe} and APP_{ind} mutations (Webster et al., 2014).

APP751SL/ PS1 KI: These transgenic mice are a cross between an over expressing human APP line, with mutations at APP_{swe} and APP_{lon} (V717I), and a PSEN1 knock-in line, with two point mutations at M233T and L235P (Webster et al., 2014)

5xFAD: These mice are transgenic for both APP and PSEN1. The APP mutations include APP_{swe}, APP_{flo} (I716V), and APP_{lon}. The PSEN1 mutations include M146L and L286V (Webster et al., 2014).

3xTg: These mice are transgenic for APP (APP_{swe}), PSEN1 (M146V), and MAPT (P301L) (Webster et al., 2014).

$APP_{swe,ind}$^: Transgenic mice that have both the APP_{swe} and APP_{ind} mutations (Webster et al., 2014).

*,^ denotes mice with the same mutation, but different names

II. Chapter 3

II.1 Establishment of the behavioural testing time point

A pilot experiment was run to establish a testing time point where Aβ-induced memory loss was observed, ranging from 48 hours post-training to 8 days post-training (Figure II.1). Animals were starved for 2 days, trained at time point 0 hours (the day after starvation completed), injected with 0.1 mM Aβ 25-35 at time point 24 hours, and tested for the conditioned feeding response every day for up to 8 days post-training. The results of this pilot experiment, along with general incubation time points used in the literature, established the testing time point as 24 hours post-injection and 48 hours post-training.

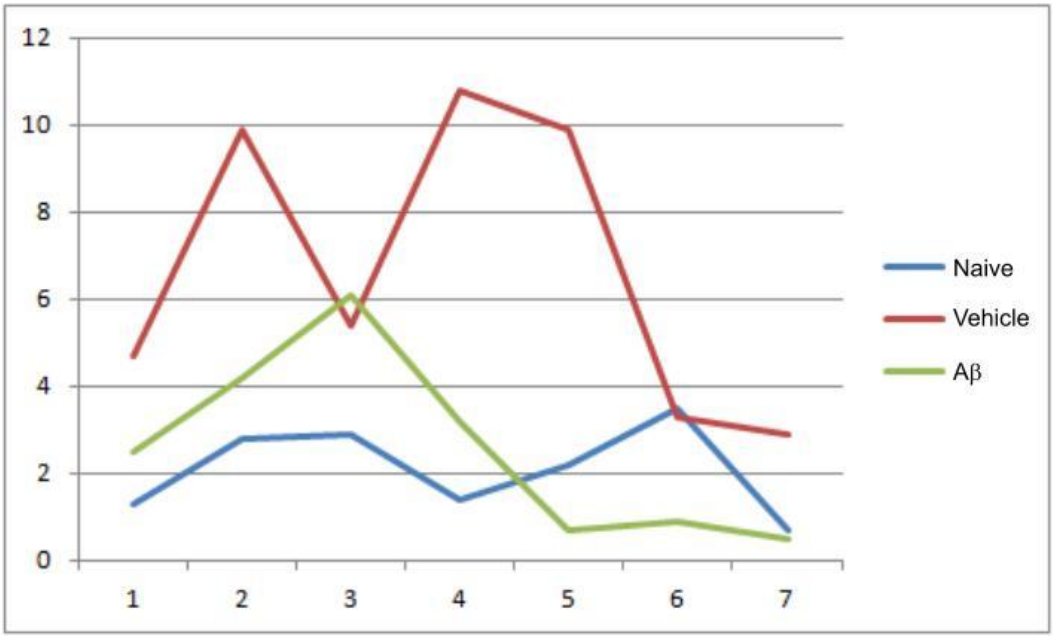

Figure II.1 Comparison of behavioural responses from day 1 to 7 after injection. Naïve, uninjected; trained, vehicle-injected; and trained, Aβ 25-35-injected animals were behaviourally tested 1, 2, 3, 4, 5, 6, or 7 days after animals were injected. The average behavioural response of each group is represented for each day.

III. Chapter 6

III.1 NMDAR1 antibody studies

As NMDAR1 antibodies have not been used successfully in *Lymnaea*, a sequence alignment between *Lymnaea* and rat NMDAR1 was compared for areas of high homology (Figure III.1A). Discrepancies between the two sequences were found in all antigens of commercial antibodies. The first antibody studied, Anti-NMDAR1 (Abcam, aa 869-882), is a polyclonal antibody and exhibited banding at different weights in the rat sample (Figure III.1B). However, the predominant bands were not at the predicted weight of ~120kD. Unsurprisingly, since non-specific banding appeared throughout the rat sample, the *Lymnaea* sample was a long smudge of incomprehensible signal. Even with a lot of optimisation, this antibody is unlikely to offer decent results for *Lymnaea*, considering the poor results in the rat sample. A new antibody, NMDAR1 (Novus Bio, aa 1-564), was compared in a similar manner to assess usefulness in *Lymnaea*. Unlike the Abcam antibody, the Novus Bio antibody only showed banding at two weights in the rat sample, one of which is the predicted weight of NR1 at 120 kD, but with a more dominant band at a lower molecular weight (Figure III.1B). *Lymnaea* signal with the Novus Bio antibody is contained to the 200-100 kD region, showing no equivalent banding to the non-specific band in the rat sample. The downside of this antibody is in how *Lymnaea* displays its banding. It is again largely smudgy, with no crisp band appearing. A great amount of optimisation, along with a pre-absorption study, would be needed to determine if this antibody is useful in *Lymnaea*. If determined useful, the antibody should be used to label surface expression of NNMDARs, as surface levels have been found to change, but total levels have not (Lacor et al., 2007; Snyder et al., 2005) after Aβ treatment. The preliminary data suggests this antibody may be used successfully; however, will need to be further investigated.

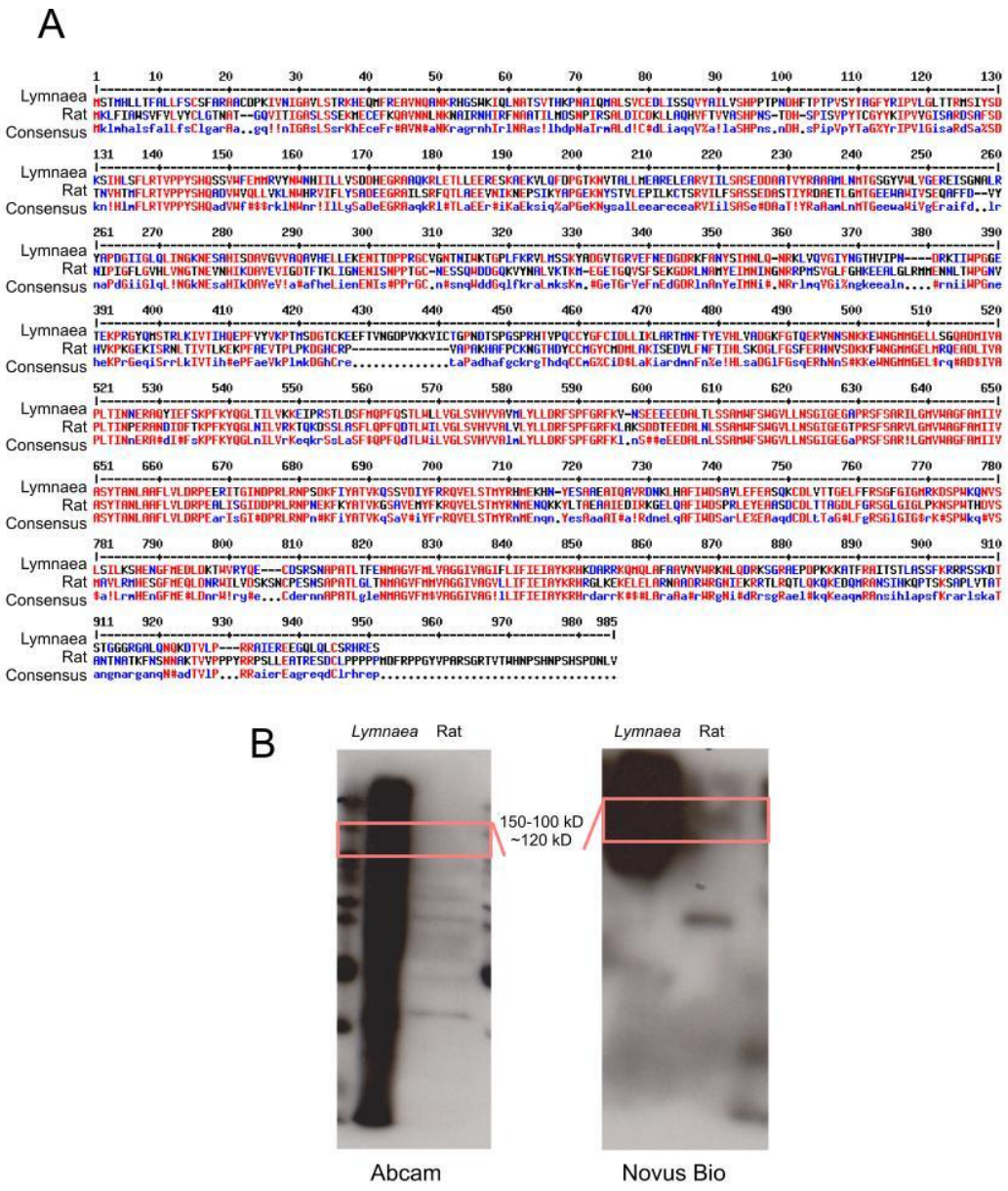

Figure III.1 NR1 comparisons between *Lymnaea* and rat indicate discrepancies in protein sequences. (**A**) NR1 amino acid sequence alignment between *Lymnaea* and rat. Consensus amino acids are shown in red, discrepancies are shown in blue. (**B**) Western blots of two different NR1 antibodies; Abcam (left) and Novus Bio (right). *Lymnaea*, rat, and protein ladders are run side-by-side on a gel and western blotted with the appropriate NR1 antibody. Pink boxes indicate 150-100 kD regions, with particular interest in finding a 120 kD band.

III.2 α7-nAChR antibody studies

nAChR antibodies, like NMDAR1, have not been used successfully in *Lymnaea* (aa 365-384). Similarly, a sequence alignment between *Lymnaea* and rat was made (Figure III.2) to find an appropriate antibody that had an antigen within the high homology range.

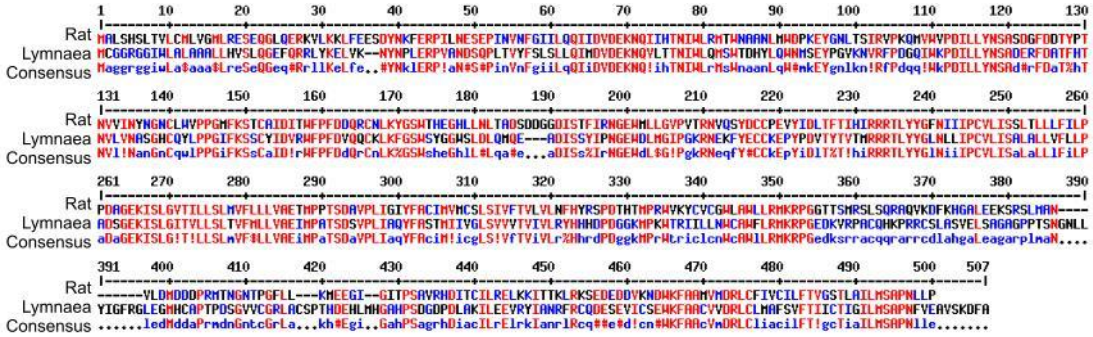

Figure III.2 α7-nAChR sequence alignment (**A**) nAChR A subunit in *Lymnaea* and α7-nAChR in rat amino acid sequence alignment. Consensus amino acids are shown in red, discrepancies are shown in blue.

III.3 Adenylyl cyclase antibody studies

An adenylyl cyclase mammalian antibody has not yet been used successfully in *Lymnaea* so, similarly to the NR1 and nAChR studies, a sequence alignment was used to compare areas of high homology between *Lymnaea* and rat. A commercially available mammalian adenylyl cyclase antibody was selected (range 250-300). However, the antigen had low alignment and the antibody was not successful when *Lymnaea* and rat sample were run side-by-side on a gel and western blotted with the antibody (Appendix III.3).

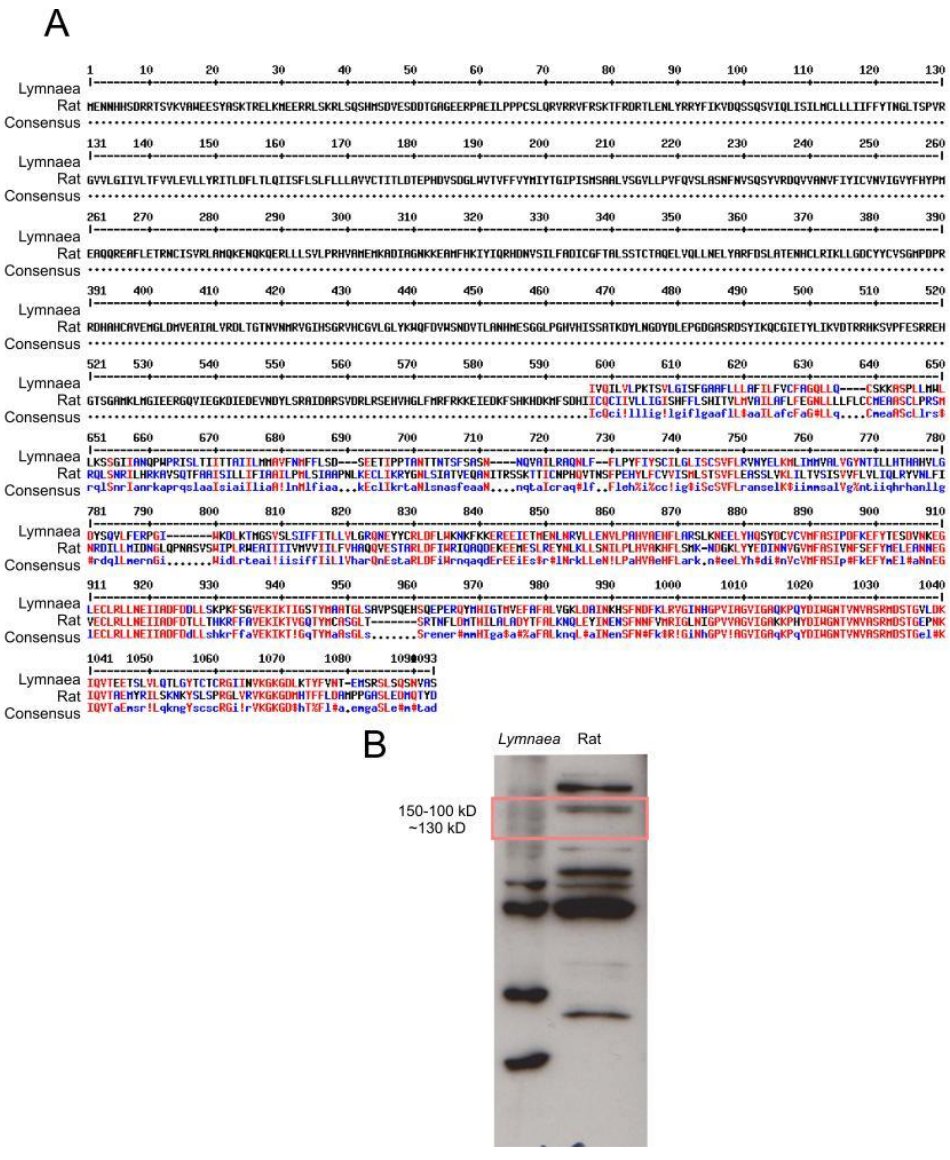

Figure III.3 An adenylyl cyclase mammalian antibody does not match well to *Lymnaea* adenylyl cyclase. (**A**) Adenylyl cyclase in *Lymnaea* and rat amino acid sequence alignment. Consensus amino acids are shown in red, discrepancies are shown in blue. (**B**) Western blots of *Lymnaea* and rat samples, run side-by-side on a gel and western blotted with an adenylyl cyclase antibody. Pink box indicates 150-100 kD regions, with particular interest in finding a 130 kD band.

III.4 PKC antibody studies

Like the other studies in this section, an appropriate sequence alignment was used to find a mammalian PKC antibody that may be used in *Lymnaea* (Appendix III.4A). Once a PKC antibody was selected with perfect alignment between the *Lymnaea* sequence and the antigen (range 499-697), samples from *Lymnaea* and rat were run side-by-side on a gel and western blotted with the PKC antibody (Figure III.4B). The bands match up exactly at 80 kD, with very strong signal in both and no other signal at non-specific sites.

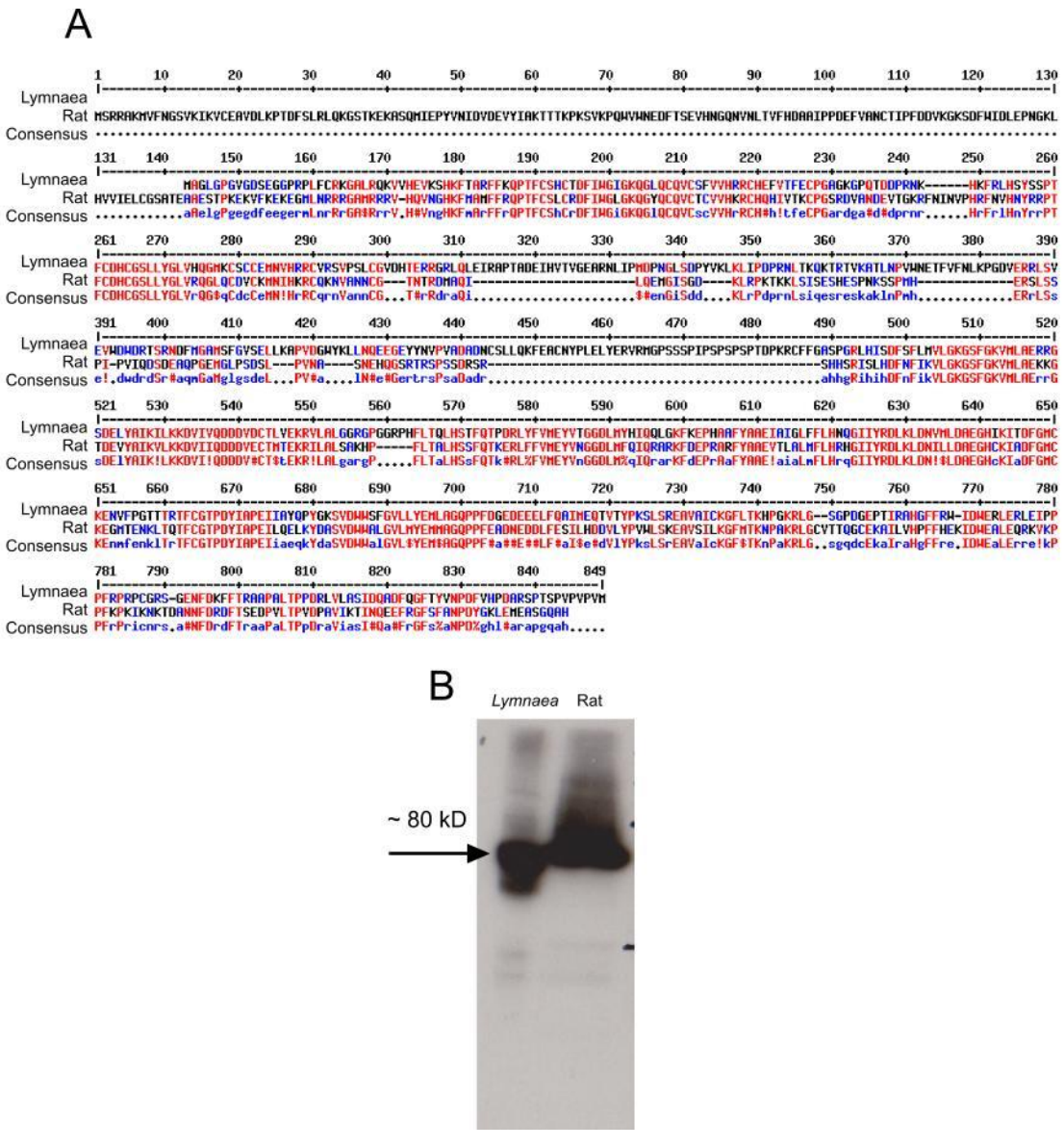

Figure III.4 A mammalian PKC antibody can be used successfully in *Lymnaea* studies. (**A**) PKC in *Lymnaea* and rat amino acid sequence alignment. Consensus amino acids are shown in red, discrepancies are shown in blue. (**B**) Western blot of *Lymnaea* and rat samples, run side-by-side on a gel and western blotted with a PKC antibody. Arrow indicates 80 kD.